



UNIVERSITÀ  
DEGLI STUDI  
DI PADOVA

UNIVERSITA' DEGLI STUDI DI PADOVA

**Dipartimento di Ingegneria Industriale DII**

Corso di Laurea Magistrale in Ingegneria Meccanica

**DEVELOPMENT OF A SUITABLE MODELLING  
APPROACH FOR THE ROBOT ASSISTED  
POLISHING PROCESS**

Relatore: Bruschi Stefania

Correlatore: Bissacco Giuliano

Federico Mazzucato, 626275

Anno Accademico 2012/2013







# CONTENTS

CONTENTS .....	5
ABSTRACT .....	9
CHAPTER ONE: Grinding, Lapping, Polishing .....	10
1.1. Introduction .....	10
1.2. Grinding .....	10
1.3. Lapping .....	15
1.4. Polishing .....	17
1.5. Conclusion .....	18
CHAPTER TWO: Examples of Polishing systems .....	21
2.1. Introduction .....	21
2.2. Diamond Polishing .....	21
2.3. Abrasive Flow Finishing .....	22
2.4. Chemical Mechanical Polishing .....	24
2.5. Elastic Emission Machining .....	26
2.6. Magnetic Abrasive Finishing .....	27
2.7. Magneto-Rheological Finishing .....	28
2.8. Magneto-Rheological Abrasive Flow Finishing .....	30
2.9. Magneto Float Polishing .....	32
2.10. Conclusion .....	34
CHAPTER THREE: Roughness: main parameters and measuring instruments .....	36
3.1. Introduction .....	36
3.2. Main Roughness Parameters .....	39
3.3. Measuring instruments .....	41
CHAPTER FOUR: The theoretical models .....	44
4.1. Introduction to the models .....	44
4.2. Introduction to the first theoretical model .....	45
4.3. Introduction to the second theoretical model .....	58

4.4.	Introduction to the third theoretical model.....	79
CHAPTER FIVE: The implemented MATLAB program.....		92
5.1.	Introduction .....	92
5.2.	Implemented MATLAB program structure .....	93
CHAPTER SIX: The experimental planning.....		103
6.1.	Introduction to the variables of the process .....	103
6.2.	The experimental planning .....	108
6.2.1.	Experimental planning variables.....	108
6.2.2.	Assignment of the levels for the chosen polishing process.....	111
6.2.3.	Number of repetitions of the experimental tests and timing intervals ...	116
6.2.4.	Configuration of the samples.....	117
CHAPTER SEVEN: Uddeholm Sleipner® HRC 59.....		121
7.1.	Introduction to the polishing material .....	121
7.2.	Preparation of the samples.....	122
7.3.	Mechanical properties tables of the UDDEHOLM SLEIPNER .....	124
CHAPTER EIGHT: Measurements of the samples before the experimental tests....		126
8.1.	Introduction .....	126
8.2.	Hommel Stylus Instrument T1000 .....	126
8.3.	Measurement operation .....	131
8.4.	Results of the measurements.....	137
CHAPTER NINE: Robot Assisted Polishing machine (RAP).....		145
9.1.	Introduction .....	145
9.2.	RAP control system and RAP tools .....	147
9.3.	RAP benefits .....	150
CHAPTER TEN: The experimental tests .....		151
10.1.	Introduction.....	151
10.2.	Preliminary settings .....	152
10.3.	Experimental methodology .....	155
10.3.1.	Introduction to the experimental procedure.....	155

10.3.2.	Understanding and measuring of the reachable final roughness value ..	157
10.3.3.	The issue of the paste refresh .....	158
10.3.4.	Summary of the experimental procedure and results correlated with the made measurements to evaluate $T4$ .....	166
10.4.	Observations related to the first measurements done to estimate $T4$ .....	175
CHAPTER ELEVEN: Measurements of the samples after the experimental tests .....		177
11.1.	Introduction.....	177
11.2.	Measurements with Hommel .....	177
11.3.	Conclusion.....	179
CHAPTER TWELVE: Analysis of the data.....		180
12.1.	Introduction.....	180
12.2.	Roughness analysis.....	180
12.6.1.	Introduction.....	180
12.6.2.	Arithmetical mean roughness ( $Ra$ ) analysis .....	182
12.6.3.	Maximum profile valley depth ( $Rv$ ) analysis.....	198
12.6.4.	Average maximum height of the profile ( $Rz$ ) analysis.....	212
12.6.5.	Conclusion.....	224
12.3.	DOE analysis.....	225
12.6.1.	Introduction.....	225
12.6.2.	Preliminary regression model .....	225
12.6.3.	Analysis of the full factorial design (3 factors and 2 levels each).....	229
12.6.4.	Conclusion regarding the full factorial analysis .....	244
12.6.5.	DOE analysis adding the central point .....	245
12.6.6.	Analysis deriving by all the parameter combinations employed in these experimental tests .....	252
12.4.	Correlation between the roughness behavior and the number of strokes made by the pad during the process .....	256
12.5.	Fitting of the preliminary regression model .....	259

12.6.	Creation of an empirical regression model using the experimental results ....	267
12.6.1.	Formulation of the empirical model .....	267
12.6.2.	Comparison between two empirical regression model created from the same experimental data but with different starting considerations .....	278
12.6.3.	Roughness behavior evaluation of the empirical model .....	280
12.6.4.	Comparison of predictions between the preliminary empirical model and the last empirical model .....	288
12.7.	MRR analysis .....	291
12.7.1.	Alignment of the profiles .....	291
12.7.2.	Computation of the experimental amount of material removal caused by the polishing process .....	297
12.7.3.	Comparison between the experimental data and the prediction of the first theoretical model .....	302
12.7.4.	Comparison between the experimental data and the prediction of the second model .....	306
12.7.5.	Comparison between the experimental data and the prediction of the third model .....	311
12.7.6.	Conclusion regarding the verification of the three theoretical models for the MRR .....	314
12.8.	Analysis of the overlap zone .....	316
	CHAPTER THIRTEEN: Conclusion .....	320
	References .....	324
	Acknowledgements .....	326



# ABSTRACT

This work is a master thesis born by a collaboration project between the Mechanical Engineering Department of Technical University of Denmark (DTU) and STRECON A/S company.

The dealt argument regards the analysis of the roughness behavior of the UDDEHOLM SLEIPNER material during a Polishing process in flat kinematics conditions. This particular machining condition has been possible to realize thanks to the employment of the Robot Assisted Polishing machine, common called RAP, that is a property of STRECON.

To understand how and which parameters affect the roughness behavior during the process some experimental tests have been run, checking the time required to reach the final roughness value. An empirical model capable to describe the roughness behavior as function of the most important polishing variables is purposed. Moreover, some theoretical models regarding the amount of material removal caused by the process are verified thanks the use of a MATLAB program realized by the collaboration of Roman Wechsler during his internship program in DTU.

Moreover, the behavior of the process in presence of overlapping is analyzed, detecting how the track left by the pad on the polished surface looks like.

In the end, the conclusions about the detected roughness behavior and MRR analysis are introduced and explained. Finally, some considerations about the polishing process in flat kinematics conditions and prospective new experimental tests are discussed.

# CHAPTER ONE

## Grinding, Lapping, Polishing

### 1.1. Introduction

Grinding, Lapping and Polishing are three important mechanical processes used to obtain the desired researched dimension, surface finishing, and very fine shapes of the machining workpiece, causing a little amount of material removal.

For these three techniques, the mechanisms employed to machine the workpieces could seem very similar (for example a rotating wheel which rubs against a wafer is common both in Lapping and in Polishing), but the aims remain distinct for each other. In fact, they are three different mechanical processes with different characteristics each other, and each of them has to be employed to obtain a precise result. An example of this is that these three techniques may belong to a mechanical machining sequence to achieve the desired final roughness value, or a free-damage surface of the machining part (in this particular case, the Grinding process is applied firstly on the workpiece and then Lapping and Polishing follow). Nevertheless, the design specification may require tolerances or sizes that a grinding wheel is capable to obtain, without the employment of the other two. Or, it could happen a mechanical machining which requires a great material removal in the beginning, but a close roughness tolerance in the end because these are the required specifications of the design. In this last case, the workpiece has to be firstly machined with a Grinding process to remove a large amount of material, and then with a Polishing process in the end to satisfy the requests.

But to better understand what are the characteristics and the capabilities of each of them and to see where and how these particular processes are employed in the mechanical field, they will be introduced above.

### 1.2. Grinding

Grinding is a material removal process, where rapid material removal occurs [1]. This technique is usually employed to remove big irregularities from the sample surface or to reduce the beginning workpiece sizes to desired dimensions [1].

Generally the used velocity of the grinding wheel is very high, and this is not the correct process to obtain very fine final roughness surface values or free-damage superficial condition. In fact, to achieve better surface conditions, Lapping or Polishing process usually follow Grinding.

In this technique, fixed bonded abrasive is employed with a grain size that is usually bigger than 40  $\mu\text{m}$  [1]. The common employed abrasives are: aluminum oxide, silicon carbide, cubic boron nitride and diamond [1]. With this kind of abrasives related to their grain size the  $R_a$  values of the reached final roughness surface are usually included between 1.6 and 0.1  $\mu\text{m}$  (lower values are unusual but possible to reach).

MATERIAL	HARDNESS (KNOOP 100)	DENSITY	STRUCTURE
SILICON CARBIDE (SiC)	2450	3.22	BLOCKY, SOLID, SHARP
ALUMINA (Al <sub>2</sub> O <sub>3</sub> )	2000	3.97	BLOCKY, SOLID, ANGULAR
BORON CARBIDE (B <sub>4</sub> C)	3000	2.51	BLOCKY, SOLID, SHARP
DIAMOND (C)	6000	3.51	SHARP, ANGULAR, SOLID

**TABLE 1.1.** Typologies of abrasive typically employed [1].

The dynamics of Grinding is simple. A grinding wheel is rotated at high speeds against the machining workpiece surface. The abrasive is situated in the grinding wheel that is pushed against the surface. In this way, the abrasive can scratch the part and cause the material removal. Big grain size of the abrasive granules and high speeds involve an high material removal.

The risk in this process is given by the increment of the temperature in the contact zone. In fact, high velocities together with the force applied by the wheel involve high temperatures which could affect the surface properties of the workpiece. The high local reached temperatures could cause changing in the chemical properties of the material, distortions of itself, and dangerous residual stresses. Fortunately, much of the heat generated in the contact zone is carried out by the chip formation [2].

Regarding the grinding wheel, they are responsible for the abrasion of the workpiece surface. In fact, they bring the abrasive in touch with the machining part. They can be distinguished by the typology of employed abrasive. If the abrasive is conventional, that is, aluminum oxide or silicon carbide is employed, the grinding wheels are called “conventional grinding wheels”, whereas if the employed abrasive is cubic boron nitride

or diamond, they are called “superabrasive grinding wheels” [3]. The choice between the two different typologies of wheels mainly depends on three factors:

- Physical and chemical characteristics of the work material (for example, the diamond is not indicated to machine ferrous alloy) [3];
- Grinding conditions [3];
- Type of grinding (stock removal grinding or form finishing grinding) [3].

Some configurations for conventional or superabrasive grinding wheels are shown in the picture below:

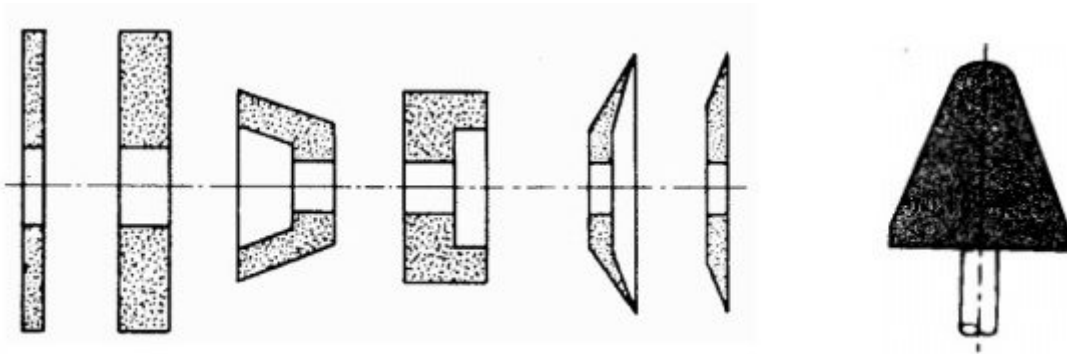


**FIGURE 1.1.** Examples of conventional grinding wheels [3].

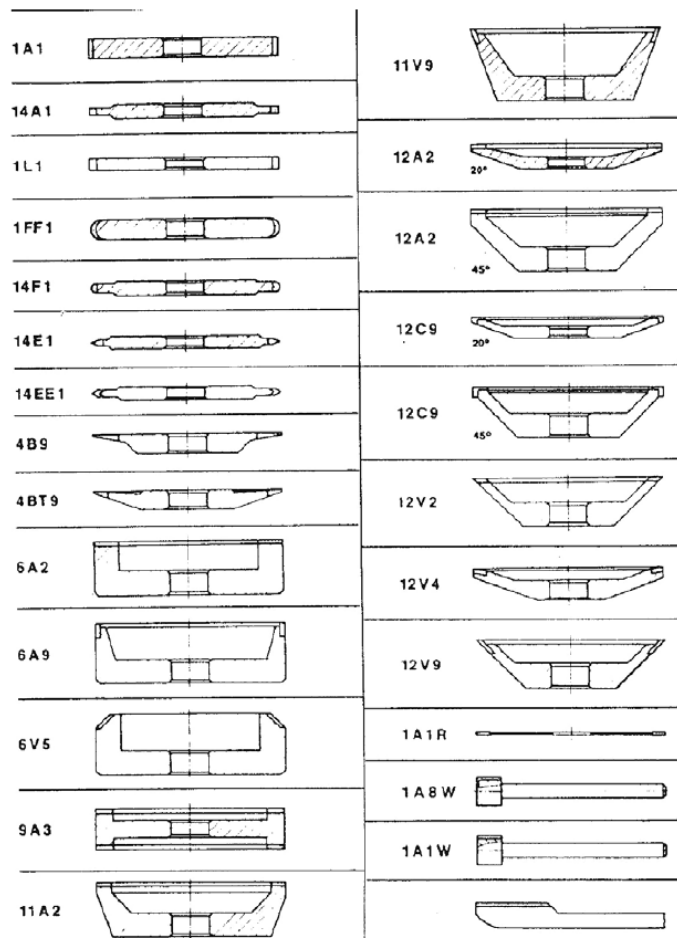


**FIGURE 1.2.** *Examples of superabrasive grinding wheels [3].*

As it can be seen in the previous pictures, every code defines a particular shape of the grinding wheels. This is because the Grinding process depends on the shape of the machining part, on the specifications required for that, and on the size of the workpiece. In fact, the Grinding process can be divided in surface grinding, cylindrical grinding, internal grinding, or centerless grinding operations. The differences between these typologies of grinding processes depend on the relative position between machining part and wheel, shape of the workpiece, shape of the wheel, and clamping system of the workpiece.












	External cylindrical	Internal cylindrical	Plan	Rotation
Peripheral plunge grinding				
Peripheral longitudinal loops				
Side plunge grinding				

FIGURE 1.3. Examples of grinding processes [4].

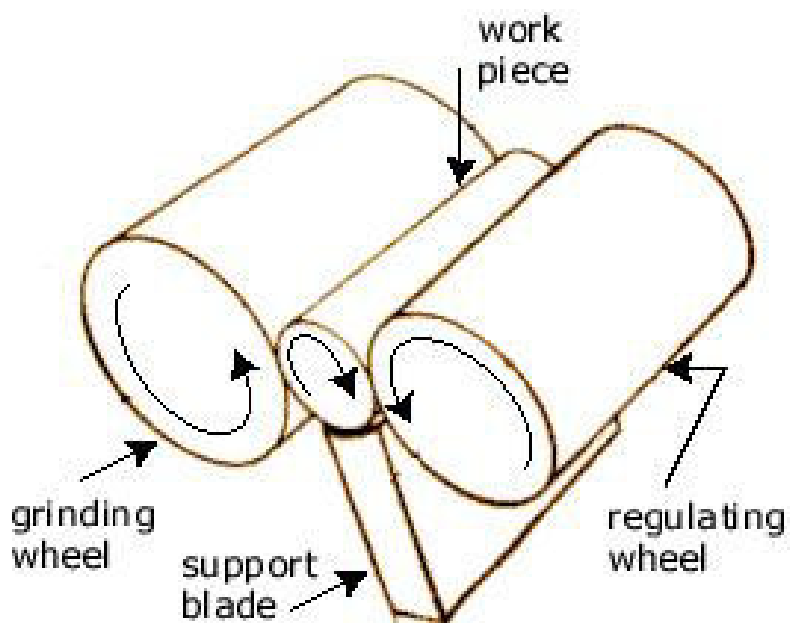


FIGURE 1.4. Centerless grinding [5].

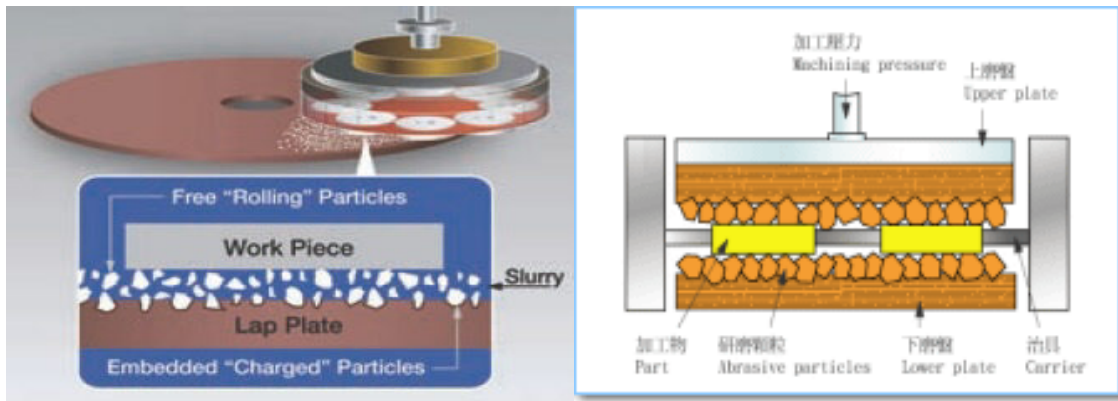
### 1.3. Lapping

Lapping is a material removal machining process that produces smooth and flat surfaces. The magnitude of the generated material removal is lower than that one generated by Grinding. The obtainable ranges of the final roughness values are between the 0.2 and 0.025  $\mu\text{m}$ . This technique is usually used to obtain dimensionally accurate specimens to high tolerances [1]. The reached speeds of the lapping plates are usually lower than that ones of the grinding wheels (less of 80 rpm [1]) and the employed abrasive size is between the 5-20  $\mu\text{m}$  [1]. Lapping process is mainly used to produce the desired flatness of the machining part.

Lapping can be run in two different regime: free abrasive Lapping and fixed abrasive Lapping [1] (in both cases, the caused surface damage is lower than Grinding).

In fixed abrasive Lapping, two plates rub together (one of them is the workpiece) and the abrasive is bounded on the polishing plate surface. This process can be seen very similar to the Grinding process, but the employed grain size and speed in Lapping are higher and the final effect on the part surface result very different.

The most used regime is the free abrasive lapping. In this case, two plates rotate but do not touch each other. The abrasive is free to move, roll and scratch the surface without a preferential way. The admission of the abrasive occurs towards an application of slurry that acts as lubricant and in the same time moves the abrasive on the lapping surface, washing out the chips of material. This is the most accurate method for producing specimens and causes the least amount of damage [1]. Anyway, it is noteworthy that in the end of this process the lapped surface does not have directional marks [6].



a

b

**FIGURE 1.5.** General scheme of a lapping process. a) [6]; b) [7].

Some example of lapping machines are shown below:



a

b

**Figure 1.6.** Examples of lapping machines. a) [8]; b) [9].



And in the table below some diamond lapping example are listed:

	Seal Ring	Pump Slider	Hot Water Seal	Chuck
Ceramic material	99.7% alumina	Alumina	Alumina	Alumina nitride
Surface area	49 in <sup>2</sup>	0.35 in <sup>2</sup>	1.5 in <sup>2</sup>	104 in <sup>2</sup>
Removal rate	.0018 in./hr	.0024 in./hr	.0038 in./min	.0005 in./hr
Diamond size	6 micron	3 micron	15 micron	3 micron
Slurry type	Water-based	Water-based	Water-based	Water-based
Plate type	HY iron composite	HY copper	HY copper	HY ceramic
Surface finish	5.7 μin	1.7 μin	6.5 μin	6 μin

**TABLE 1.2.** Materials usually employed in diamond lapping [6].

#### 1.4. Polishing

Polishing process is the material removal machining technique that is employed to obtain scratch-free, specular surface [1]. Here the produced material removal is very low and it is usually used to create very fine surfaces after a grinding or lapping process.

The abrasive is not fixed, but it is free to move between the pad and the workpiece surface and it is applied on the surface between a slurry that can have a lubricant function. This process is not cable to make flat surfaces because the applied force and the reached speed of its wheel are very low.

The employed abrasives is very fine (they are usually <15 μm) and the pad is very soft to allow to incorporate the abrasive particles that scratch the machining surface (for example wood or polyurethane pad are typically employed in polishing).

This process is very used to machine hard materials like glass or ceramics [1].

Some polishing machines are shown below:

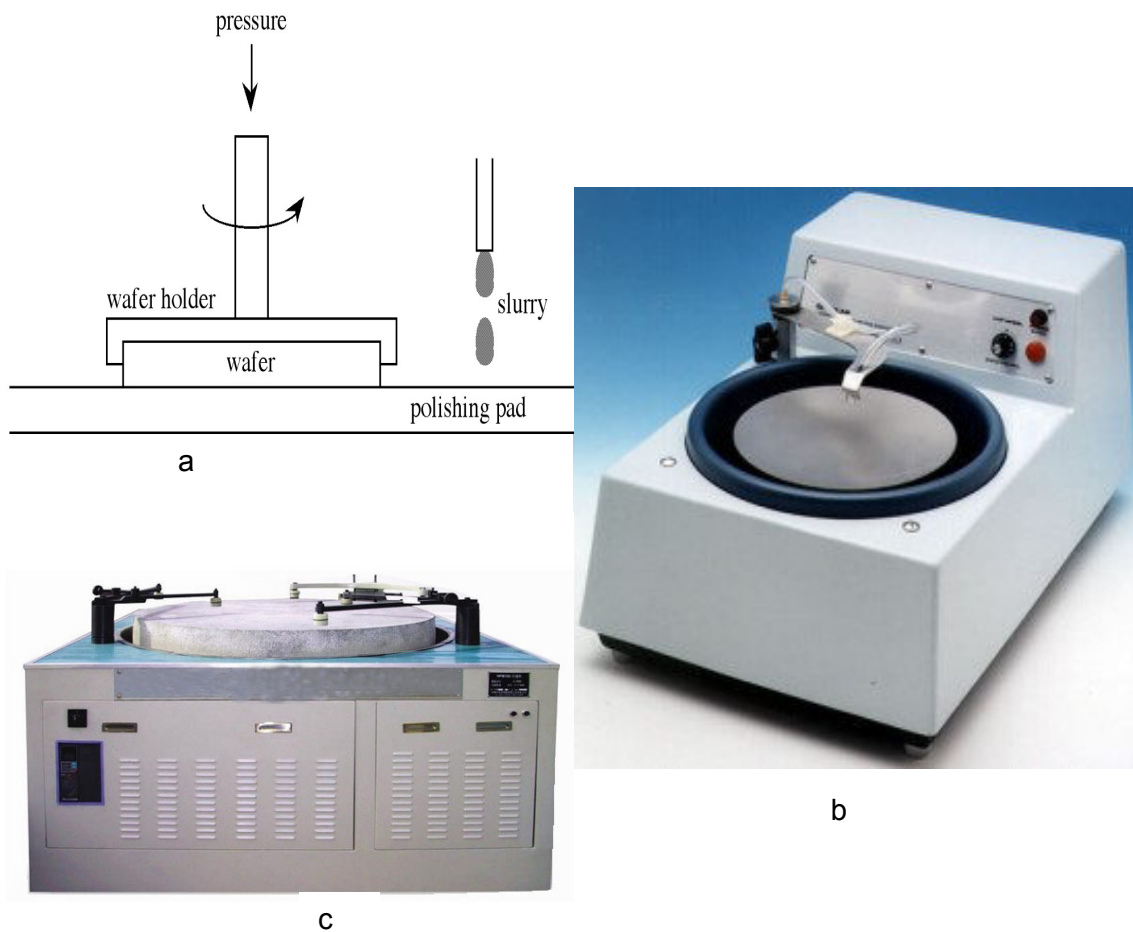


**FIGURE 1.7.** Example of polishing machines. a) [10]; b) [11]; c) [12].

## 1.5. Conclusion

These are the three important techniques for precise material removal processes. They are very important to reach the desired specification of the products. Anyway, these techniques are not fast in machining the parts and they are not suitable to process a high volume of products. This fact makes them very expensive.

A table is introduced below, where some example of mechanical processes and their final achievable roughness are listed:

<b>Manufacturing</b>		<b>Roughness, Ra (<math>\mu\text{m}</math>)</b>													
<b>Group</b>	<b>Description</b>	<b>0.006</b>	<b>0.012</b>	<b>0.025</b>	<b>0.05</b>	<b>0.1</b>	<b>0.2</b>	<b>0.4</b>	<b>0.8</b>	<b>1.6</b>	<b>3.2</b>	<b>6.3</b>	<b>12.5</b>	<b>25</b>	<b>50</b>
<b>Melting</b>	Sand casting														
	Casting														
	Die casting														
	Microcasting														
<b>Forming</b>	Forging														
	Rolling														
	Stuffing														
	Extrusion														
	Coinage														
	Lamination														
<b>Material removal</b>	Cutting														
	Cylindrical tuning														
	Facing tuning														
	Throat tuning														
	Shaving														
	Filing														
	Drilling														
	Boring														
	Widening														
	Smoothing														
	Milling														

TABLE 1.3. a) Usual final roughness achievable with machining process. [13].

<b>Manufacturing</b>		<b>Roughness, Ra (<math>\mu\text{m}</math>)</b>													
<b>Group</b>	<b>Description</b>	<b>0.006</b>	<b>0.012</b>	<b>0.025</b>	<b>0.05</b>	<b>0.1</b>	<b>0.2</b>	<b>0.4</b>	<b>0.8</b>	<b>1.6</b>	<b>3.2</b>	<b>6.3</b>	<b>12.5</b>	<b>25</b>	<b>50</b>
<b>Material removal</b>	Broaching														
	Cylindrical grinding														
	Facing grinding														
	Surface grinding														
	Frosting														
	Superfinishing														
	Lapping														
	Polishing														
	Tumbling														

**TABLE 1.3. b)** Usual final roughness achievable with machining process. [13].

# CHAPTER TWO

## Examples of Polishing systems

### 2.1. Introduction

In this chapter we want to introduce some polishing processes which are typical in the engineering environment and are capable to produce surface very smooth, shiny and damage-free as the traditional machining processes (as for example Grinding and Lapping) are not. These processes are capable to produce surface roughness values of eight nanometers or lower and they are often called Micro-/nano-machining (MNM) [6]. Moreover, a medium with loose abrasive particles are employed in each one [6]. Their main characteristics as operating principles, technology, employed material, and results are explained below.

The discussed polishing systems will be eight:

- Diamond Polishing;
- Abrasive Flow Finishing (AFF);
- Chemical Mechanical Polishing (CMP);
- Elastic Emission Machining (EEM);
- Magnetic Abrasive Finishing (MAF);
- Magneto-Rheological Finishing (MRF);
- Magneto-Rheological Abrasive Flow Finishing (MRAFF);
- Magnetic Float Polishing (MFP).

### 2.2. Diamond Polishing

In this process system the main features are the pad, the abrasive particles, the workpiece, and the interactions between them. The pad is usually softer than the workpiece material, for example polymers can be used, and the employed abrasive particles are diamond particle, but when the surface integrity and the chemical composition of the workpiece are negatively affected by the diamond abrasives these last ones may be substituted by cubic boron nitride grains (this could happen with ferrous alloys for examples).

An example is shown in the figure below:

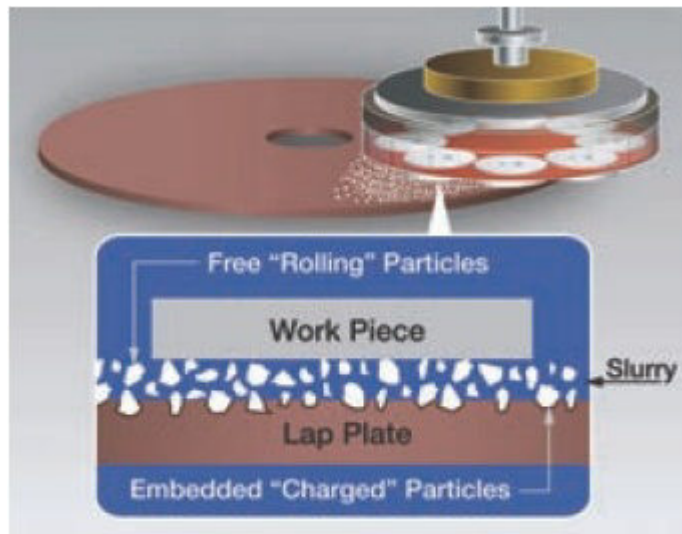


**FIGURE 2.1.** Diamond Polishing scheme.[6].

In literature some models exist to describe this process and they are usually based on the interactions between lap, workpiece, and the abrasive involved in the process.

During the diamond polishing process, the diamond abrasives are embed in the soft lap and scratch the workpiece surface causing material removal. The amount of material removal and the final surface roughness of the workpiece usually depend on: applied down pressure and its distribution on the contact area, grain size, employed slurry, workpiece material, mechanical characteristics of the pad.

### **2.3. Abrasive Flow Finishing**

The Abrasive Flow Finishing (AFF) is one of the polishing process where there is not external control of forces acting on the workpiece. In fact, this polishing system employs two vertical apposed cylinders and extrudes a medium containing the abrasive particles forward and backward between some holes situated between the workpiece and the tooling[14]. Therefore, the workpiece is located between the two cylinders so that it can be polished by the medium (*figure 2.2*).

Regarding the abrasive particles, they are blended in the medium[14]. This one is usually a special viscoelastic polymer that changes its viscous behavior when forced to

flow through a restrictive passage as a hole for example[14]. This polishing process is capable to reach excellent results for both surface accuracy and geometrical dimensions, though the workpiece is geometrically complex [14]. This is possible because the medium may follow and adapt to any geometry. This is the motivation because the medium is called as “self deformable stone” too [14]. In fact, it achieves two tasks: it assumes the shape of the polished workpiece for first and polishes the surface of the interested part (*figure 2.2*). Therefore, AFF can be applied to a large range of finishing operations that require uniform and repeatable results, for example this process is particularly used for deburring and finishing critical hydraulic and fuel system components of aircraft[14].

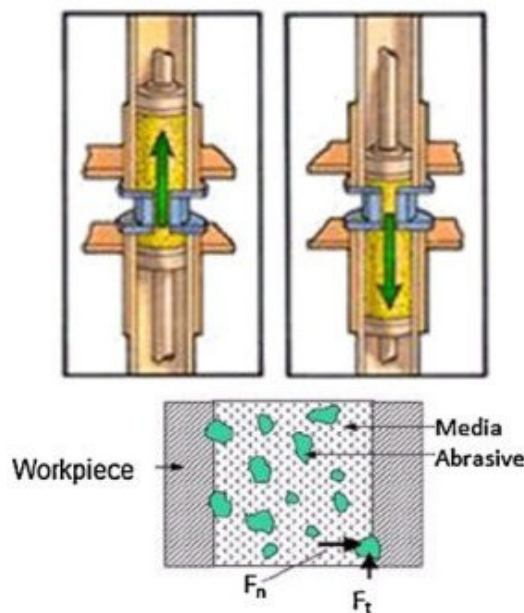


**FIGURE 2.2.** Abrasive Flow Polishing scheme.[14].

It has been shown by experimental tests that the material removal rate in AFF depends on some important process variables as: the position where an abrasive particle strikes the workpiece, the axial force, the radial force, the number of active grain in the medium and the grain depth of indentation[14]. Finally, it has been found that in AFF an increase in viscosity of the medium results in an increase in material removal rate, but in a decrease of the surface roughness[14].

## 2.4. Chemical Mechanical Polishing

Chemical Mechanical Polishing is a particular, expensive, but increasingly important category of loose abrasive finishing process; in fact, it is often used in semiconductor manufacturing [14]. This happens because with CMP it is possible to achieve two important targets for this industrial sector: reliable interconnects between two parts and a uniform thickness of the machined piece. The application of this CMP technology is primarily used to generate high quality, high form accuracy and high surface integrity, that is very difficult to be obtained by the traditional process. In fact, CMP is capable to overcome many problems of surface damage associated with hard abrasives as for example: pitting, dislodgement of grain, damage free surface [14]. With this process it is possible to machine both ductile and brittle materials. Moreover, as well as AFF, an external control on the force acting on the workpiece is not possible here.

In Chemical Mechanical Polishing two different reactions coexist affecting the process: a chemical reaction between the workpiece surface and the slurry, and a mechanical action between the abrasive particles and the new layer generated by the first reaction. The amount of material removal and the quality of the surface roughness depend on this two reactions. The kinematics of this polishing process can be rotational (*figure 2.3*) or linear (this is the case of analyzed in the following chapter). In the first case, a circular rotational pad is employed and it is usually held down on a workpiece; in the second one, the workpiece is usually fixed and the pad move on it with a determined feed and frequency.

For example, an example of this process is the Tungsten CMP. It is basically a combination of four main factors: the pad, the slurry, the abrasive particles and the workpiece. Here the chemical reaction occurs between tungsten and the slurry, whereas the mechanical action occurs between the abrasive particles carried by the slurry and the new superficial layer generated by the first reaction. The material removal rate depends on both chemical reaction rate and mechanical reaction rate. In fact, the two reactions are connected: the second one cannot exist without the first one, and for high MRR both reactions have to be high, because if one of them is low the other one is limited.

In literature some models exist that describe a CMP process and in the chapter four some examples will be introduced. Anyway no one is a general model capable to describes all the possible typologies of CMP processes. In fact, every model refers to the particular case that it wants to describe, but if one factor is changed (as for example the slurry composition, or the concentration of the abrasives) the model



becomes ineffective. A global model that describes all the different kinds of CMP process is still an actual challenge. However, to formulate a general model is not simple, because the considering variables are numerous and each one can affect the process in different way.

The main variables in CMP process are:

- Slurry;
- Abrasive (hardness, composition, size, shape, concentration);
- Relative velocity between the wafer and the part;
- Frictional forces and lubrication;
- Pad (fiber structure, pore size, elastic and shear modulus, hardness, thickness, Young's modulus, surface geometry, etc);
- Geometry of the part;
- Part size.
- Temperature;
- Pressure.

And the usual outputs of interest are:

- Material removal;;
- Planarization rate;
- Surface damage;
- Surface quality, in particular the surface roughness.



**FIGURE2.3.** General Chemical Mechanical Process employing rotational kinematic. [14].

## 2.5. Elastic Emission Machining

Elastic Emission Machining is the last polishing process here discussed where there is not external control on the force acting on the workpiece. EEM is a particular technological system capable to remove material at the atomic level and to get crystallographically and physically untouched finished surface [14]. A great dimensional accuracy and an high surface finish are obtainable by this polishing process.

EMM employs a soft ball as polishing pad, it is usually polyurethane (see *figure 2.4*). A load is applied on the soft ball which is always monitored by the control system of the machine. The abrasive is situated on the slurry which is put under the rotating pad (*figure 2.4*). The abrasive particles are very fine, and the material removal is very precise because it occurs to atomic level. The very precise material removal is followed by a very precise size dimensions.

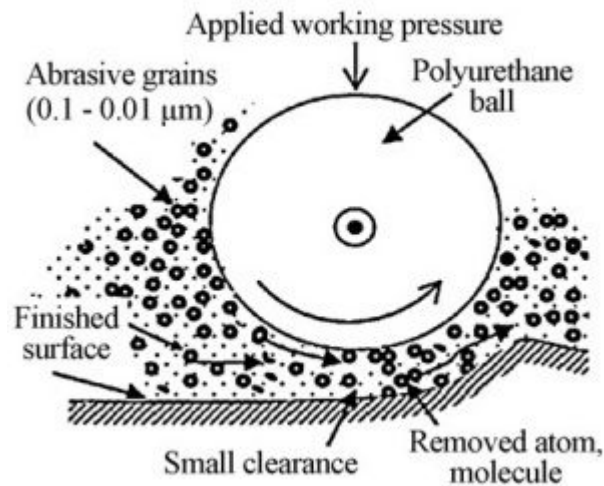


**FIGURE 2.4.** Elastic Emission Machining process. [14].

## 2.6. Magnetic Abrasive Finishing

Magnetic Abrasive Finishing is a polishing process where an external control of the force acting on the workpiece is possible and, in particular, MAF is capable of precision finishing of workpieces made of hard-to-machine material, obtaining nano-level surface finish [14]. This is the main reason because MAF is widely used in the industrial sector.

In this process, the magnetic field plays a fundamental role. In fact, it is capable to control the finishing process because the fine abrasive particles employed (as for example diamond or alumina) are sintered with ferromagnetic particles. The result of the sintering of both are particular particles named ferromagnetic abrasive particles [14]. These particles are formed and driven by the magnetic field. In fact, it acts as a bond and keeps the ferromagnetic abrasive particles in the machining gap [14]. In the gap zone, the magnetic force can be divided in two components: a normal one that is responsible for abrasive penetration inside the workpiece surface, and a tangential one that summed with the tangential force of the rotational motion of the ferromagnetic abrasives, is responsible to remove material in the form of tiny chips (*figure 2.5*) [14]. Therefore, the tasks of the magnetic field in MAF are two: to form and bring the ferromagnetic abrasive particles in the gap zone, and scratch the workpiece surface with the abrasives. In other hands, the magnetic field is responsible for both material removal, surface finishing and position of the ferromagnetic abrasive particles to the workpiece. Under this last point of view, the slurry with the ferromagnetic abrasive particles can be seen as a flexible abrasive brush [14] (*figure 2.5*).

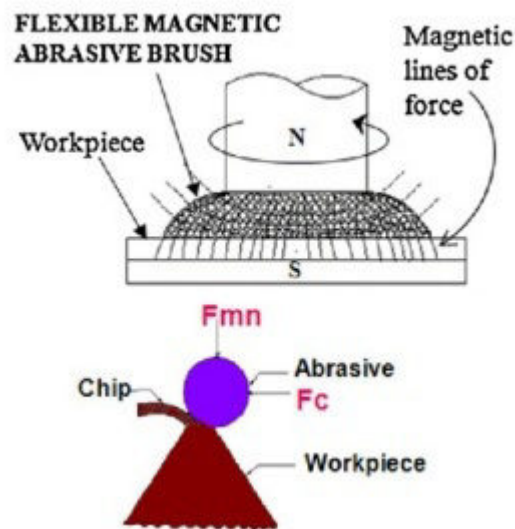


**FIGURE 2.5.** Magnetic Abrasive Finishing, where  $F_{mn}$  is the magnetic normal force and  $F_c$  is the tangential force. [14].

The process is highly efficient. The material removal rate and finishing rate depend on vary variables as: the workpiece circumferential speed, magnetic flux density, working gap, workpiece material properties, and size, type and volume fraction of abrasives [14]. The  $R_a$  reached values are in the order of nanometer.

MAF is mainly a polishing process, but it can be employed in other mechanical processes as removing of thin oxide film from high-speed rotating shafts, or in micro-deburring processes [14].

## 2.7. Magneto-Rheological Finishing

Magneto-Rheological Finishing is a finishing process that uses the property of Magneto-Rheological fluids (or MR fluids) to polish a workpiece and it has been developed to overcome the difficult encountered in finishing the lens [14]. The MR fluids are particular because they change their viscosity when a magnetic field is applied. They are constituted by a suspension of deionized water, iron particles, abrasive particles and stabilizing agents [14]. The presence of a magnetic field changes the rheological behavior of the MR fluid that becomes a non-Newtonian fluid, whereas without electro-magnet its behavior is Newtonian [14].

During this polishing process, the MR fluid is constantly kept in circulation and alternatively changes its physical phase, depending on its position in the circuit. In fact, if the fluid is close to the electro-magnet, it becomes solid, whereas if it is not, it exhibits its liquid phase.

In MRF, first the magneto-rheological fluid is carried on the rim of a rotating wheel, and then this wheel brings the MR fluid in the polishing zone. When the MR fluid is on the wheel it becomes solid, because its rheological behavior changes in presence of a magnetic field, since the rotating wheel is connected with the electro-magnet. Therefore, in this condition, the MR fluid arrives to the polishing zone in its solid phase. Even the workpiece is in the polishing zone and it is held down in contact with the rotating wheel in the CNC machine (*figure 2.6*). In this way, it can be polished by the abrasive particles carried by the MR fluid. As well as in EEM, the amount of material removal is controlled by the dwell time, but otherwise the external force on the workpiece is controllable [14].

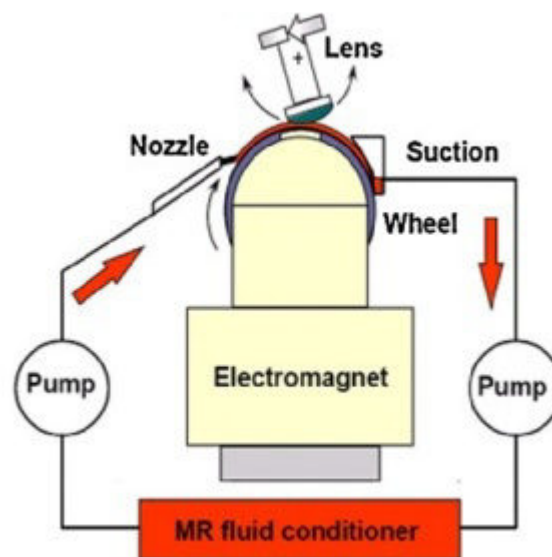


**FIGURE 2.6.** *Magneto-Rheological Finishing process.* [14].

What happens in the contact zone is shown in the *figure 2.7*. Due to the magnetic field applied on the polishing zone, the magnetic particles arrange themselves on the wheel surface, while the non-magnetic particles are pushed by them in contact with the workpiece surface [14]. This layout of the particles causes the polishing of the interested part. The material removal depends on the surface penetration of the

abrasive particle in the workpiece, that depends on the normal magnetic force of the electric-magnet, and on the relative motion between abrasive particles and workpiece [14].

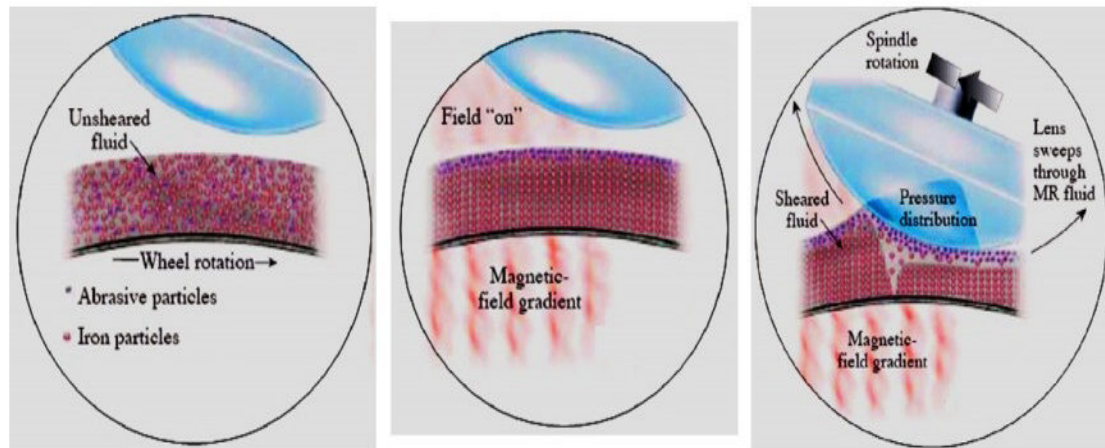


**FIGURE 2.7.** Polishing contact zone, between the MR-fluid and the workpiece. [14].

MRF is mainly employed in processes which machine brittle materials as finishing optical glasses or finishing glass ceramics, but it can be used for ductile material as plastics too [14].

## 2.8. Magneto-Rheological Abrasive Flow Finishing

The Magneto-Rheological Abrasive Flow Finishing is a polishing process that results from the sum of Abrasive Flow Finishing (AFF) and Magneto-Rheological Finishing (MRF). In other hands, it is an hybrid process developed to preserve the advantages of both processes: versatility of AFF, and determinism and controllability of rheological properties of MRF [14]. This process is capable to polish complex geometries, both internal and external, since it employs an abrasive mixed viscous base medium that is called “self deformable stone” as occurs MRF [14](figure 2.8).

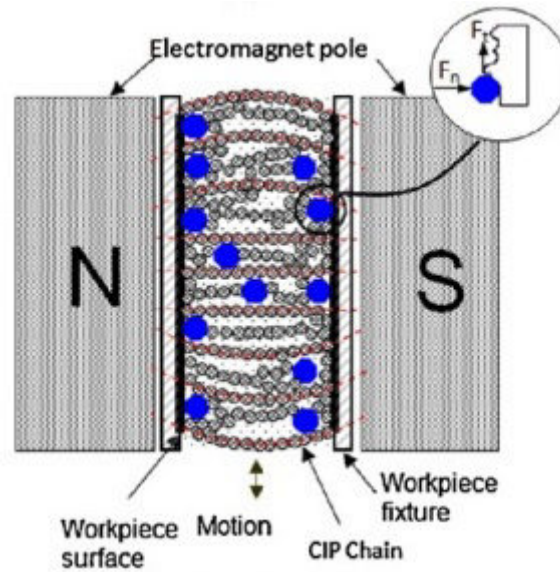


**FIGURE 2.8.** Magneto-Rheological Abrasive Flow Finishing process. [14].

The used medium in MRAFF is a MR-fluid, as in MRF, and fine abrasive particles are dispersed in it. When a magnetic field is applied, the rheological properties of the fluid change and some columnar structures are shaped where the magnetic field is applied [14] (figure 2.9). These structures are formed by the ferromagnetic abrasive particles and they produce the abrasion of the workpiece surface and shear the peaks from it [14]. As in the MRF process, the function of the magnetic field in MRAFF is fundamental. In fact, he acts as a bond and confers a certain resistance to the structures containing the abrasive particles. Therefore, in this process, the amount of material removal is strongly affected by the bonding strength produced by the magnetic field, and by the applied pressure which holds down the workpiece [14].

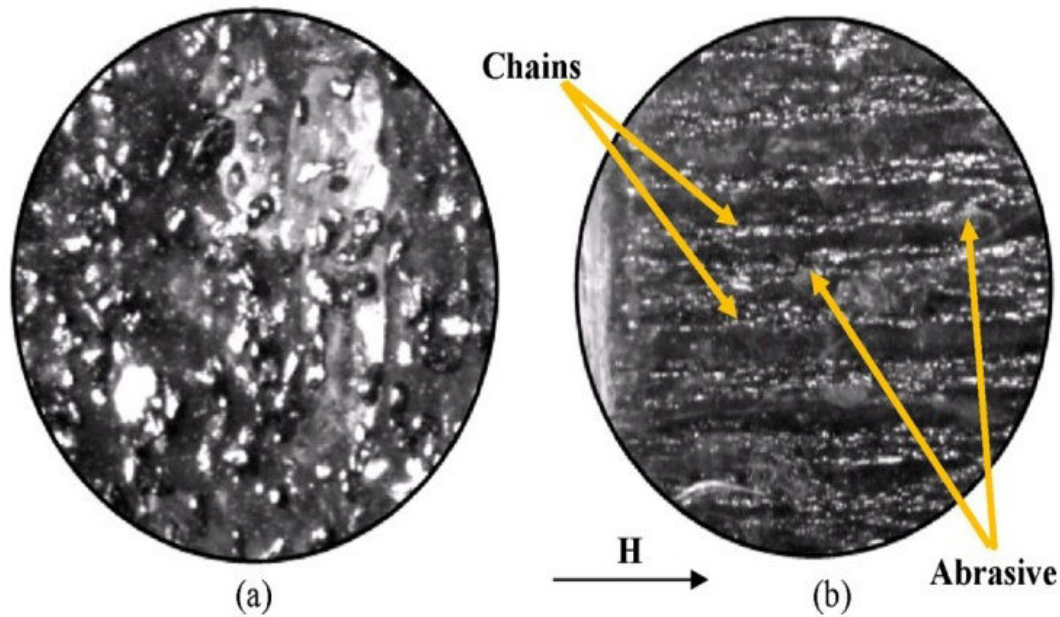


**FIGURE 2.9.** The chain structure shaped during the exhibition to a magnetic field: a) MR-fluid in a “normal” situation; b) MR-fluid under the influence of magnetic field. [14].

MRAFF process can reach the nano-level surface roughness value and for its particular flexibility to machine complex internal and external surface, it is capable to polish shaped 3D components [14]. In this process the external control of the force acting on the workpiece is possible as in MRF.

## 2.9. Magneto Float Polishing

The Magnetic Float Polishing has been developed for finishing of spherical surfaces as for examples bearing rollers. In fact, in the processes showed previously that kind of finishing manufacture was not possible. As in MAF, MRF and MRAFF, a magnetic field is here present too and it drives the abrasive slurry during the polishing process.

MFP is based on the ferro-hydrodynamic behavior of magnetic fluid [14]. In fact, when a magnetic field is applied, the non magnetic float and the abrasive particles presented in the fluid levitate on the surface of the fluid [14]. In this way, the abrasive particles are in contact with the workpiece and the polishing process can begin. As well as in the polishing processes which use the application of a magnet, in MFP the applied magnetic field plays an important role too. The levitation force applied in this process is fundamental.



In fact, when a magnetic field is present, the magnetic material in the magnetic fluid is attracted to the area of higher magnetic field, whereas the non magnetic materials (as abrasive particles and acrylic float) are pushed toward the area of lower magnetic field. This latter force applied on the non magnetic material can be named “buoyant force” and it is highly controllable, in fact it is proportional to the magnetic field gradient [14].

The structure of a MFP machine is simple (*figure 2.10*). A group of electromagnets are placed under the main chamber where the magnetic fluid, the abrasive particles, and the workpiece are located [14]. The magnets are the source of the magnetic field and for this reason the magnetic material goes down in the chamber, because it is attracted by them. Therefore, the non magnetic materials goes up and gets in touch with the workpiece. The down force necessary to hold the abrasives-workpiece contact is provided by a drive shaft that push the polishing parts down [14]. The level of down force can be controlled.

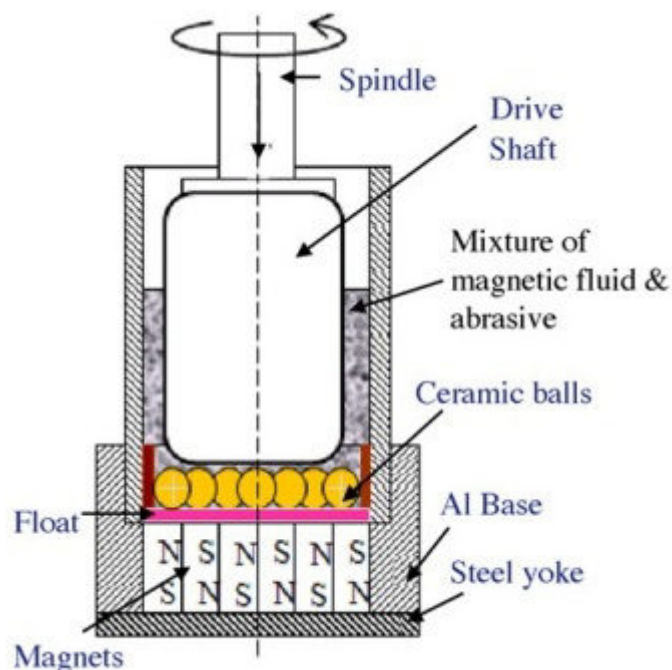


**FIGURE 2.10.** Magneto Float Polishing process.[14].

The workpieces are polished due to the relative motion between them and the abrasive particles under the influence of levitation force and down force.

## **2.10. Conclusion**

In conclusion, some polishing processes have been introduced. Not all these processes will be the aim of this thesis, but only the Chemical Mechanical Polishing will be discussed in the next pages. However, all these processes reach fine surfaces with roughness value in the nano-millimeter range. They achieve workpieces with high dimensional accuracy and free damage surface. They are very important when the workpiece or a part of it requires an optimal roughness values or free damage surfaces, as for example in the optical or mechanical environment (the application of mechanical components proof to the mechanical fatigue are an example).

The main disadvantages are two: these processes need much time to machine the workpiece and therefore they are very expensive, and not all have a theoretical model that can describe how the material removal varies with the input parameters and, principally, how the roughness varies with the time and the process variables; in other hands, not all these processes are completely automatic but depend on the skills of the operator.

A table is provided below where the eight polishing processes and their main applications are shown:

<b>POLISHING PROCESS</b>	<b>BEST REACHED ROUGHNESS</b>	<b>MACHINED PARTS</b>
<i>Diamond Polishing</i>	<i>100÷10 nm</i>	<i>glass, non ferrous alloys, ceramics</i>
<i>Abrasive Flow Finishing</i>	<i>~50 nm</i>	<i>hydraulic and fuel tube, hollow components</i>
<i>Chemical Mechanical Polishing</i>	<i>~5 nm</i>	<i>thin film transistor, IC wafer, semiconductor device</i>
<i>Elastic Emission Machining</i>	<i>&lt;5 nm/sub-nanometer</i>	<i>optical mirrors, optical surfaces</i>
<i>Magnetic Abrasive Finishing</i>	<i>~8 nm</i>	<i>mechanical and electronic components, high-speed rotating shaft</i>
<i>Magneto-Rheological Finishing</i>	<i>~10 nm</i>	<i>optical glasses, glass ceramics, plastics</i>
<i>Magneto-Rheological Abrasive Flow Finishing</i>	<i>~10 nm</i>	<i>optical glasses, complex 3D shaped parts, electronic parts</i>
<i>Magnetic Float Polishing</i>	<i>~4 nm</i>	<i>ceramic balls, bearing rollers</i>

**TABLE 2.1.** Roughness values achievable by the previously processes. [14].

# CHAPTER THREE

## Roughness: main parameters and measuring instruments

### 3.1. Introduction

The roughness is an important parameter and issue in many mechanical applications. It is determinant in mechanical conditions where friction, wear, lubrication, and good surface conditions affect both the life of the part during its working life and the good dimensional results related to the shape of the desired product. This means that the roughness interests a wide range of materials, from the metals, to the ceramics, and polymers as well, and a big range of mechanical fields.

In fact, the roughness is directly related to the surface conditions of the products, and this means that it is a good factor that clarify on the presence of scratches or scrapes on the part. In particular, scratches and scrapes weaken the products, decreasing the resistance of the itself under static loads and under dynamic loads (that is, they badly affect the fatigue life of the stressed part). In fact, they act as stress concentration points which bring to premature rapture of product under stress.

Moreover, having bad condition of the part surface could bring big problems when sliding surfaces are involving. In fact, if the roughness of the involved surfaces is not low, the relative motion between the two part could increase the heating between them causing large local temperature. This means that the life of the two parts would be shorter because the chemical surface conditions of the interested parts would be affected by the heating itself, causing local chemical changing of the surface or local melting.

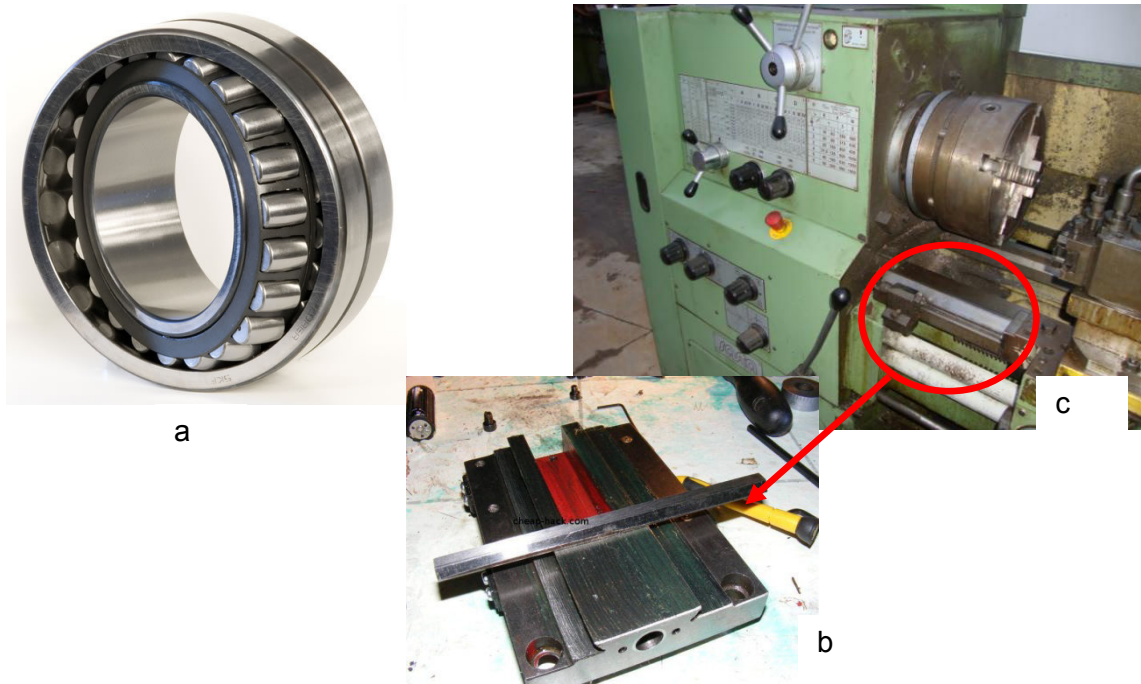


**FIGURE 3.1.** Sliding surfaces. a) [15]; b) [16]; c)[17].

Another field where the roughness plays a very important role is when the thermal and electrical conduction become an important characteristic for the use of the interested part. This happens for example in the electric conduction, where the contact between the devices has to be very high to guarantee a high electrical conductivity[18]. In this case, if the roughness is high, the contact between the two surfaces will happen only in few located zones, determining a contact area smaller than which should be. This means that the electrical conductivity field would be locally modify. This can be seen in the picture below:

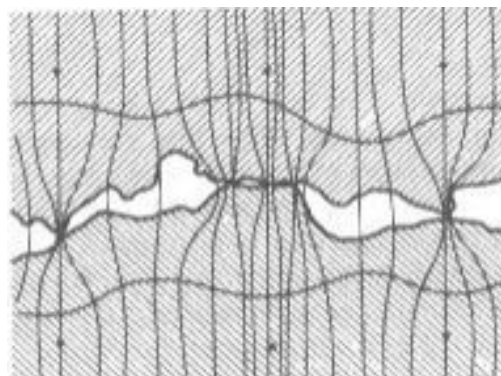


**FIGURE 3.2.** Local contact between two surfaces. [18].

Regarding the lubrication, the presence of high picks on the part surface could break the hydrodynamic fluid film that is important in system where the relative movement between two parts is required, but the contact between the two different surfaces is not desired. In this case, if the roughness condition is not good, the film might break and the contact between the two parts occurs, causing serious damages to the mechanical system.

Another important field that is interested by the roughness conditions is the tolerance field. Here if the sizes and the surface conditions of the part do not respect the required tolerances, the part will be scrapped, with consequent loss of money. An example of this case is the coupling cylinder-piston or the molds for polymer products.



**FIGURE 3.3.** Plastic molding. a) [19]; b) [20].

The roughness plays an important role in the chemical attack too. In fact, the smooth surfaces are more difficult to be attacked by chemical agents, guaranteeing a part's life and superficial integrity longer on the time than the rough ones. Also this means that the printing or the application of protective coating on these surfaces will be more difficult to make, because they tend to slip away.

Besides these mechanical applications, the roughness surface condition is important in the optical field, in the fluid dynamics and in the noise-vibration control too [18].

### 3.2. Main Roughness Parameters

As it can be read in these few rows, the roughness is a very important factor for a wide range of application especially in the mechanical field. For this reason it is necessary to describe the main parameters that are employed to define it.

The first one and one of the most in use is the *Arithmetical Mean Roughness* or commonly abbreviated  $R_a$ . This is defined as:

$$R_a = \frac{1}{l} \int_0^l |y(x)| dx$$

**FORMULA 3.1.** *Ra definition.*

Where  $l$  indicates the evaluation length where the roughness is computed. An example of roughness profile is shown below:

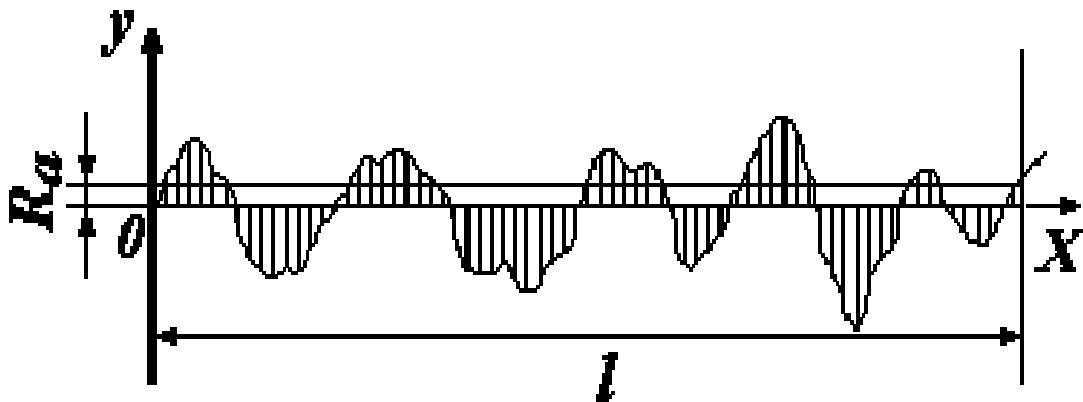


**FIGURE 3.4.** *Example of roughness profile. [21].*

The  $R_a$  represents the average roughness amplitude of the analyzed surface. This parameter is highly robust under a statistical point of view, but it does not give information about the presence of high peaks or deep valleys that could compromise a low value of the arithmetical mean roughness. For this reason, another important parameter has been defined to take into account the presence of undesired peaks and

valleys. This is the *Maximal Roughness Amplitude* or *Ten-Point Mean Roughness*, commonly abbreviated  $R_z$ . This parameter is defined as:

$$R_z = \frac{|Y_{p1} + Y_{p2} + Y_{p3} + Y_{p4} + Y_{p5}| + |Y_{v1} + Y_{v2} + Y_{v3} + Y_{v4} + Y_{v5}|}{5}$$

**FORMULA 3.2.** *Rz definition.*

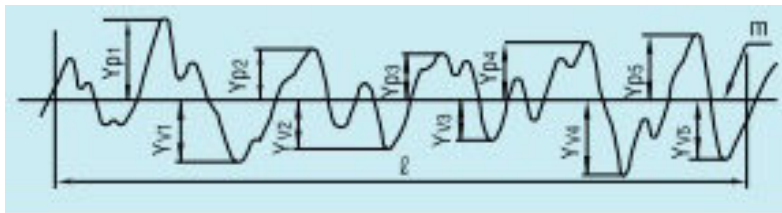


**FIGURE 3.5.** *Rz visualization.* [22].

The maximal roughness amplitude is particularly useful to characterize the surface defects when it is very important, for example in optical.

The two parameters previously described are the most employed to analyze the surface condition of the interested part and to do a general quality control of itself. But other parameters can be used as for example:

- *Root Mean Square Roughness* or commonly called  $R_q$ : this is an important parameter more sensitive than  $R_a$  employed to describe large deviation from the mean line of the profile. The equation that describes this value is:

$$R_q = \sqrt{\frac{1}{l} \int_0^l \{y(x)\}^2 dx}$$

**FORMULA 3.3.** *Rq definition.*

- *Maximum Height Of Peaks* or commonly called  $R_p$ : it is equal to the maximum peak of the profile over the mean line.



- *Maximum Depth Of Valleys* or commonly called  $R_v$ : it is equal to the maximum valley of the profile below the mean line.
- *Maximum Height Of The Profile* or commonly called  $R_t$ : it is equal to the sum between the highest peak of the profile and the deepest valley. In other hands:

$$R_t = R_p + R_v$$

**FORMULA 3.4.** *Rq definition.*

Other roughness parameters exist to describe the roughness but these six parameters are the most employed when a surface condition has to be characterized. However the first two of them ( $R_a$  and  $R_z$ ) are the most used when the surface quality control has to be checked and when the surface tolerances have to be respected.

### 3.3. Measuring instruments

To understand if during a Grinding or Lapping or Polishing process, or to check if the surface condition of a part respect the required tolerances, some measurement instruments are used. These are defined depending on their way to identify the roughness value. In fact, they can touch the measuring surface with a diamond tip for example (this is the case of a profilometer) or not (for example towards an optical system). Each of them can affects the measuring surface and has some strong and weak points. Below the most useful measurement instruments will be introduced:

- *Stylus instruments*: they are instruments which come in contact with the measuring surface. A diamond tip is usually employed to come in touch with the surface. The stylus makes a certain load on the tip which has to stay in contact with the surface. The tip runs across the surface for a determined length called “evaluation length” and records the vertical displacements of the surface profile. The vertical displacement of the tip is usually translated by a transducer which sends a signal to the software that elaborates it in roughness

parameter.

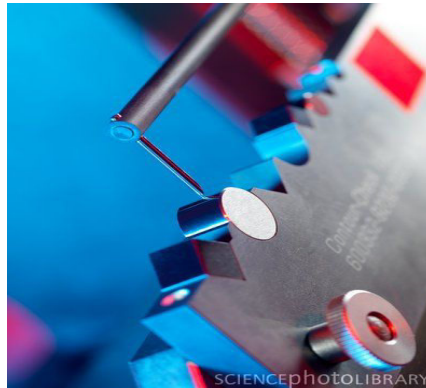


**FIGURE 3.6.** Examples of Stylus instruments. [23].

The problems related with this kind of measurement instruments are mainly two: the first one is that the type of employed transducer affects the measurement, and the second one is that in the contact zone between the tip and the surface a plastic deformation occurs and thus the beginning surface conditions are modified.

- *Optical instruments:* this kind of instruments do not come in contact with the measuring surface. In fact, they do not use a tip to find out the vertical displacement of the surface but “take a picture” of the analyzing region. The principle with that these measure instruments work is simple. A beam of radiation is reflected by the interested surface. Depending on the surface roughness the reflected light can specular, diffuse, specular and diffuse. Depending on the amount of specular or diffuse radiation the roughness surface is estimated.



**FIGURE 3.7.** ALICONA. Example of optical instrument. [24].

The main problem with these measurement instruments is that the roughness of too smooth surface is difficult to measure, because in this case the radiation is reflected back with a very small angle of deviation.

- *Microscopy*: these optical instruments are usually employed to investigate the surface, or in other hands to see how the part looks like. It is the most employed instrument to detect scratches, grooves, superficial texture, superficial phase changes and other visual defects that can be observed. Anyway, some microscopes exist now which are capable to investigate the roughness value of the part surface as for example the Scanning Tunneling Microscopy (STM), and the Atomic Force Microscopy (AFM).

# CHAPTER FOUR

## The theoretical models

### 4.1. Introduction to the models

The first important step in achieving the purposes of our thesis is that of searching in the literary resources (as in the online DTU library, or in specialized texts, or in specialized articles for example) some preexisting models, which describe the material removal behavior during a polishing process.

The best result of this literary search would be to find out some models which refer to a polishing process employing flat kinematics condition, since this polishing condition is replicated in STRECON when the RAP machine is used to machine flat surfaces. Unfortunately, the required typology of wished model has not been found, but only models with rotational kinematics have been dealt by the examined documents. For this reason, the models explained in the following chapters will discuss a CMP polishing process where both the pad and wafer rotate around their own axis. In a later stage, the rotational kinematics of these models will be adjusted to adapt the theoretical models to the linear kinematics of the pad encountered in our polishing tests. These models then will be implemented in the MATLAB program, so that it will be possible to see if the theoretical prediction is verified by the experiments or not.

This particular and important research has been a month and an half long, and has brought to focus on three models discussing the Material Removal Rate. These three models are discussed in three different articles which are titled: "*A Plasticity-Based Model of Material Removal in Chemical-Mechanical Polishing (CMP)*" written by Guanghui Fu, Abhijit Chandra, Sumit Guha and Ghatu Subhash [25], and called "*Model 1*" in the created program of analysis; "*Material Removal Mechanism in Chemical Mechanical Polishing: Theory and Modeling*" written by Jianfeng Luo and David A. Dornfeld [26], and reported as "*Model 2*"; "*Effect of particle size, polishing pad and contact pressure in free abrasive polishing*" written by Yongsong Xie and Bharat Bhushan [26], and called "*Model 3*" in the MATLAB program.

All these model cannot predict the exact amount of material removal encountered during the polishing process, but they give a proportional factor that is directly related to the Material Removal Rate. Obviously, this factor differs from model to model (for example the model one calculates the overall reduction area of the workpiece surface,

the model two finds out the reduction of the thickness, whereas the model three calculates the total wear coefficient). To predict the exact MRR, the theoretical models require some experimental data to estimate it. Therefore, once having run the test and measured the profiles required to detect the material removal, part of the MRR data calculated will be filled in the MRR database of the models, and from these the proportional factor for each model will be calibrated. In this way, the theoretical model will be able to formulate a prediction of the MRR for the other experimental data which have not been put in the database. Therefore, the verification of the models could be made with the comparison between the theoretical prediction and the experimental results.

Regarding the roughness behavior of the workpiece surface, no models have been found from the literary research. Indeed, only some information about the variables which affect the roughness behavior of the surface has been extracted from the analyzed documents. These variables are: down pressure, abrasive size, abrasive size distribution, relative velocity between pad and wafer, chemical reactions, mechanical property of the wafer and pad, shape of the abrasive particles. Anyway in these articles, no information about how these parameters affect the roughness behavior has been extracted. Then this argument should be detected after having run with the experimental tests.

In the following subchapters, the three analyzed theoretical models for the MRR will be introduced.

## **4.2. Introduction to the first theoretical model**

The first implemented model has been extracted by “A Plasticity-Based Model of Material Removal in Chemical-Mechanical Polishing (CMP)”, an article written by Guanghui Fu, Abhijit Chandra, Sumit Guha, and Ghatu Subhash [25].

The aim of this model is to understand the influence of various design parameters on the Material Removal Rate (MRR) and provides a theoretical formula that predicts the amount of MRR during a Chemical Mechanical Polishing process. This is not easy, because CMP is not a conventional material removal technique and because in this process the MRR is caused by two different reactions which affect each other: a chemical one and a mechanical. Both are important and affect the process; the chemical reaction, for example, occurs between the wafer and the slurry and changes the chemical characteristics of the polishing material surface that become softer and

easier to work, whereas the mechanical reaction occurs between the wafer surface and the abrasives and causes the material removal from the workpiece. The full knowledge on how and how much the chemical reaction affects the process and how the two reactions affect each other is not known to date, so for this reason some simplifications are necessary. The theoretical assumptions assumed in this model are the following:

- Due to the chemical reaction, an hydroxylated interface layer is produced. There is not sure information on this layer, but the workpiece surface becomes softer. For this reason the model assumes that this layer has a perfectly plastic behavior (*figure 4.1*) [25];
- The pad is soft, therefore when a load is applied, it deforms, and its deformation between two consecutive abrasive particles can be approximated as the bending of a elastic beam (*figure 4.1 and 4.4*) [25];
- Understanding and predicting the distribution of the abrasive particles in the contact zone is not easy, because many factors influence the motion of the particles in the slurry. Therefore, their distribution is assumed to be uniform over the wafer [25];
- When the abrasive particles hit the surface of the wafer, the yield stress point is supposed to be reached. For this reason, it is supposed to be completely enveloped in a perfectly plastic solid (*figure 4.2 and 4.3*) [25];
- The particles are assumed to be rigid and they are harder than pad and the hydroxylated layer [25].

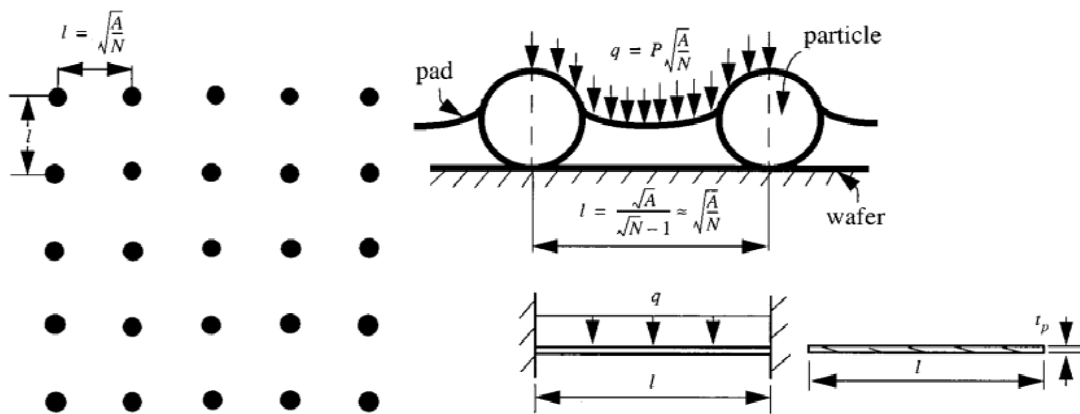


**FIGURE 4.1.** Distribution of the abrasives in the contact area and of the load between two particles [25].

As said above, the CMP process is not a well known process as the conventional material removal techniques. This is the reason because a great number of variables have to be taken into account to predict the MRR or other output values of interest (as for example the final roughness of the machined part). In particular, this great number of variables includes both process parameters (as pressure, relative velocity between pad and wafer, etc), and geometric variables (as the shape of the particles), and mechanical variables (as hardness of the pad, hardness of the wafer, etc). Anyway, the considered variables in this model will be introduced step by step with the main equation used to represent the process.

The complete model discussed in the article takes into account two different shapes for the abrasive particles: one sharp (*figure 4.3*) and one spherical (*figure 4.2*), and from this two different shapes it develops two different equations and, therefore, two different models. Anyway, for our purpose, only the case with spherical abrasive particles will be considered. This can be seen as another assumption for our model. In fact, the particles in the slurry are free to move everywhere and to assume every position that they want, and usually they attack the workpiece surface with a negative rake angle. For this reason the assumption of spherical abrasive particles is not so restrictive, though the shapes of the particles located in a slurry is various.

Anyway, for a full explanation of the model and of its concepts and for a better understanding, the case of sharp particles will be explain below, but in the MATLAB program only the case with spherical particles will be implemented and run.

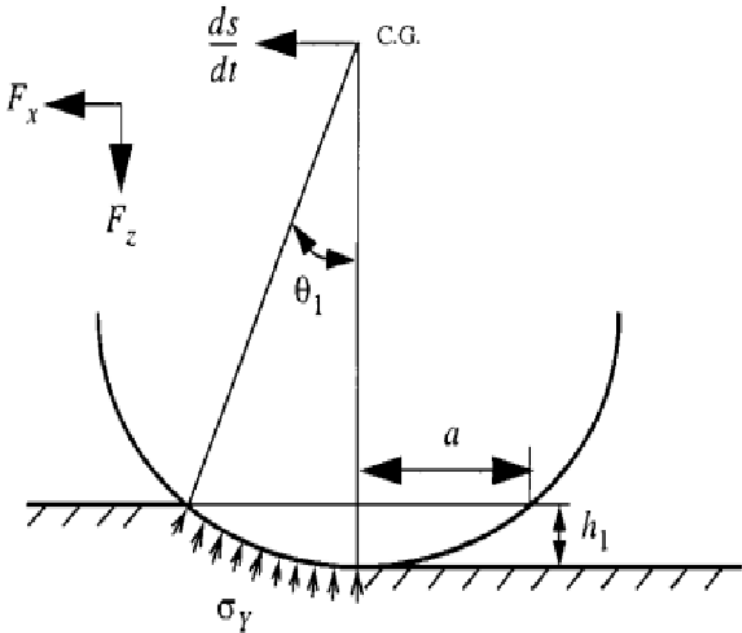


FIGURE4.2. Plastic contact between a spherical particle and the surface of the workpiece [25].

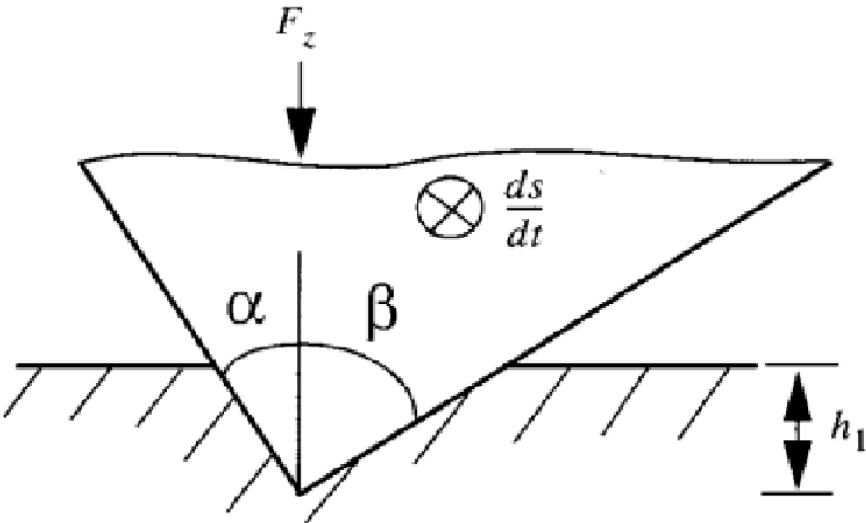


FIGURE4.3. Plastic contact between a sharp particle and the surface of the workpiece [25].



After having introduced the principal assumptions of this model, the first equation regarding the representation and description of CMP process can be reported below. In the beginning the total volume removed during the process is defined. If the previous theoretical assumption are taken into account and  $N$  abrasive particles are considered participating in the CMP process, the total volume removed ( $\Delta V$ ) can be expressed as:

$$\Delta V = N \times A_s \times \Delta s$$

**FORMULA 4.1.** [25].

where  $A_s$  represents the cross-sectional area, orthogonal to the movement of the abrasive particles, of the contact volume and  $\Delta s$  represents the abrasive motion of the  $N$  particles. After having defined  $\Delta V$ , the overall reduction area ( $\frac{dH}{dt}$ ) over an area  $A$  can be found. The steps to derive it are shown below:

$$\frac{\Delta V}{\Delta t} = N \times A_s \times \frac{\Delta s}{\Delta t}$$

**FORMULA 4.2.** [25].

$$\frac{dV}{dt} = N \times A_s \times \frac{ds}{dt}$$

**FORMULA 4.3.** [25].

$$\frac{\Delta V}{A \times \Delta t} = \frac{N}{A} \times A_s \times \frac{\Delta s}{\Delta t}$$

**FORMULA 4.4.** [25].

$$\frac{dH}{dt} = \frac{N}{A} \times A_s \times \frac{ds}{dt}$$

**FORMULA 4.5.** [25].

The *equation 4.5* is the starting one to define the MRR equations in different process situations. In fact, the overall reduction area formula is the base of the whole model and it will be adjusted depending on the circumstance and will be extended introducing the variables of the process.

Now, both for spherical and for sharp particles two different physical conditions are analyzed: the first one is when the wafer and pad do not touch each other, and this condition is implemented like a CMP process employing a stiff pad and high abrasive concentration; the second one is when there is an extended contact between the wafer and the pad, and this condition is implemented like a CMP process employing a soft pad and low abrasive concentration.

The CMP process with spherical abrasive particles is analyzed for first. In this condition, the first step is to define the acting forces on the abrasive between the pad and the surface of the workpiece. The forces on the contact zone are two, one in the vertical direction ( $F_z$ ) and one horizontal one ( $F_x$ ), and they are expressed as (*figure 4.2*):

$$F_z \sim \int_0^\pi \int_0^{\theta_1} \sigma_Y \times \cos \theta \times R^2 \times \sin \theta \, d\theta \, d\varphi = \frac{\pi}{2} \times \sigma_Y \times R^2 \times \sin^2 \theta_1$$

**FORMULA 4.6.** [25].

$$F_x \sim \int_0^\pi \int_0^{\theta_1} \sigma_Y \times \sin \theta \times \sin \varphi \times R^2 \times \sin \theta \, d\theta \, d\varphi = \sigma_Y \times R^2 \times \left[ \theta_1 - \frac{1}{2} \times \sin(2\theta_1) \right]$$

**FORMULA 4.7.**[25].

In the equations shown above,  $\theta_1$  represents the angle of contact and  $R$  is the radius of the abrasive grain. A double integral is necessary because it is computed over the part of the spherical surface where contact is made.

At this point, some new assumptions can be made. In fact, if the contact angle  $\theta_1$  is supposed small, the sine of it can be considered equal to that angle ( $\sin(\theta_1) = \theta_1$ ) and, therefore, referring to the *figure 4.2*,  $\theta_1$  can be approximated as  $\sqrt{2h_1/R}$ , where  $h_1$  is the depth of penetration of the abrasive particle in the workpiece surface.

With the previous assumptions, the equations representing the two forces  $F_z$  and  $F_x$  can be simplified and written again as:

$$F_z \sim \sigma_Y \times R \times h_1$$

**FORMULA 4.8.**[25].

$$F_x \sim \sigma_Y \times R^{1/2} \times h_1^{3/2}$$

**FORMULA 4.9.**[25].

Now, the usual employing pressure in a CMP process is not high, moreover the size of the abrasive particles is not large, but it reaches only some micrometers. Therefore, in this condition, the penetration  $h_1$  can be estimated small and the radius of the contact impression  $a$  can be written as:

$$a = \sqrt{R^2 - (R - h_1)^2} = \sqrt{2R \times h_1 - h_1^2} \sim \sqrt{2R \times h_1}$$

**FORMULA 4.10.**[25].

And the cross-sectional area  $A_s$  becomes to be equal to:

$$A_s \sim \frac{2}{3} \times 2a \times h_1 = \frac{4}{3} \times a \times h_1 = \frac{4}{3} \times (\sqrt{2R \times h_1} \times h_1) = \frac{4}{3} \times \sqrt{2} \times R^{1/2} \times h_1^{3/2}$$

**FORMULA 4.11.**[25].

From this latter expression, and using the equation found out to estimate the force  $F_z$  (formula 4.8), the formula for the cross-section area can finally be written as:

$$A_s \sim R^{1/2} \times \left( \frac{F_z}{\sigma_Y \times R} \right)^{3/2}$$

**FORMULA 4.12.**[25].

At this point, the cross-section area  $A_s$  and the forces system acting on the abrasives,  $F_z$  and  $F_x$ , have been found. From these parameters it is now possible to find out the pressure acting on the workpiece surface by each abrasive particle. In fact, using the equations 4.12 and recalling the assumptions formulated in the first pages of this chapter, for a CMP process employing spherical abrasive particles in a stiff pad and high abrasive concentration regime, the required average pressure is equal to:

$$P = \frac{N \times F_z}{A}$$

**FORMULA 4.13.**[25].

From this equation the force  $F_z$  can be expressed as:

$$F_z = \frac{P \times A}{N}$$

**FORMULA 4.14.**[25].

Substituting the *equation 4.14* in the *4.12*, the cross-section area is found to be as:

$$A_s \sim R^{1/2} \times \left( P \times \frac{A}{N} \times \frac{1}{\sigma_y \times R} \right)^{3/2}$$

**FORMULA 4.15.**[25].

If the *equation 4.15* is substituted in turn into the *equation 4.5*, the formula for MRR can be written as:

$$\frac{dH}{dt} \sim \frac{1}{\sigma_y^{3/2}} \times \left( \frac{A}{N} \right)^{1/2} \times \frac{1}{R} \times P^{3/2} \times \frac{ds}{dt}$$

**FORMULA 4.16.**[25].

What has been exactly found in the *equation 4.16* is not the exact MRR (as it has been said in the introduction of the model) but the usual overall reduction area introduced in the sentences above. Choosing this parameter to represent the MRR is not wrong, because it is proportional to MRR and estimates correctly the behavior of the material removal rate depending on the process parameters.

At this moment, another assumption can be done. In fact, if it is supposed that both the pad and the wafer are rigid for the same concentration (wt%) of abrasive particles in the slurry, it can be written that:

$$\begin{aligned} wt\% &= \frac{\rho_{particle} \times V_{particle}}{\rho_{fluid} \times V_{fluid} + \rho_{particle} \times V_{particle}} = \frac{1}{\frac{3}{2\pi} \times \left( \frac{\rho_{fluid}}{\rho_{particle}} \right) \times \frac{1}{R^2} \times \frac{A}{N} + \left( 1 + \frac{\rho_{fluid}}{\rho_{particle}} \right)} \\ &= constant \end{aligned}$$

**FORMULA 4.17.**[25].

Moreover, if some simplifications are done, it is observed that:

$$\frac{1}{R^2} \times \frac{A}{N} = \text{constant}$$

**FORMULA 4.18.**[25].

Therefore, after this consideration, the overall reduction area expressed in *equation 4.16* can be simplified and written as:

$$\frac{dH}{dt} \sim \frac{1}{\sigma_y^{3/2}} \times P^{3/2} \times \frac{ds}{dt}$$

**FORMULA 4.19.**[25].

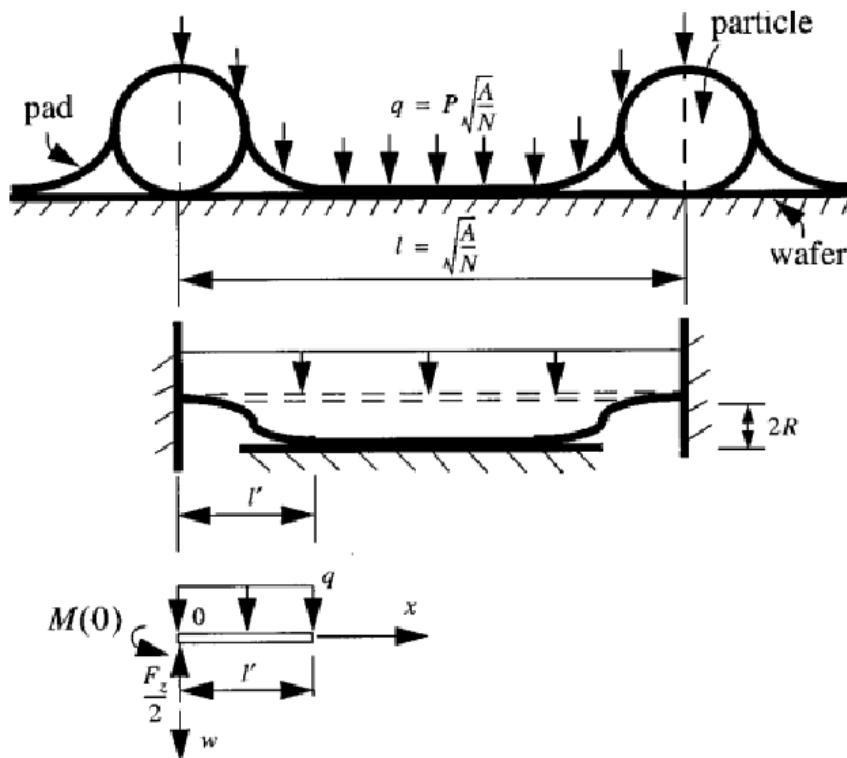


**FIGURE 4.4.** Pad modeled as a fixed-fixed beam.[25].

Before analyzing the condition with a soft pad and a low abrasive concentration, it is noteworthy to derive the condition where the *equation 4.19* is valid. In fact, only when the pad and the wafer do not touch each other the previous formulation can be used. For this purpose, the assumption formulated in the beginning of this explanation that considers the span of the pad between two abrasive particles ( $l$ ) as a fixed-fixed beam (*figure 4.4*), has to be resumed. This consideration permits to express the maximum deflection occurring as:

$$\omega_{max} = \frac{q \times l^4}{384 \times E_p \times l}$$

**FORMULA4.20.**[25].

To satisfy the condition that the pad and wafer do not touch each other, it is required that:

$$\omega_{max} < 2R$$

**FORMULA4.21.**[25].

Substituting *equation 4.20* into *4.21*, it is obtained that:

$$\frac{P}{64E_p \times t_p^3} < \left(\frac{N}{A}\right)^2 \times R$$

**FORMULA4.22.**[25].

This is the condition for that the *equation 4.19* is valid, where  $E_p$  represents the Young's modulus of the pad and  $t_p$  is its thickness.

Anyway, normally in CMP process, it is usual to employ a soft pad with a low abrasive concentration and in this case a extended contact between the pad and the wafer occurs. Under this conditions, the system forces acting on the contact zone is different

from the first one, where two forces  $F_z$  and  $F_x$  acted only on the abrasive particles. In fact, in this new condition only a fraction of the total force is carried by the abrasives, whereas the other one is directly carried by the pad on the contact zone between the workpiece and the pad itself.

As done in the first case with stiff pad and high abrasive concentration, the force system is calculated for first. Even this time, the beam theory is used to calculate the required parameter and to define boundary conditions where the equations are valid.

After this brief introduction, the force  $F_z$  can be expressed as shown below:

$$\begin{aligned}
 F_z &= \frac{4}{3} \times (144R \times q^3 \times E_p \times l)^{1/4} \\
 &= \frac{4}{3} \times \left[ 144R \times \left( P \times \sqrt{\frac{A}{N}} \right)^3 \times E_p \times \left( \frac{1}{12} \times \sqrt{\frac{A}{N}} \times t_p^3 \right) \right]^{1/4} \\
 &= \left( \frac{4^5}{3^3} \right)^{1/4} \times \left[ E_p \times t_p^3 \times R \times \left( \frac{A}{N} \right)^2 \times P^3 \right]^{1/4}
 \end{aligned}$$

**FORMULA4.23.[25].**

Where the load  $q = P \times \sqrt{A/N}$ [25] is a distributed load per unit length of the beam.

Therefore the overall reduction area can be found to be equal to:

$$\frac{dH}{dt} \sim \frac{1}{\sigma_y^{3/2}} \times (E_p \times t_p^3)^{3/8} \times \left( \frac{N}{A} \right)^{1/4} \times \frac{1}{R^{5/8}} \times P^{9/8} \times \frac{ds}{dt}$$

**FORMULA4.24.[25].**

With this latter equation, the case of CMP employing spherical abrasive particles has been completed. Now the case employing sharp particles can be introduced (*figure 4.3*).



For this geometry, the cross-sectional area is not equal to the other one for spherical particles, but it is expressed as:

$$A_s = \frac{1}{2} \times h_1 \times (h_1 \times \tan \alpha + h_1 \times \tan \beta) = \frac{\tan \alpha + \tan \beta}{2} \times h_1^2 \sim h_1^2$$

**FORMULA4.25.[25].**

Now, as in the two previous situations (spherical abrasive particles with stiff pad and high abrasive concentration, and with soft pad and low abrasive concentration) the system force is calculated first. Noting that for sharp particles  $F_z = \sigma_Y \times h_1^2$  and using the *equation 4.5*, the overall reduction area in this case is equal to:

$$\frac{dH}{dt} \sim \frac{N}{A} \times \frac{F_z}{\sigma_Y} \times \frac{ds}{dt}$$

**FORMULA4.26.[25].**

The *equation 4.26* is the starting point to analyze the MRR in the two different conditions presented previously.

In the first condition where the wafer and the pad do not touch each other (stiff pad and high abrasive concentration), as well as for spherical particles, the load is transferred from the pad to the wafer surface only by the abrasives. Then, the overall reduction area (*equation 4.26*) becomes:

$$\frac{dH}{dt} \sim \frac{N}{A} \times \frac{F_z}{\sigma_Y} \times \frac{ds}{dt} = \frac{1}{\sigma_Y} \times \frac{F_z \times N}{A} \times \frac{ds}{dt} = \frac{1}{\sigma_Y} \times P \times \frac{ds}{dt}$$

**FORMULA4.27.[25]**

When instead an extended contact between the pad and the wafer is expected (soft pad and low abrasive concentration), the overall reduction area is expressed as:

$$\frac{dH}{dt} \sim \frac{N}{A} \times \frac{F_z}{\sigma_Y} \times \frac{ds}{dt} \sim \frac{1}{\sigma_Y} \times \frac{N}{A} \times \left[ (E_p \times t_p^3) \times R' \times \left(\frac{A}{N}\right)^2 \times P^3 \right]^{1/4} \times \frac{ds}{dt} \sim \frac{1}{\sigma_Y} \times \left(\frac{N}{A}\right)^{1/2} \times (E_p \times t_p^3)^{1/4} \times R'^{1/4} \times P^{3/4} \times \frac{ds}{dt}$$

**FORMULA 4.28.** [25].

Where  $R'$  is assumed to be the equivalent size of the sharp particles.

With the *equation 4.28* the explanation of the first model has been presented. The aim of this first model is to analyze and understand how the CMP process parameters (like pressure, relative velocity, abrasive shape, concentration, and size, pad stiffness, shape of the abrasive, wafer hardness) and their variations during the process influence the Material Removal Rate values, to get more control over the process and to obtain a good MRR prediction.

### 4.3. Introduction to the second theoretical model

The second implemented model was extracted by “Material removal mechanism in chemical mechanical polishing: theory and modeling”, an article written by Jianfeng Luo and David A. Dornfeld [26].

In this article, differently from the first model where two different conditions between pad and wafer have been discussed, the proposed theoretical model describes a Chemical Mechanical Polishing process where the contact between the polishing pad and the wafer is always present. In fact, in a normal CMP system the pad and wafer surface are not separated but they contact each other directly and then some new considerations have to be formulated.

In fact, the interactions that happen between wafer, pad and abrasive particles are quite different from those in the conventional techniques due to the small pad hardness and the different size scales among the pad asperity and the polishing abrasives. The employed pad in CMP are usually made of polymers, this means that they are softer than the polishing material (that is usually ceramic or steel) and therefore the direct

contact between the pad and the polishing surface is possible and it affects the process, conditioning the mechanism of material removal. An example of this is provided on how the load is applied on the abrasive particles (*figure 4.6*). In fact, in a process employing an hard pad, the force acting on the abrasives is totally supported by abrasive particles and it is equal to:

$$F_1 = P \times \frac{B}{N}$$

**FORMULA 4.29.**[26].

Where  $N$  is the number of active particles,  $F_1$  is the main force on each particles,  $P$  is the down pressure and  $B$  the area of the asperity (*figure 4.6b*). In this case, it can be noted that the force acting on each particles is independent from the abrasive size. If a CMP process is analyzed, where a soft pad is employed, the equation for the force changes, and it becomes equal to:

$$F_2 = 0.25\pi \times x^2 \times P$$

**FORMULA 4.30.**[26].

Where  $x$  is the diameter of the particles (*figure 4.6a*). As we can see, in this latter equation the force does not depend on the abrasive number but it is affected by the pressure and abrasive size. In fact, in this latter condition the contact mode is changed. The whole load is now supported by both asperities of the pad and abrasives, unlike what happened before; this is due to compression of the pad's asperities which embed the abrasive particles.

This fact is fundamental and implies that Young's modulus of the pad, hardness of the pad and contact area between wafer and pad are important parameters which have to be taken into account in defining the theoretical model.

But other variables in addition to those listed above have to be taken into account. In fact, the shape of the pad, its roughness and the distribution of abrasive size play a significant role in CMP too. This is due to the small size of the abrasives. In fact the

employed nanoscale polishing abrasives are much smaller than the microscale height of the pad asperities, and this influences the process, because not all the abrasive particles can be embedded in the pad and scratch the workpiece.

As it has been done in the first model, the beginning point is to formulate some assumptions with whom the realistic problem can be simplified in an easier analytical one. The main assumptions are:

- A plastic contact over the wafer-abrasive interface and pad-abrasive interface is supposed. This assumption is important, and it is made after some microscopic observations of polished surfaces which have shown that material removal in CMP occurs as a consequence of a combination of chemical reaction of the slurry with the wafer surface, and mechanical action of the abrasives with the surface (indentations, scratches, rollings) [26];
- The force applied on the wafer surface by the fluid flow is neglected, but the contact is assumed purely solid-solid contact[26];
- The real size distribution of the abrasive particles is not known, so the problem is simplified supposing a normal distribution of abrasive size[26];
- Even the real profile of the pad is not known. It takes time in measuring and anyway it would be different from pad to pad. Therefore its detection is without meaning. For this reason a periodic rough surface of the polishing pad is supposed, with a uniform distribution of the summits over the rough surface with known density  $D_{SUM}$  of summit per unit area and known radius  $R$  (*figure 4.7*) [26];
- The elastic modulus of asperities is supposed small, this imply that all the asperities deform under down pressure and can contact the wafer[26];
- To ensure the solid-solid contact mode, a large down pressure and a low relative velocity between wafer and pad are supposed. This condition do not permit

the formation of a thin fluid film and so the hydrodynamical contact mode cannot happen (*figure 4.5*) [26];

- The real area of contact is a small fraction of the apparent contact area and it is determined by the down pressure value and the shape of the contact surfaces of the two solids[26];
- The hardness of the pad is much smaller than that of the wafer and the abrasives are almost embedded statically in the pad[26];
- The shape of the abrasives is assumed to be spherical (*figure 4.8*)[26];
- The contact between polishing pad/pad asperities and abrasive particle is assumed to be quasi-static indentation[26];
- The penetration depth of the spherical indenter into the wafer and the pad surface is smaller than the diameter of the abrasives (*figure 4.8*)[26];
- The number of abrasives captured over the wafer-pad contact area (both active and inactive) is independent on the down pressure, but it is dependent on the roughness of the pad[26];
- The particles which are not in the contact area will not be involved in two-body abrasion and the material removed by them is negligible, because they are assumed to be involved in three-body abrasion or inactive[26];
- Most of the contact in CMP is direct contact between the wafer and the pad asperity without abrasive present[26].

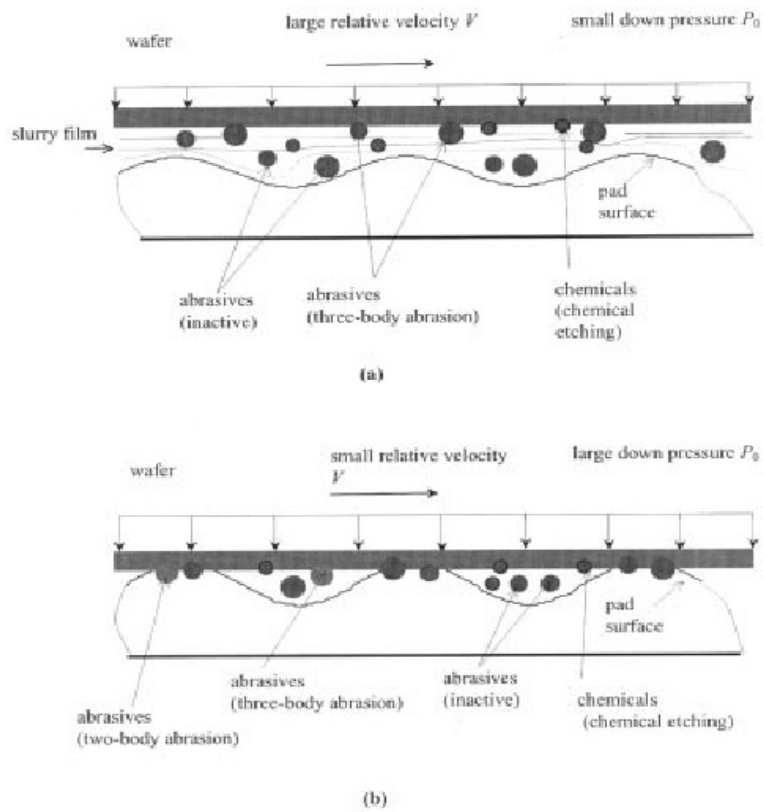


**FIGURE 4.5.** a) Hydro-dynamical contact mode is represented; b) Solid-solid contact mode is represented [26].

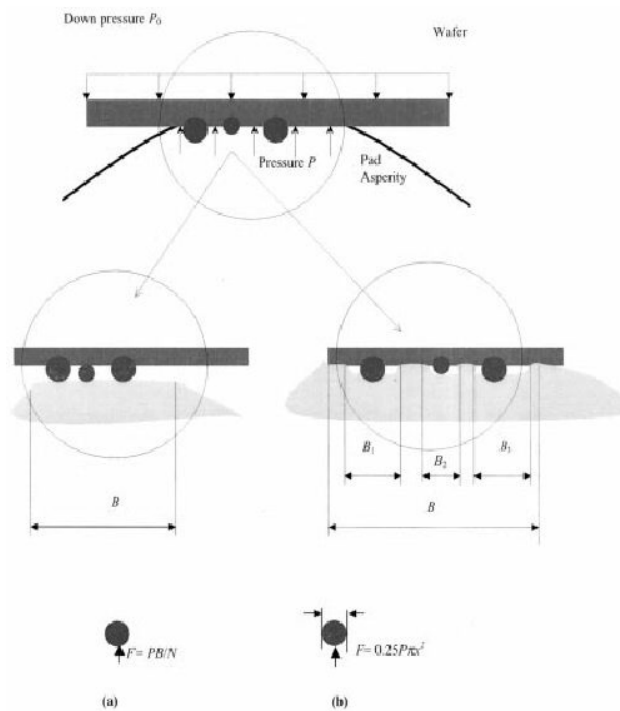


**FIGURE 4.6.** a) Conventional polishing process using hard pad; b) CMP process using soft pad [26].

After having introduced the assumptions of the model, the first step to do for deriving the final equation for MRR is to calculate the apparent contact area  $A_0$ . This parameter is important because other process parameters as mean pressure, volume removed and MRR depend on this one. Then the apparent contact area can be written as:

$$A_0 = \frac{1}{4}\pi \times D^2$$

**FORMULA 4.31.**[26].

Where  $D$  is the diameter of the wafer. From the above equation the real contact area (that is the real portion of pad that gets in touch with the wafer surface. This happens because the surface of the pad is not smooth, but a periodic rough distribution of its surface is supposed) can be found as:

$$A = b \times A_0 = \pi \times \left( \frac{3R}{4D_{SUM}} \times \frac{P_0}{E^*} \right)^{2/3} \times D_{SUM} \times A_0 = b_1 \times \left( \frac{P_0}{E^*} \right)^{2/3} \times A_0$$

**FORMULA 4.32.**[26].

From the *equations 4.31 and 4.32*, the mean pressure can now be found. In fact it is equal to:

$$P = \frac{P_0 \times A_0}{A} = \frac{P_0}{b} = \frac{1}{b_1} \times E^{*2/3} \times P_0^{1/3}$$

**FORMULA 4.33.**[26].

Where  $P_0$  is the down pressure applied on the wafer and  $b_1$  is a constant value equal to:

$$b_1 = \pi(3R/4)^{2/3} \times D_{SUM}^{1/3}$$

**FORMULA4.34.**[26].

Whereas  $b$  is the ratio of the real contact area with the apparent contact area. This parameter after some simplifications can be written as:

$$b = b_1 \times (P_0/E^*)^{2/3}$$

**FORMULA4.35.**[26].

Where the symbol  $E^*$  is called equivalent modulus of elasticity, and it is equal to:

$$E^* = \frac{1}{(1 - \nu_w^2/E_w)} + (1 - \nu_p^2/E_p)$$

**FORMULA4.36.**[26].

Where  $E_w$  and  $\nu_w$  are respectively the Young's modulus and Poisson's ratio of the wafer and  $E_p$  and  $\nu_p$  are the Young's modulus and Poisson's ratio of the pad. But it can be simplified. In fact, since the Young's modulus of the wafer is larger than the Young's modulus of the pad, if the Poisson's ratio of the pad is assumed to be closed to 0.5 (for polymer material for example), the  $E^*$  is approximately equal to:

$$E^* = \frac{4}{3}E_p$$

**FORMULA4.37.**[26].



This assumption it is usually true, because the Young's modulus of the pad is much smaller than that of the wafer. Therefore, with this assumption the force applied on an abrasive can be written as:

$$0.25\pi \times P \times x^2 = 0.25\pi \times \frac{1}{b_1} \times \left(\frac{4}{3}\right)^{2/3} \times E_p^{2/3} \times P_0^{1/3} \times x^2$$

**FORMULA4.38.**[26].

An important observation can be underlined in the above equation. In fact, it can be seen that the pressure dependence does not linearly vary with the applied force. This is a direct consequence of the fact that the pad gets in touch with the workpiece surface and that all the load is not wholly supported by only the abrasive particles (as it was introduced in the assumptions of the model).

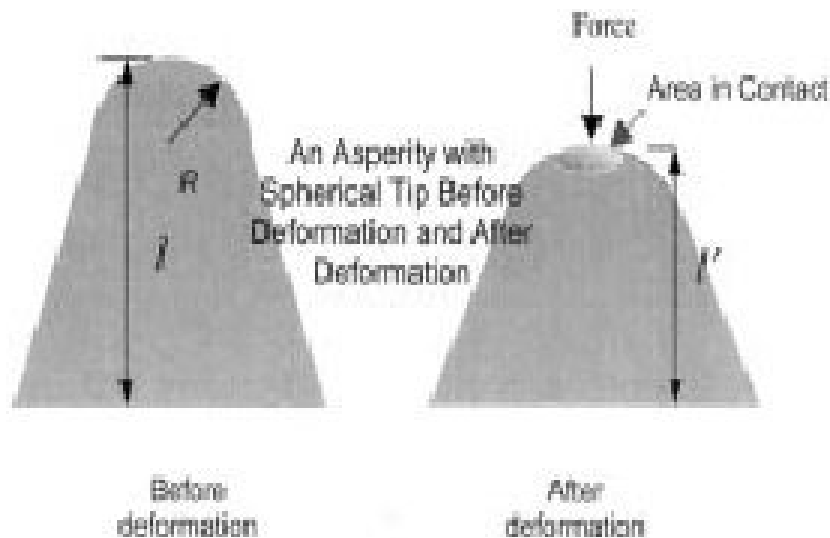


**FIGURE4.7.** Assumed geometry of the pad asperity before and after deformation [26].

This means that a plastic deformation happens too. Therefore if a plastic contact zone between the abrasives and the wafer and between the abrasives and the pad is

assumed (see the assumptions of the model), the penetration depth in each case respectively is equal to (*figure 4.8*):

$$\Delta_1 = a_1^2 = \frac{2F}{\pi \times x \times H_w}$$

**FORMULA4.39.**[26].

$$\Delta_2 = a_2^2 = \frac{F}{\pi \times x \times H_p}$$

**FORMULA4.40.**[26].

Where  $F = 0.25\pi \times P \times x^2$ , whereas  $a_1$  and  $a_2$  are the radii of the cross-sectional area of contact between the spherical particle and the wafer and the pad surface. These radii are shown in the *figure 4.8* and they are equal to:

$$a_1 = \sqrt{2F/(\pi \times H_w)}$$

**FORMULA4.41.**[26].

$$a_2 = \sqrt{F/(\pi \times H_p)}$$

**FORMULA4.42.**[26].

Where  $H_w$  and  $H_p$  respectively represents the hardness of the wafer and the pad.

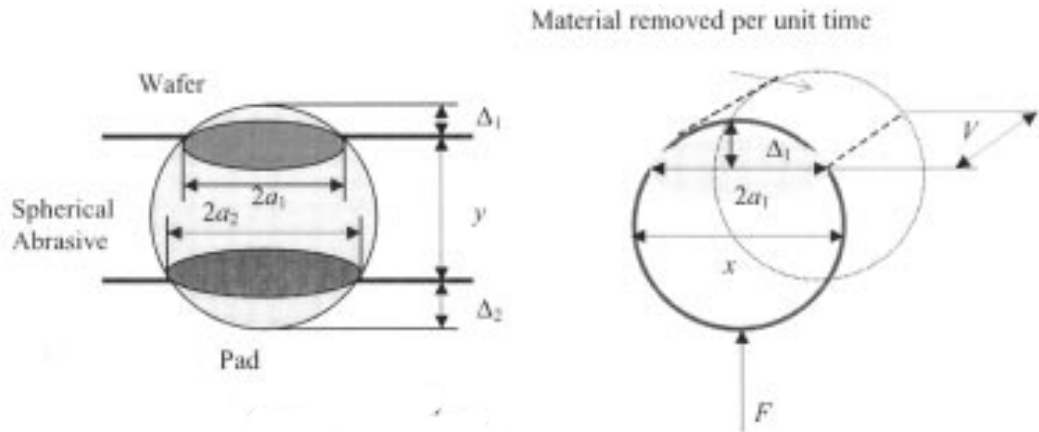


**FIGURE 4.8.** The penetration depth of the abrasives relatively the wafer and the pad [26].

The equations 4.39 and 4.40 can be used to determine the deformation of two contact points between the wafer surface and abrasive particle and polishing pad and abrasive. This deformation is equal to the sum of the two different penetration depth:

$$\Delta = \Delta_1 + \Delta_2 = \frac{F}{\pi \times x} \times \left( \frac{2}{H_w} + \frac{1}{H_p} \right) = 0.25P \times x \times \left( \frac{2}{H_w} + \frac{1}{H_p} \right)$$

**FORMULA 4.43.** [26].

As it was supposed and as it is simple to imagine, from this latter equation a second observation can be done, since it is clearly shown that the deformation is larger when the pad and wafer are softer. Therefore, more the pad is soft, more the abrasive is embedded in it, and more the workpiece is soft, more the MRR increases.

Now it is noteworthy that the mean value of cutting depth  $\Delta_1$  is approximately equal to the final roughness  $R_a$  of the polished wafer. In fact, the value  $\Delta_1$  is the track that an abrasive leaves on the surface of the machined part, therefore it is not wrong to compare that track with the final roughness reached in the end of the process.

So to estimate the pressure  $P$  applied on the polishing pad and the ratio  $b$  of contact area, in the beginning the roughness of the wafer surface has to be measure. From this

information and from the knowledge of the average sizes of the active abrasives, the pressure may be expressed as:

$$P = \frac{\Delta_1 \times H_w}{0.5x_{avg-a}} = \frac{R_a \times H_w}{0.5x_{avg-a}}$$

**FORMULA4.44.**[26].

And the ratio of contact area as:

$$b = \frac{P_0}{P} = \frac{0.5P_0 \times x_{avg-a}}{R_a \times H_w}$$

**FORMULA4.45.**[26].

Where  $x_{avg-a}$  is the average size of the active abrasives (*figure 4.10*). Obviously the average size of the active abrasives will change with the down pressure, because the penetration depth changes and consequently the distance between wafer and pad. At this point, the third observation can be introduced. In fact, if the number of total abrasives captured in the contact zone (both active and inactive) does not depend on the applied down pressure, but only on the shape of the pad's profile, it is not the same for the active abrasive particles which instead depend on the applied down pressure and on the hardness of the pad. This is an important observation, because the MRR depends only on the active abrasive particle.

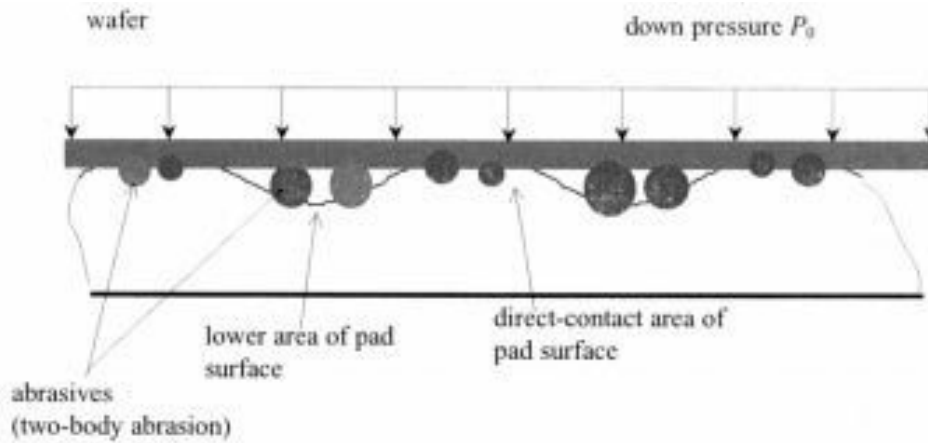


**FIGURE 4.9.** Two and three body abrasion coexist [26].

Now, the equation for MRR can be estimated. In fact, if a down pressure  $P_0$ , a relative velocity  $V$ , and a mean size  $x_{avg-a}$  of active abrasives are supposed, the mean volume removed by a single abrasive per unit time is:

$$\begin{aligned}
 Vol_{removed} &= \Delta_1 \times a_1 \times V = \frac{2\sqrt{2} \times F}{\pi \times x_{avg-a} \times H_w} \times \sqrt{F/\pi \times H_w} \times V \\
 &= \frac{\sqrt{2}}{4} \times x_{avg-a}^2 \times \left(\frac{P}{H_w}\right)^{3/2} \times V = \frac{\sqrt{2}}{3} \times \frac{x_{avg-a}^2 \times E_p}{(b_1 \times H_w)^{3/2}} \times \sqrt{P_0} \times P
 \end{aligned}$$

**FORMULA 4.46.**[26].

Where  $P$  is given by the *equation 4.33*. The *equation 4.46* is the first step to formulate the MRR expression, anyway it can well represent its trend. Before reaching the final equation for MRR, some other considerations have to be introduced.

As discussed above, not all the particles on the contact area will be involved in material removal, moreover, the particle which are not in the contact area will not be involved in two-body abrasion, but in three-body abrasion so that their material removal rate can be neglected. Therefore, it is important to understand how many abrasive particles are active in the contact zone to quantify the amount of the material removal rate during

CMP process. To determine the number of active abrasives, it is supposed a normal distribution of abrasive particles size (*figure 4.10*):

$$p\{x = x_a\} = p(x_a) = \frac{1}{\sqrt{2\pi}} \times \exp \left[ -\frac{1}{2} \times \left( \frac{x - x_{avg}}{\sigma} \right)^2 \right]$$

**FORMULA4.47.**[26].

And:

$$p\{x \leq x_a\} = \Phi \times \left( \frac{x_a - x_{avg}}{\sigma} \right) = \frac{1}{\sqrt{2\pi}} \times \int_{-\infty}^{(x_a - x_{avg})/\sigma} e^{-(1/2)t^2} dt$$

**FORMULA4.48.**[26].

Where  $x_{avg}$  is the mean abrasive diameter and  $\sigma$  the standard deviation.

If it is supposed that the number of active abrasives increases with the decrease of the separating distance or the increase of the deformation  $\Delta$  (that is with the increase of the pressure) (*figure 4.10 and 4.11*), they can be defined as:

$$\begin{aligned} N &= n \times \left( \Phi \times \left( \frac{x_{max} - x_{avg}}{\sigma} \right) - \Phi \times \left( \frac{x_{max} - \Delta - x_{avg}}{\sigma} \right) \right) \\ &= n \times \left( \Phi \times \left( \frac{x_{max} - x_{avg}}{\sigma} \right) - \Phi \times \left( \frac{x_{max} - x_{avg} - \frac{F}{\pi \times x} \times \left( \frac{2}{H_w} + \frac{1}{H_p} \right)}{\sigma} \right) \right) \end{aligned}$$

**FORMULA4.49.**[26].

Where  $n$  is the number of all particles (active and inactive) captured over the wafer-pad contact area.

Now, in most situations some simplifications are possible; for example  $(x_{max} - x_{avg})/\sigma$  can be approximated as 3 and consequently  $\Phi \times ((x_{max} - x_{avg})/\sigma)$  as 1 and then the force  $F$  in *equation 4.49* may be approximately equal to the pressure  $P$  times the size of the largest particles. Therefore, after some substitutions the *equation 4.49* can be simplify as:

$$N \sim n \times \left\{ 1 - \Phi \times \left[ 3 - \frac{0.25x_{max} \times \left( \frac{1}{H_p} + \frac{2}{H_w} \right)}{\sigma} \times P \right] \right\}$$

$$= n \times \left\{ 1 - \Phi \times \left[ 3 - \frac{0.25 \times \left( \frac{4}{3} \right)^{2/3} \times (x_{avg} + 3\sigma) \times \left( \frac{1}{H_p} + \frac{2}{H_w} \right)}{\sigma} \times \frac{E_p^{2/3}}{b_1} \times P_0^{1/3} \right] \right\}$$

**FORMULA4.50.**[26].

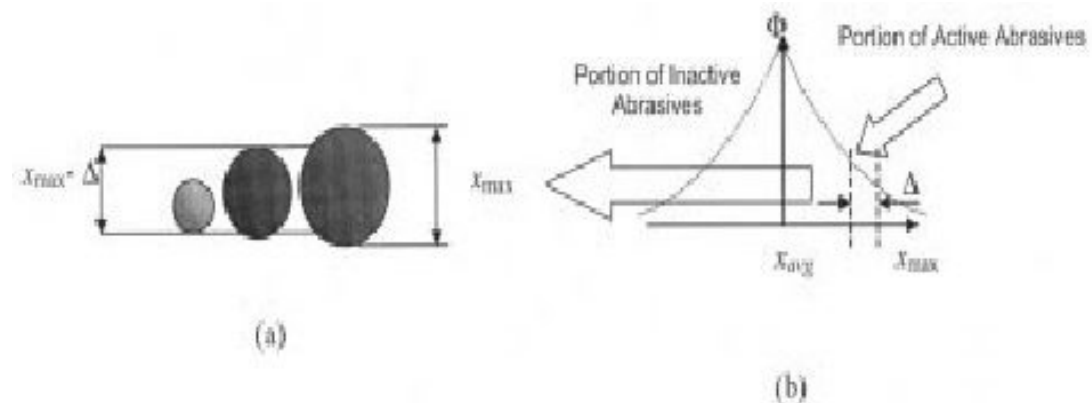


**FIGURE4.10.** a) Variance in the grain size of abrasive particles; b) Portion of active and inactive abrasive particles [26].

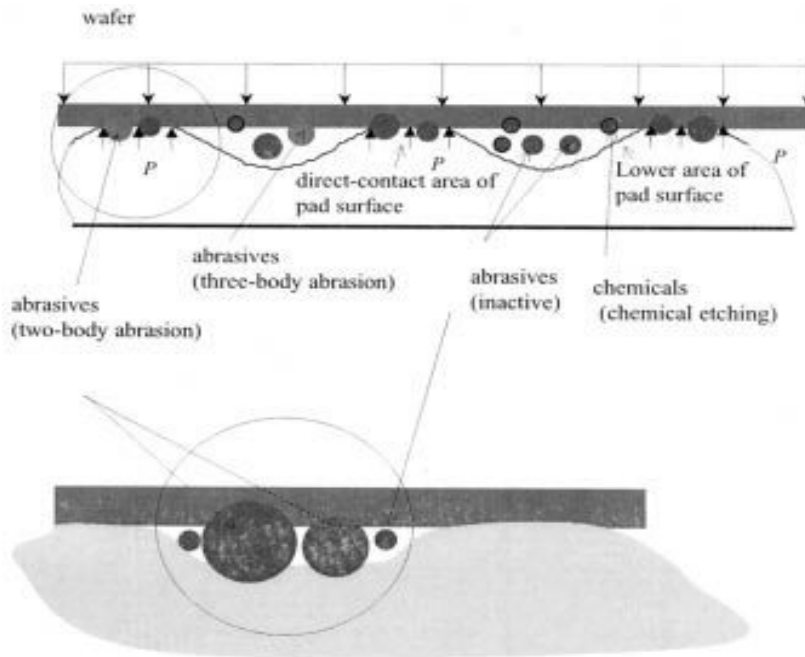


**FIGURE 4.11.** Varies positions between pad and wafer in the contact area [26].

In particular the average size  $x_{avg-a}$  of active abrasive is supposed to change with the down pressure, and this fact can be seen from the following equation (figure 4.10):

$$\begin{aligned}
 x_{avg-a} &= x_{avg} + \frac{\sigma \times p \times \left( \frac{x_{max} - \Delta - x_{avg}}{\sigma} \right)}{1 - \Phi \times \left( \frac{x_{max} - \Delta - x_{avg}}{\sigma} \right)} \\
 &= x_{avg} + \frac{\sigma \times p \times \left[ 3 - \frac{0.25 \times \left( \frac{4}{3} \right)^{2/3} \times (x_{avg} + 3\sigma) \times \left( \frac{1}{H_p} + \frac{2}{H_w} \right) \times \frac{E_p^{2/3}}{b_1} \times P_0^{1/3}}{\sigma} \right]}{1 - \Phi \times \left[ 3 - \frac{0.25 \times \left( \frac{4}{3} \right)^{2/3} \times (x_{avg} + 3\sigma) \times \left( \frac{1}{H_p} + \frac{2}{H_w} \right) \times \frac{E_p^{2/3}}{b_1} \times P_0^{1/3}}{\sigma} \right]}
 \end{aligned}$$

**FORMULA 4.51.**[26].

The last step consists in defining the number of all the abrasives captured over the wafer-pad interface:  $n$ . To find out that, the number of all abrasives over the wafer-pad



interface when there is a certain distance between them has to be defined first and it is equal to (figure 4.12):

$$n_{all} = G \times A_0 \times l'$$

**FORMULA4.52.**[26].

Where  $G$  is the concentration of the abrasives in the slurry and  $l'$  is the gap between wafer and pad. If a down pressure is applied, and the gap between wafer and pad becomes smaller, the number of abrasive in the fluid changes because the asperities of the pad undergo a deformation, and it becomes (the concentration of the abrasive particles  $G$  is considered constant):

$$n_f = G \times (A_0 - A'_a) \times l'$$

**FORMULA4.53.**[26].

Where  $A'_a$  is the mean area of all asperities after deformation.

From equations 4.52 and 4.53, the number of abrasives captured by the asperities on the contact area can be found, and it is equal to (figure 4.12):

$$n = n_{all} - n_f = G \times A'_a \times l' = G \times Vol'$$

**FORMULA4.54.**[26].

Where  $Vol'$  is the volume of the asperities. In other hands,  $n$  is supposed to be equal to the number of abrasive particles which do not flow out from the wafer-pad interface after deformation.

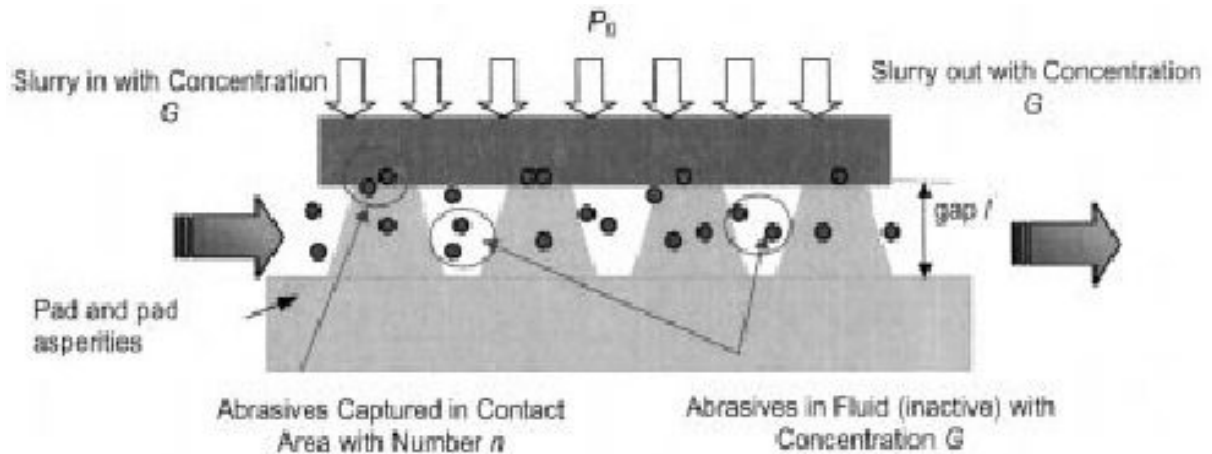


**FIGURE 4.12.** Active and inactive abrasive particles between wafer and pad asperities [26].

Now the *equation 4.54* can be modified. In fact, the usual pads employed during a CMP process are made in soft material as polymer for example. In this case, the volume  $Vol'$  may be approximately constant because the Poisson's ratio of polymer materials is close to 0.5. So  $n$  can be expressed as:

$$n = G \times A_o \times D_{SUM} \times a \times l$$

**FORMULA 4.55.**[26].

Where  $a$  is the mean area of a single asperity and  $l$  the mean height of a single asperity.

If the concentration of the abrasive particles are expressed as:

$$G = \frac{d_s \times \rho_s \times m_{s-a}}{\rho_a \times Vol_a} = \frac{d_s \times \rho_s \times m_{s-a}}{\rho_a \times \frac{\pi}{6} \times x_{avg}^3}$$

**FORMULA 4.56.**[26].

Where  $d_s$  is the dilution ratio of slurry to DI water [ $volume\ of\ slurry / (volume\ of\ slurry + DI\ water)$ ],  $\rho_s$  is the density of the slurry before dilution,  $m_{s-a}$  is the concentration of slurry before dilution [ $(weight\ of\ abrasive\ in\ slurry) / (weight\ of\ liquid\ in\ slurry)$ ],  $\rho_a$  is the density of the abrasive, and  $Vol_a$  is the average volume of a single abrasive. The number of abrasives captured over the wafer-pad contact area can be written as (figure 4.12):

$$n = G \times D_{SUM} \times A_0 \times a \times l = \frac{d_s \times \rho_s \times m_{s-a} \times A_0}{\rho_a \times \frac{\pi}{6} \times x_{avg}^3} \times D_{SUM} \times a \times l$$

**FORMULA 4.57.**[26].

With this latter equation the formulation for the active abrasive particles can be completed. In fact, the equation 4.50 becomes:

$$N \sim \frac{d_s \times \rho_s \times m_{s-a} \times A_0}{\rho_a \times \frac{\pi}{6} \times x_{avg}^3} \times D_{SUM} \times a \times l \times \left\{ 1 - \Phi \times \left[ 3 - \frac{0.25 \times \left(\frac{4}{3}\right)^{2/3} \times (x_{avg} + 3\sigma) \times \left(\frac{1}{H_p} + \frac{2}{H_w}\right)}{\sigma} \times \frac{E_p^{2/3}}{b_1} \times P_0^{1/3} \right] \right\}$$

**FORMULA 4.58.**[26].

To find out the expression for the number of active abrasive particles and its dependence from controllable variables has been important because the material removal rate depends on it. Therefore, now the equation for MRR can be introduced:

$$MRR_{mass} = \rho_w \times N \times Vol_{removed} \times C_0$$

**FORMULA 4.59.**[26].

Where  $\rho_w$  is the density of the wafer material,  $N$  is the number of active abrasive particles,  $Vol_{removed}$  is the volume removed by a single abrasive in unit time, and  $C_0$  is the material removal due to chemical etching. Now, in CMP process the mechanical reaction and chemical reaction are both important and substantially influence the process, but the chemical contribute  $C_0$  used in the MRR *equation 4.59* cannot be measured directly from static etching of the wafer. Anyway, in CMP process with solid-solid contact between wafer and pad the MRR induced from chemical interactions is much smaller than that one caused from the mechanical interaction between pad, abrasive particles and wafer. For this reason, and to simplify the problem, the direct chemical etching yields is ignored. Therefore, if into 4.59, the equations find out previously are substituted, one for the mean volume removed by a single abrasive per unit time  $Vol_{removed}$  (*equation 4.46*) and one for the active abrasive particles  $N$  (*equation 4.58*), the MRR becomes:

$$MRR_{mass} = \rho_w \times A_0 \times k^2 \times \frac{2\sqrt{2}d_s \times \rho_s \times m_{s-a} \times D_{SUM} \times a \times l}{\rho_a \times \pi \times x_{avg}} \times \frac{E_p}{(b_1 \times H_w)^{3/2}} \\ \times \left\{ 1 - \Phi \times \left[ 3 - \frac{0.25 \times \left(\frac{4}{3}\right)^{2/3} \times (x_{avg} + 3\sigma) \times \left(\frac{1}{H_p} + \frac{2}{H_w}\right) \times \frac{E_p^{2/3}}{b_1} \times P_0^{1/3}}{\sigma} \right] \right\} \\ \times \sqrt{P_0} V$$

**FORMULA4.60.**[26].

Now some constants can be introduced to simplify the MRR expression, as:

$$MRR_{mass} = C_1 \times \left[ 1 - \Phi \times \left( 3 - C_2 \times P_0^{1/3} \right) \right] \times \sqrt{P_0} \times V$$

**FORMULA4.61.**[26].

Where:

$$C_1 = \rho_w \times k^2 \times A_0 \times \frac{2\sqrt{2}d_s \times \rho_s \times m_{s-a} \times D_{SUM} \times a \times l}{\rho_a \times \pi \times x_{avg}} \times \frac{E_p}{(b_1 \times H_w)^{3/2}}$$

**FORMULA4.62.[26].**

$$C_2 = \frac{0.25 \times \left(\frac{4}{3}\right)^{2/3} \times (x_{avg} + 3\sigma) \times \left(\frac{1}{H_p} + \frac{2}{H_w}\right)}{\sigma} \times \frac{E_p^{2/3}}{b_1}$$

**FORMULA4.63.[26].**

$C_1$  is the constant that reflects the effect of the slurry chemicals, slurry abrasives, wafer size, wafer density, wafer hardness, pad material, and pad roughness;  $C_2$  is the constant that reflects the effect of slurry abrasives (average size and size distribution), wafer and pad hardness, and pad roughness. Both constants should be independent on the down pressure  $P_0$  and the relative velocity  $V$ .

The MRR expressed as in *equation 4.61* is not the only one expression for it, but it sometime can be indicated as:

$$\begin{aligned} MRR_{thickness} &= \frac{MRR_{mass}}{\rho_w \times A_0} = \frac{C_1 \times \left[1 - \Phi \times \left(3 - C_2 \times P_0^{1/3}\right)\right] \times \sqrt{P_0} \times V}{\rho_w \times A_0} \\ &= C_3 \times \left[1 - \Phi \times \left(3 - C_2 \times P_0^{1/3}\right)\right] \times \sqrt{P_0} \times V \end{aligned}$$

**FORMULA4.64.[26].**

Where:

$$C_3 = \frac{C_1}{\rho_w \times A_0} = \frac{2\sqrt{2}d_s \times k^2 \times \rho_s \times m_{s-a} \times D_{SUM} \times a \times l}{\rho_a \times \pi \times x_{avg}} \times \frac{E_p}{(b_1 \times H_w)^{3/2}}$$

**FORMULA 4.65.**[26].

Also  $C_3$  is a constant independent of pressure  $P_0$  and relative velocity  $V$ . The *equation 4.64* has been introduced because in most situation the material removal rate is approximated by the thickness removed per unit time.

As written before, the direct chemical etching yields  $C_0$  is ignored in the MRR equation because the MRR caused by chemical interactions is smaller than that caused by mechanical ones, but the enhancing effect of chemical etching on the mechanical material removal is reflected by density  $\rho_w$  and hardness  $H_w$  of the workpiece surface. This is because it is believed that a softened layer with material properties different from those of the wafer will be formed continuously on the wafer surface due to chemical reactions. This “new” layer formed on the wafer surface is softer than the previous wafer surface and it is then removed by abrasive particles. Anyway, the hardness value of the “new” layer cannot be measured directly using static chemical etching since CMP is a dynamical process with a continuous interaction between chemical removal and mechanical removal, so it has to be fitted.

As for the first model implemented, this second one wants to predicts the MRR during a CMP process, keeping under control the process variables. As it is possible to see by the MRR equations, a lot of variables have to be considered to understand the process and to formulate a good prediction of MRR, as for example: the number of abrasive particles captured over the wafer-pad contact area and the number of active abrasive particles, the force acting on the abrasives during polishing and calculated based on down pressure, the hardness of pad, volume of pad asperities and distribution of abrasive size, shape of pad, density and hardness of “new” layer on the wafer surface, size and geometry of the abrasive particles.

More attention has been done for the abrasive distribution and for the pad profile respect to the first model. In fact, here there is a distinction between inactive and active

abrasive particles, and these last ones have been identified as the responsible for the material removal rate.

#### 4.4. Introduction to the third theoretical model

The third implemented model was extracted by “Effect of particle size, polishing pad and contact pressure in free abrasive polishing”, an article written by Yongsong Xie, Bharat Bhushan [27].

As well the two previous theoretical models, this one has been developed to predict the material removal rate during a CMP process. Precisely, the aim of this model is to create an equation which estimates the wear rate. In fact, here the MRR is indicated with a dimensionless parameter (wear rate) depending on polishing parameters as particle size, mechanical and geometrical characteristics of the soft pad, mechanical and geometrical characteristics of the workpiece and nominal contact pressure.

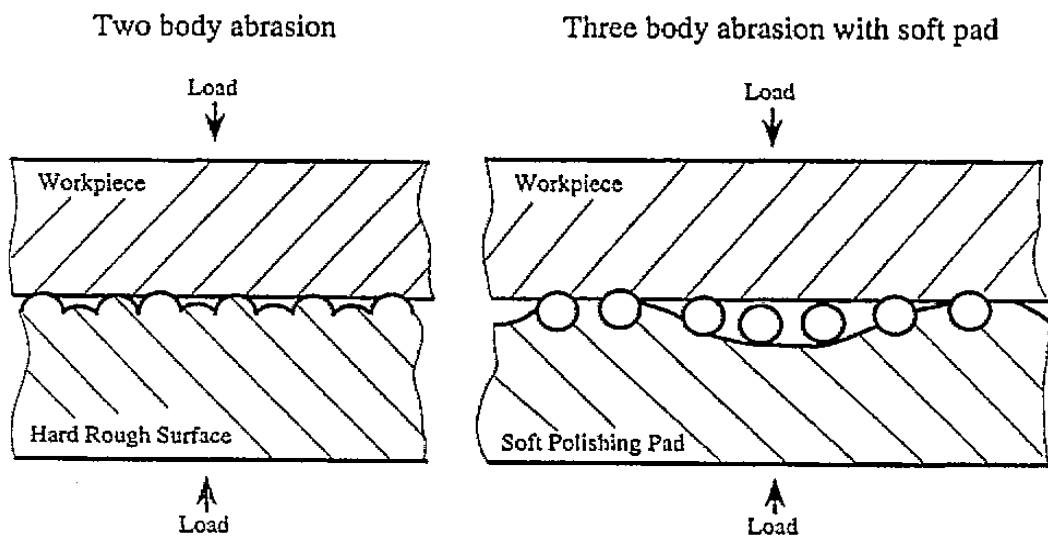


**FIGURE 4.1.** Two body abrasion and three body abrasion [27].

This new model has been formulated because, as in the two previous situations, a new theory to predict the MRR in a CMP process is necessary. In fact the models used to describe a conventional process with fixed abrasive particles are not adequate for a process employing free abrasives, or, in other hands, using three-body abrasion interaction and not two-body abrasion interaction (*figure 4.13*).

In fact, although the mechanism of material removal in two-body abrasion and in free abrasive polishing are the same (there are always some abrasive particles which scratch the polishing part), there are some differences between the two methods. For example, two of the most important differences are: how the abrasive particles are held from the pad against the polishing surface and hence how the load is transferred from the pad to the workpiece surface, and the effect of particles size on wear rate which is usually smaller in a process with a free abrasives than that employed in a fixed abrasive particles process. Moreover, the contact between abrasives and workpiece results more complex in the first one than in the second one, because in CMP the abrasive particles are free to move in the slurry, whereas in the conventional processes they are fixed in a wheel for example.

The introduction and the explanation of this model follow those done for the other two. Therefore, the assumptions considered are explained now:

- Abrasive particles are supposed to be harder than both workpiece and polishing pad [27];
- The abrasive particles can deform elastically only during contacts [27];
- The down pressure is supposed to be low (in CMP the down pressure values are usually low) [27];
- As consequence of low down pressure, the contact between the polishing pad and the polished surface is supposed to be purely elastic [27];
- Only the contact between the abrasive particles and the workpiece, or between the abrasive particles and the pad can be plastic, due to very high local stress that could be reached [27];
- Polishing particles are spherical in shape (this assumption may not cause significant error because the particles may orient themselves during contact to assume small attack angles on the leading edges) [27].



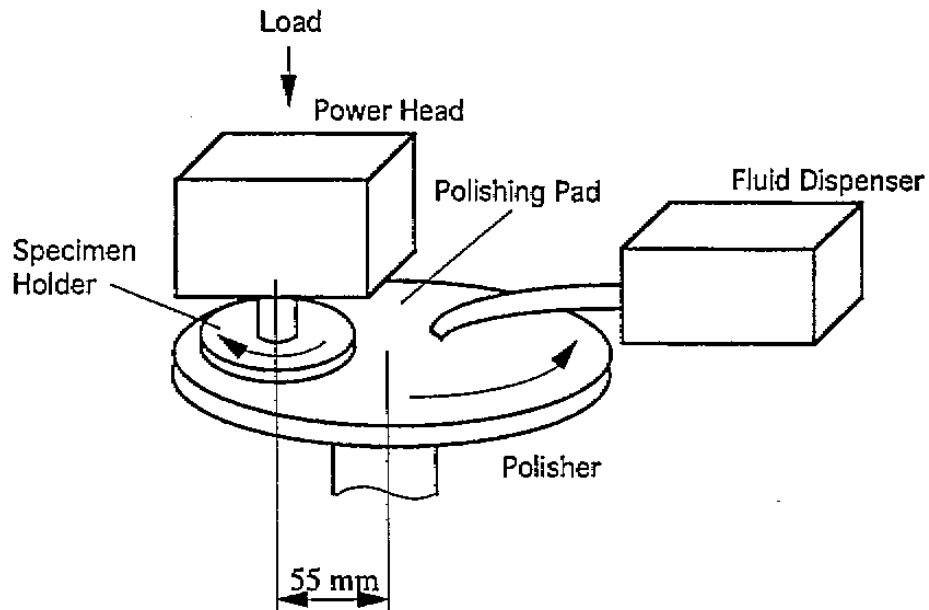


**FIGURE 4.2.** Polishing system [27].

Regarding the last assumption, where the shape of the abrasive particles is discussed, it is necessary to underline that indeed the particles can be assumed various shapes (spherical or sharp in general). Nevertheless, this assumption is not heavy and does not imply a significant error in the model because the particles are free to move and orient themselves during the contact as they want, and in this action they usually assume small attack angle. Therefore, for the point of view of the contact between the workpiece and the abrasive particles, they can be considered spherical.

After having introduced the assumptions of the model, the analysis which leads to the formulation of the MRR equation can be started. The mechanism of contact between abrasive particles and workpiece is analyzed for first. In fact, when a load  $\Delta P$  is applied on a particle (*figure 4.14*), the contact could be either plastic or elastic. If it is supposed that the contact between abrasive particle and workpiece is plastic, but also that one between the particle and the pad, the formula for the applied load  $\Delta P$  can be written as:

$$\Delta P = H_w \times S_w = H_p \times S_p$$

**FORMULA 4.66.**[27].

Where  $H$  is the hardness and  $S$  the plastically deformed surface area of the workpiece and polishing pad (the subscript  $w$  indicates the wafer, whereas  $p$  indicates the pad). Now, for the previous assumptions, the shape of the abrasive particles is spherical, so in this condition  $S_w$  and  $S_p$  can be written as:

$$S_w = 2\pi \times R \times \delta_w$$

**FORMULA4.67.**[27].

$$S_p = 2\pi \times R \times \delta_p$$

**FORMULA4.68.**[27].

Where  $R$  is the radius of the spherical particles,  $\delta_w$  and  $\delta_p$  are the interferences between the particle and the two surfaces. If these equations are substituted in *equation 4.66*, it is found that:

$$\frac{\delta_w}{\delta_p} = \frac{H_p}{H_w}$$

**FORMULA4.69.**[27].

Now, from this last equation and from the geometrical relation  $2R = \delta_w + \delta_p + h$  derived by *figure 4.15*, the interference between the particle and the wafer (in other hands the depth of cut if the contact is plastic) can be expressed as:

$$\delta_w = \frac{H_p}{H_w + H_p} \times (2R - h)$$

**FORMULA4.70.**[27].

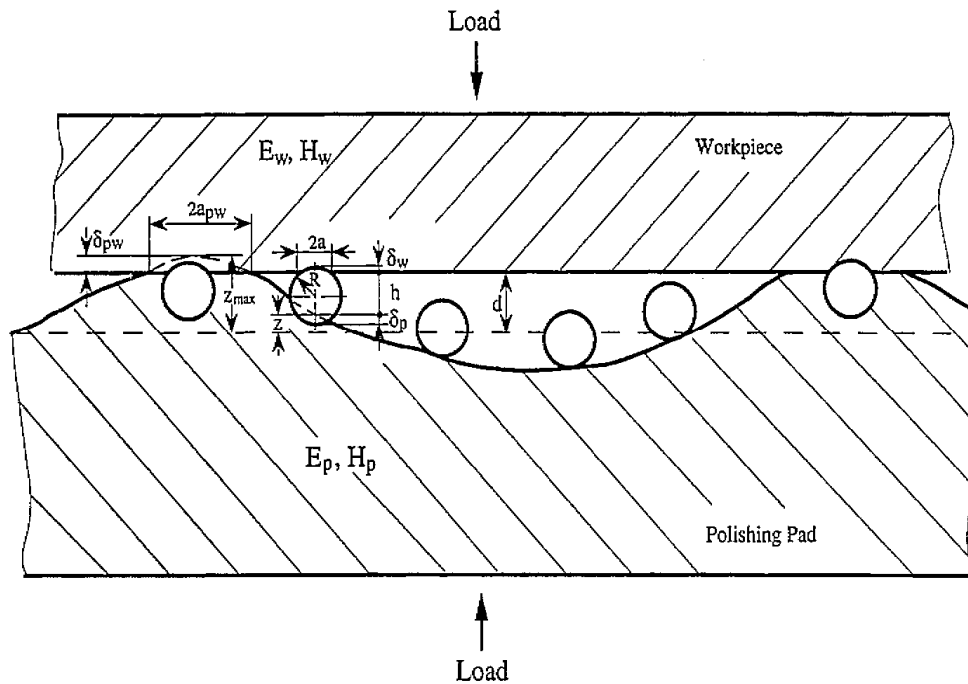


**FIGURE 4.3.** Distribution of the abrasive particles in the contact area [27].

Now,  $\delta_w$  is an important parameter in this model, because with that the contact between the abrasive particle and the wafer can be defined (figure 4.15). In fact, if  $\delta_w$  is small enough, for example, the contact is elastic and the wear rate will be negligible, but if  $\delta_w$  is quite deep, the contact become plastic and  $\delta_w$  becomes the depth of cut.

The interference between the particle and the wafer can be expressed using the Hertzian expression too, and it is like:

$$\delta_w = \left( \frac{3\pi \times p}{4E^*} \right)^2 \times R$$

**FORMULA 4.71.**[27].

This last expression of the interference will be used to derive the equation for MRR because the pressure appears inside as variable, and the pressure is an easy parameter to check during the process.

Anyway  $p$  is defined as the mean contact pressure between the abrasive particle and the polished surface and  $E^*$  is the contact elastic modulus given by:

$$\frac{1}{E^*} = \left(1 - \frac{\nu_a^2}{E_a}\right) + \frac{(1 - \nu_w^2)}{E_w}$$

**FORMULA 4.72.**[27].

Where  $E$  and  $\nu$  are elastic modulus and Poisson's ratio of the abrasive particle and workpiece (the subscript  $a$  is for the particle, whereas  $w$  means the workpiece) (figure 4.15).

To define the maximum elastic interference  $\delta_{we}$ , beyond which the contact becomes plastic, the boundary condition has to be analyzed. This condition is defined when the mean contact pressure is equal to the hardness of the wafer,  $p = H_w$ .

Under this condition the *equation 4.71* becomes:

$$\delta_{we} = \left(\frac{3\pi \times H_w}{4E^*}\right)^2 \times R$$

**FORMULA 4.73.**[27].

Therefore, from this last one and from the *equation 4.70*, the maximum separation  $h_e$ , between the polished surface and the polishing pad where the elastic contact is still valid, can be found to be equal to:

$$h_e = R \times \left[2 - \left(\frac{3\pi \times H_w}{4E^*}\right)^2 \times \left(\frac{H_w}{H_p} + 1\right)\right]$$

**FORMULA 4.74.**[27].

This found distance  $h_e$  is the boulder for the elastic contact, but it is also the starting point for the plastic contact. With the *equation 4.74*, the boundary conditions have been

defined. Now, the plastic contact and therefore the condition where the MRR can occur will be analyzed.

If the condition of plastic contact between pad and polished surface is supposed ( $\delta_w$  becomes the depth of cut), the contribution of a particle to the wear coefficient is:

$$\Delta K = \frac{\Delta V}{L} = \frac{c \times \Delta S \times L}{L} = c \times \Delta S$$

**FORMULA4.75.[27].**

Where  $K$  is the wear rate of the polished surface (the wear rate is a factor proportional to the material removal rate) defined as the volume of material removal from the surface  $\Delta V$ , divided by the sliding distance  $L$ ;  $c$  is a fraction of displaced material which becomes loose wear debris and is a constant related to material property;  $\Delta S$  is the cross sectional area of the grooves caused by the particle.

Now, the depth of the groove,  $\delta_w$ , is very small compared with the radius of the particle, so under this condition it may be written:

$$\Delta S \sim a \times \delta_w$$

**FORMULA4.76.[27].**

$$\frac{\delta_w}{a} \sim \frac{a}{R}$$

**FORMULA4.77.[27].**

Where  $a$  is the radius of the circular cross section area caused by the abrasive particle on the surface of the polishing part. With these last considerations (equations 4.76 and 4.77) the equation for the wear rate (equation 4.75) can be modified as:

$$\begin{aligned}\Delta K &= c \times \Delta S = c \times a \times \delta_w = c \times \sqrt{R \times \delta_w} \times \delta_w = c \times \sqrt{R \times \delta_w^3} \\ &= c \times \sqrt{R \times \left( \frac{H_p}{H_w - H_p} \times (2R - h) \right)^3}\end{aligned}$$

**FORMULA 4.78.**[27].

Now the wear rate coefficient has been found, but not all the abrasive particles get in touch with the surface of the workpiece and, therefore, not all cause MRR. Thus it is important to define which particles are active in the MRR. Regarding that, it is supposed a surface height distribution density of the polishing pad called  $\phi_1(z)$  and a randomly distribution of the  $N$  particles on unit area in the gap located between the pad and the wafer, called  $N_{\phi_1}(z) dz$ .

After these assumptions, the total wear coefficient related to the active particles is equal to:

$$\begin{aligned}K &= \int_{d-h_e}^{z_{max}} \Delta K \times N \times \phi_1(z) dz = \int_{d-h_e}^{z_{max}} c \times N \times \sqrt{R \times \left( \frac{H_c}{H_w + H_p} \times (2R - h) \right)^3} \times \phi_1(z) dz \\ &= c \times N \times \left( \frac{H_p}{H_w + H_p} \right)^{1.5} \\ &\quad \times \left[ \int_{d-h_e}^d R^{0.5} \times (2R - h)^{1.5} \times \phi_1(z) dz + \int_d^{z_{max}} 2^{1.5} \times R^2 \times \phi_1(z) dz \right]\end{aligned}$$

**FORMULA 4.79.**[27].

But these considerations are not enough. In fact, not all the particles captured in the contact zone can be considered active. That is, not all the particles are in a position

$z < d - h_e$  and only those particular abrasive particles can scratch the polishing material and be held by the pad. This happens because not all the abrasive particles have the same size, but there is a certain standard deviation of that.

To take into account this fact, a constant  $A$  is introduced in the *equation 4.79*:

$$K = A \times c \times N \times \left( \frac{H_p}{H_w + H_p} \right)^{1.5} \times \left[ \int_{d-h_e}^d R^{0.5} \times (2R - h)^{1.5} \times \phi_1(z) dz + \int_d^{z_{max}} 2^{1.5} \times R^2 \times \phi_1(z) dz \right]$$

**FORMULA4.80.**[27].

In this way, not all abrasive particles participate at the polishing process.

To simplify again the analytic model, another assumption is made. In fact, it is assumed that the particles can only polish the surface once, and after scratching the counterface the particles are moved away from the initial position by the centrifugal force.

The number of single scratches per unit area is:

$$N = \frac{3C_v \times u \times \Delta t}{4\pi \times R^3}$$

**FORMULA4.81.**[27].

Where  $C_v$  is the slurry concentration per unit volume of spherical particles with uniform size,  $\Delta t$  is the time interval between two polishing contacts, and the settling velocity of individual spheres in a viscous fluid is given by Stokes equation:

$$u = \frac{2(\rho_a - \rho_l) \times g}{9\eta} \times R^2$$

**FORMULA4.82.**[27].

Where  $\rho_a$  is the density of the spheres,  $\rho_l$  is the density of the fluid,  $g$  is the acceleration of gravity,  $\eta$  is the dynamic viscosity.

Anyway, the *equation 4.82* is not always valid. In fact, for very small abrasive particles (as the CMP employs), that formulation has to be modified, because when the abrasive particles are in a slurry, they attract each other, forming some particles agglomerates. In particular, more the particles are small, more they tend to agglomerate. This fact modifies the behavior of the particles that is not well described by the *equation 4.82*. For this reason, in these cases, the using formula is:

$$u = \frac{2(\rho_a - \rho_l)g}{9\eta} \times R_{max}^{0.7} \times R^{1.3}$$

**FORMULA4.83.**[27].

And if this last equation is substituted in the *equation 4.81*, it becomes:

$$N = \frac{C_v \times \Delta t \times (\rho_a - \rho_l) \times g \times R_{max}^{0.7}}{6\pi \times \eta \times R^{1.7}} = B \frac{C_v}{R^{1.7}}$$

**FORMULA4.84.**[27].

Where  $B$  is a constant determined by the physical property of the slurry and the operating conditions; it is equal to:

$$B = \frac{\Delta t \times (\rho_a - \rho_l) \times g \times R_{max}^{0.7}}{6\pi \times \eta}$$

**FORMULA4.85.**[27].



After this brief consideration, the nominal contact pressure  $P$  can be calculated. It is equal to:

$$P = \int_d^{z_{max}} \pi \times a_{pw}^2 \times p \times N_p \times \phi_2(z) dz$$

**FORMULA 4.86.**[27].

Where  $a_{pw}$  is the radius of a circular contact area and  $p$  is the mean contact pressure equal to:

$$p = \frac{4E_p \times \sqrt{\delta_{pw}/R_p}}{3\pi}$$

**FORMULA 4.87.**[27].

Whereas  $R_p$  represents the radius of curvature on the top of the pad asperities,  $N_p$  is the density of the asperities of the pad, and  $\phi_2(z)$  is the peak height distribution density of the polishing pad. Anyway, the *equation 4.86* is true, if it is assumed that all the load is undertaken by the pad-workpiece contact and the deformation of the pad asperities is elastic.

The radius of a circular contact area  $a_{pw}$  can be expressed as:

$$a_{pw}^2 = R_p \times \delta_{pw}$$

**FORMULA 4.88.**[27].

Where  $\delta_{pw}$  is the interference between the pad and the workpiece which is equal to  $z - d$ .

Now, from the *equations 4.87* and *4.88*, if the elastic modulus of the polishing pad is  $E_p$ , the *equation 4.86* for the contact pressure can be expressed as:

$$P = \frac{4}{3} N_p \times E_p \times R_p^{0.5} \times \int_d^{zmax} (z - d)^{1.5} \times \phi_2(z) dz$$

**FORMULA4.89.**[27].

All the variables in the *4.89* are known except one, the peak height distribution density of the polishing pad  $\phi_2(z)$ . This last parameter can be supposed and if for the surface height distribution and the peak height distribution of the polishing pad it is assumed a Gaussian distribution, the distribution density function will be equal to:

$$\phi_1(z) dz = \phi_2(z) dz = \frac{1}{\sqrt{2\pi} \times \sigma} \times \exp\left(-\frac{z^2}{2\sigma^2}\right)$$

**FORMULA4.90.**[27].

Where  $\sigma$  is the standard deviation of the distribution and the reference plane is the center plane of the surface.

Finally, substituting the *equation 4.90* into the *4.89*, the contact pressure  $P$  becomes:

$$P = \frac{4N_p \times E_p \times R_p^{0.5}}{3(2\pi)^{0.5} \times \sigma} \times \int_d^{zmax} (z - d)^{1.5} \times \exp\left(-\frac{z^2}{2\sigma^2}\right) dz$$

**FORMULA4.91.**[27].

And the wear rate  $K$  is found to be:

$$K = \frac{A \times B \times c \times C_v}{(2\pi)^{0.5} \times \sigma \times R^{1.2}} \times \left( \frac{H_p}{H_w + H_p} \right)^{1.5} \\ \times \left[ \int_{d-h_e}^d (2R - h)^{1.5} \times \exp\left(-\frac{z^2}{2\sigma^2}\right) dz + \int_d^{zmax} (2R)^{1.5} \times \exp\left(-\frac{z^2}{2\sigma^2}\right) dz \right]$$

**FORMULA 4.92.**[27].

In this model a distribution of the abrasive in the slurry and of the asperities of the pad profile is considered to analyze the model, as well as in the model two. Moreover, not all the abrasive particles in the contact zone are taken into account because not all are active and participate to the material removal. These considerations are important but involve a larger computational work.

The considered shape of the abrasives is only one (spherical). The chemical effects are not considered, but in solid-solid contact mode they can be neglected.

This model, as the other two previous models and otherwise to the conventional process, takes into account an important number of variables like: mechanical characteristics of the pad, mechanical characteristics of the wafer, particles size, down pressure, number of active abrasive particles, geometry profile of the pad surface.

# CHAPTER FIVE

## The implemented MATLAB program

### 5.1. Introduction

Once completed the research in the literature of some models that well represent a Chemical Mechanical Polishing process, the second step has been to implement the three chosen theoretical models with MATLAB software to check if their MRR predictions were in agreement with our experimental results. This work of implementation has been done by Roman Wechsler, a German student from Monaco of Bavaria engaged in an internship at the Department of Mechanical Engineering of the Technical University of Denmark.

Nevertheless, the comparison between the theoretical previsions and the experimental results obtained by the experimental tests is not the only task of this new program. In fact, it is capable to create some empirical models which are able to fit for example some data resulting from some experimental tests. In our case, this capability of the program will be employed to create an empirical model which describes the roughness behavior of the polished samples.

MATLAB (*figure 4.1*) is a well known “high level technical computing language and interactive environment for algorithm development, data visualization, data analysis, and numerical computation” [29]. This is a flexible system and a large gamma of applications can be done, as for example: “signal and image processing, communications, control design, test and measurements, financial modeling and analysis, and computational biology” [29]. Moreover, the MATLAB environment can be extended with some special-purpose functions to solve particular classes of problems [29]. In our case, particularly, the program will be employed to predict the Material Removal Rate using the analytical equations found out from the literature and to create some empirical models which predict the surface roughness behavior in a polishing process.

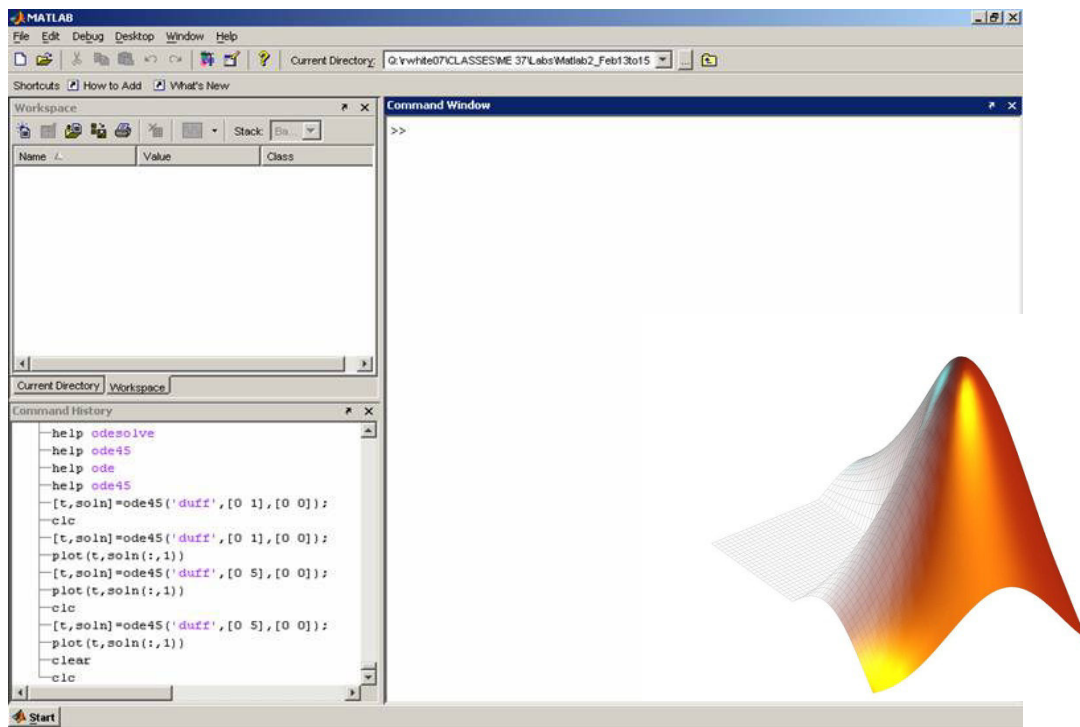


**FIGURE 5.1.** Starting page of MATLAB [29].

MATLAB is particularly suitable for our work of analysis and research, because it “supports the entire data analysis process, from acquiring data from external devices and databases, through preprocessing, visualization, and numerical analysis, to producing presentation-quality output” [29]. All these features make the program complete and fast to work.

## 5.2. Implemented MATLAB program structure

The program built by Roman Wechsler has two main aims:

- The first one is in to help in finding empirical models which predict the surface roughness behavior during a polishing process, using the extracted experimental data;
- The second one is to determine the Material Removal Rate (MRR) produced by a polishing process in dependence on various input parameters, as for example: down pressure, grain size, relative velocity between pad and wafer, etc.

Regarding the first purpose, the MATLAB program employs regression algorithms to find out some regression coefficients of mathematic functions which describe the surface roughness behavior as output depending on some input parameters (as time, down pressure, relative velocity between pad and wafer, etc). To create an empirical model, the first step is to run the m-file “Start\_program” (figure 5.2) and then to choose the first link “Create new empiric model” on the “GUI\_mainMenu” window (figure 5.3).

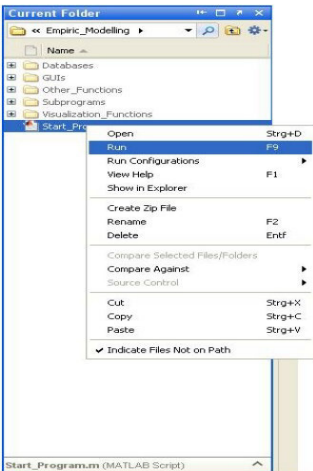


FIGURE5.2. First step to run the program [28].

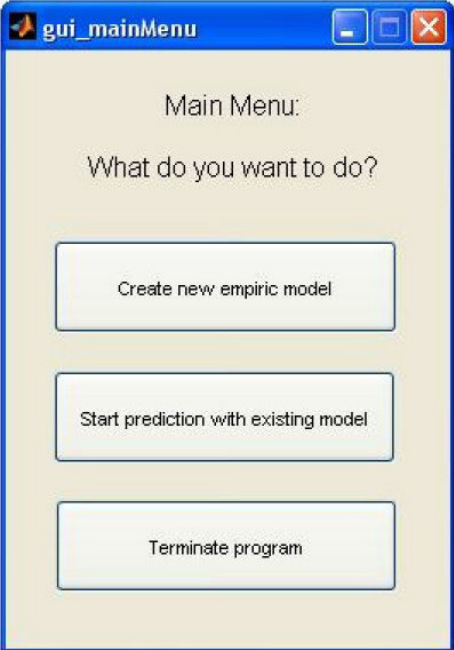


FIGURE5.3. GUI\_mainmenu [28].

When a left click on “GUI\_mainMenu” is done, a new window “gui\_createModel\_predObserv” opens and there the predictors (input parameters) and the observations (output values) have to be entered inside. Both predictors and observations have to be chosen from the database containing the experimental data (figure 5.4). This means that this database has to be created before starting with the creation of the model.

	A	B	C	D	E	F	G	H	I
1	IDENTIFIER_BEGIN	Observation name	Passes	Force on pad [N]	Abrasives's radius [ $\mu$ m]	Frequency [1/min]	Stroke [mm]	Response: Roughness	IDENTIFIER_END
2	ID_begin	observation_name	passes	force	radAbr	frequency	stroke	roughn_resp	ID_end
3	TRUE	exampleData_exp_5_obs_1	0	500	10	2500	1	1,5	TRUE
4	TRUE	exampleData_exp_5_obs_2	10	500	10	2500	1	1,2	TRUE
5	TRUE	exampleData_exp_5_obs_3	20	500	10	2500	1	0,9	TRUE
6	TRUE	exampleData_exp_5_obs_4	40	500	10	2500	1	0,6	TRUE
7	TRUE	exampleData_exp_5_obs_5	70	500	10	2500	1	0,5	TRUE
8	TRUE	exampleData_exp_5_obs_6	0	1000	20	2500	2	1,5	TRUE
9	TRUE	exampleData_exp_5_obs_7	10	1000	20	2500	2	1,1	TRUE
10	TRUE	exampleData_exp_5_obs_8	20	1000	20	2500	2	0,85	TRUE
11	TRUE	exampleData_exp_5_obs_9	40	1000	20	2500	2	0,55	TRUE
12	TRUE	exampleData_exp_5_obs_10	70	1000	20	2500	2	0,5	TRUE
13	TRUE	exampleData_exp_5_obs_11	0	500	5	1500	2	1,5	TRUE
14	TRUE	exampleData_exp_5_obs_12	10	500	5	1500	2	1,15	TRUE
15	TRUE	exampleData_exp_5_obs_13	20	500	5	1500	2	0,85	TRUE
16	TRUE	exampleData_exp_5_obs_14	40	500	5	1500	2	0,6	TRUE
17	TRUE	exampleData_exp_5_obs_15	70	500	5	1500	2	0,55	TRUE
18	TRUE	exampleData_exp_5_obs_16	0	1000	15	1500	1	1,5	TRUE
19	TRUE	exampleData_exp_5_obs_17	10	1000	15	1500	1	1,05	TRUE
20	TRUE	exampleData_exp_5_obs_18	20	1000	15	1500	1	0,75	TRUE
21	TRUE	exampleData_exp_5_obs_19	40	1000	15	1500	1	0,45	TRUE
22	TRUE	exampleData_exp_5_obs_20	70	1000	15	1500	1	0,4	TRUE

**FIGURE 5.4.** Example of Database.

In particular, the number and the name of the predictors and the number of observations taken into account have to be remembered, because this information will be required in the next steps and it is fundamental to create the new empirical model. When the predictors and the observations has been chosen from the database, the next step is to select or create a mathematic function that represents the process.

The structure of the function is equal to:

$$y = f(\vec{x}, \vec{\beta})$$

**FORMULA 5.1.**[28].

Where  $y$  is the response of the model and  $\vec{x}$  is the vector of the chosen predictors:

$$\vec{x} = \begin{pmatrix} x_1 \\ x_2 \\ \cdot \\ \cdot \\ x_p \end{pmatrix}$$

**FORMULA 5.2.**[28].

And  $\vec{\beta}$  is the vector of the regression coefficients:

$$\vec{\beta} = \begin{pmatrix} \beta_1 \\ \beta_2 \\ \cdot \\ \cdot \\ \beta_n \end{pmatrix}$$

**FORMULA 5.3.**[28].

The program permits us to define either a predefined function, or a personal function using a linear regression, or a personal function using a non linear regression. Nevertheless, before doing that, it is necessary to define the method by which the program has to optimize the regression coefficients. The possible methods are two: the least squares method, or the robust regression method. The first one minimizes the sum of the squares of the errors made in solving every single equation, whereas the second one uses the squares of the residual but iteratively weights them, so in this way



the outliers are weighted less than valid measurements and the method results more robust against the outliers. Therefore, it is important to choose one of these methods before to define an equation. The least squares method or the robust regression method can be chosen in the “*gui\_createModel\_modelFcn*” window where the model function can be chosen too.

When one of the two previous methods is chosen, it is possible to define a function for the empirical model. As mentioned earlier, three are the typologies of functions which can be chosen.

If a predefined function is chosen, the construction of the empirical model is simpler, because we already have a defined structure for our function, but we obtain least control on the process. Anyway, four predefined functions can be chosen and they are listed below:

- *Linear function*: it is structurally the simplest function. A constant value is present and there are  $p$  linear terms. The formula is:

$$y_{linear}(\vec{x}) = \beta_1 + \sum_{i=1}^p \beta_{i+1} \times x_i$$

**FORMULA 5.4.**[28].

In this case the number of regression coefficients  $n$  is one more than the number of predictors  $p$ .

- *Interaction function*: it contains a constant term, a linear term and a pairwise interaction term. That is:

$$y_{interaction}(\vec{x}) = y_{linear}(\vec{x}) + \sum_{i,j=1}^p \beta_{ij} \times x_i \times x_j; i \neq j$$

**FORMULA 5.5.**[28].

The number of regression coefficients is equal to:

$$n = p + 1 + \sum_{i=1}^p (p - 1).$$

- *Quadratic function*: it contains a constant term, a linear term, an interaction term and a quadratic term. The formula is:

$$y_{quadratic}(\vec{x}) = y_{linear}(\vec{x}) + y_{interaction}(\vec{x}) + \sum_{i=1}^p \beta_{i^2} \times x_i^2$$

**FORMULA 5.6.**[28].

In this case the number of regression coefficients is:

$$n = p + 1 + \sum_{i=1}^p (p - i) + p.$$

- *Purequadratic function*: it only consists of the constant term and the linear and quadratic term. The formula is:

$$y_{purequadratic}(\vec{x}) = \sum_{i=1}^p \beta_{i^2} \times x_i^2$$

**FORMULA 5.7.**[28].

Here the number of regression coefficients is:  $n = p + 1 + p$ .

If the personal function is chosen, an own personalized function can be defined. To do that, the link “*Edit function database*” has to be selected, and a new window opens, called “*gui\_edit\_databaseFcn*” (figure 5.5).

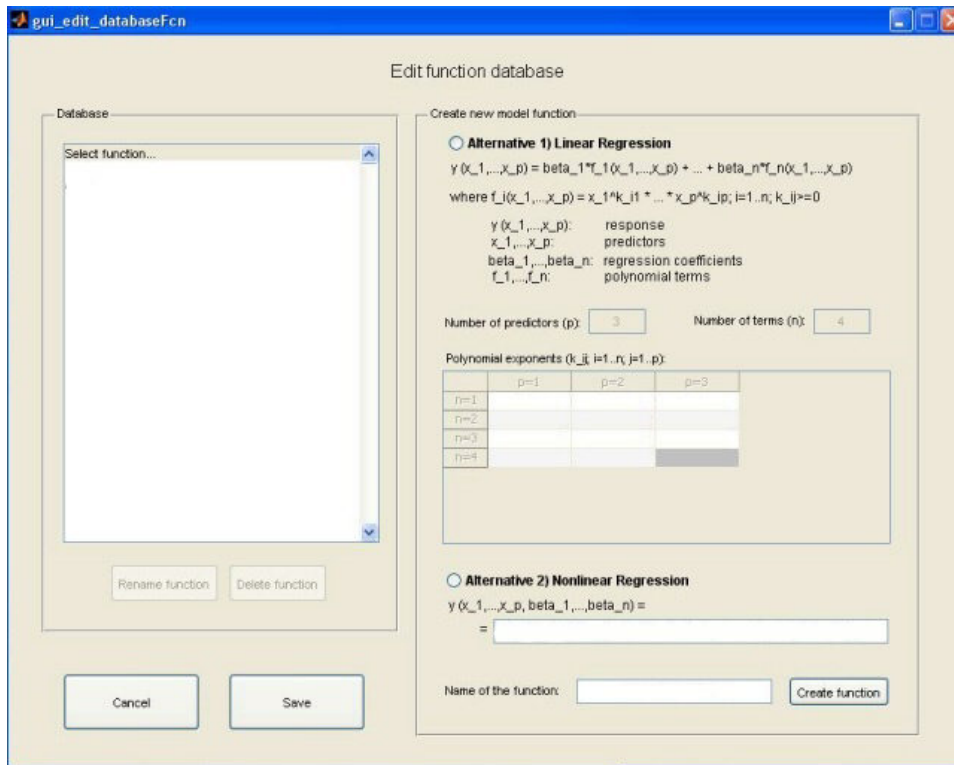


FIGURE 5.5. In the `gui_edit_databaseFcn` a new function can be formulated [28].

In this new window we can create our new function in two different ways. In fact, we can decide if we want to make a linear regression function or a non linear regression function. For the first alternative, the option “*alternative 1) Linear Regression*” has to be chosen. In this case, the program needs to know the number of predictors ( $p$ ) and the number of additive terms or regression coefficients ( $n$ ). It is noteworthy that the numbers of  $p$  and  $n$  have to be the same as the numbers chosen in the previous window “`gui_createModel_predObserv`”. After this information, the program needs to know the polynomial exponents which we want to employ in the new function. To do that, we have to fill a matrix where each column represents one predictors, while the rows represent the regression coefficients or additive terms. Once the matrix and the fields of predictors and terms are filled, the program will be capable to define a linear polynomial function that represent our process. If we click on the “*Alternative 2) Nonlinear Regression*” option, the second alternative is chosen and any kind of function can be defined (non linear regression function). Unlike the first alternative, in this one we need to have an estimation of the regression coefficients, because the program requires one to create an empirical equation. For this reason this alternative is more elaborate to define, but permits us to have more control on the process and on its response. To use this option, once having chosen the link “*Alternative 2) Nonlinear*

*Regression*”, we have to enter any valid MATLAB expression in the empty field, naming the regression coefficient with the symbol  $\beta_i$  and the predictors with the symbol  $x_i$ . Once defining the structure of the expression, we can click on “*Create function*” and then on “*Save*”. Only for this last alternative, when the equation is created, a new window opens called “*gui\_createModel\_initialValues*” where we have to enter the estimates for the regression coefficients. After this last operation, the expression is defined and ready to be employed.

When a new empirical model has been defined we can start with the prediction of the output values, employing the created model. To do that, in the first window “*gui\_mainMenu*” (figure 5.3) the link “*Start prediction with existing model*” has to be selected. From this one, a new window opens, called “*gui\_prediction\_chooseModel*”, where the models previously defined can be chosen. But before to run the selected model, the variables of our empirical equation have to be chosen. That is, the predictors (maximum two) in the form of vectors have to be defined to obtain some results by the model. These vectors are defined as a range of values and therefore we have to put in a maximum value, a minimum one and an increment which defines the resolution of the numerical calculation. Depending on the kind of chosen vectors (predictors) the trend of the response is different.

When the vectors have been chosen, the model can run and the final outputs are shown graphically as well as numerically. The graphical outputs are two graphs, where in the first one the response is a 3D surface along the z axis and the x and y axes are the two chosen predictors, whereas in the second one the response is shown with isolines. The resolution of these graphs depends on the chosen increment of the vectors defined previously. The numerical output is located in the MATLAB workspace and there we can find a matrix with the response data, a cell array with the values of the input values and a file with the information about the used model.

The first and empirical purpose of this program has been explained above, but the verification of the three implemented theoretical models is also possible. In fact, the second purpose of the MATLAB program is to calibrate the three implemented models so that a comparison between the predictions and the experimental data can be done, and therefore the verification of the model can be made.

To use this function of the program, the file “*Start\_Simulation*” has to be run, in this way a new window opens, where the three models can be found (figure 5.6). Once a model has been chosen, the empty fields for the input parameters have to be filled (figure 5.7). The input parameters to put in the model are shown in the window and they are

process parameters (as frequency, stroke, force on the pad, feed speed), abrasives parameters (as mean radius), resolutions parameters (as time, axial, tangential), pad parameters (as Young's modulus, hardness, standard deviation of the surface profile, length, width) and workpiece parameters (as surface, hardness, rotational speed, diameter) (*figure 5.7*). Unlike what has been done for the empirical models, here only one of these input values has to be defined as vector, with a maximum value, a minimum value and a desired increment, to fit the trend of the response.

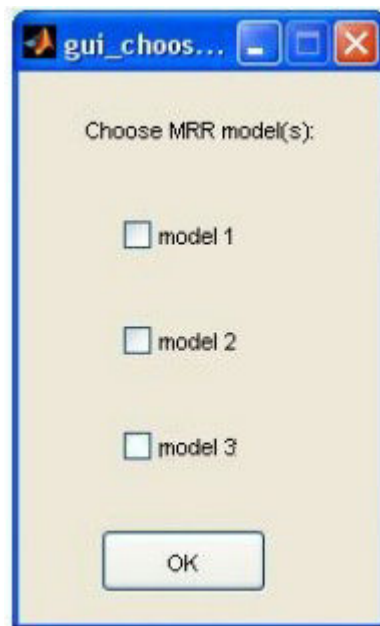


**FIGURE 5.6.** The window where the three models can be chosen is shown [28].

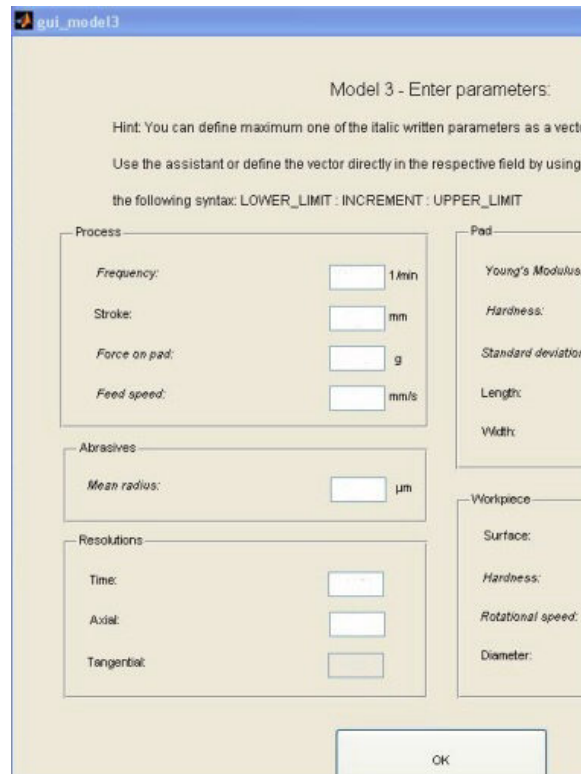


**FIGURE 5.7.** Process parameters which the program requires to run [28].

When the input parameters have been typed in the appropriate fields, the program will ask whether a calibration of the model's output with the experimental data located in a database is necessary or not. If the calibration of the output is done, a new window opens, called "*gui\_calibration\_search*", where the experimental data for the calibration have to be chosen. As well as in creating an empirical model, the outputs are delivered graphically and numerically. In the two opened figures the response is shown as a surface in one of them, and with isolines in the other one. Instead the numerical results are stored in the MATLAB workspace and they are a matrix with the response data of MRR, a matrix with the MRR proportionality factor and the proportionality factor that was determined during the calibration, that is  $MRR = MRR_{prop} \times propFact$ .

# CHAPTER SIX

## The experimental planning

### 6.1. Introduction to the variables of the process

After a depth study and analysis of the polishing process system and of the problem connected with it, and after the analysis of the chosen theoretical model describing a polishing process, some variables have been identified influencing the material removal and the variation of the roughness behavior as well as the final reached value. From these considerations an experimental planning was formulated.

These variables or input parameters are very numerous and they can be divided between two families: the parameters which affect the material removal (that is, in other hands, the input parameters for the theoretical models), and those which effect the roughness behavior. These two typologies of parameters can be completely different each other or can be the same, but anyway in this last case they could have different influences on the analyzed outputs. That is, for example, if the down force acting on the workpiece is considered, it affects both the material removal and the roughness behavior, but with two different influences for each. In fact, when the material removal is considered, an increase of down pressure causes an increase of MRR, whereas when the roughness behavior is analyzed the influence of the pressure is ambiguous (this fact is shown in the experimental results related to the third model [27]).

For this reason, to better understand what are the variables which affect a polishing process, and how they affect the material removal and the roughness behavior of the workpiece surface, two different lists will be introduced to distinguish the two different families.

Firstly, the variables regarding the MRR are listed:

- Yield stress of the workpiece;
- Hardness of the workpiece;
- Young's modulus of the pad;
- Length of the pad;
- Width of the pad;
- Thickness of the pad;
- Hardness of the pad;

- Mean radius of the asperities summits;
- Density of the summits;
- Mass ratio of abrasive to liquid;
- Dilution ratio to ID water;
- Density of the abrasive in the slurry;
- Mean abrasive size;
- Standard deviation of the size;
- Down pressure;
- Relative velocity among pad and workpiece.

Whereas, the found variables which affect the roughness behavior are:

- Hardness of the pad;
- Hardness of the wafer;
- Mean grain size;
- Concentration of the abrasive in the slurry;
- Standard deviation of the grain size;
- Down pressure acting on the workpiece;
- Feed rate of the pad;
- Frequency of the pad;
- Stroke of the pad in the direction of the oscillations;
- Polishing time.

As said previously, the considering variables are very numerous, but each of them affects the process and therefore they have to be considered in our analysis. The meaning and the role of each variable will be explained below. But it is noteworthy to define, before starting with the exposition of the variables, what is meant with the term “oscillation”. In this case and in all the following analysis, it has the meaning of frequency. In fact the term “oscillation” is used in this work only because it is employed by STRECON, and its unit of measure is 1/min.

*Yield stress of the workpiece:* this mechanical characteristic of the machining material is important because it primarily affects the material removal. In fact, more the Yield stress value is high, more is difficult to have a plastic deformation of the surface and a higher down force is required to reach the threshold condition between the elastic behavior of the machined material and the plastic one. In fact, it is noteworthy that all the analyzed MRR models assume a perfectly plastic behavior of the workpiece on the



contact area with the abrasive particles and only after having reached or exceeded the Yield stress value, the material removal can occur.

*Hardness of the workpiece:* this variable is important both for the material removal and for the roughness behavior of the workpiece. In fact, more the hardness is high, more the abrasive particles find difficulty into penetrating the workpiece surface. Consequently, they find more resistance in scratching and wresting material from the surface. On the opposite, the penetration of the abrasives into a soft material is easier, and the material removal increases, but the scratches will be more marked and the final roughness value could increase. But this could not be the only influence that the hardness of the workpiece has on the roughness. In fact, it could affect the roughness behavior of the machined material modifying the curve shape of the roughness itself on the time, determining a descent to the convergence value more or less pronounced. This means that for hard materials, the final roughness could be better than a softer one, but the required timing to reach it could be longer. Anyway, this is only a supposition which has to be verify with the experimental tests.

*Young's modulus of the pad:* in our considerations and analysis the pad is always considered softer than the workpiece. Nevertheless, some experimental results [27] show that soft pads with an higher rigidity work better than soft pad with a lower rigidity. This "work better" means that with the first kind of pads the material removal is higher and the left track on the surface by the pad is more definite with well-defined edges. This means also that the reached roughness field on this zone is more homogeneous. This happens because the rigid pads are more stable during the polishing process and they do not undergo important deformation during the process, so that the pressure distribution during the motion of the pad is more stable and constant compared to what occurs when a pad with a lower rigidity is employed.

*Length, width and thickness of the pad:* these three variables define the geometry of the pad and the size of the contact zone between pad and workpiece. The size of the contact zone surface is important because it is another variable on which the pressure distribution is dependent. In fact, geometrical size, down pressure value, and Young's modulus are the main variables that influence the pressure distribution on the contact zone between pad and workpiece and, consequently, they affect both material removal and roughness behavior. Anyway, for a stable pressure distribution, more the size of the pad are big (length and width in particular), more the material removal is high and larger zone will be interested by a reduction in roughness value.

*Hardness of the pad:* this is an important parameter for the process itself. In fact, the considered polishing process required a pad which is capable to catches the abrasives on its surface. This action can be done only by soft pad which can incorporate the abrasive particles when the contact between pad-workpiece-abrasives occurs. If the abrasives are not incorporated on the pad surface, they will not can scratch the workpiece or a less efficient three-body abrasion occurs in the polishing zone. This is the main reason because the pad are softer than both the abrasives and workpiece.

*Mean radius of the asperities summits or mean area of single asperity:* this parameter, as the following one, is directly linked with the hardness of the pad. In fact hardness of the pad, mean radius of the asperities summits, and density of the summits are responsible of the real size of the contact between pad and wafer and of the number of abrasives incorporated into the pad surface. If the radius of the asperities summits is big, the contact zone will be big and there will be more likely to incorporate abrasive particles. This means that if the number of the involved abrasives is high, the material removal will be high and the polishing process will require less time to reach the final roughness value.

*Density of the summits:* as introduced above, this parameter is one of those parameters important to determine the size of the contact zone and consequently the number of incorporated abrasives in the pad. Similar considerations done for the previous chapter are valid for this parameter as well.

*Mass ratio of abrasive to liquid, Dilution ratio to ID water, Density of the abrasive in the slurry:* these parameters are employed to describe the slurry and the presence of the abrasives into it. In fact, the diamond paste used during the experimental tests is a compound of diamond, where its concentration plays a fundamental role both in the material removal and in the timing to reach the final roughness. In fact, more the concentration of the abrasives is high, more abrasive particle can scratch the workpiece surface, bringing an increment in the material removal rate and in a decrease of the timing required to reach the expected value for that abrasive size.

*Mean abrasive size:* this is an important parameter both for the material removal and for the final roughness value. In fact, two of the three theoretical models show that with the increment of the grain size the material removal increases (second and third model), whereas for the first model the opposite happens. For the roughness behavior the mean abrasive size seems to determine the final roughness value achievable with that polishing process. This means that the abrasive size decides the minimum value reached by the polishing surface, but not the timing to obtain it.

*Standard deviation of the size:* low standard deviation of the grain size implies that more or less all the abrasive particles have the same radius (if they are assumed spherical). This means that for a given down force more particles will be incorporated in the pad surface because more abrasives will have the same size (this does not happen if the standard deviation is very high. In fact, in this case the larger particles prevent the smaller ones of sinking into the pad surface) and therefore the material removal and the roughness on the polished area will be more homogeneous.

*Down pressure acting on the workpiece:* the down pressure is one of the most important parameters in this process. Regarding the material removal, all the three theoretical models agree in saying that with an increment of the down pressure the material removal increases. This because the abrasive particles are pushed into the material and during the motion they leave deeper scratches. Otherwise, the influence of the pressure on the roughness is not well-known. In fact, the article where the third theoretical model is introduced [27], exposes some experimental results where the influence of the pressure on the roughness behavior is ambiguous. In fact, for some tests an increment of pressure brings to decrease the reached final roughness, whereas for other ones it brings to increase the roughness value. The role of the pressure, therefore, has to be verified and understood running the experimental tests.

*Feed rate of the pad and Frequency (Oscillation) of the pad:* these two parameters define the kinematics conditions of the pad. The analyzed theory for the material removal says that with an increase of the relative velocity between the pad and the wafer the MRR increases, whereas for the roughness nothing has been found. Anyway, it is sure that feed rate and oscillation define the motion of the pad and for this reason they define the track which is left by the pad on the workpiece surface. This is directly connected with the roughness behavior but its influence has to be determined.

*Stroke of the pad:* this parameter determines the oscillation amplitude of the pad. This means that the stroke gives a contribution in determining the shape of the pad motion too (as it occurs for feed rate and frequency of the pad). But this is not all. The strokes influences the pressure distribution as well due to the imposed motion to the pad. So it is expected to influence both material removal and roughness behavior, in particular on the edge of the pad track.

*Polishing time:* this is maybe the most important parameter of the process. In fact, the whole cost of the polishing process depends on this factor. More the timing increases, more the pad has time for polishing the interested part, but more the cost of the process increases and this is a great problem that has to be minimized. Then the

understanding of the optimal combination of parameters to obtain the shortest time to polish the part and the understanding when the process has to be stopped because the final roughness value has been reached, are two important purpose to improve a polishing process itself.

## 6.2. The experimental planning

### 6.2.1. Experimental planning variables

After this briefly presentation of the variables taken into account to analyze the polishing process in flat kinematics condition, the experimental planning can be introduced.

Some of the variables previously introduced have been locked by some choices of process defined in agreement with the company and with the required timing to run the tests themselves. In fact, regarding the pad, its length, width, and thickness have been locked because defined sizes are required by the RAP clamping system employed to hold the pad, whereas hardness and all those characteristics concerning the surface condition of the pad (as for example asperities distribution) have been locked as well, because a wood pad has been employed for all the experimental tests.



**FIGURE 6.1.** Image related to wood pad with its clamping system in the end of the polishing arm.

Regarding the variables related to the workpiece, they have been all locked because the polishing material has been decided to be UDDEHOLM SLEIPNER ® HRC59 (see chapter seven related to the polishing material). This means that Yield stress point and hardness have been defined.

Regarding the abrasive particles, a diamond paste of 14  $\mu\text{m}$  has been employed for the experimental tests (figure 6.2). The name of the paste was “JOKE MAGIC®” diamantpaste 14  $\mu\text{m}$ . This means that concentration, mean size and standard deviation of the grain size have been locked as well as dilution ratio and density of the abrasives in the slurry.



**FIGURE 6.2.** Diamond paste.

The last variable to be locked has been the stroke of the pad. This was established to be 0.5 mm because this value is usually used by STRECON operators.

In the end, the only free variables from the initial parameters were three:

- The down force acting on the workpiece;
- The feed rate of the pad;
- The frequency (oscillation) of the pad.

From these three variables an experimental planning has been programmed.

Below it is possible to see a summary where the free and locked variables are reassumed:

<b>VARIABLES</b>	<b>LOCKED/FREE</b>
<b>Yield stress point of the workpiece</b>	<i>Locked</i>
<b>Hardness of the workpiece</b>	<i>Locked</i>
<b>Young modulus of the pad</b>	<i>Locked</i>
<b>Length, width, thickness of pad</b>	<i>Locked</i>
<b>Hardness of the pad</b>	<i>Locked</i>
<b>Mean area of single asperity</b>	<i>Locked</i>
<b>Density of the summits</b>	<i>Locked</i>
<b>Density of the abrasive in the slurry</b>	<i>Locked</i>
<b>Mean abrasive size</b>	<i>Locked</i>
<b>Standard deviation of the grain size</b>	<i>Locked</i>
<b>Stroke of the pad</b>	<i>Locked</i>
<b>Down pressure</b>	<i>Free</i>
<b>Feed rate of pad</b>	<i>Free</i>
<b>Frequency of pad</b>	<i>Free</i>

**TABLE 6.1.** *Process variables.*

Since the free variables were only three and the tests have been supposed to take a large time to reach the final desired roughness, the experimental planning has been built following a full factorial design with three parameters and two levels each. This means that the overall number of runs has been eight. In fact, for the full factorial design the number of runs is given by:

$$(\text{levels})^{(\text{parameters})} = \text{number of runs}$$

$$2^3 = 8$$

Now, due to the length of the initial bar 1030 mm from where the samples of Sleipner have been obtained and due to the RAP clamping system which constrained the size of the samples themselves to be 60 mm × 80 mm, thirteen samples have been obtained from the initial bar.

In other hands, five more samples were available to be machined. For this reason and to extend the experimental planning employing these samples, remembering that one of them will be polished to detect the overlap effect, it has been decided to polish one of the four samples (four because five samples less the sample required for the overlapping test) assuming as process parameters the central values between the two extreme levels for each parameter (for this reason this samples will be called “central point” as well during the thesis, because here a set of central values is employed), whereas the remaining three samples have been machined assuming one of the three free parameters on its central value and maintaining the other two locked on their highest level (this choice is shown in *table 6.4*).

This choice has been done to understand more about the roughness behavior between the employed limit values. In fact, since a full factorial design with three level steps has been not possible to plan (for two reasons: the first one was the long required time to run the tests and this fact could create operative problems for STRECON because the machine would have been busy for many days, and the second one was that the samples were not enough to run a plan like that. In fact, a full factorial design with three levels for each parameter requires in our case twenty-seven runs or, in other hands, twenty-seven samples), and since the full factorial employing two levels does not give information about how the model response varies between the two limit value assumed by the polishing parameters, the settings of parameters chosen for the four additional samples will be useful to extract some more information about the behavior of the response when the parameters assume values belonging to the their range of variation. In this way, at the end of this analysis, it will be possible to understand firstly how the chosen parameters affect the response of the model, and secondly it will be possible to obtain a first indication on how the behavior of the response itself is when the parameters are change along their interval of variation.

#### 6.2.2. Assignment of the levels for the chosen polishing process

Therefore, when the experimental planning to follow was defined, the second step has been to decide which values had to be assigned to the considered parameters. To make this, some considerations were done. Some information has been asked to STRECON regarding which parameters were usually used by them for a polishing process in flat kinematics conditions and which ranges for pressure, feed rate, and oscillations the RAP machine could reach. These data have been important to understand which limits were possessed by the machine and how the skilled company

worked in this situations, formulating in this way some reference points for our experimental tests. The answer of STRECON company is summarized in the table below:

PARAMETER	RANGE OF THE RAP		EMPLOYED VALUE	UNIT OF MEASUREMENT
	MINIMUM	MAXIMUM		
Pressure	100	3000	500	g
Feed rate	0.1	10	1	mm/s
Frequency	3.33	83.33	50	1/s

TABLE 6.2. Maximum and minimum values achievable by RAP and employed parameters by STRECON [30].

Referring to the usual values employed by STRECON, some observations have been done. In fact, if those values are assumed and if the motion of the pad is thought sinusoidal, the journey of the pad itself can be represented more or less as the picture below:

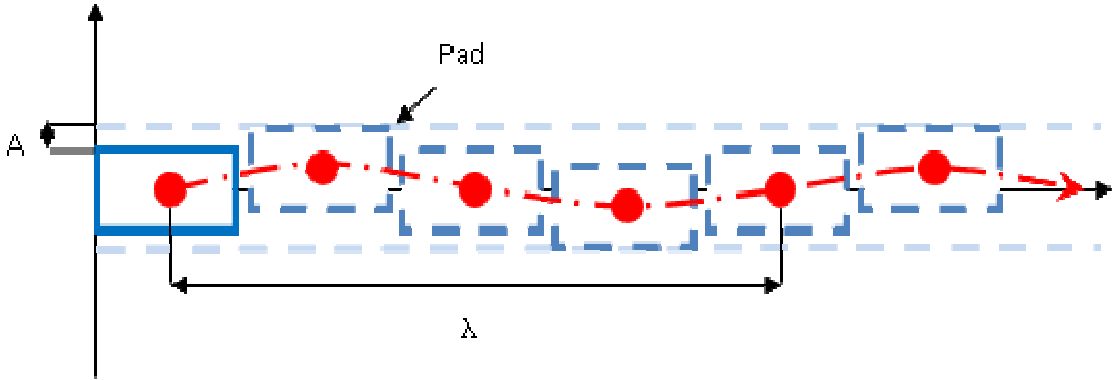


FIGURE 6.3. Sinusoidal motion of the pad.



This means that for feed rate of 1 mm/s and an oscillation of 3000 pulses per minute (frequency of 50 1/s), the wave length of the pad journey is equal to 20  $\mu\text{m}$ . In fact, we have:

$$\text{feed rate} = 1 \frac{\text{mm}}{\text{s}}$$

**FORMULA 6.1.**

$$\text{frequency} = f = \frac{3000}{\text{min}} = 50 \frac{1}{\text{s}}$$

**FORMULA 6.2.**

$$\text{period} = T = \frac{1}{f} = \frac{1}{50} = 0,02 \text{ s}$$

**FORMULA 6.3.**

$$\lambda = T \times (\text{feed rate}) = 0,02 \times 1 = 20 \mu\text{m}$$

**FORMULA 6.4.**

If  $A$  represents the amplitude of the sinusoidal journey of the pad (in this case the amplitude is equal to the employed stroke of 0.5 mm), it could be supposed that more or less all the abrasive particles captured by the pad will follow the journey represented in *figure 6.3* and therefore they will have the same wave length.

From this observation, it has been supposed to confer to the parameters values that kept constant the wavelength found out by the equations above. This is important because, acting in this way, we will be able to understand from the results of the experimental tests if the roughness behavior of the workpiece surface depends on the polishing time or on the distance made by the pad during the polishing process and, therefore, from these conclusions the empirical models for the roughness can be formulated, valuating if the main variable to take in account is the time or the distance.

Then, the choice of the parameter values in our experimental planning has two great meanings: the definition of the experimental planning itself and the future evaluation of the empirical models.

Regarding this, for the frequency the value of 8.33 1/s and 58.33 1/s (that is oscillation of 500 1/min and 3500 1/min respectively) has been chosen. This option has been done because the employed frequency by STRECON of 50 1/s was wanted to be belonged into the used experimental range for this variable, for understanding in this way if the chosen parameters by this company are a good choice or can be improved.

The chosen options for the frequency have implied that the values were locked for the feed rate. In fact, if the wavelength of 20  $\mu\text{m}$  is kept constant, the levels for the feed rate become 0.167 mm/s (for an oscillation of 500 1/min) and 1.167 mm/s (for an oscillation of 3500 1/min).

Regarding the pressure, being the only parameter independent from the wavelength, its two values have been chosen setting the same considerations done for the oscillations, and that is, the two pressure levels have been selected so that the employed value by STRECON was included in the experimental range. In other hands the two pressure levels has been 100 g and 900 g (the STRECON usual value is 500 g).

After that, the experimental planning is almost finished. The parameters and their levels are summarized below:

	<b>PRESSURE (g)</b>	<b>FEED RATE (mm/s)</b>	<b>FREQUENCY (1/s)</b>
<b>MAX VALUE</b>	900	1.167	58.33
<b>MIN VALUE</b>	100	0.167	8.33
<b>CENTRAL VALUE</b>	500	0.667	33.33

**TABLE 6.3.** Levels for the experimental planning.

In the last row of *table 6.3*, the central parameter values that will be employed for the central tests have been reported. They are nothing more than the average between the maximum value and the minimum one of each parameter.

To complete the experimental planning, the order to run the tests has to be established. To make this, the *MINITAB* software has been employed. This program permits us to build our experimental planning if the starting inputs and their value levels are known, and helps us to analyze the consequent results coming from the experimental tests. Moreover, *MINITAB* gives us the order to run the experiments. This order is particular because it is random. In fact, the randomization permits us to suppose a normal distribution of the noise factor so that we can imagine its influence is negligible on the experimental results.

Once the inputs and their levels have been introduced in the program the results was the following summarized in the table below:

<i>RUN</i>	<i>PRESSURE</i> (g)	<i>FEED RATE</i> (mm/s)	<i>FREQUENCY</i> (1/s)	<i>NUMBER OF</i> <i>SAMPLE</i>
<u>1</u>	900	0.167	8.33	<u>1</u>
<u>2</u>	900	1.167	8.33	<u>2</u>
<u>3</u>	900	1.167	58.33	<u>3</u>
<u>4</u>	100	1.167	8.33	<u>4</u>
<u>5</u>	100	1.167	58.33	<u>5</u>
<u>6</u>	100	0.167	8.33	<u>6</u>
<u>7</u>	100	0.167	58.33	<u>7</u>
<u>8</u>	900	0.167	58.33	<u>8</u>
<u>9</u>	500	0.667	33.33	<u>9</u>
<u>10</u>	900	1.167	33.33	<u>10</u>
<u>11</u>	900	0.667	58.33	<u>11</u>
<u>12</u>	500	1.167	58.33	<u>12</u>
<u>13</u>	500	0.667	33.33	<u>13</u>

**TABLE 6.4.** *The complete experimental planning.*

After this last step the experimental planning is complete and ready to be run.

### 6.2.3. Number of repetitions of the experimental tests and timing intervals

Besides determining the order of the runs relating with the chosen parameters for the tests, the number of repetitions for each test and the number of timing intervals have to be decided.

Regarding the number of repetitions to do for each test, it has been decided that for a same set of parameters the test had to be repeated three times. In this way, a result more reliable for each test can be obtain and the factor of error influencing our tests can be understood.

Regarding the timing intervals, these are important to understand how the roughness behavior varies on the time and four timing points have been chosen to evaluate this. From the literary study, it is expected that the roughness behavior curve is steep in the beginning when the polishing process has just started, and more or less flat when the convergence roughness value is close to be reached. In other hands, the roughness behavior is expected to be as in the *figure 6.4*:

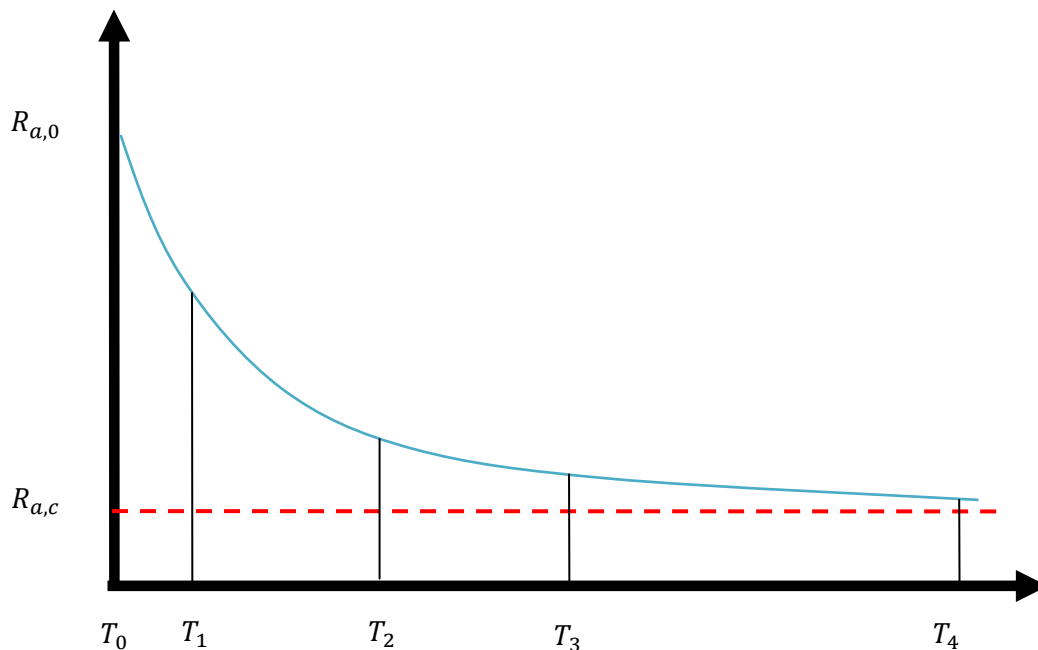


**FIGURE 6.4.** Expected roughness behavior.

In the *figure 6.4*, the four timing intervals are  $T_1$ ,  $T_2$ ,  $T_3$ ,  $T_4$ , whereas  $T_0$  is the starting moment when the polishing surface has its starting roughness  $R_{a,0}$ . The employed

methodology to define the four timing intervals is simple. Firstly, the  $T_4$  has to be found out. In fact,  $T_4$  is the required time for the process to reach the convergence roughness value for a precise setting of parameters ( $R_{a,c}$ ). Once this time is determined, the other three are defined as  $T_3 = 0.5T_4$ ,  $T_2 = 0.3T_4$ , and  $T_1 = 0.1T_4$ . These choices have been done because the variation of the roughness is more important in the starting phase of the polishing process. Therefore more points are required to better fit the shape of the roughness curve.

These considerations are not true for the samples twelve. In fact, only the overlap effect has to be analyzed and then the four timing intervals are not required, but only the profile of the polished zone has to be analyzed to understand what effect the overlap has on the surface when it is present. Therefore, only in this case the polishing surfaces will be worked for a time equal to  $T_4$ , and to better use the free surface in the samples, six repetitions and not three will be run. The chosen combination of parameters for this sample has been equal to that one employed for the sample 0, that is: pressure=500 g, feed rate=0.667 mm/s; frequency=33.33 1/s.

Then, in the end, for each parameters combination previously defined in the experimental planning, four timing intervals have to be get out and for each of these combinations three repetitions have to be run. This means that the overall number of test to do are equal to  $12 \times 3 \times 4 + 6 = 150$ , [(*number of parameter combinations*)  $\times$  (*repetitions*)  $\times$  (*timing intervals*) + (*six repetitions for the overlap effect*)].

#### 6.2.4. Configuration of the samples

The last step has been to define the size of the polishing area in each sample. Since that the size of the pad is three millimeters by six millimeters and the feed rate motion in the direction of the length of the pad (that is 6 mm) is usually employed to be perpendicular to the frequency motion (it is in the direction of the width of the pad), the shape of the polishing areas has been decided to be rectangular with size four millimeters by twenty millimeters. This is not true for the sample 0 and for the sample 12. In fact, for the sample 0 the length of the polishing area is smaller because the sizes of this sample is smaller. For this reason the size of the polishing areas have been decided to be four millimeters by fifteen millimeters. Regarding the sample 12, where the overlap effect is investigated, the sizes of the polishing areas have to be different because the overlap implies a bigger width of the polishing areas. For this

reason, in this case the sizes have been decided to be five millimeters and an half by twenty millimeters (an pad overlap of 50% has been employed).

The layout of the polishing areas can be seen in the following figures.

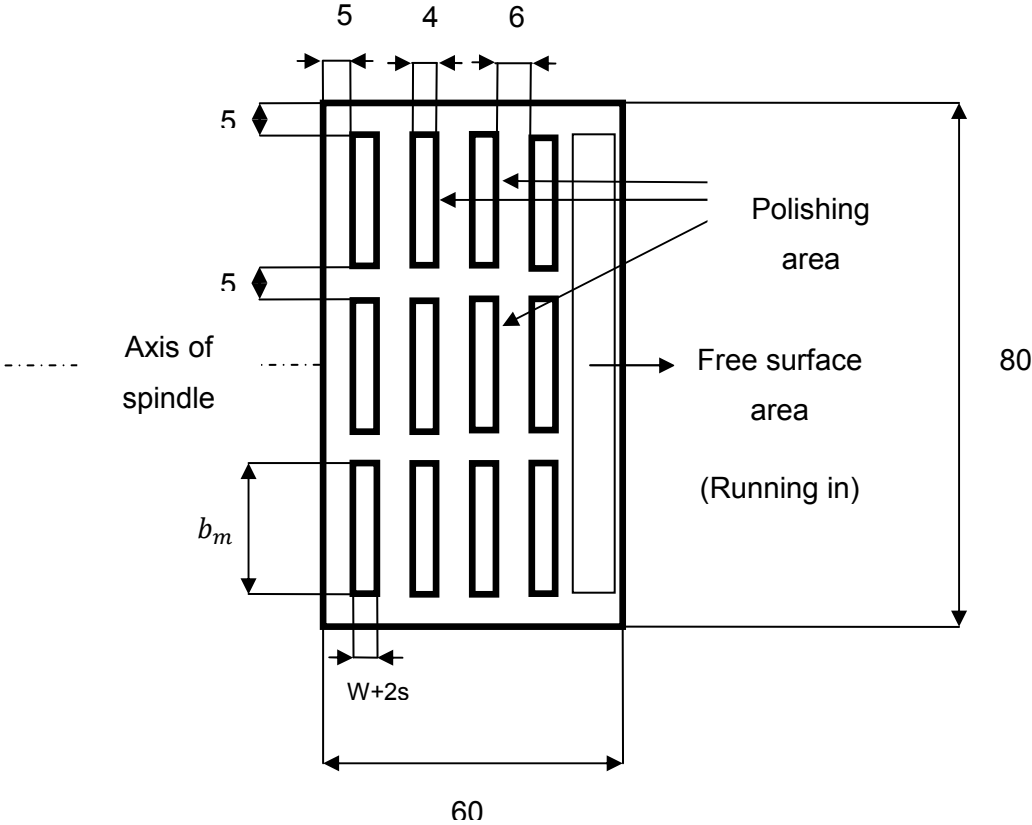


**FIGURE 6.5.** General layout of the samples.

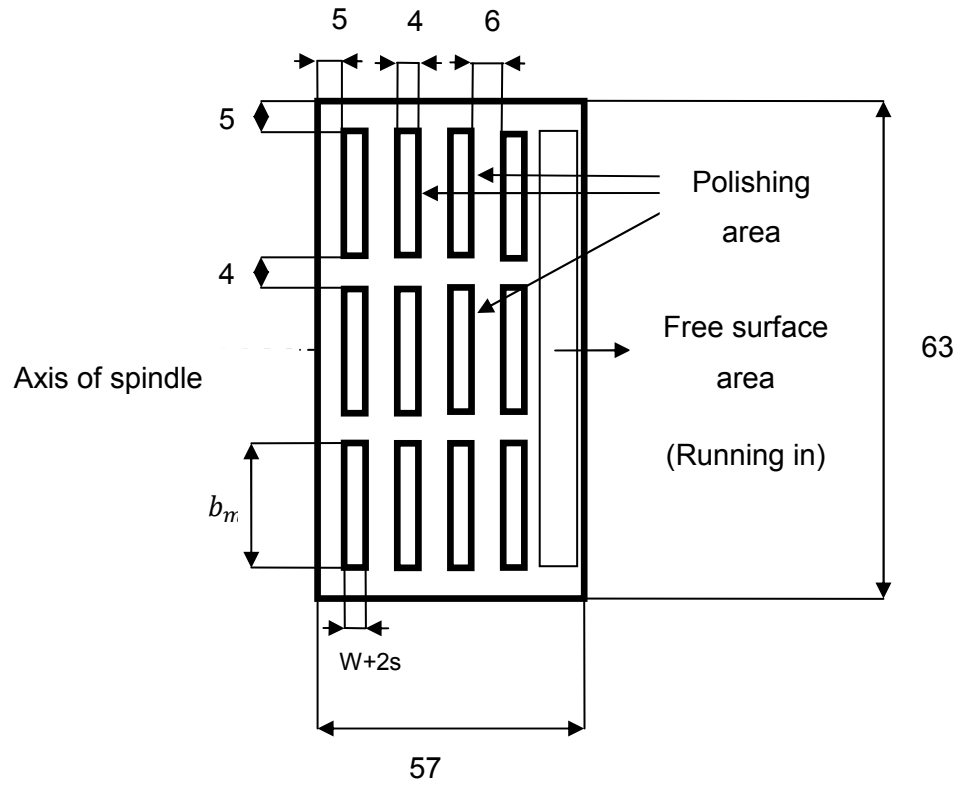


FIGURE 6.6. Layout of the sample 0.

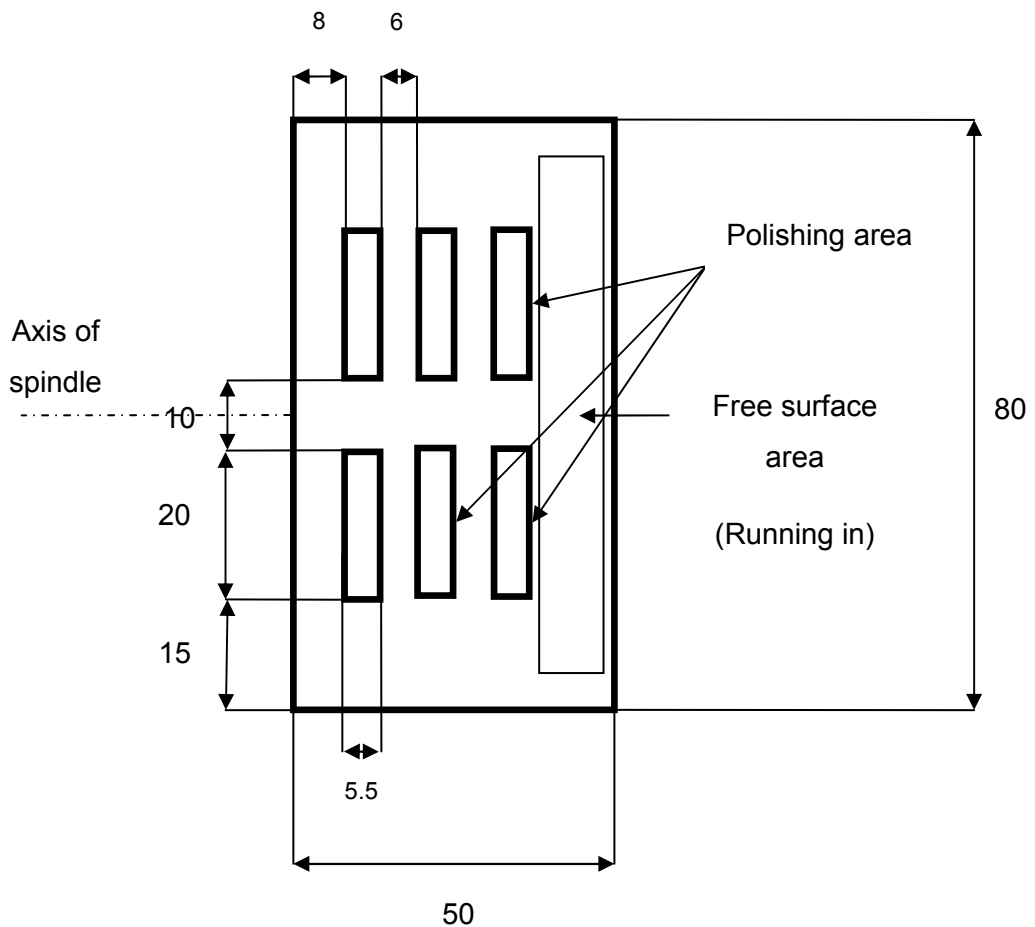


FIGURE 6.7. Layout of the sample 12 where the overlap effect is analyzed.

Therefore, in this way, every sample corresponds to a set of parameters with its three repetitions and its four timing intervals. This means that in every sample a complete roughness behavior curve can be estimated and the effects of the parameters can be easily seen.

The two important outputs to analyze after the experimental tests are: firstly the reached final roughness value and the required timing to obtain it, and towards the DOE analysis it will be possible to understand how the polishing parameters affect the roughness behavior and what is the best parameter setting to reach the best final roughness value in a shorter timing, secondly the amount of material removal caused by the process.

In conclusion, with this full factorial design with three factors and two levels, we will be able to understand which is the influence of each parameter on the roughness behavior and what are the interactions between the chosen inputs. Moreover, these tests will permit us to see if there is some dependence of the roughness behavior on the distance made by the pad during the polishing process or if only the polishing time is determinant in affecting the surface behavior of the workpiece. Moreover the amount of material removal rate for each sample will be detected and compared with the predictions of the theoretical models.

To do this, 150 tests in thirteen samples are required to obtain reliable experimental data.



# CHAPTER SEVEN

## Uddeholm Sleipner® HRC 59

### 7.1. Introduction to the polishing material

The material employed for the experimental tests has been the steel UDDEHOLM SLEIPNER® HRC 59 [31].



**FIGURE 7.1.** Sleipner's samples before grinding.

Uddeholm Sleipner HRC 59 is a product of the Swedish steelworks Uddeholm, a company which is born in the 1668 and it is one of the world's leading supplier of tooling material [31].

This steel is a chromium-molybdenum-vanadium alloyed steel. The typical concentration of chromo, molybdenum and vanadium are summarized in the *table 7.1*.

<b>Element</b>	<b>C</b>	<b>Si</b>	<b>Mn</b>	<b>Cr</b>	<b>Mo</b>	<b>V</b>
<b>Concentration %</b>	0.9	0.9	0.5	7.8	2.5	0.5

**TABLE 7.1.** Typical Sleipner composition [31].

The usual application of the Sleipner is as a general purpose steel for cold work tooling and it is employed for medium run tooling applications due to its high resistance to mixed or abrasive wear and good resistance to chipping [31]. These two last characteristics make the Sleipner particularly suitable for cold working and bring it to substitute the previously employed steels [31].

It is interesting to see what are the main characteristics of this material. They are listed below:

- Good wear resistance [31];
- Good chipping resistance [31];
- High compressive strength [31];
- High hardness after high temperature tempering [31];
- Good through-hardening properties[31] ;
- Good stability in hardening [31];
- Good resistance to tempering back[31] ;
- Good WEDM properties [31];
- Good machinability and grindability [31];
- Good surface treatment properties[31].

As it can be seen from the previous list, these characteristics make Sleipner an excellent steel for tooling application, as blanking, shearing, forming, coining, cold forging, cold extrusion, thread rolling, drawing, powder pressing [31].

## 7.2. Preparation of the samples

Regarding the samples, in the beginning a pre-machined rectangular bar of Sleipner of size  $10\text{mm} \times 60\text{mm} \times 1030\text{mm}$  has been got by Strecon. From this bar, thirteen samples have been obtained.

Once the samples have been cut, they have undergone a hardening process. After that, Strecon have sent them to the Mechanical Department of DTU, where they have been ground until a theoretical  $R_a$  of  $0.14\ \mu\text{m}$ , before of the polishing tests.

Therefore, the starting samples for the test have been thirteen samples of Uddeholm Sleipner which were cut from a whole rectangular bar of material and then hardened and ground until a theoretical roughness of  $0.14\ \mu\text{m}$ .

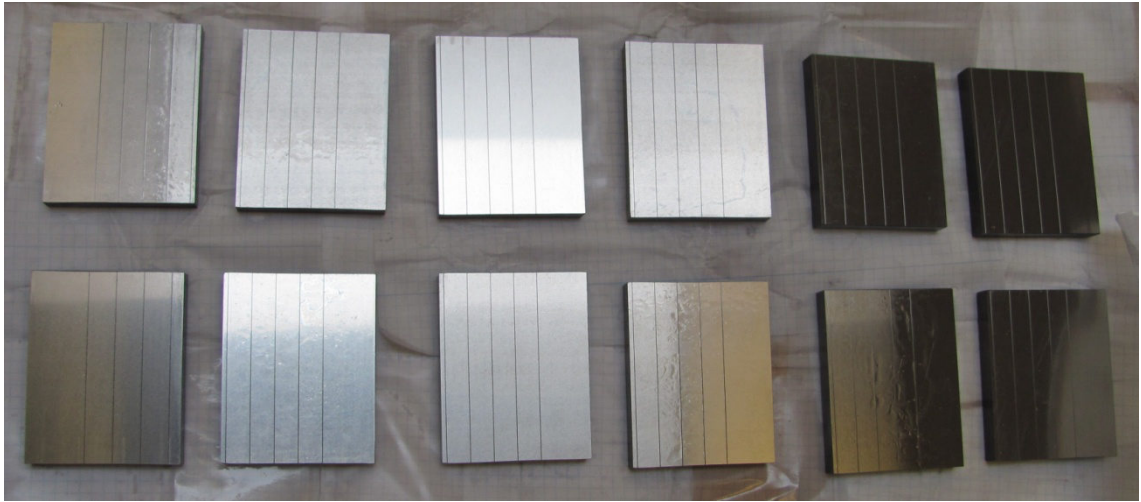


**FIGURE 7.2.** *Twelve of the thirteen samples employed for the experimental tests.*

### 7.3. Mechanical properties tables of the UDDEHOLM SLEIPNER

In the following tables the physical and mechanical properties of the Sleipner will be summarized:

<b>Temperature</b>	<b>20°C</b>	<b>200°C</b>	<b>400°C</b>
<b>Density [kg/m<sup>3</sup>]</b>	7730	7680	7620
<b>Modulus of elasticity [MPa]</b>	205000	190000	180000
<b>Coefficient of thermal expansion [after low temperature tempering (60 HRC) per °C from 20°C]</b>		$12.7 \times 10^{-6}$	
<b>Coefficient of thermal expansion [after high temperature tempering per °C from 20°C]</b>		$11.6 \times 10^{-6}$	$12.4 \times 10^{-6}$
<b>Thermal conductivity [W/m+°C]</b>		20	25
<b>Specific heat [J/kg C]</b>	460		

TABLE 7.2. Physical data. This table reports values for Sleipner 62 HRC [31].

<b>Tempering temperature</b>	<b>Hardening temperature</b>		
	<b>1870°F</b>	<b>1920°F</b>	<b>1960°F</b>
<b>1020°F</b>	58-60 HRC	59-61 HRC	61-63 HRC
<b>1070°F</b>	53-51 HRC	52-54 HRC	53-55 HRC

TABLE 7.3. Hardening and tempering recommended temperatures [31].

<b>Hardness HRC</b>	<b>Compressive Yield strength <math>R_{c0,2}</math> [MPa]</b>
50	1700
55	2050
60	2350
62	2500
64	2650

**TABLE 7.4.** Compressive strength [31].

# CHAPTER EIGHT

## Measurements of the samples before the experimental tests

### 8.1. Introduction

For understanding the variation of the roughness on the workpiece surface caused by the analyzed polishing process and for calculating the material removal induced by the interactions between pad, abrasive particles, and surface of the samples, it has been necessary to measure both the profile of each polishing area for each sample and the starting roughness surface on it. In other hands, it has been required to extrapolate more of twelve profiles for each sample (because the polishing surfaces are twelve for each specimen) and valuate the starting roughness surface for each one. Regarding the starting roughness, it has not been necessary to get more of twelve measurements in as many different zones of the sample, but only eight measurements have been adequate. This is because the samples have been grinding until an expected  $R_a$  of 0.14  $\mu\text{m}$  before running with the polishing process, and after this type of machining process the roughness surface conditions are more or less the same on the whole ground area of the part and less reference points are so required to estimate it.

### 8.2. Hommel Stylus Instrument T1000

For this reason, the first step of our experimental planning is to measure the samples resulting from the Grinding process. To do that, a profilometer present in the metrology lab has been employed. The name of this measurement instrument is “*Hommel Stylus Instrument T1000*” (figure 8.1a and 8.1b. See figure 8.2 for the technical specifications); it is a profilometer which uses a tip of diamond to measure the profile and the roughness surface of the analyzing part. The action of this measurement machine is simple. In fact, on the top of the Hommel there is a small automatic arm with a diamond tip in the end (called stylus) which goes in contact with the analyzing surface and with a horizontal movement it is able to extrapolate the shape of the surface, and therefore to memorize the profile of the surface and its roughness parameters. This device is simple, but not fast. Anyway it is very efficient and the final results is a graph with the profile of the surface and a report list with the most significant parameters for the waviness and for the roughness, as for example: the

arithmetical mean roughness ( $R_a$ ), the maximum peak ( $R_y$ ), the ten-point mean roughness ( $R_z$ ), maximum roughness depth ( $R_{max}$ ), the total height of the profile ( $R_t$ ), the root mean square average ( $R_q$ ), and other values that characterize the waviness and the roughness of the workpiece surface (they are listed in the table of *figure 8.2*).



**FIGURE 8.1a.** The Hommel Stylus T1000.

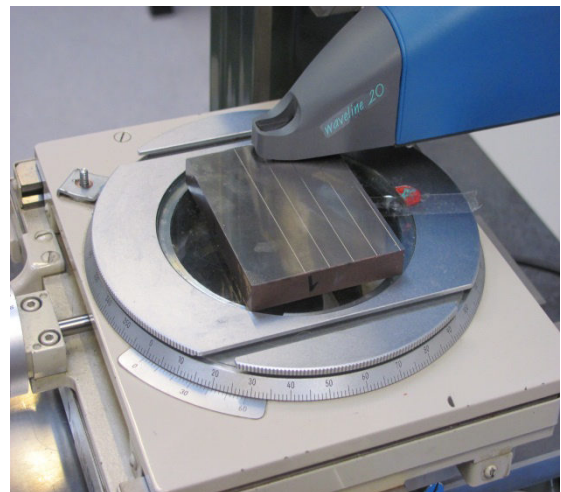
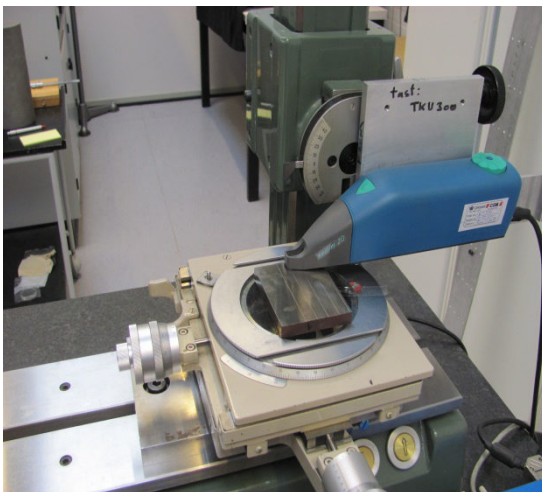


**FIGURE 8.1b.** Hommel Stylus during the measurements of the samples.

## HOMMEL TESTER T1000 – Technical specifications

HOMMEL TESTER T1000	basic	top	wave
Display	Rear-illuminated graphic display 240 x 160 dots		
Power source	Ni-Metallhydrid-Battery, Rechargeable 24V/2.5 A, automatic select 90-240 V		
Battery capacity	approx. 500 measurements		
Operating temperature	0-50°C, max. 85% relative humidity		
Interfaces	V24, RS232		
Data storage	200 profiles, 999 measurements		
Measurement programmes	5 measurement programmes		
PCMCIA drive	-	integrated	Optional
Compact Flash Memory Card	-	integrated (32 MB)	Optional (32 MB)
Dimensions W x D x H	253 x 193 x 80 mm		
Weight	1,600 g		
Measurement type	Skid measurement		Skid/skidless measurement
Total deviation as per DIN 4772	Class 1		
Measurement ranges/resolution	+/- 80 µm / 0.01 µm; +/- 320 µm / 0.04 µm		
Instrument set-up	automatic or manual		
Filter	Gauss (M1) digital filter (mm): 0.025 / 0.08 / 0.25 / 0.8 / 2.5 / 8 – selectable in 1 Cut-off stages		
ISO 11562, Part 1 (50% Gauss)	M2 (Rk parameter)		
ISO 13565-1	Polynomfit		
Traverse length lt (mm)	0.48 / 1.5 / 4.8 / 15; max. 16		0.48 / 1.5 / 4.8 / 15; max. 20
ISO 4288/1 2085 (Motif)	variable 0.48 – 16 mm		variable 0.05 – 20 mm
Sampling length ln ISO 4287	1.25 / 4.0 / 12.5		
Individual traverse length lr, lw, lp ISO 4287	1 – 5 selectable		
Traverse speed (mm/s)	0.15 / 0.5 / 1.0		0.1 / 0.15 / 0.5 / 1.0; variable 0.05 – 3.0
Cut-off λ (mm)	0.08 / 0.25 / 0.8 / 2.5 / 8.0		
Bandpass filter Lc/Ls ISO 3274	100; 300		
Roughness parameters ISO 4287	Ra, Rz, Rmax, Rt, Rq, Rp, RSm, RMr(c), Rp, Rv, Rpm, Rz, Rz-ISO, Rsk, Rku, R&ccaron;, Rmr%, Rmrµm; Rdq		
Core roughness parameters ISO 13565	Rk, Rpk, Rvk, Mr1, Mr2, Rpk*, Rvk*, Vo		
Waviness parameters ISO 4287			Wa, Wz, Wmax, Wt, Wpc, Wsm, Wq, Wp, Wv, Wpm, Wsk, Wku, Wdq
Profile parameters ISO 4287	Pa, Pz, Pmax, Pt, Ppc, Psm, Pmr(c), Pp, Pv, Ppm, Psk, Pku, Pq, P&ccaron;, Pmr%, Pmrµm, Pdq		
Motif parameters ISO 4287	R, Rx, AR, P&ccaron; (CR, CL, CF), Nr, Nw		W, Wx, Wte, AW
Roughness parameters JIS B0601	Rz-JIS		
Statistic	999 measurements: Range, Xcross, Max., Min., Standard deviation		
Languages	German, English, French, Spanish, Italian, Czech, Polish, Swedish		
Measuring system	µm / pinch selectable		
Tolerance limits upper/lower	adjustable for all parameters		
<b>Integrated printer</b>			
Vertical magnification	automatic up til max. 50,000-fold		
Horizontal magnification	10 / 20 / 40 / 50 / 100 / 200 / 400-fold traverse assigned		
Paper	Thermal paper 40-50 g/m <sup>2</sup> - 57.5 mm width, length 10 m		
Printing speed	30 mm/s		
Resolution	8 dots/mm		
<b>Traverse unit</b>			
	<b>LV16</b>	<b>waveline™ 20</b>	
Types of pick-up	Skid pick-up	Skidless pick-up	
Traverse length	16 mm	20 mm	
Pick-up direction	axial, perpendicular to axis traversing	axial	
Dimensions L x W x H	134 x 45 x 47 mm	242 x 54 x 74 mm	
Weight	250 g	1,100 g	
Working area	over 360°		
Operating controls	integrated start key		
<b>Surface pick-up</b>			
	<b>T1E</b>	<b>TKL 300L</b>	
Measuring range	80 µm	600 µm	
Diamond stylus tip	5 µm; 90°	5 µm; 90° large diamond	
Skid radius	lengthways 30 mm / transversal 1,9 mm	-	
For holes from	4 mm / depth 20 mm	4 mm / depth 33 mm	
Dimensions D/L	D 10 mm / L 80 mm	D 13 mm / 85,1 mm	
Weight	12 g	15 g	

FIGURE 8.2. Technical specifications [32].



The operating principle of this instrument machine is simple, it analyzes the roughness of the part for a predefined length (called evaluation length) that can be of 1.5 or 4.8 or 15 or 20 mm(ISO standard lengths). From this length, it takes five reference lengths and from these it compute the  $R_a$  and the other roughness and waviness parameters for each one. Then, when the  $R_{a1}, R_{a2}, R_{a3}, R_{a4},$  and  $R_{a5}$  have been calculated, the overall  $R_a$  of the surface is evaluated taking the average of the previous values. That is as:

$$R_a = \frac{R_{a1} + R_{a2} + R_{a3} + R_{a4} + R_{a5}}{5}$$

**FORMULA 8.1.**

Moreover, to analyze the results, the program employed by Hommel (SURSAM) can use two different filters. This is because some noise factors could affect the roughness measurements prejudicing the result with wrong data. These filters are two and they are:

- A filter for the roughness value called “short cut-off”. This filter checks the roughness values and cuts off from them those data smaller than 2.5  $\mu\text{m}$ . This is because the diamond tip has a radius of 2  $\mu\text{m}$  and it is not capable to measure lower values from a surface profile.
- The other one is for the waviness called “long cut-off”. If the shape of the profile is the purpose of the measurement, the waviness can disturb this measurement. For this reason it can be obscured by using this filter.

Regarding our measurements, the chosen filtering parameters have been:

- A LS-line for the form removal;
- 2.5  $\mu\text{m}$  for the short cut-off filter;
- 0.8 mm for the long cut-off filter;

- 4.8 mm of evaluation length for estimating the roughness;
- 15 mm of evaluation length for measuring the surface profiles.

A short cut-off filter of 2.5  $\mu\text{m}$  has been chosen because a protection against the mechanical noise resulting from the Hommel is required, whereas a long cut-off filter of 0.8 mm has been chosen because this is the classical considered value by the metrological laboratory of DTU for historical reasons. Regarding the evaluation lengths, two different lengths are required: a longer one of 15 mm, because the whole surface including the two grooves has to be included in the profile for the MRR evaluation. A shorter length than 4.8 mm is possible to choose for the roughness consideration, but this would be too short for a good representation of the surface conditions of the analyzed sample.

Anyway, this measurement instrument has two main disadvantages:

- The first one is that the diamond tip has a radius of two micron-meters. This means that it is not capable to touch the end of each valley present in the roughness profile of the surface. In fact, for valley too deep and tight it cannot completely go down following the real profile. This is shown in the figure below (*figure 8.3*):

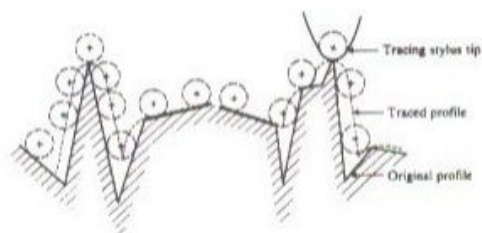


**FIGURE 8.3.** The tip of the stylus is not capable to follow completely the real profile of the surface [18].

- The second one is that the tip has an angle of ninety degrees. So it is not capable to follow perfectly the shape of the wall when a change

in the height of the profile is present (*figure 8.4* below):

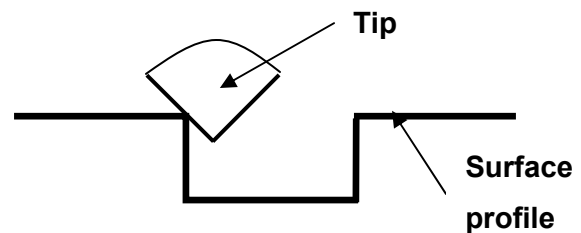


**FIGURE 8.4.** The tip of the stylus has problem to follow vertical walls as those in the figure.

### 8.3. Measurement operation

After this brief introduction of the operating principle of the employed measurement instrument, the measurement planning can be exposed.

The polishing samples have been thirteen: twelve related to the DOE analysis (the eight samples for the full factorial analysis plus the central point plus the three additional samples), and one correlated with the analysis of the overlap. For all the samples anyway, the measurements of the profiles required to compute the amount of material removal have been done.

Now, it has been important to take some reference points in the sample's surface that permitted us to characterize the roughness surface of the samples (before and after the polishing process) and to compare the profiles in the two different periods (before polishing and after polishing) for detecting the occurred material removal. Regarding this last purpose, three reference points has been identified for each polishing surface for a overall number of thirty-six reference points for each sample.

Indeed, for the special sample where the overlap effect is analyzed the reference points are not thirty-six but eighteen. They are always kept three for each polishing surface, but here the analyzing areas are not twelve but six. Anyway, now the process methodology will be exposed.

The drawings of the sample are illustrated below and the reference points for the profiles are represented (*figure 8.5, 8.6, and 8.7*). As it can see, the drawings are three, the first one (*figure 8.5*) represents the eleven sample with similar sizes; the second

one (figure 8.6) represents the sample required for the evaluation of the overlap; whereas the third one is the sample employed to evaluate the central point (figure 8.7). For this sample, the polished area had to be shorter compared to those in the other twelve samples, because in this case the overall size of the rectangular specimen were smaller. Consequently, the reference points required for the measurements have been situated in different positions.

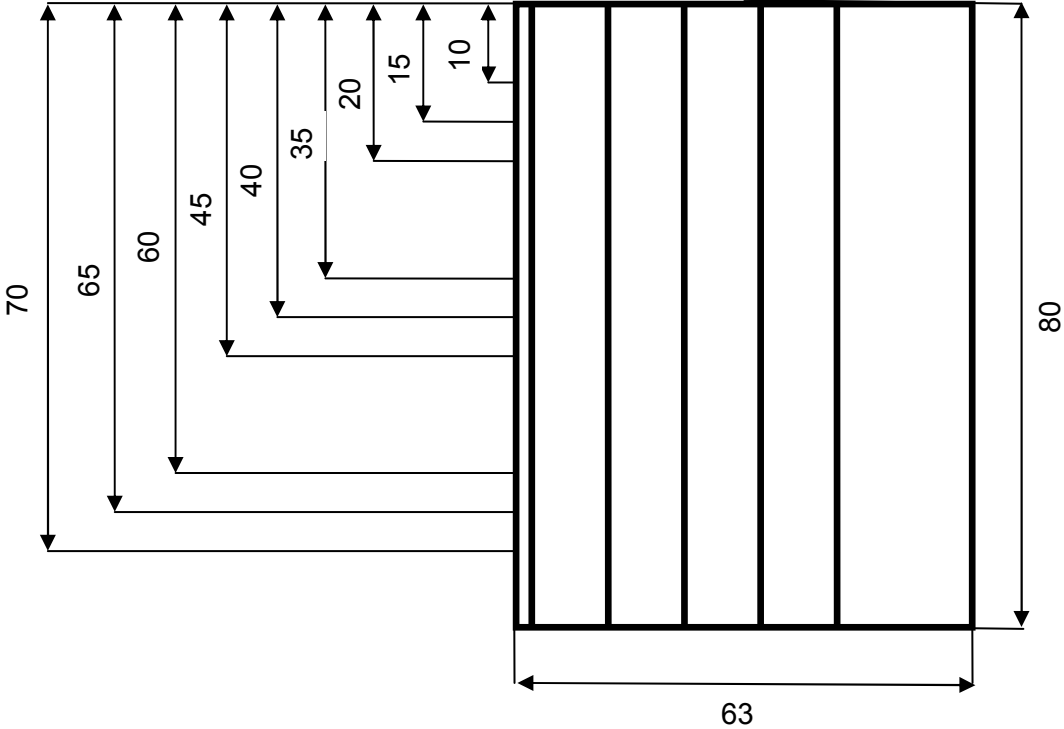


**FIGURE 8.5.** Required sample for the full factorial design plus the three additional tests.

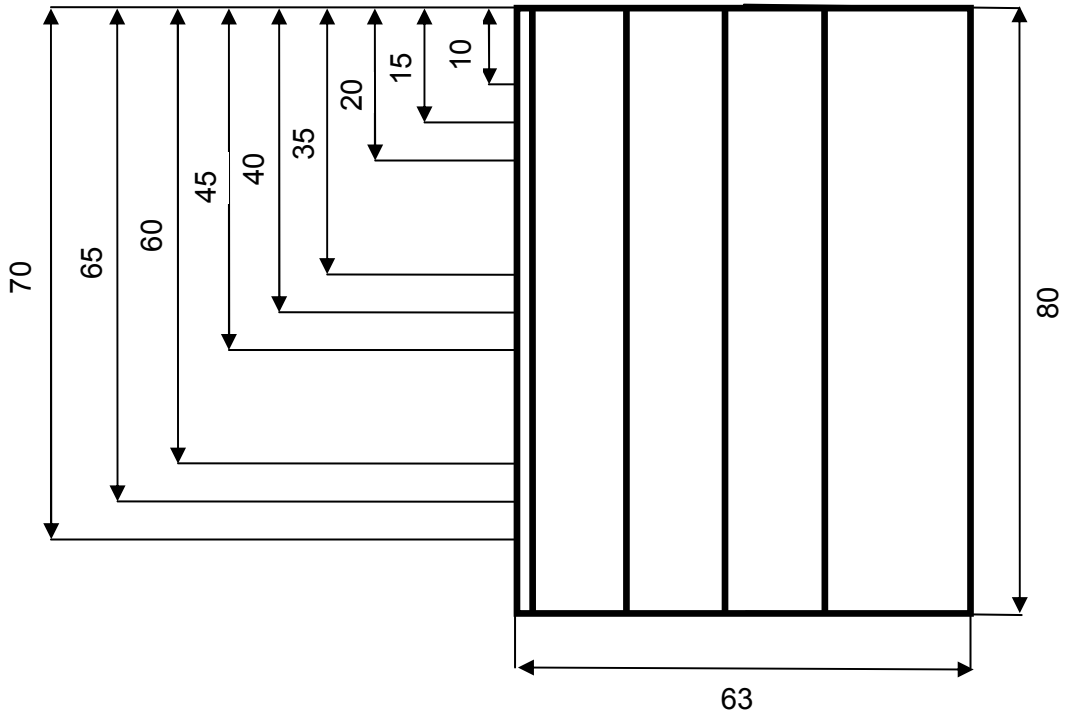


**FIGURE 8.6.** Required sample for overlapping test.

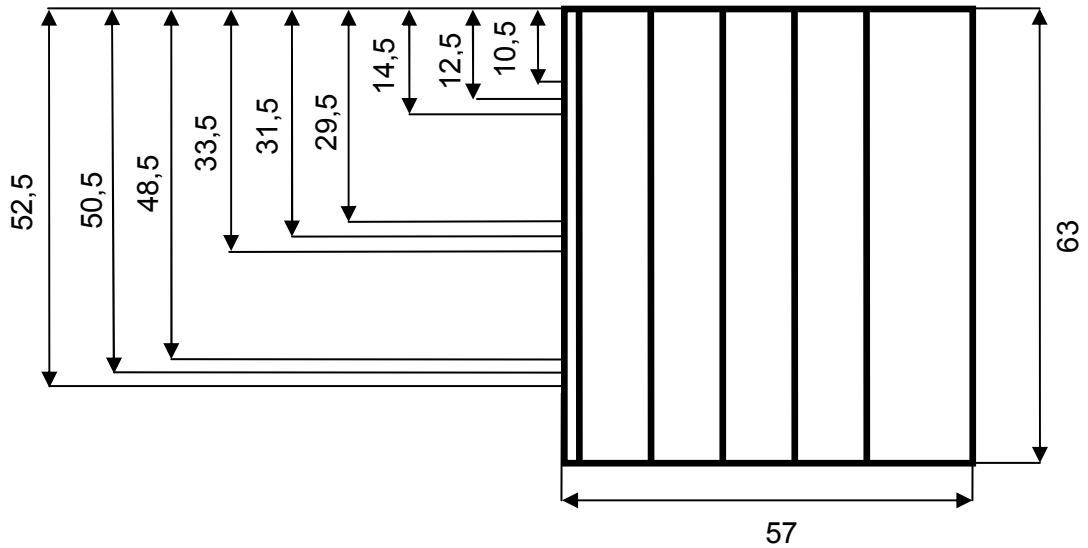


**FIGURE 8.7.** Required sample for the central point.

Firstly, the eleven samples with size  $80\text{ mm} \times 60\text{ mm}$  have been measured. The reference points, shown in *figure 8.5*, have been identified in those illustrated positions

because for each polishing surface the central point and two points moving five millimeters up and down from it have been chosen. These three measurements have been required to have a good evaluation of the polishing surface profile before the polishing process.

The same previous considerations have been done for the sample in *figure 8.6*.

Regarding the sample in *figure 8.7*, where the effect of the central point has been analyzed, the position for the measurements have been different, as it was previously said. For this sample, in fact, the reference points have been identified taking the central points for each polishing surface as well as for the other two kinds of samples, but the other two points have been chosen moving two millimeters up and down from the central point.

As said previously, the done measurements have two purpose:

- To memorize the starting profiles of the polishing surfaces, so it will be possible to compare them with the profiles of the machined surfaces for abstracting the material removal caused by the process;
- To measure the starting roughness of the samples for understanding how it varies with the variations of the input parameters and of the time.

Regarding the first aim, the measurements have been realized memorizing the profile in orthogonal way respect to the length of the samples, including in the measurements the two grooves which are close to the polishing surface itself. To clarify this important point of view, an image is presented below (*figure 8.8*):

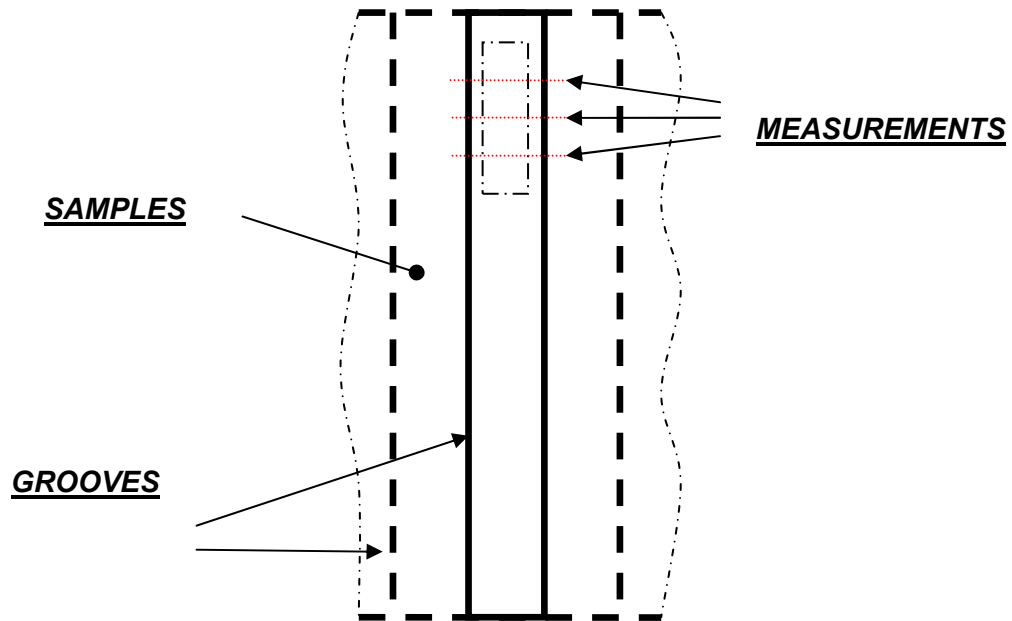


**FIGURE 8.8.** Example of measurements.

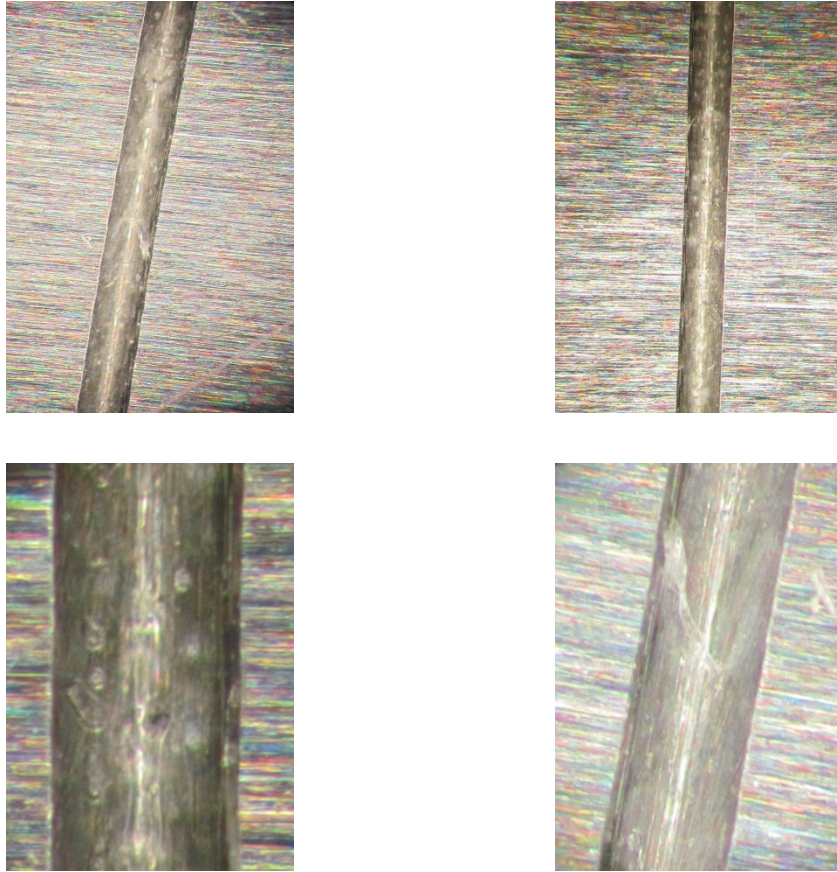


**FIGURE 8.9.** Pictures of grooves observed by microscope.

The grooves in the measurements are important. In fact, they are necessary because they permit us to take some reference point to align and compare the two different profile corresponding at the same position, detected before and after the polishing process. In other hand, we need these points to align the two different profiles measured in the same position and see how much material removal the RAP machine has caused.

Regarding the second aim, six measurements for the characterization of the roughness surface of the sample have been made. This is because, as it was exposed previously, the starting surface has undergone a Grinding process and, after that, the  $R_a$  value is more or less the same for all the machined part and less values are required to find out the beginning value. The measurements have been carried out along the same direction of the grooves. This because the sample were ground in the orthogonal direction of the grooves, that is, along the same direction followed to made the profile measurements. This means that the initial roughness was lower in this direction, whereas higher in the other one parallel to the grooves.



#### 8.4. Results of the measurements

The results from these measurements are the following:

<b>SAMPLE 0</b>							
	<i>Ra</i>	<i>Rz</i>	<i>Rzmax</i>	<i>RSm</i>	<i>Rv</i>	<i>Rp</i>	<i>Pa</i>
<b>Colm1up</b>	0.046	0.460	0.670	27.917	0.322	0.138	0.066
<b>Colm2up</b>	0.043	0.422	0.610	23.196	0.294	0.128	0.076
<b>Colm3up</b>	0.040	0.364	0.410	24.627	0.230	0.134	0.074
<b>Colm4up</b>	0.039	0.402	0.500	25.695	0.276	0.126	0.058
<b>Colm1down</b>	0.046	0.522	0.780	29.637	0.372	0.150	0.081
<b>Colm2down</b>	0.045	0.448	0.570	26.010	0.252	0.196	0.085
<b>Colm3down</b>	0.045	0.410	0.470	24.481	0.274	0.136	0.070
<b>Colm4down</b>	0.052	0.566	0.980	32.525	0.338	0.228	0.112
<b>average</b>	<b>0.045</b>	<b>0.449</b>	<b>0.624</b>	<b>26.761</b>	<b>0.295</b>	<b>0.154</b>	<b>0.078</b>
<b>std</b>	0.004	0.066	0.186	3.094	0.047	0.037	0.016
<b>std%</b>	8.8	14.8	29.8	11.6	15.9	24.1	20.8

TABLE 8.1.Data from SURSAM.

<b>SAMPLE 1</b>							
	<i>Ra</i>	<i>Rz</i>	<i>Rzmax</i>	<i>RSm</i>	<i>Rv</i>	<i>Rp</i>	<i>Pa</i>
<b>Colm1up</b>	0.031	0.332	0.450	21.824	0.228	0.104	0.088
<b>Colm2up</b>	0.034	0.356	0.480	24.422	0.234	0.122	0.065
<b>Colm3up</b>	0.034	0.318	0.380	22.888	0.212	0.106	0.074
<b>Colm4up</b>	0.036	0.402	0.580	25.226	0.290	0.112	0.076
<b>Colm1down</b>	0.037	0.406	0.590	23.378	0.294	0.112	0.061
<b>Colm2down</b>	0.035	0.402	0.640	32.233	0.290	0.112	0.088
<b>Colm3down</b>	0.036	0.394	0.530	22.741	0.278	0.116	0.059
<b>Colm4down</b>	0.037	0.418	0.630	29.172	0.242	0.176	0.069
<b>average</b>	<b>0.035</b>	<b>0.379</b>	<b>0.535</b>	<b>25.236</b>	<b>0.259</b>	<b>0.120</b>	<b>0.072</b>
<b>std</b>	0.002	0.038	0.092	3.624	0.033	0.023	0.011
<b>std%</b>	5.5	10.0	17.2	14.4	12.7	19.4	15.3

TABLE 8.2. Data from SURSAM.

<b>SAMPLE 2</b>							
	<i>Ra</i>	<i>Rz</i>	<i>Rzmax</i>	<i>RSm</i>	<i>Rv</i>	<i>Rp</i>	<i>Pa</i>
<b>Colm1up</b>	0.088	0.972	1.260	23.978	0.598	0.374	0.104
<b>Colm2up</b>	0.078	1.122	1.790	35.139	0.876	0.246	0.098
<b>Colm3up</b>	0.110	1.436	2.560	37.510	1.056	0.380	0.163
<b>Colm4up</b>	0.081	1.076	1.970	34.577	0.732	0.344	0.102
<b>Colm1down</b>	0.071	0.746	0.980	24.637	0.518	0.228	0.099
<b>Colm2down</b>	0.073	0.764	0.940	24.701	0.524	0.240	0.098
<b>Colm3down</b>	0.071	0.782	1.380	29.542	0.562	0.220	0.088
<b>Colm4down</b>	0.067	0.958	1.340	29.218	0.698	0.260	0.079
<b>average</b>	<b>0.080</b>	<b>0.982</b>	<b>1.527</b>	<b>29.913</b>	<b>0.696</b>	<b>0.286</b>	<b>0.104</b>
<b>std</b>	0.014	0.233	0.548	5.313	0.190	0.068	0.025
<b>std%</b>	17.4	23.7	35.9	17.8	27.3	23.6	24.2

TABLE 8.3. Data from SURSAM.

<b>SAMPLE 3</b>							
	<i>Ra</i>	<i>Rz</i>	<i>Rzmax</i>	<i>RSm</i>	<i>Rv</i>	<i>Rp</i>	<i>Pa</i>
<b>Colm1up</b>	0.085	0.934	1.160	24.516	0.652	0.282	0.112
<b>Colm2up</b>	0.083	0.962	1.370	26.527	0.702	0.260	0.097
<b>Colm3up</b>	0.100	1.248	1.790	29.538	0.854	0.394	0.117
<b>Colm4up</b>	0.101	1.248	1.640	31.724	0.876	0.372	0.121
<b>Colm1down</b>	0.078	1.036	1.490	26.601	0.714	0.322	0.098
<b>Colm2down</b>	0.074	0.854	1.110	23.798	0.586	0.268	0.119
<b>Colm3down</b>	0.076	0.896	1.150	25.007	0.574	0.322	0.106
<b>Colm4down</b>	0.100	1.186	2.280	41.462	0.932	0.254	0.126
<b>average</b>	<b>0.087</b>	<b>1.046</b>	<b>1.499</b>	<b>28.647</b>	<b>0.736</b>	<b>0.309</b>	<b>0.112</b>
<b>std</b>	0.012	0.160	0.400	5.819	0.136	0.053	0.011
<b>std%</b>	13.2	15.3	26.7	20.3	18.5	17.0	9.5

TABLE 8.4.Data from SURSAM.

<b>SAMPLE 4</b>							
	<i>Ra</i>	<i>Rz</i>	<i>Rzmax</i>	<i>RSm</i>	<i>Rv</i>	<i>Rp</i>	<i>Pa</i>
<b>Colm1up</b>	0.178	1.620	2.140	32.342	1.204	0.416	0.202
<b>Colm2up</b>	0.173	1.594	2.130	36.055	1.184	0.410	0.214
<b>Colm3up</b>	0.215	1.810	2.480	29.132	1.328	0.482	0.245
<b>Colm4up</b>	0.202	1.594	1.850	28.598	1.148	0.446	0.233
<b>Colm1down</b>	0.162	1.410	1.970	34.730	1.024	0.386	0.195
<b>Colm2down</b>	0.190	1.760	2.040	32.987	1.322	0.438	0.216
<b>Colm3down</b>	0.210	1.982	2.200	33.912	1.476	0.506	0.237
<b>Colm4down</b>	0.210	1.758	1.960	35.428	1.294	0.464	0.233
<b>average</b>	<b>0.192</b>	<b>1.691</b>	<b>2.096</b>	<b>32.898</b>	<b>1.248</b>	<b>0.444</b>	<b>0.222</b>
<b>std</b>	0.020	0.174	0.192	2.771	0.137	0.040	0.018
<b>std%</b>	10.3	10.3	9.2	8.4	11.0	9.0	8.1

TABLE 8.5.Data from SURSAM.

<b>SAMPLE 5</b>							
	<i>Ra</i>	<i>Rz</i>	<i>Rzmax</i>	<i>RSm</i>	<i>Rv</i>	<i>Rp</i>	<i>Pa</i>
<b>Colm1up</b>	0.189	1.642	2.080	31.656	1.138	0.504	0.227
<b>Colm2up</b>	0.198	2.246	3.690	47.790	1.702	0.544	0.244
<b>Colm3up</b>	0.196	1.912	2.710	35.486	1.390	0.522	0.233
<b>Colm4up</b>	0.190	1.694	2.180	30.589	1.264	0.430	0.207
<b>Colm1down</b>	0.170	1.640	2.160	32.079	1.196	0.444	0.195
<b>Colm2down</b>	0.189	1.996	3.290	45.726	1.452	0.544	0.226
<b>Colm3down</b>	0.202	2.040	2.460	30.736	1.534	0.506	0.226
<b>Colm4down</b>	0.210	1.844	3.390	38.320	1.316	0.528	0.230
<b>average</b>	<b>0.193</b>	<b>1.877</b>	<b>2.745</b>	<b>36.548</b>	<b>1.374</b>	<b>0.503</b>	<b>0.224</b>
<b>std</b>	0.012	0.215	0.632	6.846	0.186	0.043	0.015
<b>std%</b>	6.1	11.5	23.0	18.7	13.5	8.6	6.8

TABLE 8.6.Data from SURSAM.

<b>SAMPLE 6</b>							
	<i>Ra</i>	<i>Rz</i>	<i>Rzmax</i>	<i>RSm</i>	<i>Rv</i>	<i>Rp</i>	<i>Pa</i>
<b>Colm1up</b>	0.041	0.390	0.510	21.669	0.274	0.116	0.066
<b>Colm2up</b>	0.043	0.398	0.540	23.262	0.276	0.122	0.070
<b>Colm3up</b>	0.043	0.442	0.530	24.040	0.320	0.122	0.069
<b>Colm4up</b>	0.041	0.378	0.420	24.273	0.260	0.118	0.057
<b>Colm1down</b>	0.045	0.418	0.570	22.247	0.292	0.126	0.062
<b>Colm2down</b>	0.043	0.418	0.570	25.908	0.282	0.136	0.070
<b>Colm3down</b>	0.055	0.522	0.760	24.955	0.370	0.152	0.074
<b>Colm4down</b>	0.053	0.450	0.480	24.148	0.286	0.164	0.071
<b>average</b>	<b>0.045</b>	<b>0.427</b>	<b>0.548</b>	<b>23.813</b>	<b>0.295</b>	<b>0.132</b>	<b>0.068</b>
<b>std</b>	0.006	0.046	0.099	1.385	0.035	0.017	0.005
<b>std%</b>	12.1	10.7	18.1	5.8	11.8	13.2	8.1

TABLE 8.7.Data from SURSAM.

<b>SAMPLE 7</b>							
	<i>Ra</i>	<i>Rz</i>	<i>Rzmax</i>	<i>RSm</i>	<i>Rv</i>	<i>Rp</i>	<i>Pa</i>
<b>Colm1up</b>	0.141	1.342	1.570	27.208	0.984	0.358	0.167
<b>Colm2up</b>	0.171	1.622	1.860	30.898	1.222	0.400	0.196
<b>Colm3up</b>	0.150	1.652	2.750	30.286	1.276	0.376	0.189
<b>Colm4up</b>	0.155	1.512	2.430	31.686	1.122	0.390	0.185
<b>Colm1down</b>	0.156	1.540	1.770	28.376	1.110	0.430	0.185
<b>Colm2down</b>	0.188	1.726	2.070	32.316	1.306	0.420	0.211
<b>Colm3down</b>	0.175	1.646	1.940	29.041	1.260	0.386	0.199
<b>Colm4down</b>	0.178	1.922	2.290	35.634	1.480	0.442	0.204
<b>average</b>	<b>0.164</b>	<b>1.620</b>	<b>2.085</b>	<b>30.680</b>	<b>1.220</b>	<b>0.400</b>	<b>0.192</b>
<b>std</b>	0.016	0.169	0.385	2.632	0.150	0.029	0.013
<b>std%</b>	9.7	10.4	18.5	8.6	12.3	7.1	7.0

TABLE 8.8.Data from SURSAM.

<b>SAMPLE 8</b>							
	<i>Ra</i>	<i>Rz</i>	<i>Rzmax</i>	<i>RSm</i>	<i>Rv</i>	<i>Rp</i>	<i>Pa</i>
<b>Colm1up</b>	0.041	0.398	0.500	25.173	0.258	0.140	0.067
<b>Colm2up</b>	0.054	0.510	0.600	26.891	0.356	0.154	0.079
<b>Colm3up</b>	0.039	0.416	0.590	27.824	0.266	0.150	0.068
<b>Colm4up</b>	0.038	0.414	0.450	21.478	0.300	0.114	0.061
<b>Colm1down</b>	0.041	0.370	0.410	22.743	0.238	0.132	0.058
<b>Colm2down</b>	0.043	0.386	0.460	22.324	0.266	0.120	0.060
<b>Colm3down</b>	0.040	0.366	0.570	22.721	0.250	0.116	0.070
<b>Colm4down</b>	0.037	0.362	0.620	22.645	0.242	0.120	0.067
<b>average</b>	<b>0.042</b>	<b>0.403</b>	<b>0.525</b>	<b>23.975</b>	<b>0.272</b>	<b>0.131</b>	<b>0.066</b>
<b>std</b>	0.005	0.048	0.080	2.347	0.039	0.016	0.006
<b>std%</b>	12.8	11.9	15.2	9.8	14.3	12.0	9.8

TABLE 8.9.Data from SURSAM.

<b>SAMPLE 9</b>							
	<i>Ra</i>	<i>Rz</i>	<i>Rzmax</i>	<i>RSm</i>	<i>Rv</i>	<i>Rp</i>	<i>Pa</i>
<b>Colm1up</b>	0.049	0.532	0.720	20.650	0.372	0.160	0.066
<b>Colm2up</b>	0.054	0.496	0.630	20.713	0.324	0.172	0.091
<b>Colm3up</b>	0.057	0.548	0.880	21.864	0.398	0.150	0.094
<b>Colm4up</b>	0.054	0.600	0.800	22.223	0.442	0.158	0.067
<b>Colm1down</b>	0.048	0.446	0.500	20.228	0.300	0.146	0.069
<b>Colm2down</b>	0.057	0.552	0.640	23.235	0.384	0.168	0.092
<b>Colm3down</b>	0.058	0.640	0.990	27.482	0.368	0.272	0.086
<b>Colm4down</b>	0.060	0.626	0.720	21.969	0.462	0.164	0.079
<b>average</b>	<b>0.054</b>	<b>0.555</b>	<b>0.735</b>	<b>22.296</b>	<b>0.381</b>	<b>0.174</b>	<b>0.081</b>
<b>std</b>	0.004	0.066	0.154	2.317	0.054	0.041	0.012
<b>std%</b>	7.4	11.8	21.0	10.4	14.2	23.4	14.7

TABLE 8.10.Data from SURSAM.

<b>SAMPLE 10</b>							
	<i>Ra</i>	<i>Rz</i>	<i>Rzmax</i>	<i>RSm</i>	<i>Rv</i>	<i>Rp</i>	<i>Pa</i>
<b>Colm1up</b>	0.066	0.654	0.910	25.586	0.474	0.180	0.109
<b>Colm2up</b>	0.061	0.572	0.700	24.171	0.378	0.194	0.084
<b>Colm3up</b>	0.054	0.522	0.580	21.503	0.378	0.144	0.073
<b>Colm4up</b>	0.054	0.650	0.720	22.474	0.490	0.160	0.080
<b>Colm1down</b>	0.052	0.556	0.770	22.854	0.402	0.154	0.078
<b>Colm2down</b>	0.060	0.620	0.850	24.081	0.446	0.174	0.081
<b>Colm3down</b>	0.054	0.568	0.720	22.765	0.410	0.158	0.075
<b>Colm4down</b>	0.050	0.562	0.790	21.577	0.402	0.160	0.069
<b>average</b>	<b>0.056</b>	<b>0.588</b>	<b>0.755</b>	<b>23.126</b>	<b>0.423</b>	<b>0.165</b>	<b>0.081</b>
<b>std</b>	0.005	0.048	0.100	1.400	0.043	0.016	0.012
<b>std%</b>	9.4	8.1	13.3	6.1	10.1	9.7	14.9

TABLE 8.11.Data from SURSAM.

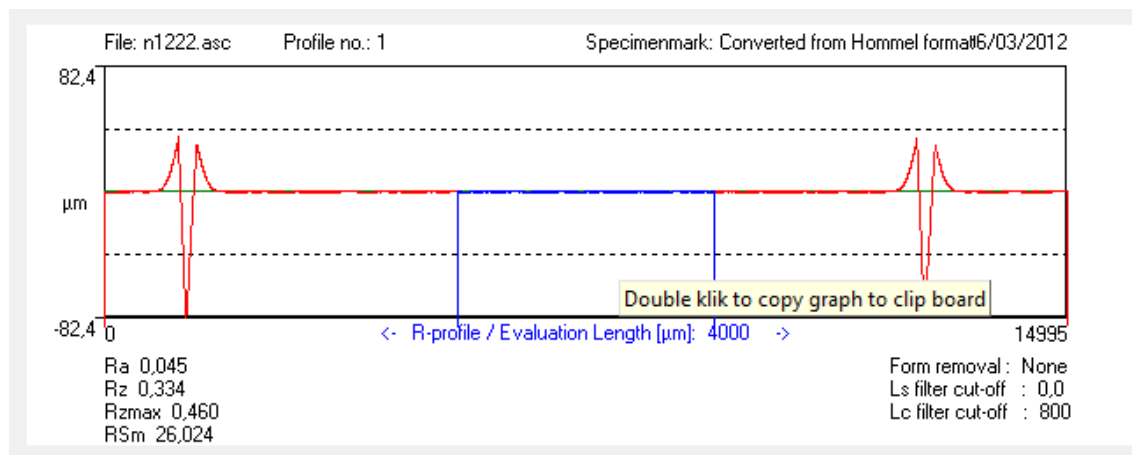
<b>SAMPLE 11</b>							
	<i>Ra</i>	<i>Rz</i>	<i>Rzmax</i>	<i>RSm</i>	<i>Rv</i>	<i>Rp</i>	<i>Pa</i>
<b>Colm1up</b>	0.049	0.522	0.640	23.576	0.384	0.138	0.090
<b>Colm2up</b>	0.048	0.442	0.640	22.381	0.302	0.140	0.065
<b>Colm3up</b>	0.057	0.630	0.790	23.402	0.492	0.138	0.082
<b>Colm4up</b>	0.059	0.664	0.870	23.868	0.492	0.172	0.087
<b>Colm1down</b>	0.053	0.570	0.680	21.765	0.410	0.160	0.077
<b>Colm2down</b>	0.052	0.510	0.590	21.707	0.334	0.176	0.083
<b>Colm3down</b>	0.060	0.650	0.890	24.780	0.478	0.172	0.077
<b>Colm4down</b>	0.063	0.678	0.930	24.572	0.520	0,158	0.108
<b>average</b>	<b>0.055</b>	<b>0.583</b>	<b>0.754</b>	<b>23.256</b>	<b>0.427</b>	<b>0.157</b>	<b>0.084</b>
<b>std</b>	0.005	0.086	0.132	1.192	0.081	0.016	0.013
<b>std%</b>	9.9	14.7	17.6	5.1	19.0	10.3	15.1

TABLE 8.12.Data from SURSAM.

<b>SAMPLE 12</b>							
	<i>Ra</i>	<i>Rz</i>	<i>Rzmax</i>	<i>RSm</i>	<i>Rv</i>	<i>Rp</i>	<i>Pa</i>
<b>Colm1up</b>	0.044	0.472	0.580	22.637	0.344	0.128	0.056
<b>Colm2up</b>	0.041	0.432	0.530	23.380	0.312	0.120	0.059
<b>Colm3up</b>	0.041	0.546	0.660	24.946	0.430	0.116	0.060
<b>Colm4up</b>	0.039	0.394	0.490	22.568	0.284	0.110	0.075
<b>Colm1down</b>	0.039	0.424	0.510	23.494	0.292	0.132	0.071
<b>Colm2down</b>	0.039	0.386	0.540	22.712	0.272	0.114	0.068
<b>Colm3down</b>	0.044	0.438	0.480	23.836	0.298	0.140	0.065
<b>Colm4down</b>	0.043	0.650	1.130	45.772	0.264	0.386	0.071
<b>average</b>	<b>0.041</b>	<b>0.468</b>	<b>0.615</b>	<b>26.168</b>	<b>0.312</b>	<b>0.156</b>	<b>0.066</b>
<b>std</b>	0.002	0.089	0.216	7.960	0.054	0.094	0.007
<b>std%</b>	5.1	19.0	35.1	30.4	17.2	60.1	10.2

TABLE 8.13.Data from SURSAM.

Whereas an example of profile is:



**FIGURE 8.10.** An example of profile measured by Hommel Stylus and displayed by SURSAM software.



# CHAPTER NINE

## Robot Assisted Polishing machine (RAP)

### 9.1. Introduction

The terminology R.A.P. means “*Robot Assisted Polishing*” and it is the name of the polishing machine employed during the experimental tests in STRECON. The whole name is “*STRECON® RAP-225 MACHINE*” (*figure 9.1*) and it is a new, alternative and flexible polishing machine tool solution that provides a qualitative and cost-effective polishing process [33].



**FIGURE 9.1.** STRECON® RAP-225 MACHINE [33].

RAP is a robot arm polishing machine and its flexibility is given by its particular movement system with 6 axis (*figure 9.2*) and by its open structure. This particular geometry permits to polish different kind of parts with different shapes as:

- Parts with 2D round and rotation-symmetric geometries (as for example inner diameter, outer diameter, tubes, sleeves, end surfaces of punches) [30];

- Parts with 3D simplified geometries (as for example dies, mono-blocks, bearing sleeve) [30];
- Flat part surfaces [30].

The rotational axis structure is shown in the picture below and it represents the movement system which RAP is capable to do:

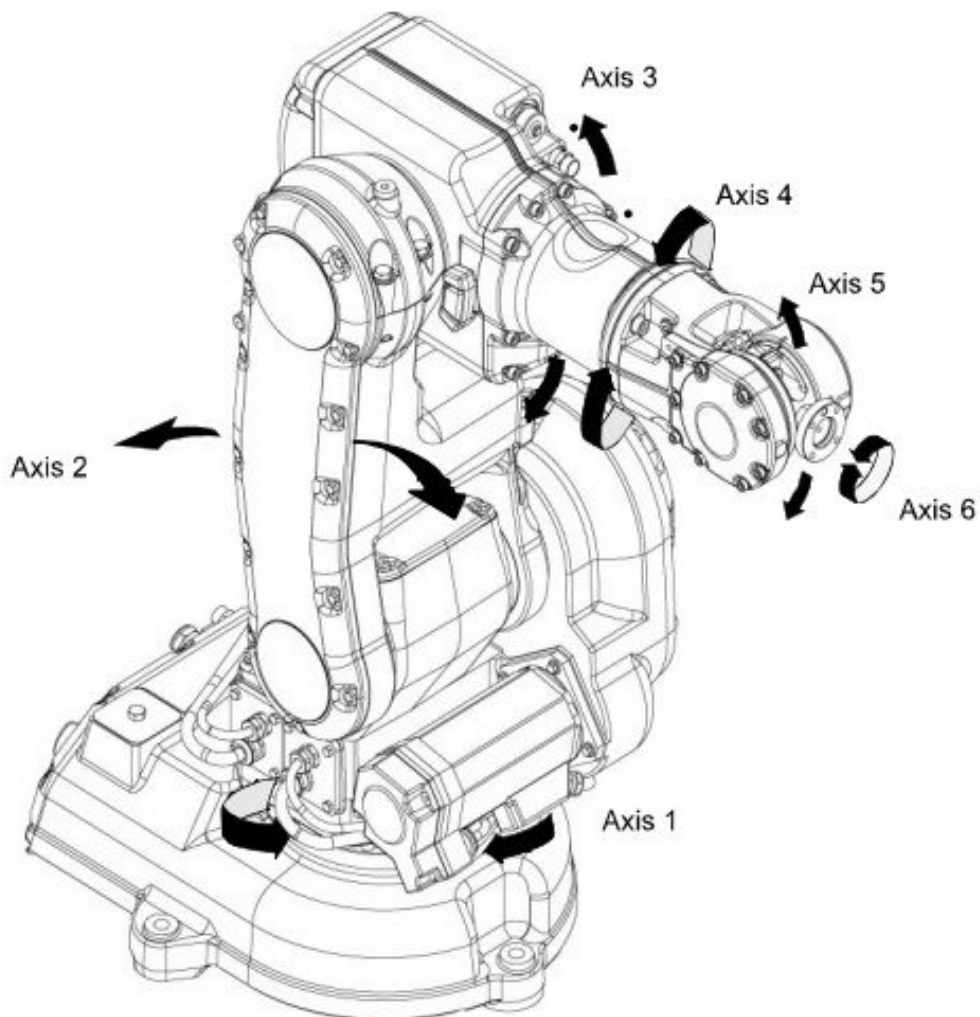


**FIGURE 9.2.** Representation of the rotational axis of the RAP [30].

## 9.2. RAP control system and RAP tools

In RAP, the control system of the polishing process is assigned by a software and carried out by a particular developed module that is mounted directly on the head of the robot (*figure 9.3*). The polishing module is an important part of the RAP machine because in this unit there are both force control and the oscillation system. Its particular features are:

- The polishing force is internally monitored by pneumatic proportional valves [30];
- The force range is between 100 g and 3000 g[30];
- The pulse oscillation frequency is fully controlled by the operator [30];
- The oscillation range of RAP is between 200 and 5000 oscillation strokes per minute [30];
- The stroke of the pulse oscillation can be adjusted/changed by the operator [30];
- The stroke length has a range of 0.5-3 mm [30];
- The polishing arm can be easily mounted to the polishing module with the help of a conical connector (*figure 9.4*) [30];

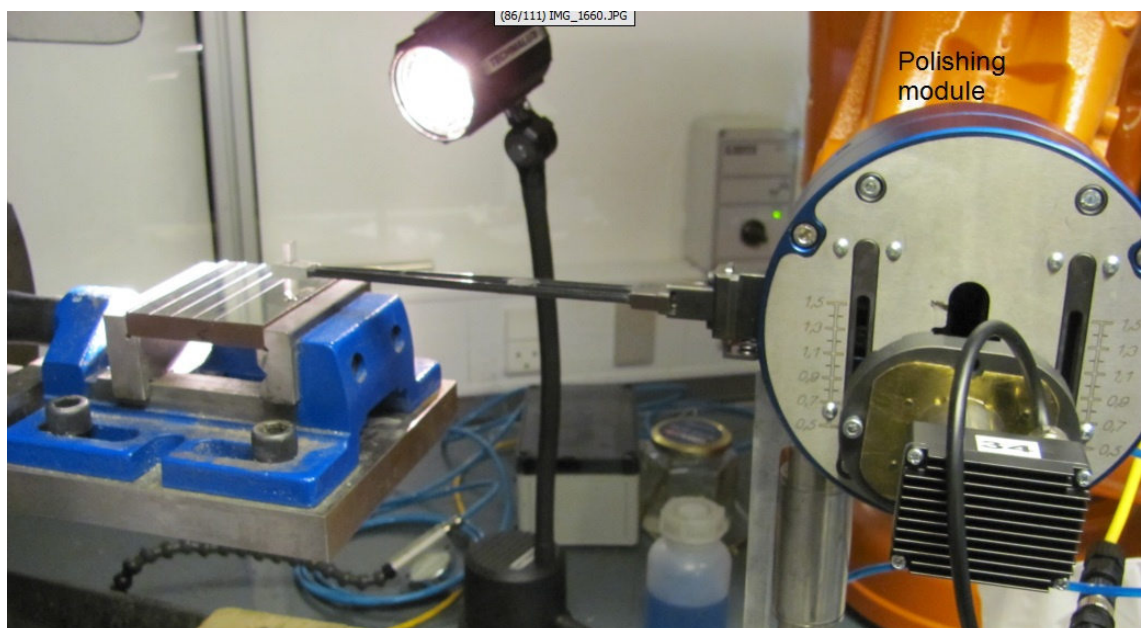


**FIGURE 9.3.** Polishing module of the RAP.

The achievable precision of RAP for some of the most important process parameters is summarized in the table below:

<b>PARAMETER</b>	<b>PRECISION</b>
<i>Coordinate (robot)</i>	$\pm 0.1 \text{ mm}$
<i>Spindle (rpm)</i>	$\pm 5 \text{ rpm}$
<i>Spindle fixed position</i>	$\pm 0.05 \text{ deg}$
<i>Pulse speed</i>	$\pm 30 \text{ rpm}$
<i>Force</i>	$\pm 100 \text{ g-typically } \pm 50 \text{ g}$

**TABLE 9.1.** Precision range of RAP [30].

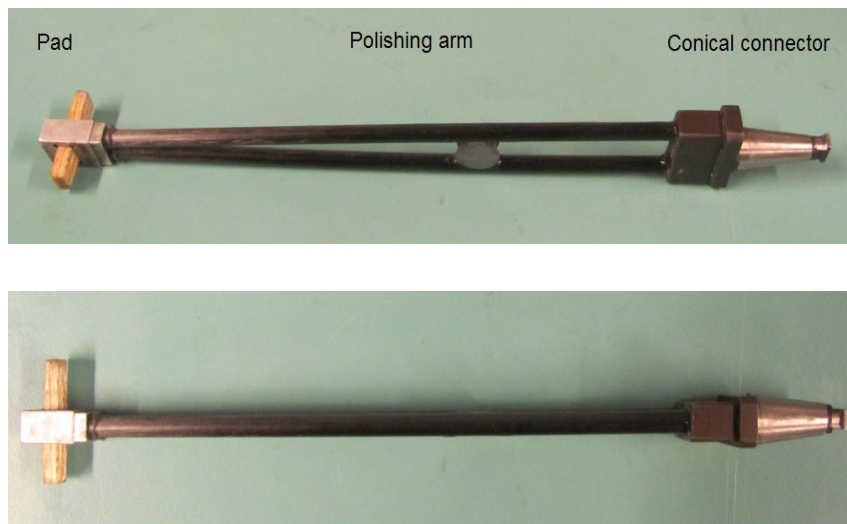


**FIGURE 9.4.** Example of polishing arm.

The polishing module is one of the most important parts forming the RAP. Anyway, this is not the only one, but the machine tool consists of:

- Machine housing [30];
- Spindle with a chuck of diameter 300 mm (this is blocked during a flat polishing process) [30];
- Robot-ABB 5 kg [30];
- Polishing module with integrated force and oscillation control. A lubrication unit takes part of the machine

- system and it is activated and controlled by the RAP program or manually (this is not activated during a flat polishing process) [30];
- Controls/PC interface for RAP programming and process control including both the robot assisted polishing process and a manual polishing mode [30];
  - Mandatory safety features in accordance with the CE directives [30];
  - A polishing arms with different lengths, thickness and shapes are available. This makes the system flexible (*figure 9.4*) [30];
  - There are different kinds of pad which can be easily mounted on the end of the arm (*figure 9.4*) [30].

Sometime some additional product features can be employed, as:

- Internal lighting in the spindle that ensures an optimal visual inspection of the inside geometry of the workpiece [30];
- A electric and robotic controls are integrated into the machine housing. This makes machine installation or move very easy [30];
- Integrated outlet for power, compressed air and drawer for tools, liquids etc [30];
- Integrated waste bin ensuring a clean work environment;
- Webcam and internet connection for internal process control and RAP Hotline [30];
- Built-in axhaust unit with filter [30].

The main characteristics of the RAP machine have been introduced. As explained previously, this kind of machine is very flexible and very easy to set up and conduct. The changing of pads and polishing arms are very easy to do and the polishing module permits a full control over the applied force and oscillation frequency.

### 9.3. RAP benefits

The benefits given by this machine can be summarized as:

- The polishing process ensures a repetitive, consistent, and uniform surface quality of the tool or workpiece [30];
- The RAP process is faster than manual polishing due to the speed of the RAP Pulse Module [30];
- The RAP machine works like a surface calibrating process ensuring a very consistent surface quality [30];
- The RAP process can easily be used to obtain mirror-like surfaces [30];
- The polishing process is specified, stored, and controlled by a program. This ensures full documentation and track records [30];
- Changes to the polishing program are easily made and securely stored [30];
- After programming, the RAP machine works on its own. In the meantime, the polisher can then do other jobs [30];
- The programming itself takes a few minutes and requires no skills in robot programming [30];
- The machine has a user-easy interface [30].

# CHAPTER TEN

## The experimental tests

### 10.1. Introduction

After having defined the experimental planning and measuring both the initial roughness of the samples and the profiles for estimating the material removal caused by the polishing process, the experimental tests can be run in collaboration and with the availability of STRECON company.

It is noteworthy that the aim of these experiments is to understand how the polishing parameters (pressure, feed rate, and frequency) affect the roughness behavior of the workpiece surface and which is the amount of material removal during a polishing process in flat kinematics conditions.

The order to run the tests is equal to that defined previously in the experimental planning and summarized below:

<b>RUN</b>	<b>PRESSURE (g)</b>	<b>FEED RATE (mm/s)</b>	<b>FREQUENCY (1/s)</b>	<b>NUMBER OF SAMPLE</b>
<b>1</b>	900	0.167	8.33	<b><u>1</u></b>
<b>2</b>	900	1.167	8.33	<b><u>2</u></b>
<b>3</b>	900	1.167	58.33	<b><u>3</u></b>
<b>4</b>	100	1.167	8.33	<b><u>4</u></b>
<b>5</b>	100	1.167	58.33	<b><u>5</u></b>
<b>6</b>	100	0.167	8.33	<b><u>6</u></b>
<b>7</b>	100	0.167	58.33	<b><u>7</u></b>
<b>8</b>	900	0.167	58.33	<b><u>8</u></b>
<b>9</b>	500	0.667	33.33	<b><u>9</u></b>
<b>10</b>	900	1.167	33.33	<b><u>10</u></b>
<b>11</b>	900	0.667	58.33	<b><u>11</u></b>
<b>12</b>	500	1.167	58.33	<b><u>12</u></b>
<b>13</b>	500	0.667	33.33	<b><u>13</u></b>

**TABLE 10.1.** Order to conduct the experiments.

## 10.2. Preliminary settings

The employed polishing machine has been the RAP machine, as anticipated in the previous chapters and kindly provided by STRECON.

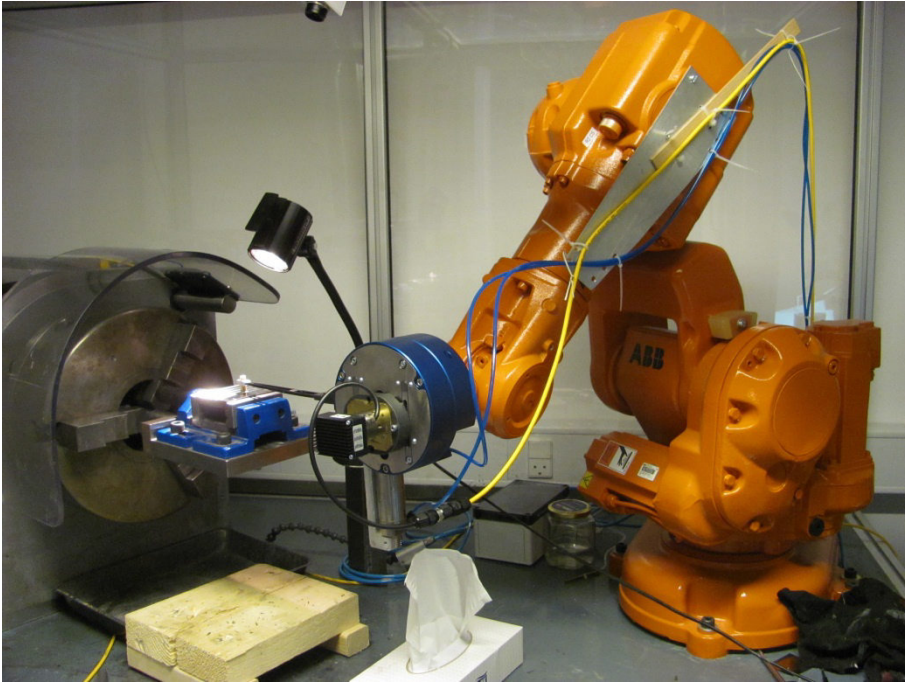


**FIGURE 10.1.** RAP machine.

The employed pad was in wood and it has been manually obtained with the help of a cutter and some sandpaper by a initial bar as shown in the *figure 10.2*:

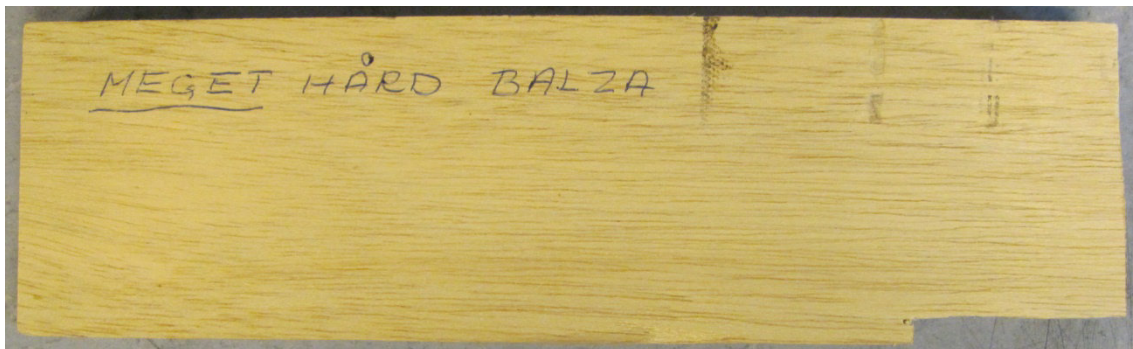


**FIGURE 10.2.** Employed material for the polishing pad.

Regarding the clamping system for the sample, the RAP machine is a polishing instrument born to polish both in rotational and flat kinematics conditions. It is provided



by a spindle that can rotated for a determined speed and that makes RAP particularly adapt to work part with circular symmetry (see *figure 10.3*).

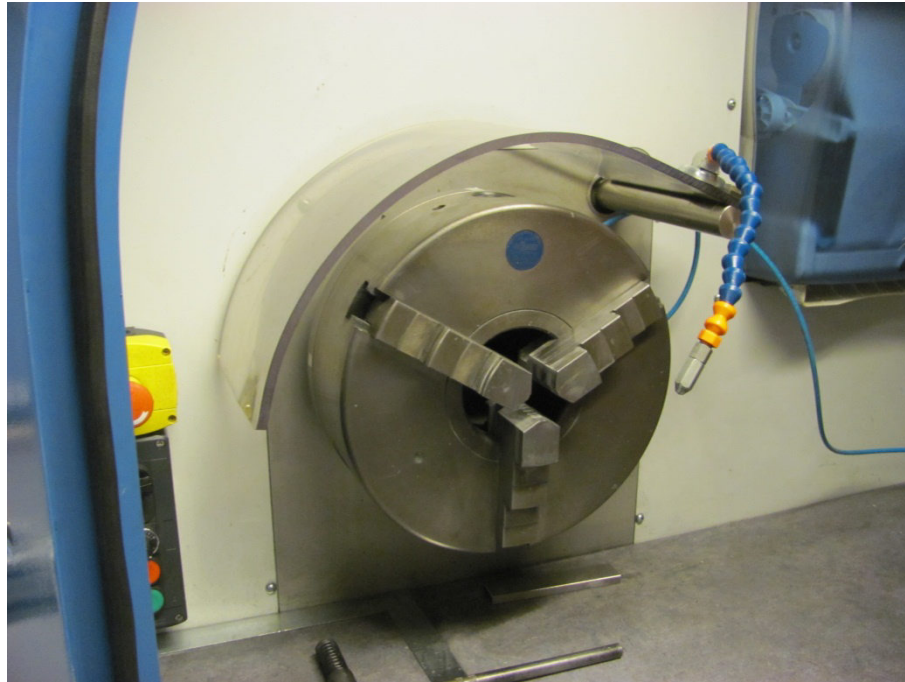


**FIGURE 10.3.** Spindle of the RAP.

To work in flat kinematics conditions, the rotation of the spindle is locked by some particular brake and a platform keeping the sample is inserted into the spindle hole that cannot rotate anymore (see *figure 10.4*).

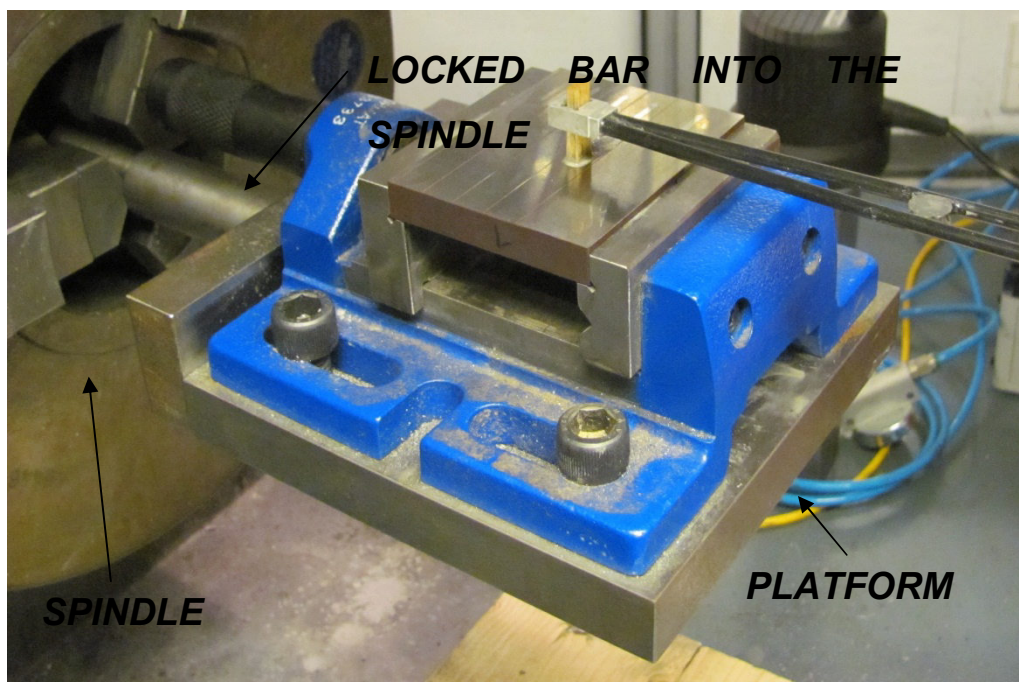


**FIGURE 10.4.** Clamping system for the sample.

In other hands, the clamping system for the sample has been formed by a locked spindle and a flat platform that is inserted into the spindle through a connecting bar. An important operation to do before running the test has been to set the height of the polishing arm and the module (z direction for RAP machine) relative to the position of the platform and the sample, to work in the best way. This operation, if the clamping system is kept in the same position for all the tests, is necessary to do only in the beginning and not every time that the sample is substituted with a new one (this because the thick is the same for all the samples).

Anyway, with this kind of clamping system, the size of the machining part is limited by the range of the lock system itself. In fact, it is possible to work only workpieces with a maximum width of eighty millimeters as shown in the *figure 10.5*. The regulation of the width is manual, through a screw that permits to tighten the clamp or release it.

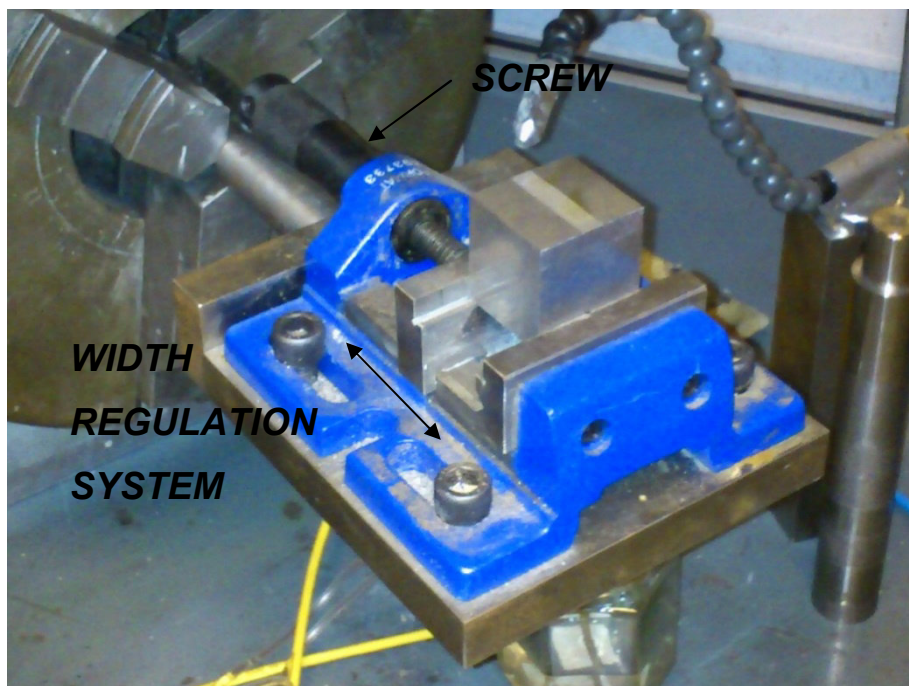


**Figure 10.5.** Regulation system in the platform.

Another important condition related to the platform where the sample has been located, is that the plane of it has to be perfectly parallel to the plane where the RAP machine works and moves. In other hands, the surface of the sample, and therefore the plane characterizing the platform, has to be parallel to the plane where the pad and the polishing arm move. This is an important point for our experiments, and this condition with the previous one related to the height of the polishing module is fundamental to

determine a good running of the experimental tests and reduce the error related to the wrong position of sample.

After these beginning preparations connected with the clamping system and the height of the polishing module relative to the position of the sample, the tests could start. Before of that, the RAP machine had to be set up. The RAP program is simple to use and understand. Firstly, when the program is on, it is necessary to enter the polishing parameters in the empty fields for the sample which has to be polished (that is, down pressure, oscillation, and feed rate). Then the coordinates where the pad is wanted to move have to be typed in. This last operation is not standard; that is, the methods to find out the correct coordinates where the pad has to move can be numerous. Nevertheless, the employed method to find out the correct position of the pad relative to the sample was the following: firstly, after having verify the correct height of the polishing module, the position ( $x = 0; y = 0$ ) has been detected (where  $x$  is in the direction of the spindle axis, and  $y$  is orthogonal to it). This has been made to understand where the zero point was relative to the real position of the sample, and how many millimeters missed to reach the correct position. After that, through a meter, the distance between the pad in the zero point and the sample has been roughly measured. Therefore, step by step, new coordinates have been typed into the program until the desired position would be reached. It is important to remember that the RAP coordinate system refers to the middle of the pad and not to the edges of it. In other hands, when the zero point is taken into account, the  $\pm 1.5 \text{ mm}$  of the pad width and the  $\pm 3 \text{ mm}$  of the pad length are not considered.

This employed method could seem rough, but this is the method followed by STRECON.

After having set up the RAP machine, the experimental tests could run.

### **10.3. Experimental methodology**

#### 10.3.1. Introduction to the experimental procedure

The experimental methodology is readily explained below:

Before polishing the defined surfaces where the roughness will be measured, it has been important to ensure that the contact surface of the pad was flat and parallel enough to the workpiece surface to guarantee a good contact between them. This because, to ensure a good contact surface between the pad and the workpiece surface

is fundamental to guarantee a good pressure distribution, a big number of active abrasive particles, and the good success of our tests. Therefore, some free polishing runs have been required in the run-in area to make this.

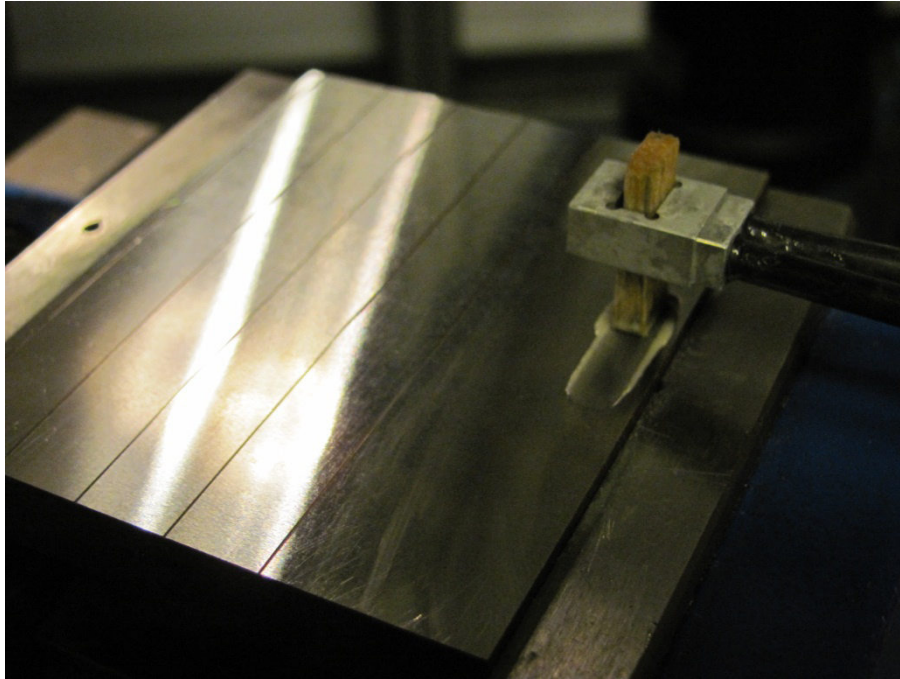


**FIGURE 10.6.** Run in area.

To polish with the pad in the run-in zone is very important, but it takes time as well. For this, to economize the required time to reach the wanted track on the surface, some rough instrument as cutter and sandpaper have been employed to “help” the pad to find out the best contact with the sample. The use of these two instrument does not have control except that the skill of the operator. Anyway, when the track left by the pad on the sample well reproduced the shape of the pad itself, the true polishing tests could begin.

Following the *table 10.1*, the first sample to be polished has been the number one (with a pressure of 900 g, a feed rate of 0.167 mm/s, and a frequency of 8.33 1/s.). As it was said in the previous chapters, each column of the same sample contained three repetitions of the same polishing surface, and each column determined a different polishing time. This means that for four columns, there has been four different intervals of timing (these intervals have been defined in the chapter six where  $T_4$  is the final time required to reach the final roughness,  $T_3$  is  $0.5 \times T_4$ ,  $T_2$  is  $0.3 \times T_4$ , and  $T_1$  is  $0.1 \times T_4$ ). Nevertheless, the timing required to reach the  $T_4$  and therefore the other intervals of

time has been estimated counting the number of pass and not the minutes corresponding. However, when the number of passes and the feed rate are know, the corresponding time is easily found.

### 10.3.2. Understanding and measuring of the reachable final roughness value

Therefore, the starting issues was: how to measure and understand if the final roughness is reached by the process? What is the achievable final roughness and when can we stop to polish the interested surface?

These have been two important questions which had to be take into account carefully. Regarding the last question, some information about the final roughness achievable from a diamond paste of 14  $\mu\text{m}$  has been searched. All the found data reported that with that typology of paste a final roughness around 50  $\text{nm}$  was obtainable. This datum is useful to understand what value of roughness is expected in the end and to decide when stopping the process. Regarding this latter points, we knew that for roughness bigger than 50  $\text{nm}$ , the polishing process was not finished yet, and it had to run more, whereas when a value around the 50  $\text{nm}$  was reached, the process could be arrested. From these considerations, it was decided that, when a value around 50  $\text{nm}$  was reached, the process could be stopped if the difference between the average of the five last consecutive measurements and the last measurement was smaller than 0.005. This assumption is shown in the equation below:

$$\frac{\text{measure1} + \text{measure2} + \text{measure3} + \text{measure4} + \text{measure5}}{5} - \text{last measurement} < 0.005$$

**FORMULA 10.1.** Assumption to arrest the polishing process in defining  $T_4$ .

This choice was done to have a good result under the statistical point of view and to make the measurement repeatable.

Regarding the first question, that is, “how to measure and understand if the final roughness is reached by the process?”, it was decided to measure the reached roughness at the moment step by step, after a certain range of time. This means that after a certain range of time, the RAP machine was stopped, the roughness value reached for that time was measured, and if the conditions explained previously were

realized, then the polishing process could machine a new surface, otherwise not. The employed instrument to measure the reached value each time was a stylus profilometer, shown in the figure below:

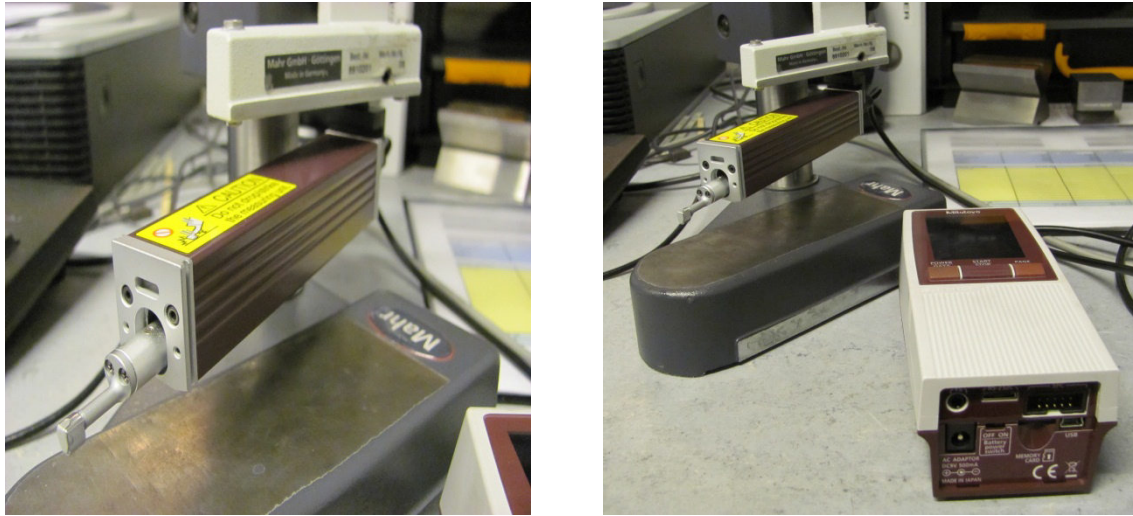


**FIGURE 10.7.** Mahr profilometer.

### 10.3.3. The issue of the paste refresh

After these considerations and assumptions, a last issue remained to be solved. It regarded the refresh of the paste. In other hands, it was important determine when stopping the process to measure the reached roughness or, better, when it was necessary to put on the sample new abrasive paste for not losing effectiveness in the process. Was it necessary to refresh the paste after a certain period of time? After a certain number of passes or strokes? Which was the parameters that affected the rest of the paste in the desired contact zone between sample and pad?

To understand this, and therefore to have more control over the process limiting the random variable regarding the refresh of the paste, some preliminary tests were run. They were run in the run-in area (luckily this was designed big enough to permit these additional tests, besides the alignment of the pad surface with the sample), twice for each combination of parameters, where the analyzing variables were time, number of passes, and number of strokes. The aim of these pre-tests was to determine if some of the mentioned previous variables affected the distribution of the abrasive on the contact zone and to understand which pressure, feed rate, and frequency have to be

assumed. The table below show which polishing parameters were chosen for these pre-tests:

<b>Abrasive paste refresh after six passes</b>	<i>Pressure</i>	900 g
	<i>Feed rate</i>	1.167 mm/s
	<i>Frequency</i>	8.331/s
<b>Abrasive paste refresh after 503 seconds</b>	<i>Pressure</i>	900 g
	<i>Feed rate</i>	1.167 mm/s
	<i>Frequency</i>	8.331/s
<b>Abrasive paste refresh after 4191.7 strokes</b>	<i>Pressure</i>	900 g
	<i>Feed rate</i>	0.167 mm/s
	<i>Frequency</i>	58.331/s

**TABLE 10.2.** Employed parameters for the preliminary tests.

As it can be seen from the table above, we have chosen to refresh after six passes (or after a 84 mm), after 503 seconds, and after 4890 strokes. These choices were arbitrary.

The results of these preliminary tests are shown below:

<b>Passes</b>	<b>Space [mm]</b>	<b>Time [s]</b>	<b>Strokes</b>	<b>Average roughness value after refresh every 4890 strokes [μm]</b>
0	0	0	0	0.081
3	42	251	14671	0.025
6	84	503	29341	0.015
9	126	754	44012	0.015
12	168	1006	58683	0.017
15	210	1257	73353	0.02
18	252	1509	88024	0.018
21	294	1760	102695	0.021
24	336	2012	117365	0.020

**TABLE 10.3.a.** Results after the preliminary tests.

Passes	Space [mm]	Time [s]	Strokes	Average roughness value after refresh every 6 passes [ $\mu\text{m}$ ]	Average roughness value after refresh every 503 seconds [ $\mu\text{m}$ ]
0	0	0	0	0.09	0.099
3	42	35.989	299.914		
6	84	71.979	599.828	0.066	
9	126	107.969	899.742		
12	168	143.958	1199.657	0.056	
15	210	179.948	1499.571		
18	252	215.938	1799.485	0.052	
21	294	251.928	2099.400		
24	336	287.917	2399.314	0.046	
27	378	323.907	2699.228		
30	420	359.897	2999.143	0.042	
33	462	395.886	3299.057		
36	504	431.876	3598.971	0.037	
39	546	467.8663	3898.886		
42	588	503.8560	4198.800	0.036	0.052
45	630	539.8457	4498.714		
48	672	575.8354	4798.628	0.037	
51	714	611.8251	5098.543		
54	756	647.814	5398.457	0.032	
60	840	719.7943	5998.286	0.033	
66	924	791.7737	6598.114	0.030	
72	1008	863.7532	7197.943	0.030	
78	1092	935.732	7797.772	0.030	
			0		
84	1176	1007.712	8397.600		0.047
126	1764	1511.568	12596.40		0.039
168	2352	2015.424	16795.201		0.032
210	2940	2519.280	20994.001		0.028
252	3528	3023.136	25192.802		0.023
294	4116	3526.992	29391.602		0.017
336	4704	4030.848	33590.402		0.019

TABLE 10.3.b. Results after the preliminary tests



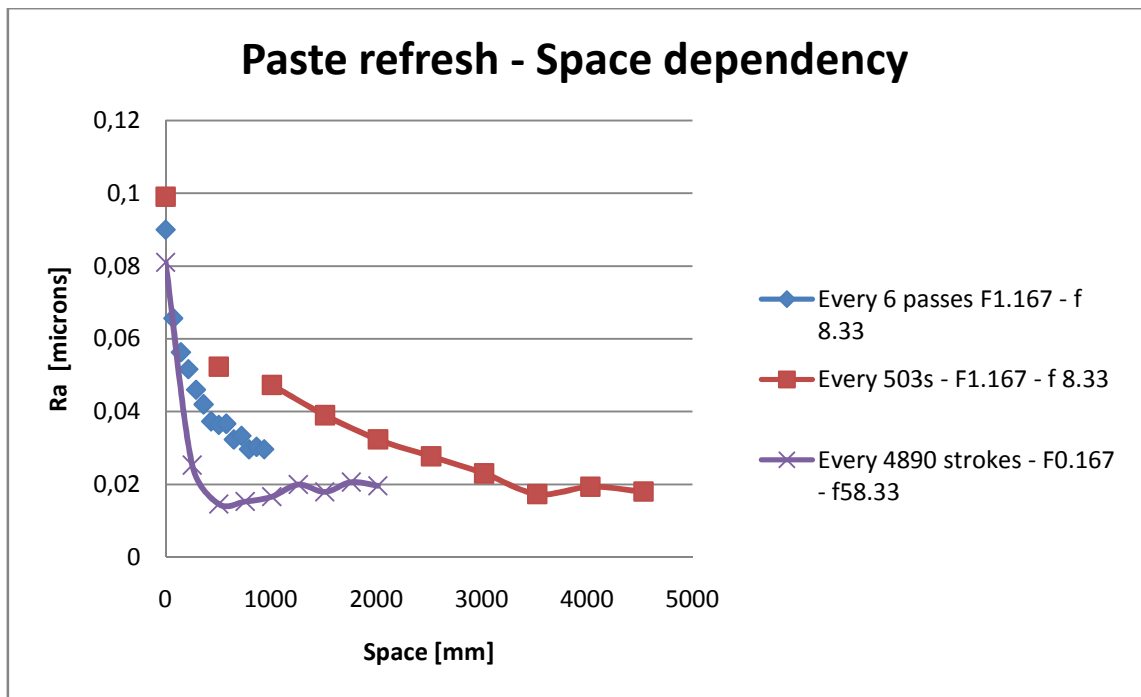


FIGURE 10.8. Abrasive paste refresh-Space dependency.

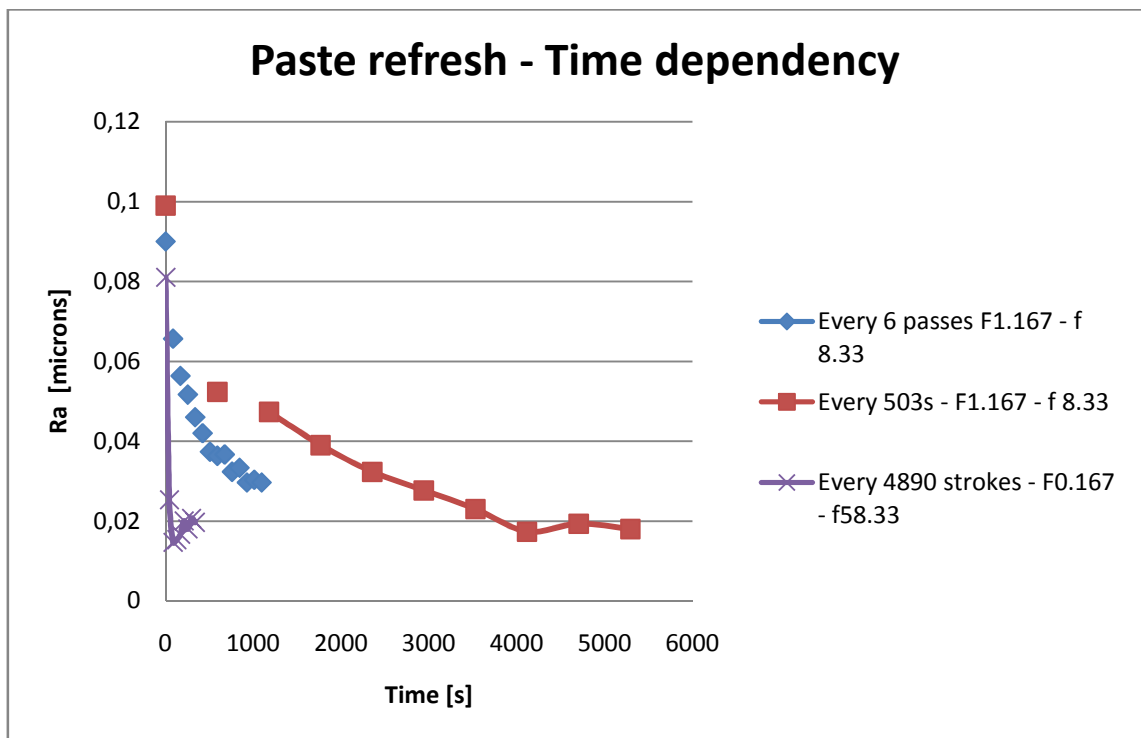
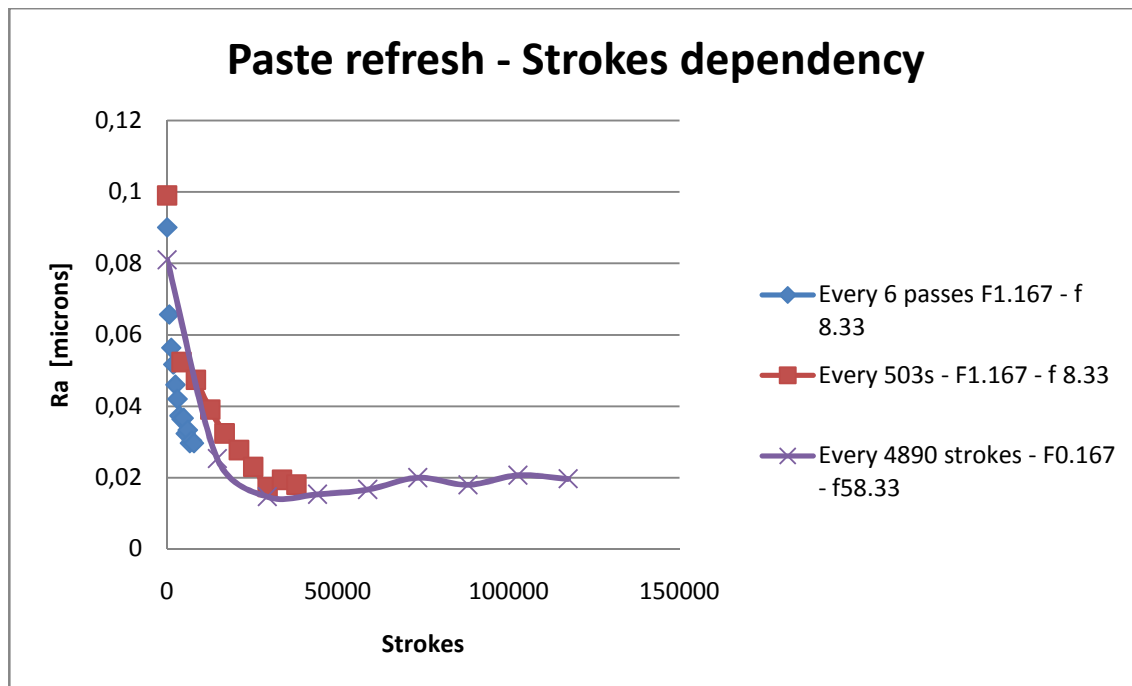


FIGURE 10.9. Abrasive paste refresh-Time dependency.



**FIGURE 10.10.** Abrasive paste refresh-Strokes dependency.

From the results of these preliminary tests, it can be seen that the most important parameters which affects the abrasive distribution on the contact zone between the pad and the sample is the frequency of the pad itself. In fact, from the three graphs above (*figure 10.8, 10.9, 10.10*) it can be seen that, in the last case where the paste refresh was checked by the number of strokes made by the pad, the three curves resulting from the tests, have a trend more similar and compact than those resulting from the other two cases (passes control and time control, *figure 10.8* and *figure 10.9* respectively). This means that if the frequency is taken into account, the number of paste refreshes does not significantly affect the roughness behavior of the sample surface. For example, if the blue and violet curves in *figure 10.10* are considered, we can see from the *table 10.3* that for the blue one the abrasive paste refresh is almost every 600 strokes, whereas for the violet is almost every 4890 strokes. This means that for a same number of strokes, for example 50000, the number of refreshes for the first one will be bigger than for the second one. But if the *figure 10.10* is analyzed this fact does not significantly affect the roughness behavior, but the two curves are very close together.

Otherwise, this does not happen for the first two graphs (*figure 10.8-10.9*) where the curves are very different each other. Here we can see that for a frequent refresh (violet curve) the roughness curve is deeper than the other two and the final roughness value

is reached after a little time (or after few passes), whereas if the paste refresh is less common (red curve), the curve will be more flat and more time or passes will be required to reach the final roughness value. Comparing the blue and the red curves, this fact is more evident. In fact, these curves have been obtained using the same process parameters ( $pressure = 900g$ ;  $feed\ rate = 1.167 \frac{mm}{s}$ ;  $frequency = 8.33\ 1/s$ ), but in the blue one the paste refresh is every 6 passes, whereas in the red one every 42, this means that in the second case the number of strokes before refreshing is seven times bigger than the first one and more paste will push outside the polishing area before putting on new abrasive again, and the polishing process it will be less efficient.

Therefore, it is clear from these preliminary tests that the frequency of the pad strongly affects the process, because it is the main cause for the evacuation of the abrasive paste from the contact zone.

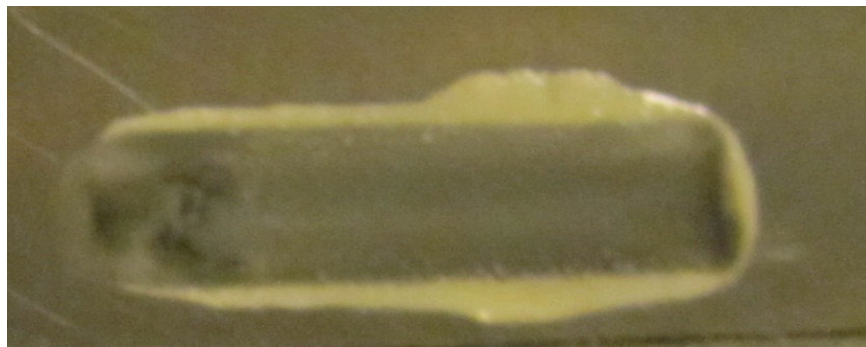


**FIGURE 10.11.** *Deposition of the paste along the margins of the track left by the pad.*

In other hands, the paste refresh have to depend on the number of strokes to have more control on the process.

Therefore, after having planned the order to run the experiments, checked the clamping system for the pad, and set up the RAP machine, the last thing made before having run with the test, has been to decide the number of strokes after that the abrasive paste refresh was necessary. The combination of parameters (only feed rate and frequency in this case because the pressure does not affect the number of strokes) taken as reference point was  $feed\ rate = 0.167 \frac{mm}{s}$ ,  $frequency = 58.33\ 1/s$  and

*number of passes* = 3. This means that the number of strokes taken as reference was 14670.66 strokes. The strokes are given by the equation below:

$$\text{strokes} = \frac{\text{passes} \times 14 \times \text{oscillation}}{\text{feed rate} \times 60}$$

**FORMULA 10.2.** Equation for the number of strokes.

The choice of these parameters is simply related to the use of the abrasive paste. In fact, the available syringe of abrasive paste was only one of 20 g (*figure 10.12*). To be sure to finish the experimental tests with the same paste the more critical condition related the paste refresh was chosen (that is  $\text{feed rate} = 0.167 \frac{\text{mm}}{\text{s}}$ ,  $\text{frequency} = 58.33 \text{ 1/s}$ ) and 3 passes were chosen, because refresh every pass was too often.

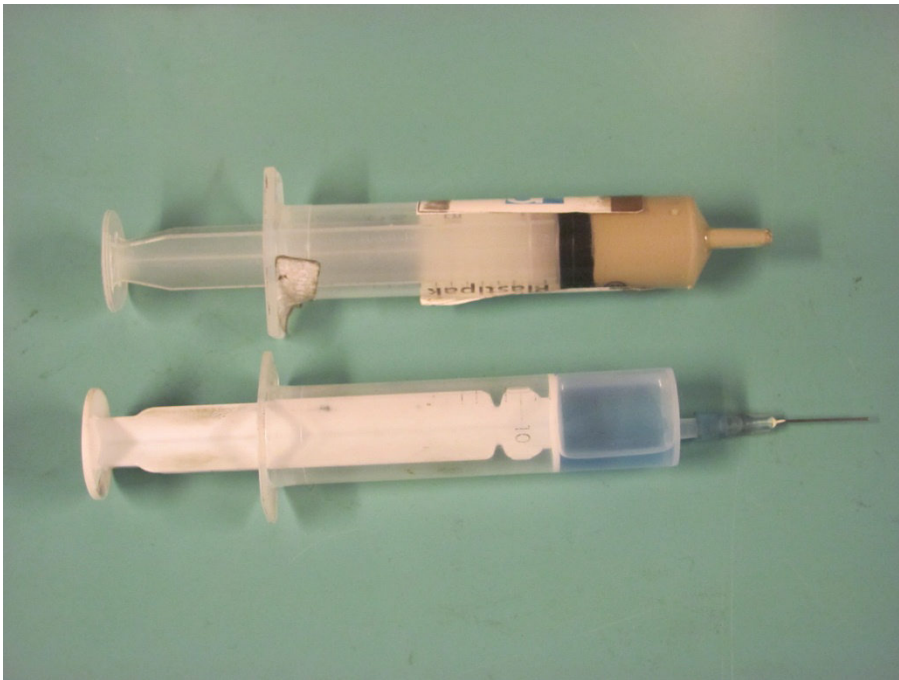


**FIGURE 10.12.** Abrasive paste and lubricant employed during the tests.

The number of passes after which the paste is necessary are listed in the table below for each sample:

<b>SAMPLES</b>	<b>PARAMETERS</b>	<b>VALUES</b>
<i>sample1/6</i>	<i>feed rate</i>	0.167 mm/s
	<i>frequency</i>	8.33 1/s
	<i>strokes</i>	14670.66
	<i>passes</i>	21
<i>sample2/4</i>	<i>feed rate</i>	1.167 mm/s
	<i>frequency</i>	8.33 1/s
	<i>strokes</i>	14670.66
	<i>passes</i>	146.749
<i>sample3/5</i>	<i>feed rate</i>	1.167 mm/s
	<i>frequency</i>	58.33 1/s
	<i>strokes</i>	14670.66
	<i>passes</i>	20.964
<i>sample7/8</i>	<i>feed rate</i>	0.167 mm/s
	<i>frequency</i>	58.33 1/s
	<i>strokes</i>	14670.66
	<i>passes</i>	3
<i>sample0/12</i>	<i>feed rate</i>	0.667 mm/s
	<i>frequency</i>	33.33 1/s
	<i>strokes</i>	14670.66
	<i>passes</i>	20.969
<i>sample9</i>	<i>feed rate</i>	1.167 mm/s
	<i>frequency</i>	33.33 1/s
	<i>strokes</i>	14670.66
	<i>passes</i>	36.687
<i>sample10</i>	<i>feed rate</i>	0.667 mm/s
	<i>frequency</i>	58.33 1/s
	<i>strokes</i>	14670.66
	<i>passes</i>	11.982
<i>sample11</i>	<i>feed rate</i>	1.167 mm/s
	<i>frequency</i>	58.33 1/s
	<i>strokes</i>	14670.66
	<i>passes</i>	20.964

**TABLE 10.4.** Number of passes for each different paste refresh.

After this last assumption the experimental tests could be run.

#### 10.3.4. Summary of the experimental procedure and results correlated with the made measurements to evaluate $T_4$

The experimental procedure is now briefly summarized:

- Firstly, the clamping system for the sample is mounted on the locked spindle. Its position is checked, because it has to be parallel to the work plane of the RAP machine;
- The height position of the polishing module relative to the clamping system is set up;
- The sample is mounted and locked on the clamping system;
- The polishing parameters (pressure, feed rate, and oscillation) are put in the RAP program;
- The correct position of the pad relative to the workpiece surface is found out and the path of the pad is set up. The path is related to the size of the polishing surface;
- Before run with polishing the true surfaces required for the test, the track of the pad have to be checked in the run-in area to avoid parallax error and to render the pad surface very flat. If the track is clearly bad, the use of sandpaper is recommended to save time;
- When the track of the pad is considered in a good condition, the  $T_4$  is found out as first;
- To find out the  $T_4$ , the interested area is polished for a number of passes listed in the *table 10.4*. After this, the roughness value reached in this area is measured with the profilometer. If the measured roughness is too high relative to expected, or if the relative error is bigger than 0.005, the polishing is repeated in the same area for a number of passes indicated in the *table 10.4*;
- To evaluate the roughness in the polishing area, the measurements with the profilometr are three. This to better characterize the overall roughness value reach in the analyzed surface;

- Every time that the polishing process is repeated on the same zone, the abrasive paste have to be refresh. A lubricant is applied on the polishing zone with the paste (*figure 10.12*);
- When the  $T_4$  is found out, the other time intervals and repetitions of the same test are a consequence of it. In this case, for the other surfaces the roughness is not measured anymore. Only the abrasive paste refresh has to be respected;
- The procedure explained before to estimated the  $T_4$  has to be respected for all the samples. Same consideration for the abrasive paste refresh.

The measurements done for each sample are listed below:

<b>SAMPLE 0</b>				
<b>Parameters</b>	<i>Pressure [g]</i>	500		
	<i>Feed rate [mm/s]</i>	0.667		
	<i>Frequency [1/s]</i>	33.33		
<b>Size of the sample</b>	63,75*57,2 (mm)			
<b>Size of the pad</b>	3*6*15 (mm)			
<b>Passes</b>	<b>T4 Value1 [<math>\mu\text{m}</math>]</b>	<b>T4 Value2 [<math>\mu\text{m}</math>]</b>	<b>T4 Value3 [<math>\mu\text{m}</math>]</b>	<b>Average [<math>\mu\text{m}</math>]</b>
0	0.055	0.068	0.05	<b>0.058</b>
21	0.019	0.016	0.017	<b>0.017</b>
42	0.014	0.012	0.013	<b>0.013</b>
63	0.019	0.013	0.014	<b>0.015</b>
84	0.013	0.012	0.013	<b>0.013</b>
105	0.016	0.013	0.013	<b>0.014</b>
0	0.055	0.068	0.05	<b>0.057</b>
21	0.019	0.016	0.017	<b>0.017</b>

**TABLE 10.5.**Measurement for each refresh

<b>SAMPLE 1</b>				
<b>Parameters</b>	Pressure [g]	900		
	Feed rate [mm/s]	0.167		
	Frequency [1/s]	8.33		
<b>Size of the sample</b>	80*63,75 (mm)			
<b>Size of the pad</b>	3*6*15 (mm)			
<b>Passes</b>	<b>T4 Value1 [μm]</b>	<b>T4 Value2 [μm]</b>	<b>T4 Value3 [μm]</b>	<b>Average [μm]</b>
0	0.048	0.042	0.046	<b>0.045</b>
21	0.028	0.03	0.031	<b>0.030</b>
42	0.022	0.02	0.022	<b>0.021</b>
63	0.02	0.022	0.022	<b>0.021</b>
84	0.013	0.019	0.013	<b>0.015</b>
105	0.014	0.014	0.016	<b>0.015</b>

**TABLE 10.6.**Measurement for each refresh

<b>SAMPLE 2</b>				
<b>Parameters</b>	Pressure [g]	900		
	Feed rate [mm/s]	1.167		
	Frequency [1/s]	8.33		
<b>Size of the sample</b>	79,35*63,75 (mm)			
<b>Size of the pad</b>	3*6*14 (mm)			
<b>Passes</b>	<b>T4 Value1 [μm]</b>	<b>T4 Value2 [μm]</b>	<b>T4 Value3 [μm]</b>	<b>Average [μm]</b>
0	0.102	0.123	0.12	<b>0.115</b>
147	0.063	0.068	0.06	<b>0.064</b>
294	0.048	0.046	0.056	<b>0.05</b>
441	0.035	0.046	0.042	<b>0.041</b>
588	0.036	0.033	0.03	<b>0.033</b>
735	0.037	0.038	0.031	<b>0.035</b>
882	0.026	0.03	0.036	<b>0.031</b>

**TABLE 10.7.**Measurement for each refresh.



<b>SAMPLE 3</b>				
<b>Parameters</b>	<i>Pressure [g]</i>	900		
	<i>Feed rate [mm/s]</i>	1.167		
	<i>Frequency [1/s]</i>	58.33		
<b>Size of the sample</b>	80,25*63,75 (mm)			
<b>Size of the pad</b>	3*6*15 (mm)			
<b>Passes</b>	<b>T4 Value1 [μm]</b>	<b>T4 Value2 [μm]</b>	<b>T4 Value3 [μm]</b>	<b>Average [μm]</b>
0	0.107	0.102	0.105	<b>0.105</b>
21	0.07	0.066	0.067	<b>0.068</b>
42	0.034	0.036	0.037	<b>0.036</b>
63	0.017	0.025	0.024	<b>0.022</b>
84	0.014	0.018	0.017	<b>0.016</b>
105	0.014	0.015	0.015	<b>0.015</b>
126	0.015	0.014	0.013	<b>0.014</b>
147	0.014	0.014	0.013	<b>0.014</b>

**TABLE 10.8.**Measurement for each refresh.

<b>SAMPLE 4</b>				
<b>Parameters</b>	<i>Pressure [g]</i>	100		
	<i>Feed rate [mm/s]</i>	1.167		
	<i>Frequency [1/s]</i>	8.33		
<b>Size of the sample</b>	80*63,75 (mm)			
<b>Size of the pad</b>	3*6*15 (mm)			
<b>Passes</b>	<b>T4 Value1 [μm]</b>	<b>T4 Value2 [μm]</b>	<b>T4 Value3 [μm]</b>	<b>Average [μm]</b>
0	0.22	0.235	0.212	<b>0.222</b>
147	0.202	0.18	0.172	<b>0.185</b>
294	0.169	0.121	0.124	<b>0.138</b>
441	0.123	0.102	0.081	<b>0.102</b>
588	0.067	0.068	0.071	<b>0.069</b>
735	0.053	0.055	0.051	<b>0.053</b>
882	0.049	0.047	0.031	<b>0.042</b>
1029	0.043	0.042	0.027	<b>0.037</b>
1176	0.031	0.042	0.044	<b>0.039</b>
1323	0.028	0.035	0.032	<b>0.032</b>

**TABLE 10.9.**Measurement for each refresh.

<b>SAMPLE 5</b>				
<b>Parameters</b>	Pressure [g]	100		
	Feed rate [mm/s]	1.167		
	Frequency [1/s]	58.33		
<b>Size of the sample</b>	78,55*63,7 (mm)			
<b>Size of the pad</b>	3*6*15 (mm)			
<b>Passes</b>	<b>T4 Value1 [μm]</b>	<b>T4 Value2 [μm]</b>	<b>T4 Value3 [μm]</b>	<b>Average [μm]</b>
0	0.213	0.215	0.225	<b>0.218</b>
21	0.146	0.149	0.147	<b>0.147</b>
42	0.126	0.131	0.133	<b>0.13</b>
63	0.117	0.119	0.117	<b>0.118</b>
84	0.087	0.112	0.109	<b>0.102</b>
105	0.077	0.084	0.109	<b>0.09</b>
126	0.074	0.084	0.099	<b>0.090</b>
147	0.066	0.073	0.084	<b>0.074</b>
168	0.067	0.066	0.078	<b>0.070</b>
189	0.063	0.066	0.071	<b>0.067</b>
210	0.063	0.064	0.067	<b>0.065</b>
231	0.06	0.061	0.062	<b>0.061</b>
252	0.046	0.057	0.058	<b>0.054</b>
273	0.055	0.055	0.05	<b>0.053</b>
294	0.038	0.052	0.051	<b>0.047</b>
315	0.04	0.052	0.05	<b>0.047</b>
336	0.045	0.045	0.049	<b>0.046</b>
357	0.042	0.05	0.047	<b>0.046</b>
378	0.034	0.038	0.038	<b>0.037</b>
399	0.04	0.04	0.041	<b>0.040</b>
420	0.034	0.037	0.04	<b>0.037</b>
441	0.036	0.039	0.039	<b>0.038</b>
462	0.039	0.037	0.038	<b>0.038</b>

**TABLE 10.10.**Measurement for each refresh.

<b>SAMPLE 6</b>				
<b>Parameters</b>	<i>Pressure [g]</i>	100		
	<i>Feed rate [mm/s]</i>	0.167		
	<i>Frequency [1/s]</i>	8.33		
<b>Size of the sample</b>	79,45*63,75 (mm)			
<b>Size of the pad</b>	3*6*15 (mm)			
<b>Passes</b>	<b>T4 Value1 [μm]</b>	<b>T4 Value2 [μm]</b>	<b>T4 Value3 [μm]</b>	<b>Average [μm]</b>
0	0.045	0.047	0.043	<b>0.045</b>
21	0.038	0.039	0.037	<b>0.038</b>
42	0.034	0.031	0.037	<b>0.034</b>
63	0.024	0.025	0.026	<b>0.025</b>
84	0.029	0.026	0.03	<b>0.028</b>
105	0.026	0.025	0.027	<b>0.026</b>

**TABLE 10.11.**Measurement for each refresh.

<b>SAMPLE 7</b>				
<b>Parameters</b>	<i>Pressure [g]</i>	100		
	<i>Feed rate [mm/s]</i>	0.167		
	<i>Frequency [1/s]</i>	58.33		
<b>Size of the sample</b>	80,1*63,7 (mm)			
<b>Size of the pad</b>	3*6*14 (mm)			
<b>Passes</b>	<b>T4 Value1 [μm]</b>	<b>T4 Value2 [μm]</b>	<b>T4 Value3 [μm]</b>	<b>Average [μm]</b>
0	0.194	0.166	0.165	<b>0.175</b>
3	0.152	0.158	0.153	<b>0.154</b>
6	0.13	0.138	0.121	<b>0.130</b>
9	0.126	0.11	0.126	<b>0.121</b>
12	0.121	0.115	0.122	<b>0.119</b>
15	0.112	0.09	0.1	<b>0.101</b>
18	0.097	0.102	0.1	<b>0.100</b>
21	0.099	0.099	0.1	<b>0.099</b>
24	0.096	0.092	0.099	<b>0.096</b>
27	0.091	0.093	0.09	<b>0.091</b>
30	0.086	0.087	0.08	<b>0.084</b>
33	0.078	0.074	0.079	<b>0.077</b>
36	0.072	0.075	0.067	<b>0.071</b>
39	0.069	0.064	0.073	<b>0.069</b>
42	0.059	0.065	0.069	<b>0.064</b>
45	0.065	0.065	0.067	<b>0.066</b>
48	0.06	0.059	0.065	<b>0.061</b>
51	0.058	0.053	0.053	<b>0.055</b>
54	0.057	0.049	0.057	<b>0.054</b>
57	0.057	0.046	0.048	<b>0.050</b>
60	0.055	0.051	0.054	<b>0.053</b>
63	0.051	0.046	0.053	<b>0.05</b>

**TABLE 10.12.**Measurement for each refresh.

<b>SAMPLE 8</b>				
<b>Parameters</b>	<i>Pressure [g]</i>	900		
	<i>Feed rate [mm/s]</i>	0.167		
	<i>Frequency [1/s]</i>	58.33		
<b>Size of the sample</b>	80*63,7 (mm)			
<b>Size of the pad</b>	3*6*15 (mm)			
<b>Passes</b>	<b>T4 Value1 [μm]</b>	<b>T4 Value2 [μm]</b>	<b>T4 Value3 [μm]</b>	<b>Average [μm]</b>
0	0.097	0.072	0.066	<b>0.078</b>
3	0.019	0.016	0.017	<b>0.017</b>
6	0.015	0.015	0.016	<b>0.015</b>
9	0.013	0.014	0.012	<b>0.013</b>
12	0.014	0.013	0.012	<b>0.013</b>
15	0.015	0.012	0.012	<b>0.013</b>

**TABLE 10.13.**Measurement for each refresh.

<b>SAMPLE 9</b>				
<b>Parameters</b>	<i>Pressure [g]</i>	900		
	<i>Feed rate [mm/s]</i>	1.167		
	<i>Frequency [1/s]</i>	33.33		
<b>Size of the sample</b>	80,6*63,75 (mm)			
<b>Size of the pad</b>	3*6*15 (mm)			
<b>Passes</b>	<b>T4 Value1 [μm]</b>	<b>T4 Value2 [μm]</b>	<b>T4 Value3 [μm]</b>	<b>Average [μm]</b>
0	0.056	0.06	0.068	<b>0.061</b>
37	0.028	0.033	0.027	<b>0.029</b>
74	0.018	0.018	0.017	<b>0.018</b>
111	0.014	0.014	0.014	<b>0.014</b>
148	0.013	0.012	0.013	<b>0.013</b>
185	0.017	0.013	0.013	<b>0.014</b>

**TABLE 10.14.**Measurement for each refresh.

<b>SAMPLE 10</b>				
<b>Parameters</b>	Pressure [g]	900		
	Feed rate [mm/s]	0.667		
	Frequency [1/s]	58.33		
<b>Size of the sample</b>	81,9*63,7 (mm)			
<b>Size of the pad</b>	3*6*15 (mm)			
<b>Passes</b>	<b>T4 Value1 [μm]</b>	<b>T4 Value2 [μm]</b>	<b>T4 Value3 [μm]</b>	<b>Average [μm]</b>
0	0.053	0.06	0.057	<b>0.057</b>
12	0.022	0.02	0.023	<b>0.022</b>
24	0.014	0.014	0.014	<b>0.014</b>
36	0.014	0.017	0.013	<b>0.015</b>
48	0.016	0.015	0.014	<b>0.015</b>
60	0.016	0.015	0.015	<b>0.015</b>

**TABLE 10.15.**Measurement for each refresh.

<b>SAMPLE 11</b>				
<b>Parameters</b>	Pressure [g]	500		
	Feed rate [mm/s]	1.167		
	Frequency [1/s]	58.33		
<b>Size of the sample</b>	79,35*63,7 (mm)			
<b>Size of the pad</b>	3*6*15 (mm)			
<b>Passes</b>	<b>T4 Value1 [μm]</b>	<b>T4 Value2 [μm]</b>	<b>T4 Value3 [μm]</b>	<b>Average [μm]</b>
0	0.062	0.06	0.06	<b>0.061</b>
21	0.02	0.023	0.024	<b>0.022</b>
42	0.019	0.017	0.018	<b>0.018</b>
63	0.015	0.018	0.018	<b>0.017</b>
84	0.015	0.02	0.019	<b>0.018</b>
105	0.02	0.019	0.016	<b>0.018</b>

**TABLE 10.16.**Measurement for each refresh.

#### 10.4. Observations related to the first measurements done to estimate $T_4$

The first observation that can be made from these tables, it is that the reached final roughness in these experiments is lower than expected from the literary data for a paste of 14  $\mu\text{m}$ . Therefore there is not agreement with them. Anyway, to be sure of the results obtained from the tests, more precise measurements will must be done in the DTU metrology lab, and deeper considerations regarding this fact will can be elaborated.

The second observation is that for the samples 4, 5, and 7 the final roughness reached in these tests was higher than for the other samples. The cause of these different values is related to the initial roughness of these samples themselves. In fact, compared to the others, the  $R_a$ ,  $R_v$ ,  $R_z$  are very high. The cause of this surface condition for these samples was due to the first transport from the DTU workshop to the lab. In fact, in that moment some scratches have been created on the surface of the samples, but in that moment, they were believed to not create complications.

Anyway, the initial roughness values have been reported in the chapter eight, but to have a quick view of them they are listed below as well:

<b>SAMPLE 4</b>				
<b><math>R_a</math></b>	<b><math>R_z</math></b>	<b><math>R_{zmax}</math></b>	<b><math>R_v</math></b>	<b><math>R_p</math></b>
0.192	1.691	2.096	1.248	0.444

**TABLE 10.17.** Starting roughness parameters. SURSAM data.

<b>SAMPLE 5</b>				
<b><math>R_a</math></b>	<b><math>R_z</math></b>	<b><math>R_{zmax}</math></b>	<b><math>R_v</math></b>	<b><math>R_p</math></b>
0.193	1.877	2.745	1.374	0.503

**TABLE 10.18.** Starting roughness parameters. SURSAM data.

<b>SAMPLE 7</b>				
<b><math>R_a</math></b>	<b><math>R_z</math></b>	<b><math>R_{zmax}</math></b>	<b><math>R_v</math></b>	<b><math>R_p</math></b>
0.164	1.620	2.085	1.220	0.400

**TABLE 10.19.** Starting roughness parameters. SURSAM data.

Moreover, for these last samples the planned down pressure of the pad was 100 grams, that is the lower level for that parameter. This means that the material removal is expected to be low and therefore the timing required to reach final roughness values similar to those reached in the other samples will be longer.

Anyway, these considerations and other more accurate analysis will be done in the following chapters, after the measurements in the DTU metrology lab.

The overall duration of the experimental tests, including the preliminary tests to determine which process parameters affected the abrasive distribution in the polishing zone, has been three weeks. In these three weeks, thirteen samples have been polished, following the experimental planning previously defined and introduced in the chapter six. The first worthy of note observations are that the final roughness value for each sample is clearly lower than expected (that is more or less 30 nanometers bigger). Whereas for the samples 4, 5, and 7 worse roughness values have been reached, probably for the bad initial surface conditions of these samples (see *table 10.17, 10.18, and 10.19* where the average roughness values for samples 4, 5, and 7 are summarized) and to have machined them with low down pressure. Anyway, every consideration and analysis will be done in the following chapters.



# CHAPTER ELEVEN

## Measurements of the samples after the experimental tests

### 11.1. Introduction

After having run with the experimental tests, the roughness and profiles measurements are required to understand what and how the samples are changed after the polishing process. Therefore, the aim of this chapter is to introduce the phase of measurements realized after the experiments with the RAP machine. The measurement instrument employed has always been the Hommel.

### 11.2. Measurements with Hommel

These measurements in this phase are very important, because two different analysis are based on them: the roughness behavior analysis, and the material removal analysis. To make the measurements in the right way is fundamental to obtain reliable analysis.

As explained in the previous paragraph, even here the Hommel is employed to detect the reached roughness in the polished surfaces and to measure the profiles of the machined zone to compute the material removal. It is noteworthy that these last measurements related to the MRR have been done for second. This to not affect the measurements related to the roughness, since the Hommel is an instrument that needs to come in contact with the surface to detect the roughness parameters, and this affects the measured zone because some local plastic deformation are made.

Regarding the roughness measurements, five measurements have been made to characterize each polished surface. This means that for a sample with twelve polished surfaces, sixty measurements are required. The length of the polished area is more or less twenty millimeters, this means that five measurements with an evaluation length of 4.8 mm will estimate the overall roughness field reached after the polishing process. The positions where the measurements have been done are shown below:

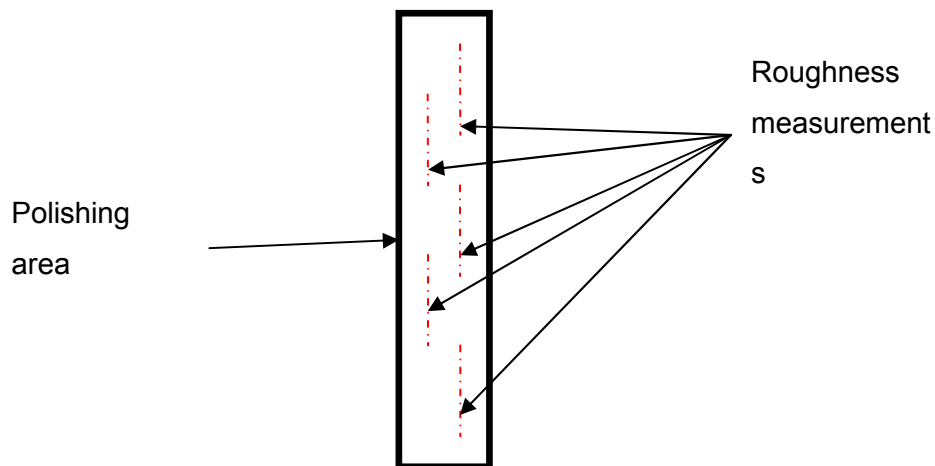


**FIGURE 11.1.** The position of the five measurements made in the same polished area.

The fundamental aspect in these last measurements is that the filters employed to estimate the roughness value in the first measurements (chapter eight) have to be kept constant for these analysis as well. This means that besides the evaluation length of 4.8 mm, the short cut-off filter has to be 2.5  $\mu\text{m}$  and the long cut-off filter has to be 0.8 mm. To keep constant these values is important to obtain comparable results.

Regarding the measurements related to the material removal, they have been done in the same position explained in the chapter eight. In fact, to keep the same position in this case is important to obtain reliable results from the comparison between the profiles before and after polishing. From these data, a profile will be extracted which will be compared with the previous one measured before the experimental tests. From this comparison the polished zone will be determined and the material removal will be computed.

### **11.3. Conclusion**

In conclusion, this part of our work is one of the most important and delicate. It has been important to define how detecting the roughness value in the polished surface, and it has been important to elaborate the obtained results employing always the same filters previously used to measure the samples before the polishing process. In fact, only in this way the measurements can be compared together.

From these data, the overall analysis regarding the material removal and the roughness behavior will be done. This means that much of what will be discussed following, will depend on the good results obtained in this phase. Overall the measurements have taken a week and an half.

# CHAPTER TWELVE

## Analysis of the data

### 12.1. Introduction

In this chapter, the results obtained by the experimental tests and detected in the measurement phase will be shown and explained. The two different analyzed arguments (roughness behavior and verification of the theoretical MRR models respectively) are separately discussed in two different subchapters.

Regarding the roughness behavior, firstly the measurements made with the Hommel on the polished surface are introduced. The main roughness parameters as  $R_a$ ,  $R_v$ , and  $R_z$  and discussed and analyzed. Then the DOE analysis regarding the optimal combination of polishing parameters to obtained the best surface condition in the shortest time is discussed. Finally, the end of this subchapter regards the estimation of some empirical models describing the roughness behavior previously analyzed.

Regarding the MRR analysis, the measured profiles are shown and compared together to determine the amount of material removal caused by the polishing process. From some of them, the amount of found material removal is employed to obtained from the models some constant values which help us to predict the MRR for the other cases that have not been implemented in the models. With this comparison between the experimental data and the predictions coming from the theoretical models (which have been “completed” with part of the experimental data themselves), the correctness of them is verified.

### 12.2. Roughness analysis

#### 12.6.1. Introduction

In the last measurement phase (see chapter eleven), each polished surface has been measured five times to have a good characterization of the overall surface condition in that zone. This means that for a sample with twelve polished surfaces (twelve because we have four timing intervals by three repetitions) the overall measurements are sixty. The direction of the measurement has been parallel to the feed rate direction of the pad. This because this direction is to higher roughness, since the starting grinding process made to prepare the samples for the experimental tests in STRECON was run

in the orthogonal way, that is along the pad oscillation direction. This means that the worse direction of roughness is precisely parallel to the grooves orientation.

Anyway, from each single measurement these roughness parameters have been detected:  $R_a$ ,  $R_z$ ,  $R_{zmax}$ ,  $R_{Sm}$ ,  $R_v$ ,  $R_p$ , and  $P_a$ .

The table below show a example of measurement made in a polished area:

	$R_a$	$R_z$	$R_{zmax}$	$R_{Sm}$	$R_v$	$R_p$	$P_a$
<b>Measurement 1</b>	0.010	0.108	0.160	15.407	0.056	0.052	0.053
<b>Measurement 2</b>	0.012	0.094	0.120	16.866	0.042	0.052	0.061
<b>Measurement 3</b>	0.030	0.288	0.370	32.413	0.202	0.086	0.073
<b>Measurement 4</b>	0.011	0.142	0.260	22.116	0.104	0.038	0.060
<b>Measurement 5</b>	0.011	0.094	0.110	15.622	0.044	0.050	0.047
<b>Measurement Average</b>	0.015	0.145	0.204	20.485	0.09	0.056	0.059
<b>Std</b>	0.009	0.082	0.110	7.202	0.068	0.018	0.010
<b>Std%</b>	58.6	56.6	54.0	35.2	75.5	32.3	16.3

**TABLE 12.1.** Measurements which are related to the sample 00  $T_2$  second repetition (column 2, repetition 2).

As it can be seen from the *table 12.1*, the five measurements have been stored in the first five rows and all the roughness parameters previously introduced have been indicated. In the last three rows, the averages of the measurements and the standard deviations of them have been reported for each parameter (the stored data come from a SURSAM analysis of the ASCII file created by Hommel).

The averages are important values in our analysis. In fact, the graphs describing the roughness behavior for each combination of parameters, and the DOE analysis have been based on these values.

Now the real roughness analysis has begun, considering for first the most common parameter employs to represent the roughness:  $R_a$ , that is equal to the parameter employed by STRECON to verify the goodness of its product. This is the main reason because the  $R_a$  is analyzed in this analysis.

#### 12.6.2. Arithmetical mean roughness ( $R_a$ ) analysis

As it has been anticipated before, from the five measurements made for each polished area, an average value and its corresponding standard deviation have been calculated and this values have been employed to represent the surface condition of the polished area itself.

An example of this is shown below, where the measurements of three polished surfaces situated in the same column are reported (the interested sample is the number 3 and the column is the number 4, corresponding to  $T_4$ ).

	$R_a$	$R_z$	$R_{zmax}$	$RSm$	$R_v$	$R_p$	$Pa$
<b>Measurement 1</b>	0.015	0.112	0.200	20.313	0.068	0.044	8.427
<b>Measurement 2</b>	0.011	0.122	0.250	21.154	0.064	0.058	5.392
<b>Measurement 3</b>	0.010	0.100	0.110	17.912	0.048	0.052	8.803
<b>Measurement 4</b>	0.008	0.074	0.090	15.002	0.034	0.040	7.822
<b>Measurement 5</b>	0.009	0.080	0.120	15.904	0.034	0.046	6.210
<b>Measurement average</b>	0.011	0.098	0.154	18.057	0.05	0.048	7.331
<b>std</b>	0.002	0.02	0.068	2.677	0.016	0.007	1.468
<b>std%</b>	22.8	21.0	44.2	14.8	32.4	14.7	20.0

TABLE 12.2. Sample 03, column 4 repetition 1.

	<i>Ra</i>	<i>Rz</i>	<i>Rzmax</i>	<i>RSm</i>	<i>Rv</i>	<i>Rp</i>	<i>Pa</i>
<b>Measurement 1</b>	0.011	0.140	0.330	33.614	0.088	0.052	5.645
<b>Measurement 2</b>	0.009	0.080	0.100	16.145	0.038	0.042	5.992
<b>Measurement 3</b>	0.009	0.064	0.070	15.229	0.028	0.036	8.570
<b>Measurement 4</b>	0.009	0.084	0.120	16.173	0.042	0.042	8.282
<b>Measurement 5</b>	0.009	0.072	0.090	14.953	0.030	0.042	1.728
<b>Measurement average</b>	0.009	0.088	0.142	19.223	0.045	0.043	6.043
<b>std</b>	0.001	0.03	0.107	8.063	0.025	0.006	2.747
<b>std%</b>	11.8	34.2	75.1	41.9	54.4	13.5	45.5

TABLE 12.3. Sample 03, column 4 repetition 2.

	<i>Ra</i>	<i>Rz</i>	<i>Rzmax</i>	<i>RSm</i>	<i>Rv</i>	<i>Rp</i>	<i>Pa</i>
<b>Measurement 1</b>	0.010	0.088	0.110	16.259	0.038	0.050	0.052
<b>Measurement 2</b>	0.020	0.170	0.360	81.272	0.114	0.056	0.092
<b>Measurement 3</b>	0.009	0.072	0.090	17.032	0.038	0.034	0.076
<b>Measurement 4</b>	0.012	0.126	0.220	19.608	0.072	0.054	0.058
<b>Measurement 5</b>	0.009	0.088	0.170	15.512	0.054	0.034	0.052
<b>Measurement average</b>	0.012	0.109	0.190	29.936	0.063	0.046	0.066
<b>std</b>	0.004	0.04	0.108	28.739	0.032	0.011	0.018
<b>std%</b>	37.5	36.4	56.8	96.0	50.1	23.7	27.0

TABLE 12.4. Sample 03, column 4 repetition 3.

In the *table 12.2, 12.3, and 12.4* the average values and standard deviation employed for the  $R_a$  analysis are underlined in yellow.

Anyway, for each polished area it has been proceeded to report the five corresponding measurements and their respective average and standard deviation. Thus, the obtained results with the corresponding graph are listed below for each combination of parameters:

<b>Sample 0</b>							
<b>Pressure=500g; Feed rate=0.667 mm/s; Frequency=33.33 1/s</b>							
<b>PASSES</b>	<b>TIME (min)</b>	<b>First repetition</b>		<b>Second repetition</b>		<b>Third repetition</b>	
		<b><math>R_{a,avg}</math> (<math>\mu m</math>)</b>	<b>Std</b>	<b><math>R_{a,avg}</math> (<math>\mu m</math>)</b>	<b>Std</b>	<b><math>R_{a,avg}</math> (<math>\mu m</math>)</b>	<b>Std</b>
0	0	0.045	0.004	0.045	0.004	0.045	0.004
11	3.023	0.017	0.002	0.016	0.005	0.021	0.003
32	8.796	0.011	0.001	0.015	0.009	0.012	0.003
53	14.568	0.014	0.001	0.01	0.001	0.011	0.001
105	28.861	0.011	0.001	0.01	0	0.01	0.001

**TABLE12. 5.** Experimental  $R_a$  results.

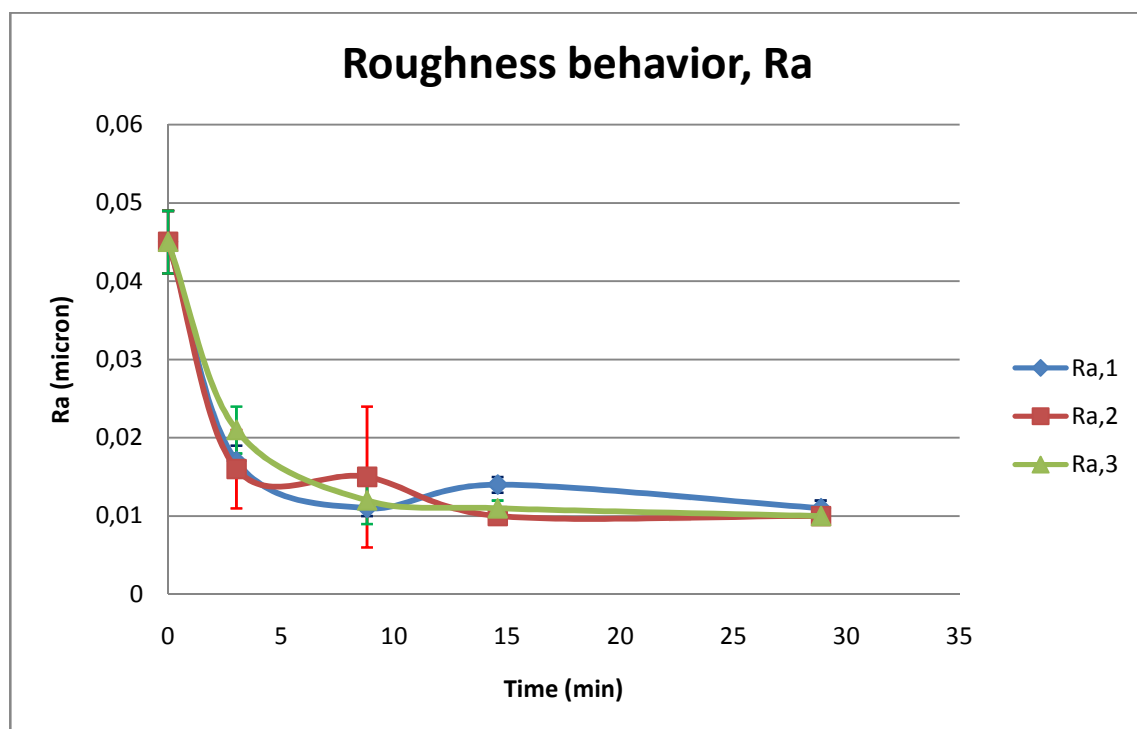


**FIGURE 12.1.** The roughness behavior for the three repetitions, employing  $P=500$  g,  $F=0.667$  mm/s;  $f=33.33$  1/s.



<b>Sample 1</b>							
<b>Pressure=900g; Feed rate=0.167 mm/s; Frequency=8.33 1/s</b>							
<b>PASSES</b>	<b>TIME (min)</b>	<b>First repetition</b>		<b>Second repetition</b>		<b>Third repetition</b>	
		<b><math>R_{a,avg}</math> (<math>\mu m</math>)</b>	<b>Std</b>	<b><math>R_{a,avg}</math> (<math>\mu m</math>)</b>	<b>Std</b>	<b><math>R_{a,avg}</math> (<math>\mu m</math>)</b>	<b>Std</b>
0	0	0.035	0.002	0.035	0.002	0.035	0.002
11	15.369	0.027	0.004	0.026	0.002	0.029	0.004
32	44.711	0.019	0.002	0.018	0.001	0.021	0.006
53	74.052	0.016	0.002	0.016	0.005	0.018	0.002
105	146.707	0.01	0.002	0.011	0.001	0.013	0.004

**TABLE 12.6.** Experimental  $R_a$  results.

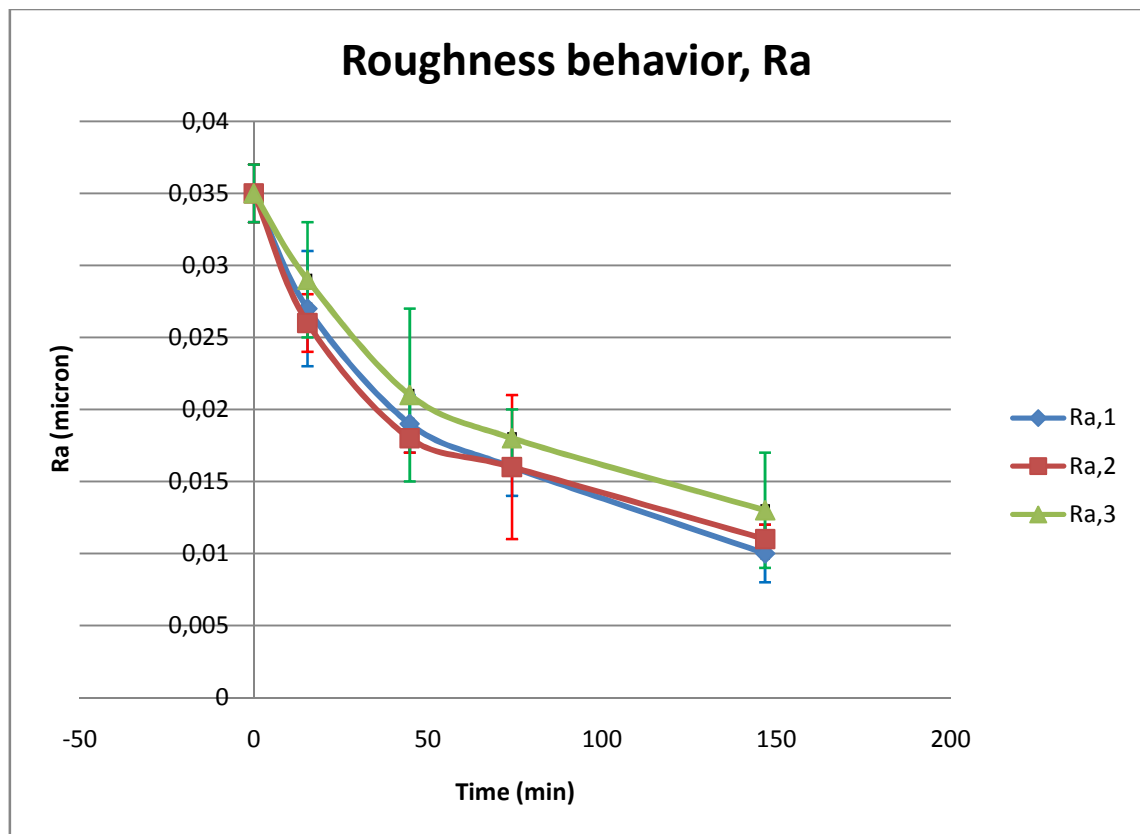


**FIGURE 12.2.** The roughness behavior for the three repetitions, employing  $P=900g$ ,  $F=0.167$  mm/s;  $f=8.33$  1/s.

<b>Sample 2</b>							
<b>Pressure=900g; Feed rate=1.167 mm/s; Frequency=8.33 1/s</b>							
<b>PASSES</b>	<b>TIME (min)</b>	<b>First repetition</b>		<b>Second repetition</b>		<b>Third repetition</b>	
		$R_{a,avg}$ ( $\mu\text{m}$ )	<b>Std</b>	$R_{a,avg}$ ( $\mu\text{m}$ )	<b>Std</b>	$R_{a,avg}$ ( $\mu\text{m}$ )	<b>Std</b>
0	0	0.08	0.014	0.08	0.014	0.08	0.014
83	16.595	0.027	0.005	0.025	0.006	0.037	0.005
265	52.985	0.023	0.007	0.014	0.001	0.024	0.005
441	88.175	0.034	0.013	0.012	0.002	0.014	0.003
882	176.35	0.022	0.006	0.009	0.001	0.015	0.003

**TABLE 12.7.** Experimental  $R_a$  results.

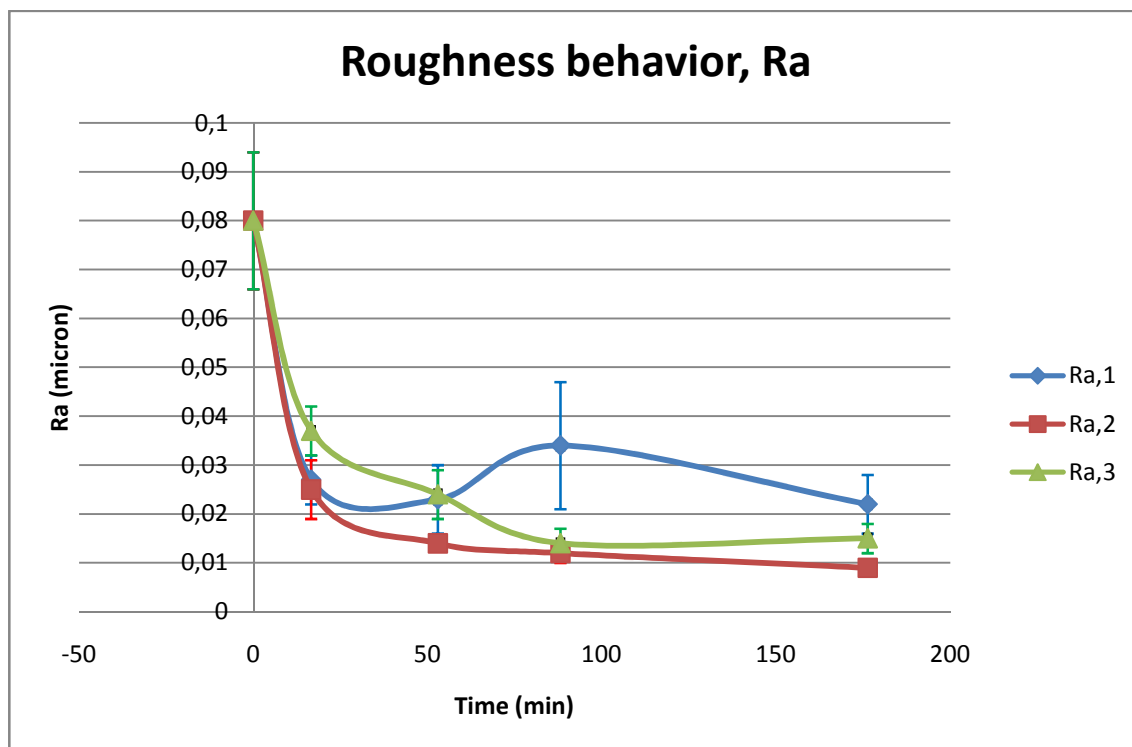


**FIGURE 12.3.** The roughness behavior for the three repetitions, employing  $P=900\text{g}$ ,  $F=1.167\text{ mm/s}$ ;  $f=8.33\text{ 1/s}$ .

<b>Sample 3</b>							
<b>Pressure=900g; Feed rate=1.167 mm/s; Frequency=58.33 1/s</b>							
<b>PASSES</b>	<b>TIME (min)</b>	<b>First repetition</b>		<b>Second repetition</b>		<b>Third repetition</b>	
		$R_{a,avg}$ ( $\mu m$ )	<b>Std</b>	$R_{a,avg}$ ( $\mu m$ )	<b>Std</b>	$R_{a,avg}$ ( $\mu m$ )	<b>Std</b>
0	0	0.087	0.012	0.087	0.012	0.087	0.012
15	2.999	0.03	0.006	0.021	0.003	0.03	0.004
45	8.997	0.017	0.005	0.015	0.003	0.021	0.009
74	14.796	0.009	0.001	0.012	0.005	0.016	0.005
147	29.391	0.011	0.002	0.009	0.001	0.012	0.004

**TABLE12. 8.** Experimental  $R_a$  results.

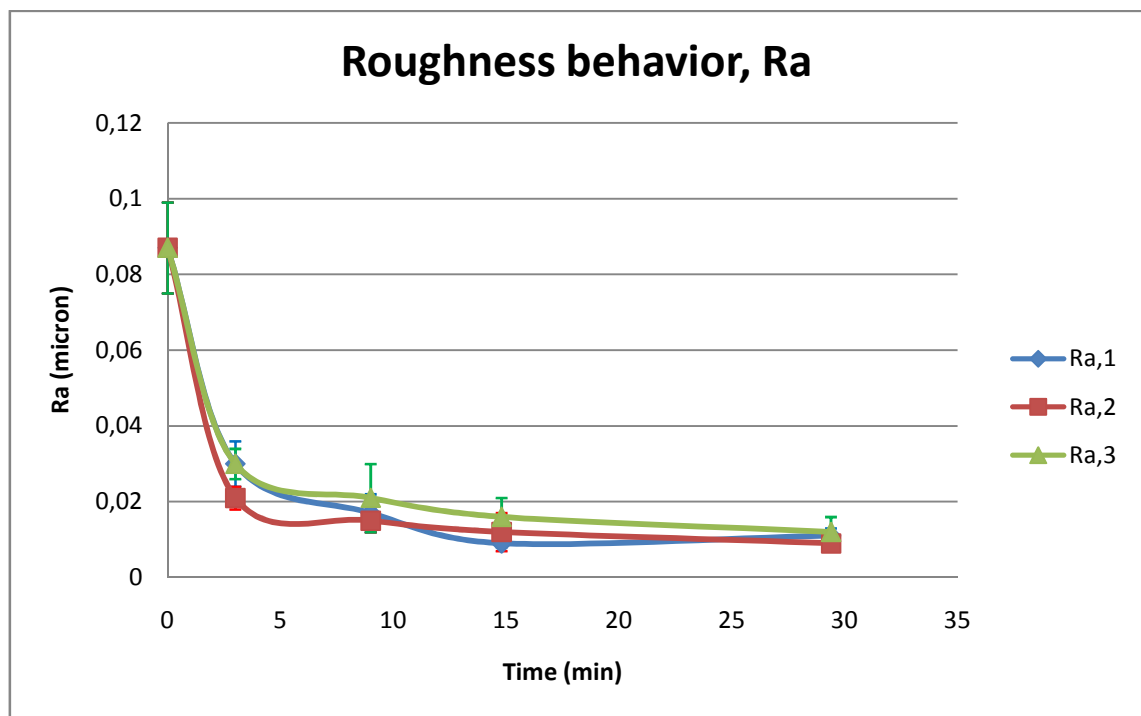


**FIGURE 12.4.** The roughness behavior for the three repetitions, employing  $P=900g$ ,  $F=1.167$  mm/s;  $f=58.33$  1/s.

<b>Sample 4</b>							
<b>Pressure=100g; Feed rate=1.167 mm/s; Frequency=8.33 1/s</b>							
<b>PASSES</b>	<b>TIME (min)</b>	<b>First repetition</b>		<b>Second repetition</b>		<b>Third repetition</b>	
		$R_{a,avg}$ ( $\mu\text{m}$ )	<b>Std</b>	$R_{a,avg}$ ( $\mu\text{m}$ )	<b>Std</b>	$R_{a,avg}$ ( $\mu\text{m}$ )	<b>Std</b>
0	0	0.192	0.02	0.192	0.02	0.192	0.02
133	26.592	0.129	0.027	0.123	0.018	0.135	0.016
397	79.377	0.112	0.005	0.104	0.006	0.09	0.033
662	132.362	0.074	0.008	0.083	0.014	0.085	0.006
1323	264.524	0.053	0.008	0.025	0.003	0.043	0.005

**TABLE 12.9.** Experimental  $R_a$  results.

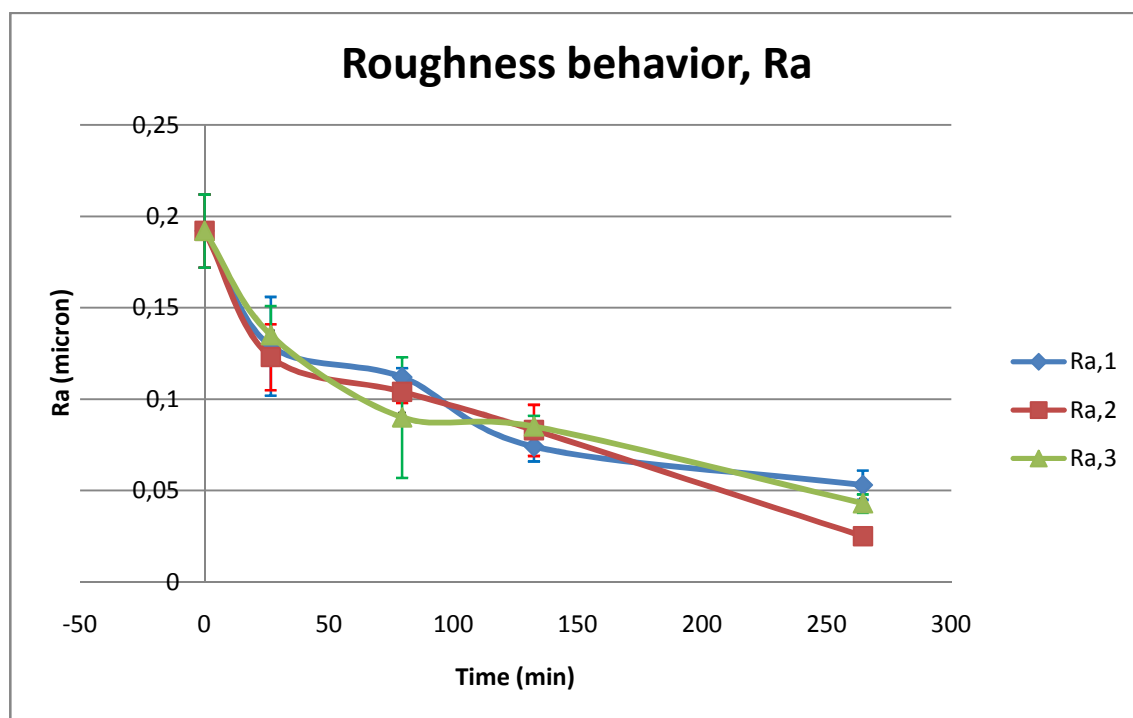


**FIGURE 12.5.** The roughness behavior for the three repetitions, employing  $P=100\text{g}$ ,  $F=1.167\text{ mm/s}$ ;  $f=8.33\text{ 1/s}$ .

<b>Sample 5</b>							
<b>Pressure=100g; Feed rate=1.167 mm/s; Frequency=58.33 1/s</b>							
<b>PASSES</b>	<b>TIME (min)</b>	<b>First repetition</b>		<b>Second repetition</b>		<b>Third repetition</b>	
		$R_{a,avg}$ ( $\mu\text{m}$ )	<b>Std</b>	$R_{a,avg}$ ( $\mu\text{m}$ )	<b>Std</b>	$R_{a,avg}$ ( $\mu\text{m}$ )	<b>Std</b>
0	0	0.193	0.012	0.193	0.012	0.193	0.012
47	9.397	0.112	0.01	0.13	0.011	0.127	0.008
139	27.792	0.072	0.009	0.077	0.004	0.09	0.014
231	46.187	0.059	0.01	0.056	0.005	0.074	0.012
462	92.374	0.034	0.003	0.044	0.005	0.05	0.007

**TABLE 12.10.** Experimental  $R_a$  results.

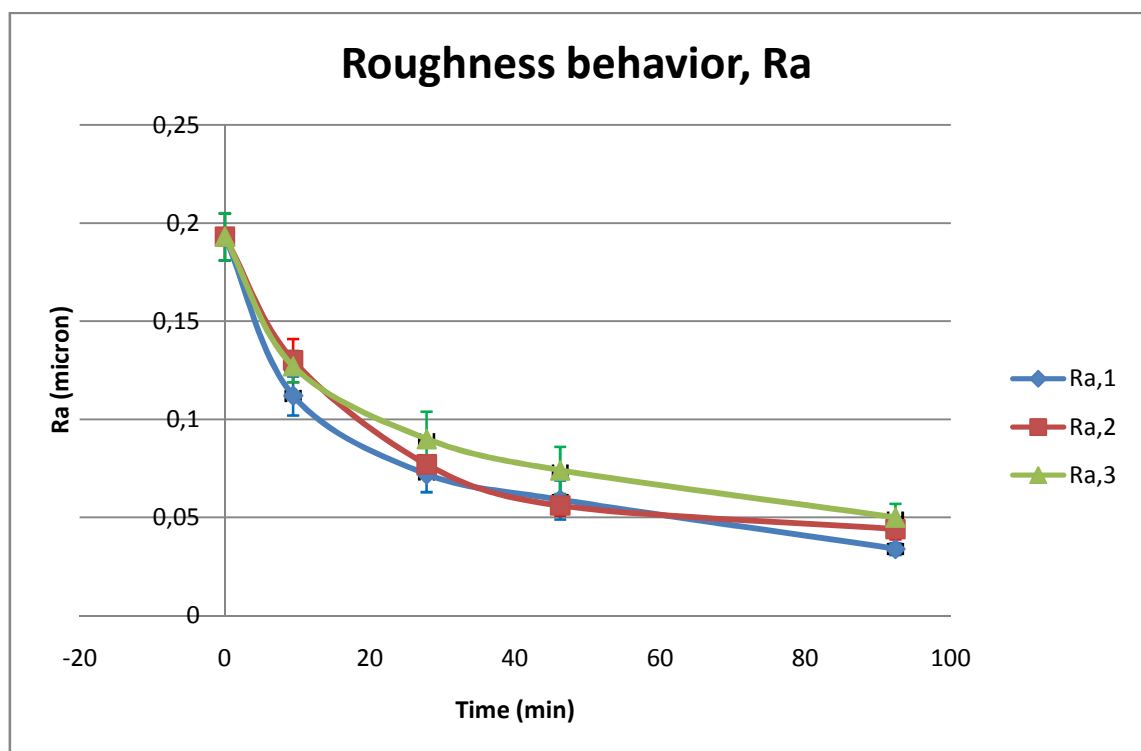


**FIGURE 12.6.** The roughness behavior for the three repetitions, employing  $P=100\text{g}$ ,  $F=1.167\text{ mm/s}$ ;  $f=58.33\text{ 1/s}$ .

<b>Sample 6</b>							
<b>Pressure=100g; Feed rate=0.167 mm/s; Frequency=8.33 1/s</b>							
<b>PASSES</b>	<b>TIME (min)</b>	<b>First repetition</b>		<b>Second repetition</b>		<b>Third repetition</b>	
		<i>R<sub>a,avg</sub></i> ( $\mu\text{m}$ )	<b>Std</b>	<i>R<sub>a,avg</sub></i> ( $\mu\text{m}$ )	<b>Std</b>	<i>R<sub>a,avg</sub></i> ( $\mu\text{m}$ )	<b>Std</b>
0	0	0.045	0.006	0.045	0.006	0.045	0.006
11	15.369	0.039	0.004	0.035	0.002	0.04	0.005
32	44.711	0.023	0.003	0.024	0.003	0.026	0.006
53	74.052	0.022	0.006	0.022	0.005	0.031	0.005
105	146.707	0.014	0.003	0.016	0.002	0.025	0.003

**TABLE 12.11.** Experimental  $R_a$  results.

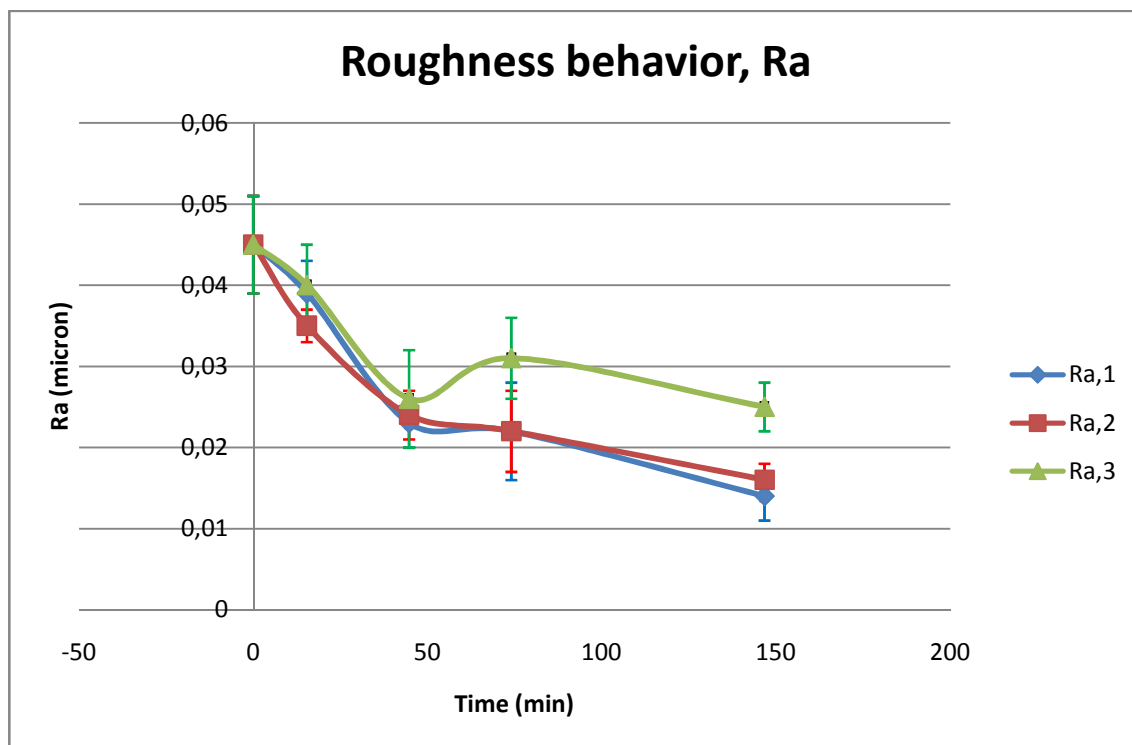


**FIGURE 12.7.** The roughness behavior for the three repetitions, employing  $P=100\text{g}$ ,  $F=0.167\text{ mm/s}$ ;  $f=8.331/\text{s}$ .

<b>Sample 7</b>							
<b>Pressure=100g; Feed rate=0.167 mm/s; Frequency=58.33 1/s</b>							
<b>PASSES</b>	<b>TIME (min)</b>	<b>First repetition</b>		<b>Second repetition</b>		<b>Third repetition</b>	
		$R_{a,avg}$ ( $\mu m$ )	<b>Std</b>	$R_{a,avg}$ ( $\mu m$ )	<b>Std</b>	$R_{a,avg}$ ( $\mu m$ )	<b>Std</b>
0	0	0.164	0.016	0.164	0.016	0.164	0.016
7	9.780	0.098	0.005	0.1	0.015	0.125	0.016
19	26.547	0.093	0.005	0.07	0.008	0.064	0.002
32	44.711	0.053	0.008	0.05	0.003	0.063	0.005
63	88.024	0.049	0.004	0.033	0.012	0.044	0.003

**TABLE 12.12.** Experimental  $R_a$  results.

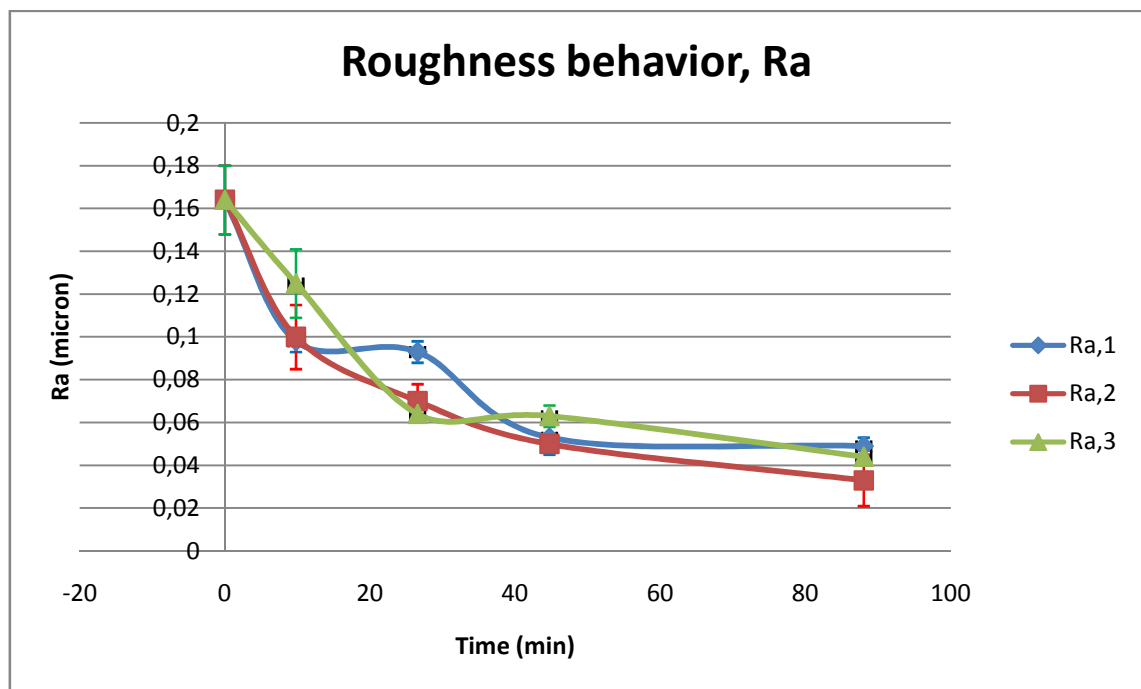


**FIGURE 12.8.** The roughness behavior for the three repetitions, employing  $P=100g$ ,  $F=0.167$  mm/s;  $f=58.33$  1/s.

<b>Sample 8</b>							
<b>Pressure=900g; Feed rate=0.167 mm/s; Frequency=58.33 1/s</b>							
<b>PASSES</b>	<b>TIME (min)</b>	<b>First repetition</b>		<b>Second repetition</b>		<b>Third repetition</b>	
		$R_{a,avg}$ ( $\mu\text{m}$ )	<b>Std</b>	$R_{a,avg}$ ( $\mu\text{m}$ )	<b>Std</b>	$R_{a,avg}$ ( $\mu\text{m}$ )	<b>Std</b>
0	0	0.042	0.005	0.042	0.005	0.042	0.005
2	2.794	0.015	0.002	0.011	0.001	0.012	0.002
5	6.986	0.012	0.004	0.01	0.001	0.011	0.004
8	11.178	0.01	0.002	0.012	0.004	0.009	0.002
15	20.958	0.013	0.001	0.011	0.003	0.01	0.002

**TABLE 12.13.** Experimental  $R_a$  results.

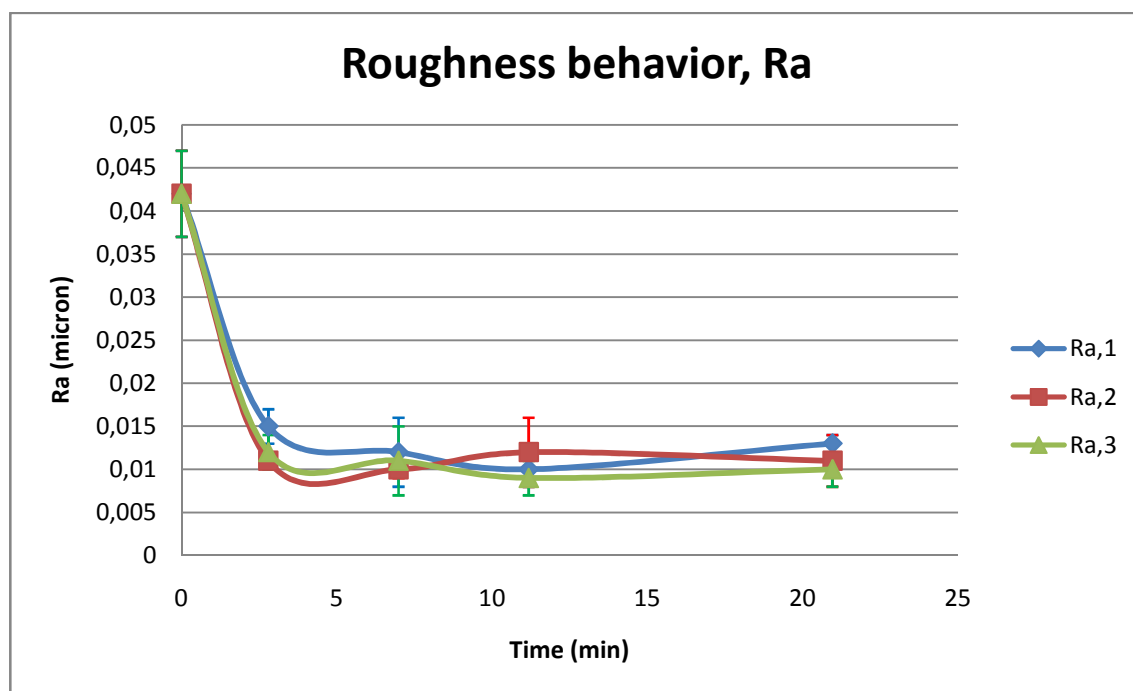


**FIGURE 12.9.** The roughness behavior for the three repetitions, employing  $P=900\text{g}$ ,  $F=0.167\text{ mm/s}$ ;  $f=58.33\text{ 1/s}$ .



<b>Sample 9</b>							
<b>Pressure=900g; Feed rate=1.167 mm/s; Frequency=33.33 1/s</b>							
<b>PASSES</b>	<b>TIME (min)</b>	<b>First repetition</b>		<b>Second repetition</b>		<b>Third repetition</b>	
		$R_{a,avg}$ ( $\mu m$ )	<b>Std</b>	$R_{a,avg}$ ( $\mu m$ )	<b>Std</b>	$R_{a,avg}$ ( $\mu m$ )	<b>Std</b>
0	0	0.054	0.004	0.054	0.004	0.054	0.004
19	3.799	0.024	0.007	0.025	0.008	0.02	0.001
56	11.197	0.012	0.004	0.017	0.007	0.015	0.004
93	18.595	0.013	0.002	0.013	0.006	0.011	0.001
185	36.989	0.01	0.001	0.011	0.002	0.009	0

**TABLE 12.14.** Experimental  $R_a$  results.

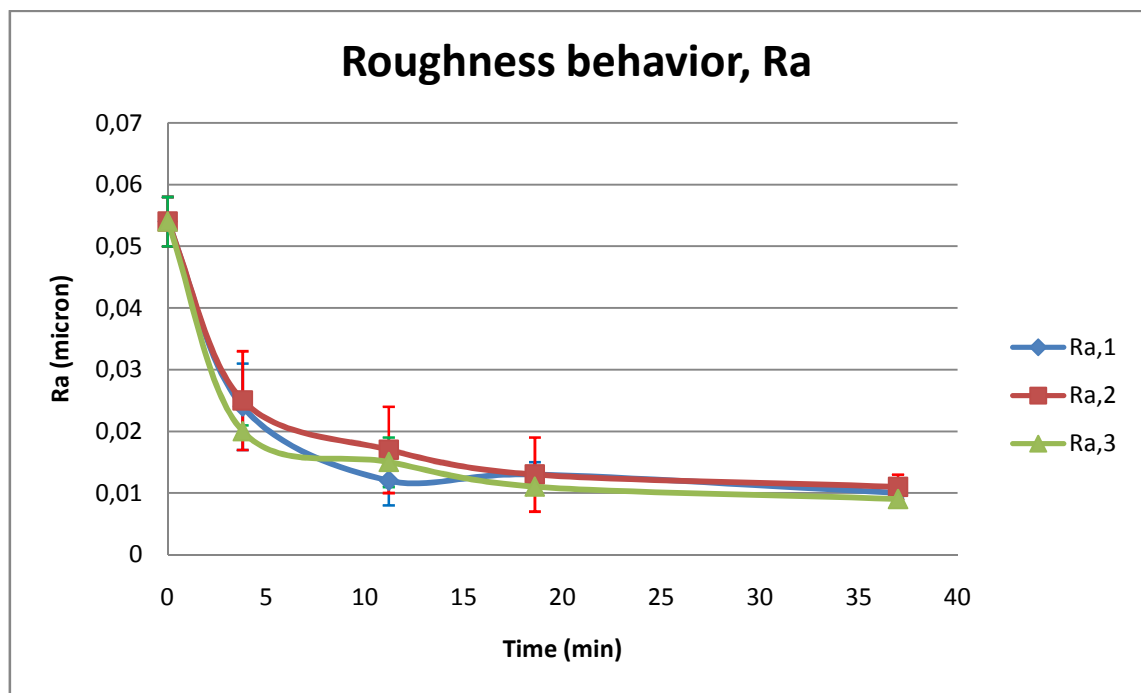


**FIGURE 12.10.** The roughness behavior for the three repetitions, employing  $P=900g$ ,  $F=1.167$  mm/s;  $f=33.33$  1/s.

<b>Sample 10</b>							
<b>Pressure=900g; Feed rate=0.667 mm/s; Frequency=58.33 1/s</b>							
<b>PASSES</b>	<b>TIME (min)</b>	<b>First repetition</b>		<b>Second repetition</b>		<b>Third repetition</b>	
		$R_{a,avg}$ ( $\mu\text{m}$ )	<b>Std</b>	$R_{a,avg}$ ( $\mu\text{m}$ )	<b>Std</b>	$R_{a,avg}$ ( $\mu\text{m}$ )	<b>Std</b>
0	0	0.056	0.005	0.056	0.005	0.056	0.005
6	2.099	0.024	0.002	0.032	0.003	0.029	0.002
18	6.297	0.015	0.001	0.015	0.001	0.016	0.004
30	10.495	0.01	0.001	0.011	0.001	0.013	0.003
60	20.99	0.015	0.003	0.015	0.003	0.01	0.001

**TABLE 12.15.** Experimental  $R_a$  results.

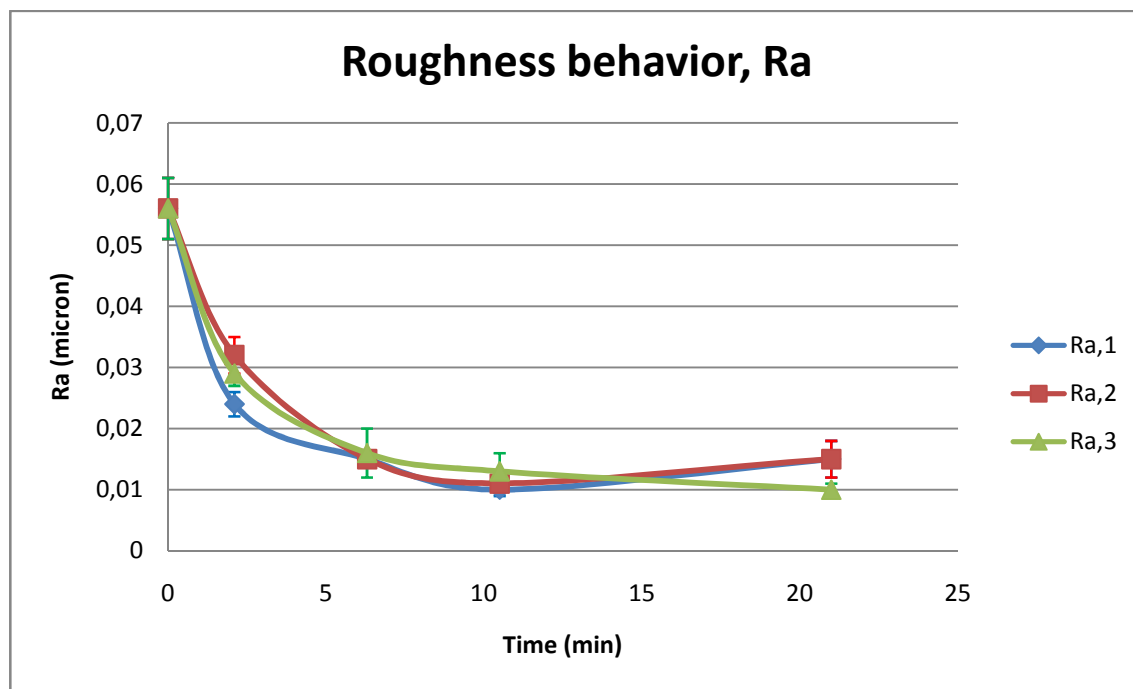


**FIGURE 12.11.** The roughness behavior for the three repetitions, employing  $P=900\text{g}$ ,  $F=0.667\text{ mm/s}$ ;  $f=58.33\text{ 1/s}$ .

<b>Sample 11</b>							
<b>Pressure=500g; Feed rate=1.167 mm/s; Frequency=58.33 1/s</b>							
<b>PASSES</b>	<b>TIME (min)</b>	<b>First repetition</b>		<b>Second repetition</b>		<b>Third repetition</b>	
		$R_{a,avg}$ ( $\mu m$ )	<b>Std</b>	$R_{a,avg}$ ( $\mu m$ )	<b>Std</b>	$R_{a,avg}$ ( $\mu m$ )	<b>Std</b>
0	0	0.055	0.005	0.055	0.005	0.055	0.005
11	2.199	0.021	0.003	0.023	0.003	0.028	0.001
32	6.398	0.016	0.001	0.015	0.002	0.017	0.001
53	10.597	0.015	0.003	0.015	0.001	0.014	0.002
105	20.994	0.014	0.002	0.013	0.001	0.015	0.002

**TABLE 12.16.** Experimental  $R_a$  results.

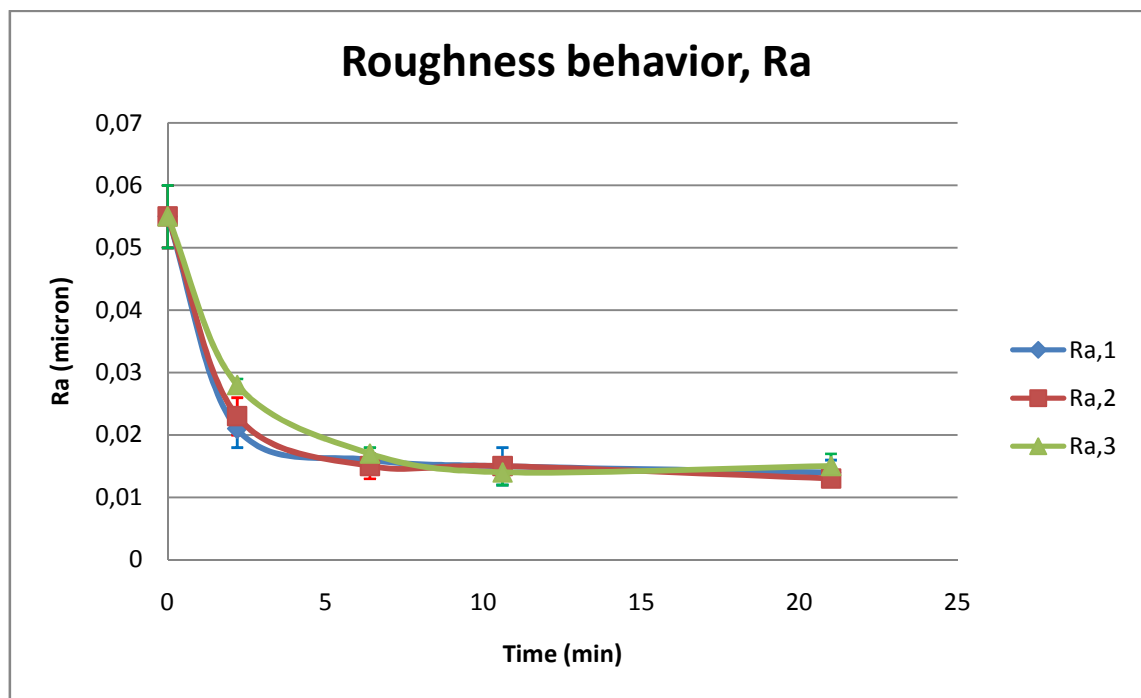


**FIGURE 12.12.** The roughness behavior for the three repetitions, employing  $P=500g$ ,  $F=1.167$  mm/s;  $f=58.33$  1/s.

As it can be seen from the *tables 12.5-12.16*, these first results say that the expected theoretical roughness behavior is respected in all the combinations of parameters, therefore the roughness curve confirms to have a rapid descend in the beginning of its life and a almost flat trend when the final roughness value is going to be reached.

Moreover, it can be seen from the tables that the theoretical starting roughness of  $0.14 \mu\text{m}$  has not been respected. In fact the starting roughness appears very far from the value of  $0.14 \mu\text{m}$  for every sample. Moreover the final roughness value is not perfectly the same for all the samples. In fact, regarding this last observation, it can be seen that for the combinations of parameters employing a down pressure of 100g (that is samples 4, 5, 6, and 7) the final roughness value is average higher than the others using pressure values from 500g to 900g. This has been mainly caused by three coexisting factors:

- The first one is related to the method employed to estimate the  $T_4$  and, therefore, to stop the polishing process for a particular machined surface (see chapter ten);
- The second one is related to the applied down pressure, in fact if the employed down pressure is very low, the amount of material removal for each pass of the pad on the machining area will be very small;
- The third one is related to the starting roughness conditions of the interested samples. In fact, they show to have the worse roughness relative to the others in the beginning of the experiments (this is not true for the sample 6).

In fact, if the starting roughness is high, this means that the considered surface is rich of higher peaks or deeper valleys relative to the other surfaces where the roughness is low. In particular, in our case, the high starting roughness of the sample 4, 5, and 7 has not been involved by the presence of high peaks (this because the samples were ground), but for the presence of deep valley caused by scratches. Therefore, to obtain a good final surface condition it is necessary to remove more material from the surface, but the employed down pressure was low and to remove a big amount of material the necessary time becomes great (in fact, polishing process is not the suitable technique to remove scratches from the surface of the part). Finally, the methodology chosen to stop with the polishing process has concurred to have a higher final roughness value too. In fact, during the process, due to the deep scratches and the low MRR, the measurements have found a stability point where the values remained more or less constant (an example is provided by the sample 7, where the last six measurements before deciding to stop the process have been:  $0.061 \mu\text{m}$ ,  $0.055 \mu\text{m}$ ,  $0.054 \mu\text{m}$ ,  $0.05 \mu\text{m}$ ,  $0.053 \mu\text{m}$ , and  $0.05 \mu\text{m}$ ). Since this stability point was on the range of 50 nanometers or less, it was decided to stop the process.

An example can be readily shown. Remembering that for the sample 6 the final roughness is close to the value reached by the most polished samples because the starting condition of the surface were very good, the average value of the main roughness parameters when the samples 4, 5, and 7 were not polished are listed below and compared with a sample where the starting surface condition were good. The chosen sample of comparison is the number 1:

<b>Samples</b>	<b>R<sub>a</sub></b>	<b>R<sub>z</sub></b>	<b>R<sub>zmax</sub></b>	<b>R<sub>Sm</sub></b>	<b>R<sub>v</sub></b>	<b>R<sub>p</sub></b>	<b>P<sub>a</sub></b>
<b>Sample 1</b>	0.045	0.449	0.624	26.761	0.295	0.154	0.078
<b>Sample 4</b>	0.192	1.691	2.096	32.898	1.248	0.444	0.222
<b>Sample 5</b>	0.193	1.877	2.745	36.548	0.374	0.503	0.224
<b>Sample 7</b>	0,164	1.62	2.085	30.680	1.22	0.400	0.192

**TABLE 12.17.** Comparison between the scratched samples and a normal one. The values are in micron.

As it can be seen from the *table 12.17*, for the three scratched samples the  $R_z$  is about four times bigger than the good one (sample 1). This means that the presence of the scratches is important and strongly affects the initial surface conditions. This is confirmed again by the presence of high values for  $R_v$  that represents the maximum valley depth. As it can be seen, this value can reach the  $1.248 \mu m$ , five time bigger than sample 1 (0.295). Moreover, the  $P_a$  value itself is very high for these samples, in fact it does not go under  $0.192 \mu m$ .

With the previous example it is clear that the three factors (low pressure, high starting roughness, and “stopping methodology”) interacting together have affected the final roughness value and the evaluation of  $T_4$ , for these three analyzed sample.

The lack of homogeneity in the starting and final roughness values of the samples imply that to do the DOE analysis some assumptions have to be done. In fact, the only output of interest has to be the time required to reach the final roughness value. Therefore, this final roughness value has to be assumed and taken as constant for all the samples. Also the starting roughness have to be assumed and kept constant. This means some preliminary regression models which describe well the roughness curves for each combination of parameters, have to be found and used to estimate the  $T_4$  required to reach a common final value from a common starting value. Anyway, this argument will be discussed when the DOE analysis will be introduced.

### 12.6.3. Maximum profile valley depth ( $R_v$ ) analysis

It is interesting to analyze how the process affects not only the average aspect of the surface, but the depth of the valleys too. In fact, the height of the peaks is very limited in this case, because the sample have been ground. The starting maximum heights of them were between the 0.100  $\mu\text{m}$  and 0.200  $\mu\text{m}$  (except for the three scratched samples where the maximum peaks are between the 0.400  $\mu\text{m}$  and 0.500  $\mu\text{m}$ , but these have been exceptions), to arrive in the end at maximum heights between 0.070  $\mu\text{m}$  and 0.050  $\mu\text{m}$  (except for the scratched samples where the maximum peaks have remained higher than 0.100  $\mu\text{m}$ ). Therefore, it does not make interest analyze the variation of them

Also because, in a process where the machining part should not have important peaks to remove, the decrease of the roughness value is mainly determined by the decrease of the depth of the present valley. This is the main reason due to the depth of the valley behavior is more interesting than the height of the peaks behavior in this case.

As it has been done for the arithmetical mean roughness parameter, now the average values for the  $R_v$  parameter with the standard deviation will be listed in the tables below.

<b>Sample 0</b>							
<b>Pressure=500 g; Feed rate=0.667 mm/s; Frequency=33.33 1/s</b>							
<b>PASSES</b>	<b>TIME (min)</b>	<b>First repetition</b>		<b>Second repetition</b>		<b>Third repetition</b>	
		$R_{v,avg}$ ( $\mu m$ )	<b>Std</b>	$R_{v,avg}$ ( $\mu m$ )	<b>Std</b>	$R_{v,avg}$ ( $\mu m$ )	<b>Std</b>
0	0	0.295	0.047	0.295	0.047	0.295	0.047
11	3.023	0.12	0.045	0.112	0.027	0.187	0.029
32	8.796	0.04	0.004	0.09	0.068	0.081	0.059
53	14.568	0.065	0.028	0.05	0.02	0.076	0.041
105	28.861	0.051	0.023	0.048	0.006	0.058	0.043

**TABLE 12.18.** Experimental  $R_a$  results.

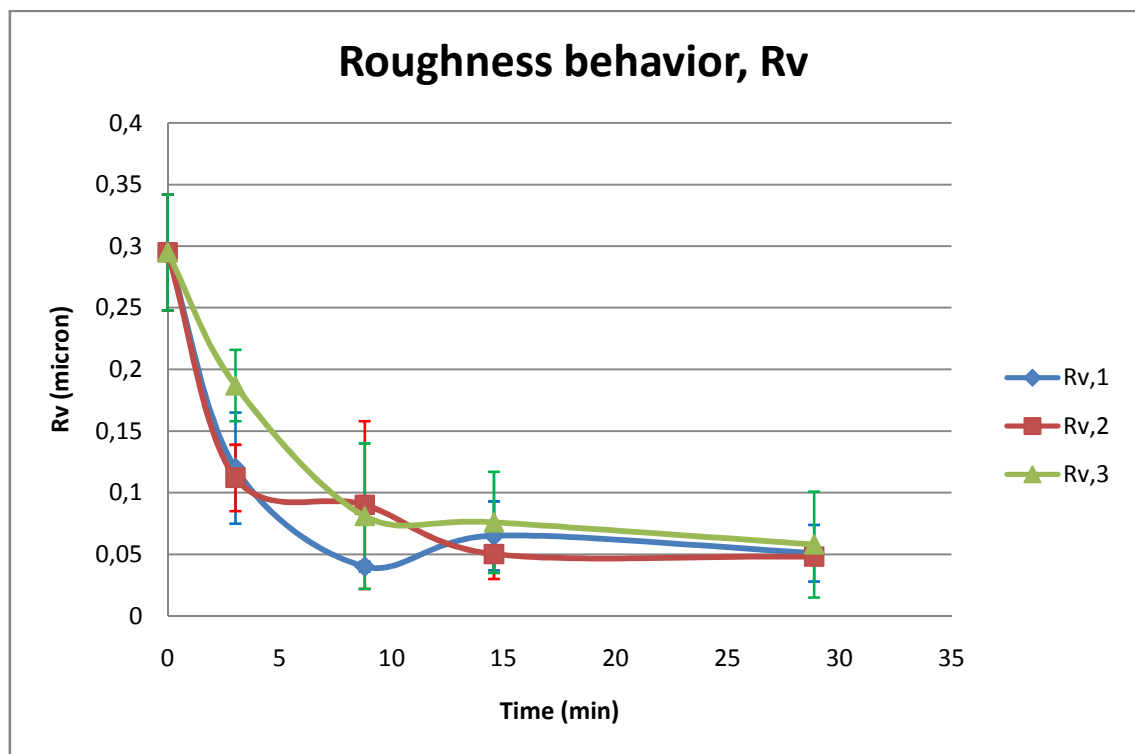


**FIGURE 12.13.** The roughness behavior for the three repetitions, employing  $P=500$  g,  $F=0.667$  mm/s;  $f=33.33$  1/s.

<b>Sample 1</b>							
<b>Pressure=900g; Feed rate=0.167 mm/s; Frequency=8.33 1/s</b>							
<b>PASSES</b>	<b>TIME (min)</b>	<b>First repetition</b>		<b>Second repetition</b>		<b>Third repetition</b>	
		$R_{v,avg}$ ( $\mu\text{m}$ )	<b>Std</b>	$R_{v,avg}$ ( $\mu\text{m}$ )	<b>Std</b>	$R_{v,avg}$ ( $\mu\text{m}$ )	<b>Std</b>
0	0	0.259	0.033	0.259	0.033	0.259	0.033
11	15.369	0.248	0.074	0.22	0.061	0.254	0.124
32	44.711	0.126	0.019	0.182	0.07	0.141	0.06
53	74.052	0.134	0.035	0.102	0.042	0.152	0.078
105	146.707	0.047	0.023	0.054	0.035	0.063	0.026

**TABLE 12.19.** Experimental  $R_a$  results.

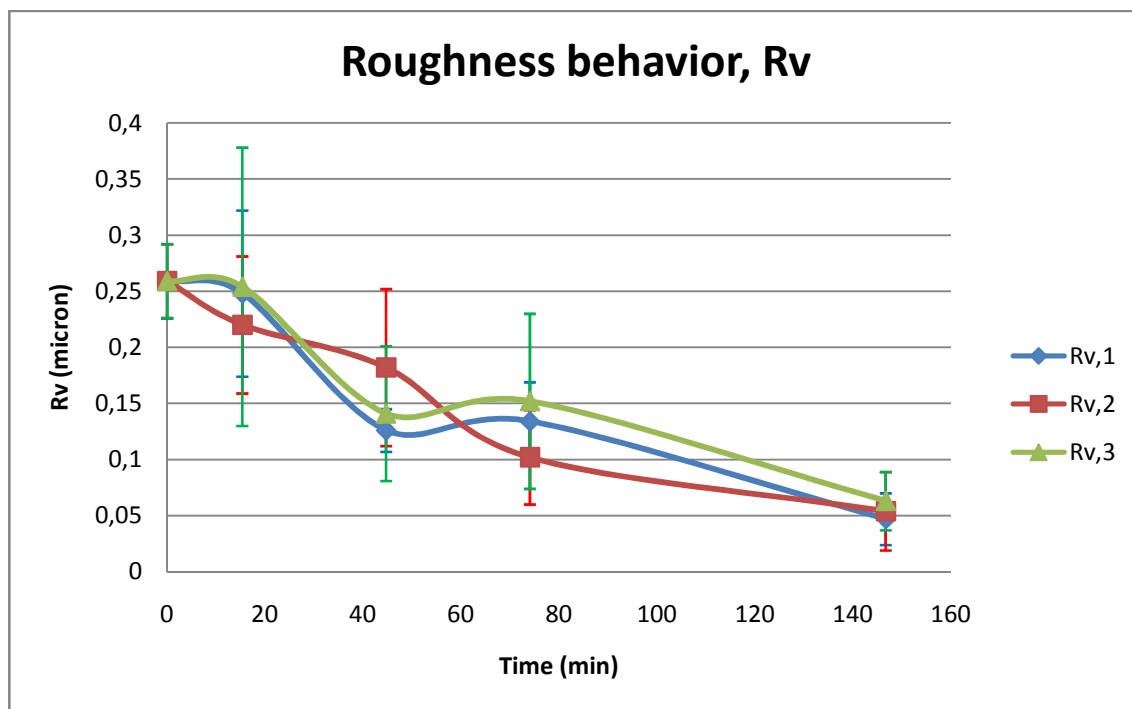


**FIGURE 12.14.** The roughness behavior for the three repetitions, employing  $P=900\text{g}$ ,  $F=0.167\text{ mm/s}$ ;  $f=8.33\text{ 1/s}$ .



<b>Sample 2</b>							
<b>Pressure=900g; Feed rate=1.167 mm/s; Frequency=8.33 1/s</b>							
<b>PASSES</b>	<b>TIME (min)</b>	<b>First repetition</b>		<b>Second repetition</b>		<b>Third repetition</b>	
		$R_{v,avg}$ ( $\mu\text{m}$ )	<b>Std</b>	$R_{v,avg}$ ( $\mu\text{m}$ )	<b>Std</b>	$R_{v,avg}$ ( $\mu\text{m}$ )	<b>Std</b>
0	0	0.696	0.19	0.696	0.19	0.696	0.19
83	16.595	0.345	0.042	0.302	0.165	0.494	0.14
265	52.985	0.372	0.169	0.196	0.086	0.367	0.181
441	88.175	0.484	0.243	0.119	0.095	0.147	0.107
882	176.35	0.198	0.178	0.044	0.025	0.137	0.081

**TABLE 12.20.** Experimental  $R_a$  results.

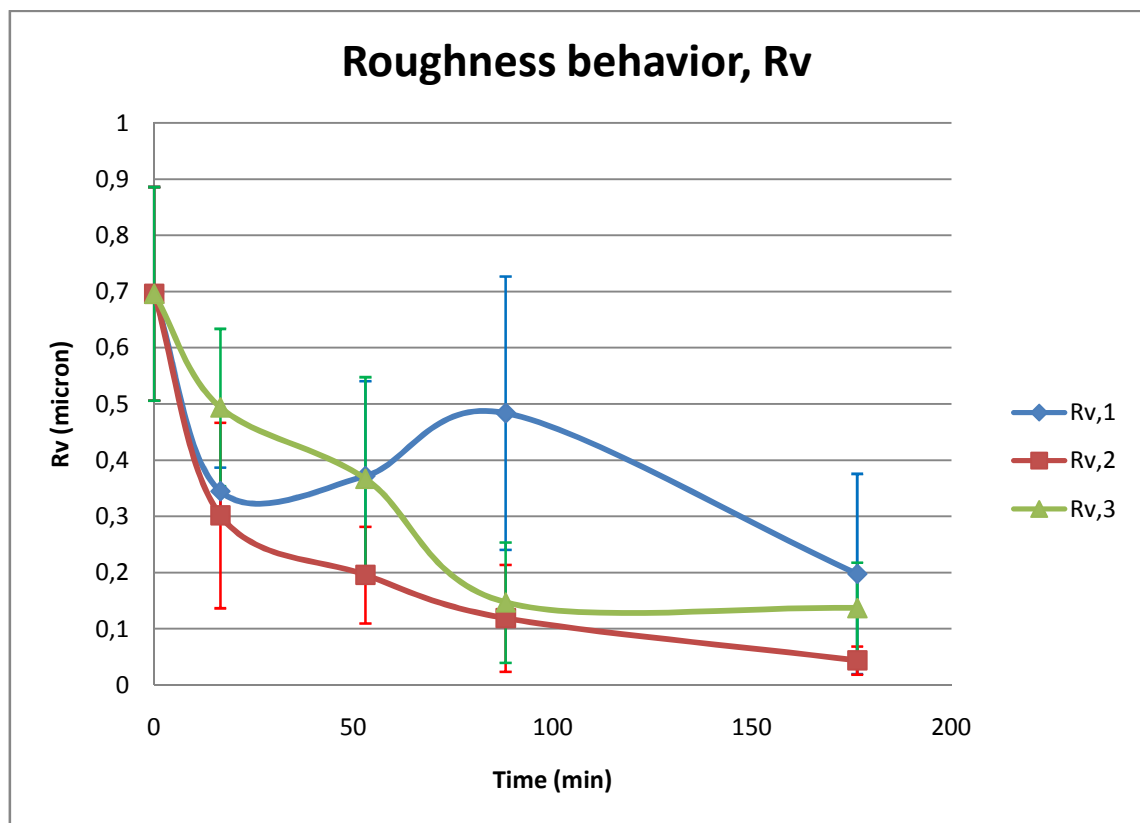


**FIGURE 12.15.** The roughness behavior for the three repetitions, employing  $P=900\text{g}$ ,  $F=1.167\text{ mm/s}$ ;  $f=8.33\text{ 1/s}$ .

<b>Sample 3</b>							
<b>Pressure=900g; Feed rate=1.167 mm/s; Frequency=58.33 1/s</b>							
<b>PASSES</b>	<b>TIME (min)</b>	<b>First repetition</b>		<b>Second repetition</b>		<b>Third repetition</b>	
		$R_{v,avg}$ ( $\mu\text{m}$ )	<b>Std</b>	$R_{v,avg}$ ( $\mu\text{m}$ )	<b>Std</b>	$R_{v,avg}$ ( $\mu\text{m}$ )	<b>Std</b>
0	0	0.736	0.136	0.736	0.136	0.736	0.136
15	2.999	0.46	0.201	0.304	0.149	0.35	0.069
45	8.997	0.204	0.171	0.182	0.123	0.237	0.182
74	14.796	0.044	0.018	0.12	0.111	0.119	0.104
147	29.392	0.05	0.016	0.045	0.025	0.063	0.032

**TABLE 12.21.** Experimental  $R_a$  results.

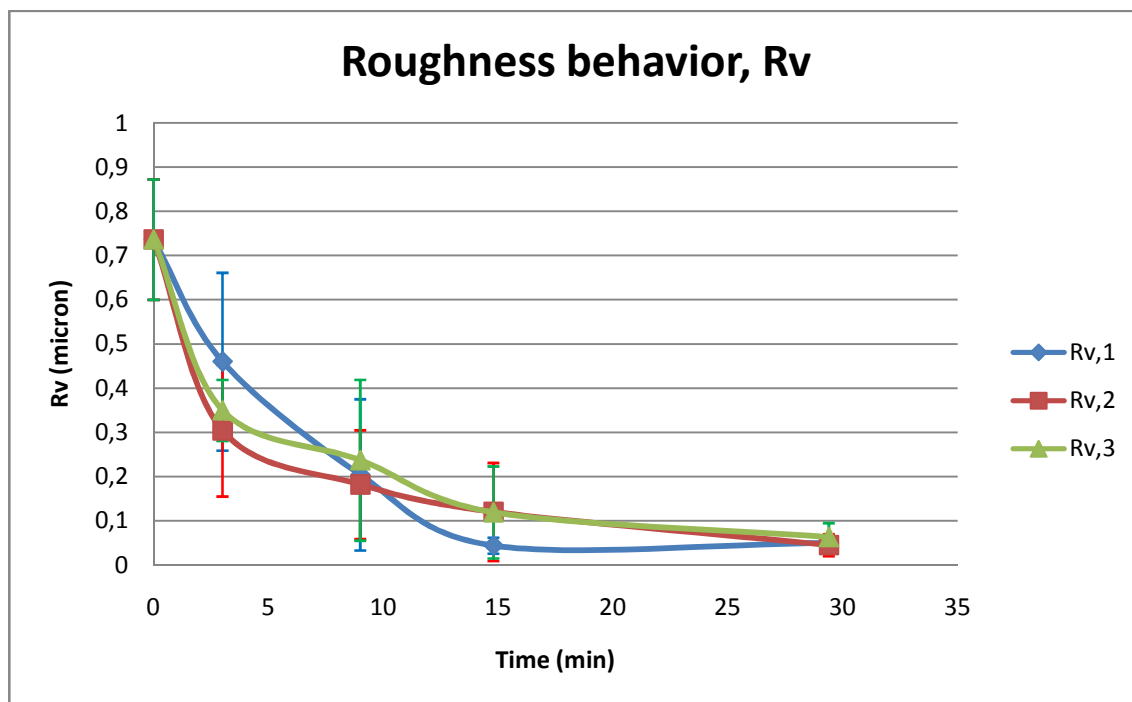


**FIGURE 12.16.** The roughness behavior for the three repetitions, employing  $P=900\text{g}$ ,  $F=1.167\text{ mm/s}$ ;  $f=58.33\text{ 1/s}$ .

<b>Sample 4</b>							
<b>Pressure=100g; Feed rate=1.167 mm/s; Frequency=8.33 1/s</b>							
<b>PASSES</b>	<b>TIME (min)</b>	<b>First repetition</b>		<b>Second repetition</b>		<b>Third repetition</b>	
		$R_{v,avg}$ ( $\mu\text{m}$ )	<b>Std</b>	$R_{v,avg}$ ( $\mu\text{m}$ )	<b>Std</b>	$R_{v,avg}$ ( $\mu\text{m}$ )	<b>Std</b>
0	0	1.248	0.137	1.248	0.137	1.248	0.137
133	26.592	1.1	0.243	1.14	0.21	1.051	0.05
397	79.377	0.942	0.107	1.161	0.052	0.816	0.202
662	132.362	0.71	0.098	1.007	0.182	0.707	0.111
1323	264.524	0.558	0.085	0.428	0.089	0.341	0.043

**TABLE 12.22.** Experimental  $R_a$  results.

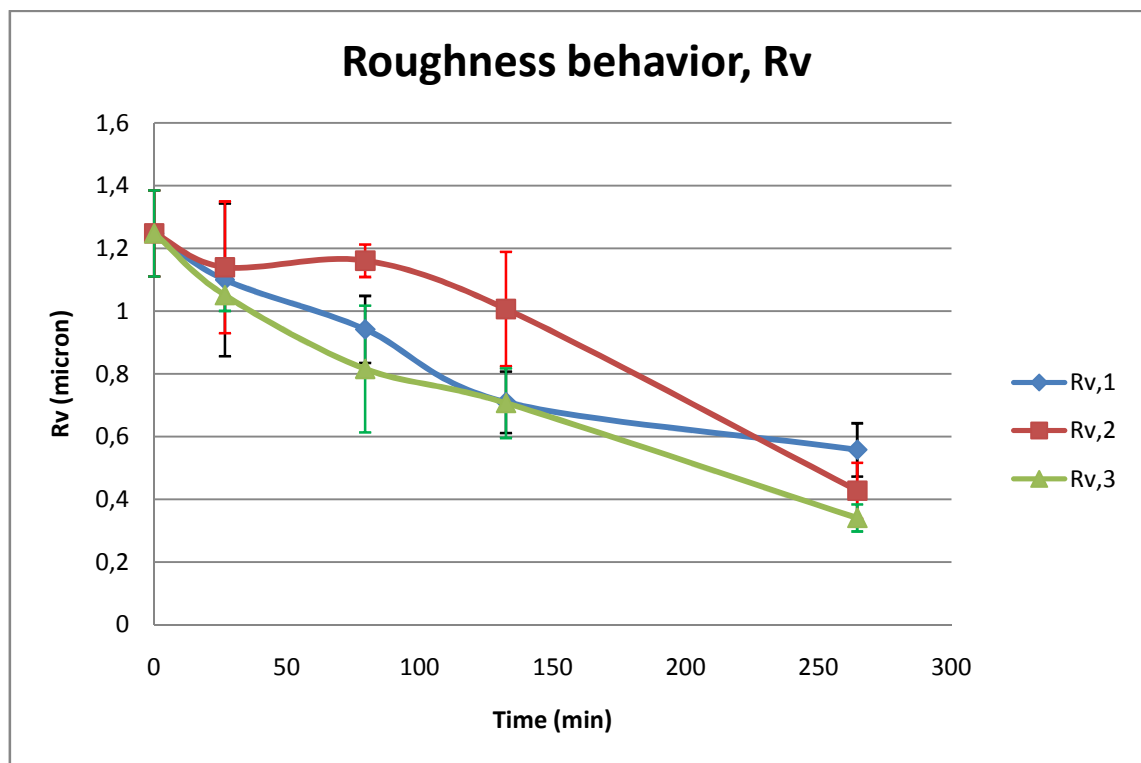


**FIGURE 12.17.** The roughness behavior for the three repetitions, employing  $P=100\text{g}$ ,  $F=1.167\text{ mm/s}$ ;  $f=8.33\text{ 1/s}$ .

<b>Sample 5</b>							
<b>Pressure=100g; Feed rate=1.167 mm/s; Frequency=58.33 1/s</b>							
<b>PASSES</b>	<b>TIME (min)</b>	<b>First repetition</b>		<b>Second repetition</b>		<b>Third repetition</b>	
		$R_{v,avg}$ ( $\mu\text{m}$ )	<b>Std</b>	$R_{v,avg}$ ( $\mu\text{m}$ )	<b>Std</b>	$R_{v,avg}$ ( $\mu\text{m}$ )	<b>Std</b>
0	0	1.877	0.215	1.877	0.215	1.877	0.215
47	9.397	0.985	0.044	1.069	0.083	1.118	0.13
139	27.792	0.865	0.159	0.847	0.052	0.909	0.085
231	46.187	0.703	0.085	0.797	0.113	0.665	0.169
462	92.374	0.644	0.184	0.564	0.084	0.278	0.1

**TABLE 12.23.** Experimental  $R_a$  results.

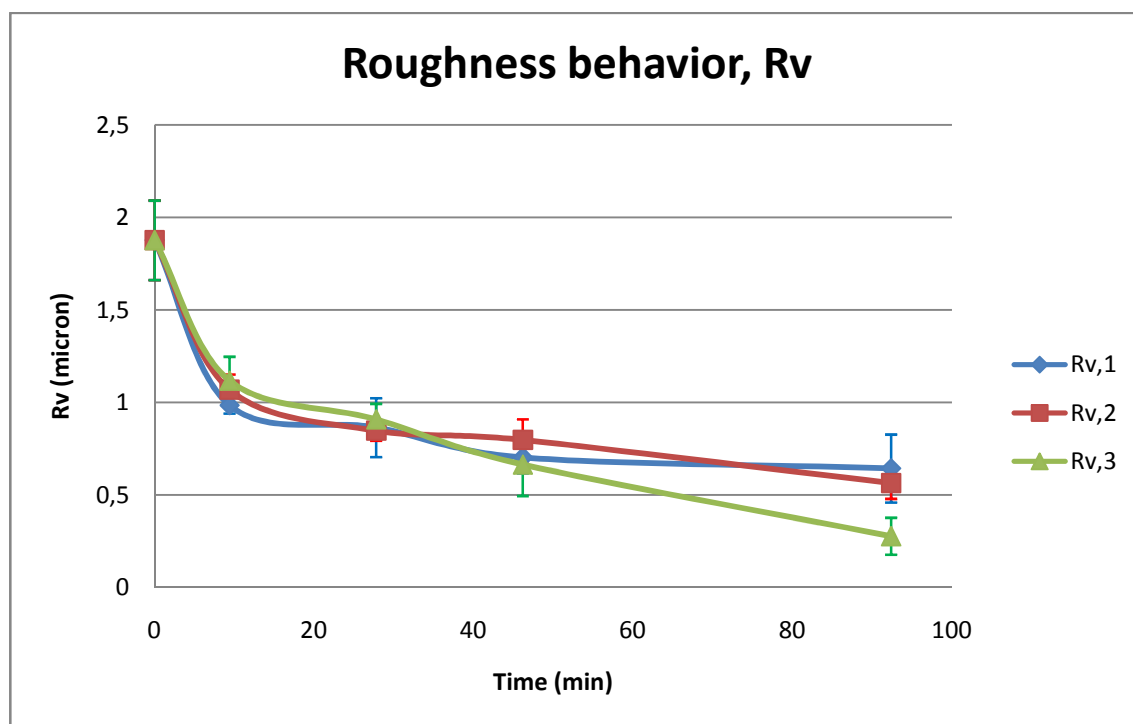


**FIGURE 12.18.** The roughness behavior for the three repetitions, employing  $P=100\text{g}$ ,  $F=1.167\text{ mm/s}$ ;  $f=58.33\text{ 1/s}$ .

<b>Sample 6</b>							
<b>Pressure=100g; Feed rate=0.167 mm/s; Frequency=8.33 1/s</b>							
<b>PASSES</b>	<b>TIME (min)</b>	<b>First repetition</b>		<b>Second repetition</b>		<b>Third repetition</b>	
		$R_{v,avg}$ ( $\mu m$ )	<b>Std</b>	$R_{v,avg}$ ( $\mu m$ )	<b>Std</b>	$R_{v,avg}$ ( $\mu m$ )	<b>Std</b>
0	0	0.295	0.035	0.295	0.035	0.295	0.035
11	15.369	0.276	0.032	0.279	0.089	0.25	0.038
32	44.711	0.243	0.129	0.178	0.021	0.167	0.059
53	74.052	0.146	0.075	0.19	0.057	0.266	0.051
105	146.707	0.094	0.069	0.11	0.018	0.236	0.07

**TABLE 12.24.** Experimental  $R_a$  results.

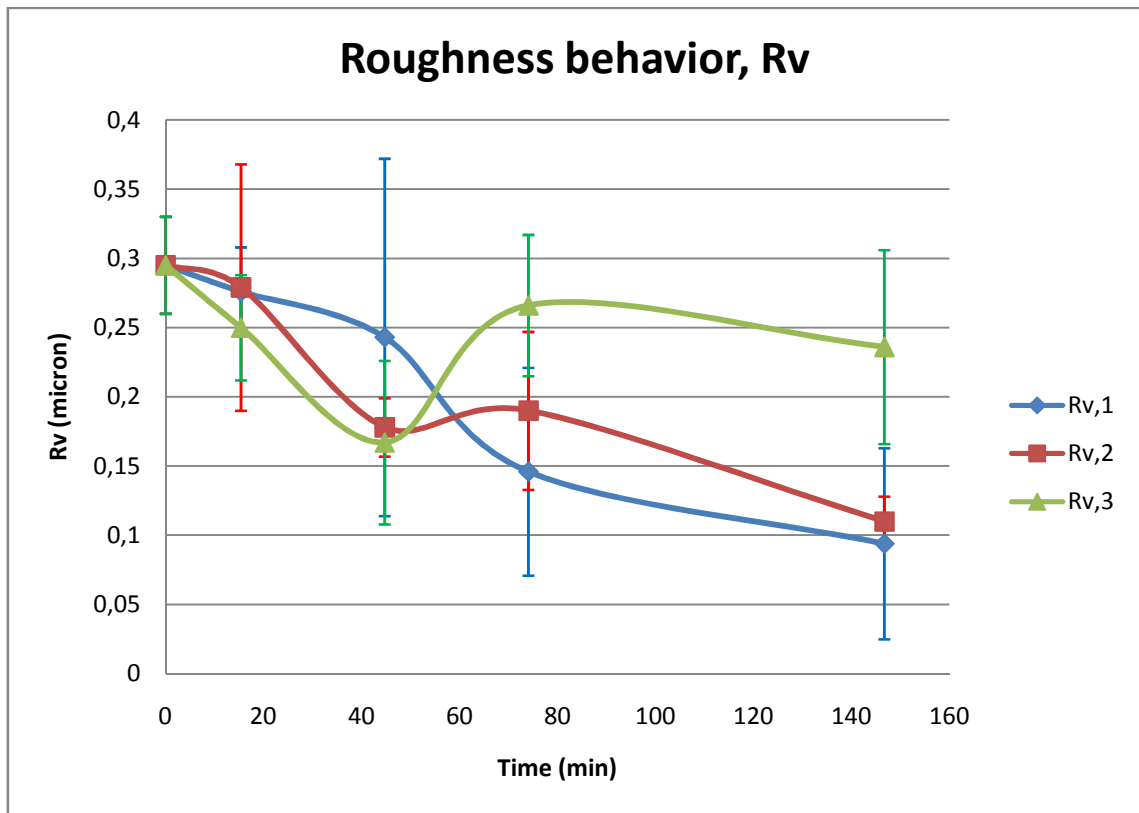


**FIGURE 12.19.** The roughness behavior for the three repetitions, employing  $P=100g$ ,  $F=0.167$  mm/s;  $f=8.33$  1/s.

<b>Sample 7</b>							
<b>Pressure=100g; Feed rate=0.167 mm/s; Frequency=58.33 1/s</b>							
<b>PASSES</b>	<b>TIME (min)</b>	<b>First repetition</b>		<b>Second repetition</b>		<b>Third repetition</b>	
		$R_{v,avg}$ ( $\mu\text{m}$ )	<b>Std</b>	$R_{v,avg}$ ( $\mu\text{m}$ )	<b>Std</b>	$R_{v,avg}$ ( $\mu\text{m}$ )	<b>Std</b>
0	0	1.22	0.15	1.22	0.15	1.22	0.15
7	9.780	0.838	0.2	0.904	0.186	0.967	0.147
19	26.547	0.682	0.078	0.604	0.098	0.58	0.075
32	44.711	0.708	0.204	0.555	0.158	0.554	0.128
63	88.024	0.387	0.1	0.394	0.244	0.516	0.122

**TABLE 12.25.** Experimental  $R_a$  results.

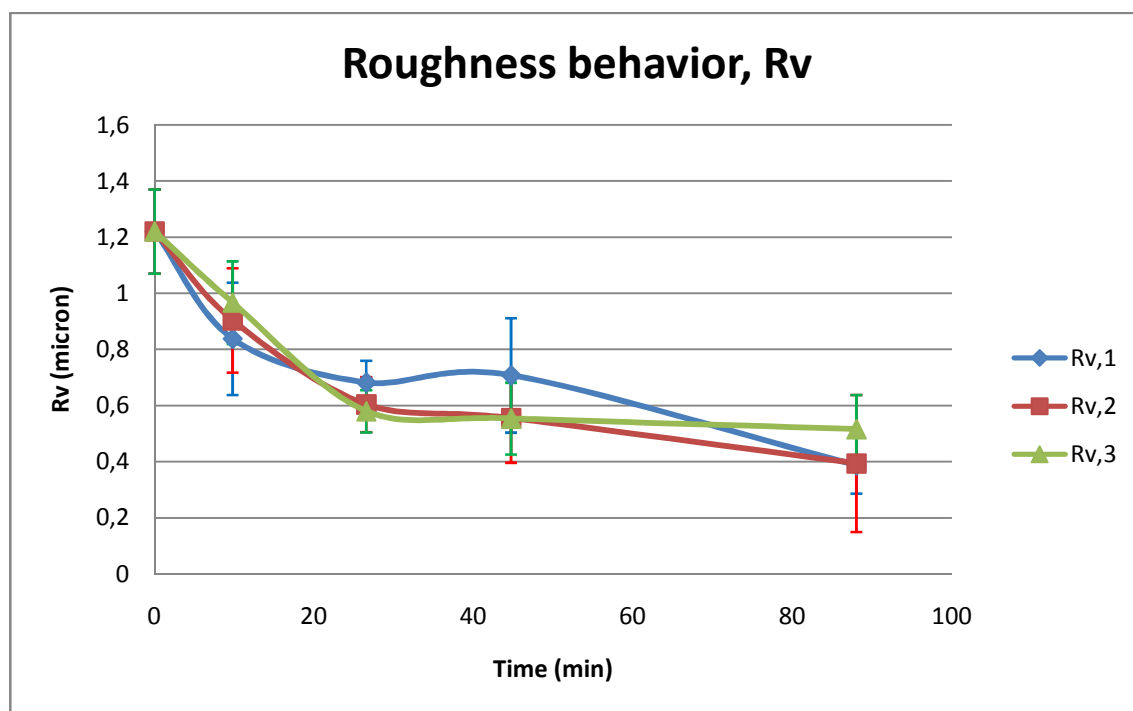


**FIGURE 12.20.** The roughness behavior for the three repetitions, employing  $P=100\text{g}$ ,  $F=0.167\text{ mm/s}$ ;  $f=58.33\text{ 1/s}$ .

<b>Sample 8</b>							
<b>Pressure=900g; Feed rate=0.167 mm/s; Frequency=58.33 1/s</b>							
<b>PASSES</b>	<b>TIME (min)</b>	<b>First repetition</b>		<b>Second repetition</b>		<b>Third repetition</b>	
		$R_{v,avg}$ ( $\mu\text{m}$ )	<b>Std</b>	$R_{v,avg}$ ( $\mu\text{m}$ )	<b>Std</b>	$R_{v,avg}$ ( $\mu\text{m}$ )	<b>Std</b>
0	0	0.272	0.039	0.272	0.039	0.272	0.039
2	2.794	0.108	0.034	0.069	0.025	0.1	0.069
5	6.986	0.067	0.055	0.039	0.006	0.177	0.221
8	11.178	0.038	0.006	0.115	0.135	0.076	0.088
15	20.958	0.052	0.01	0.098	0.126	0.093	0.109

**TABLE 12.26.** Experimental  $R_a$  results.

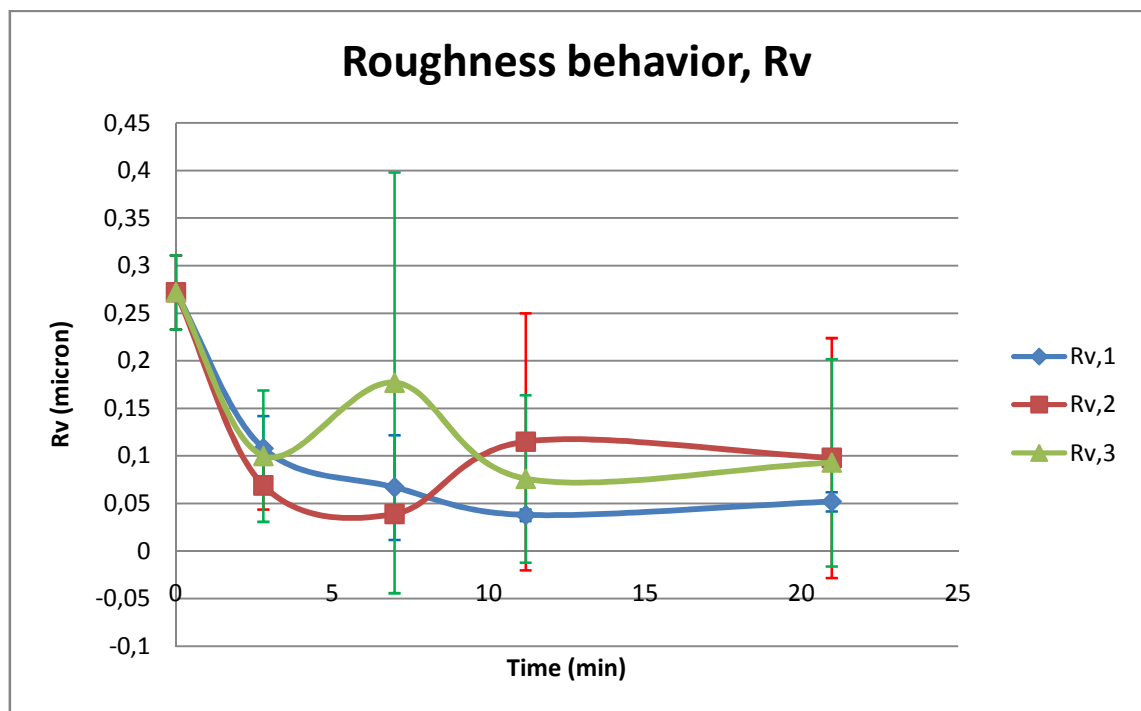


**FIGURE 12.21.** The roughness behavior for the three repetitions, employing  $P=900\text{g}$ ,  $F=0.167\text{ mm/s}$ ;  $f=58.33\text{ 1/s}$ .

<b>Sample 9</b>							
<b>Pressure=900g; Feed rate=1.167 mm/s; Frequency=33.33 1/s</b>							
<b>PASSES</b>	<b>TIME (min)</b>	<b>First repetition</b>		<b>Second repetition</b>		<b>Third repetition</b>	
		$R_{v,avg}$ ( $\mu\text{m}$ )	<b>Std</b>	$R_{v,avg}$ ( $\mu\text{m}$ )	<b>Std</b>	$R_{v,avg}$ ( $\mu\text{m}$ )	<b>Std</b>
0	0	0.381	0.054	0.381	0.054	0.381	0.054
19	3.799	0.213	0.055	0.236	0.085	0.118	0.021
56	11.197	0.111	0.124	0.121	0.081	0.078	0.04
93	18.595	0.064	0.029	0.067	0.061	0.079	0.053
185	36.989	0.04	0.012	0.084	0.078	0.039	0.005

**TABLE 12.27.** Experimental  $R_a$  results.

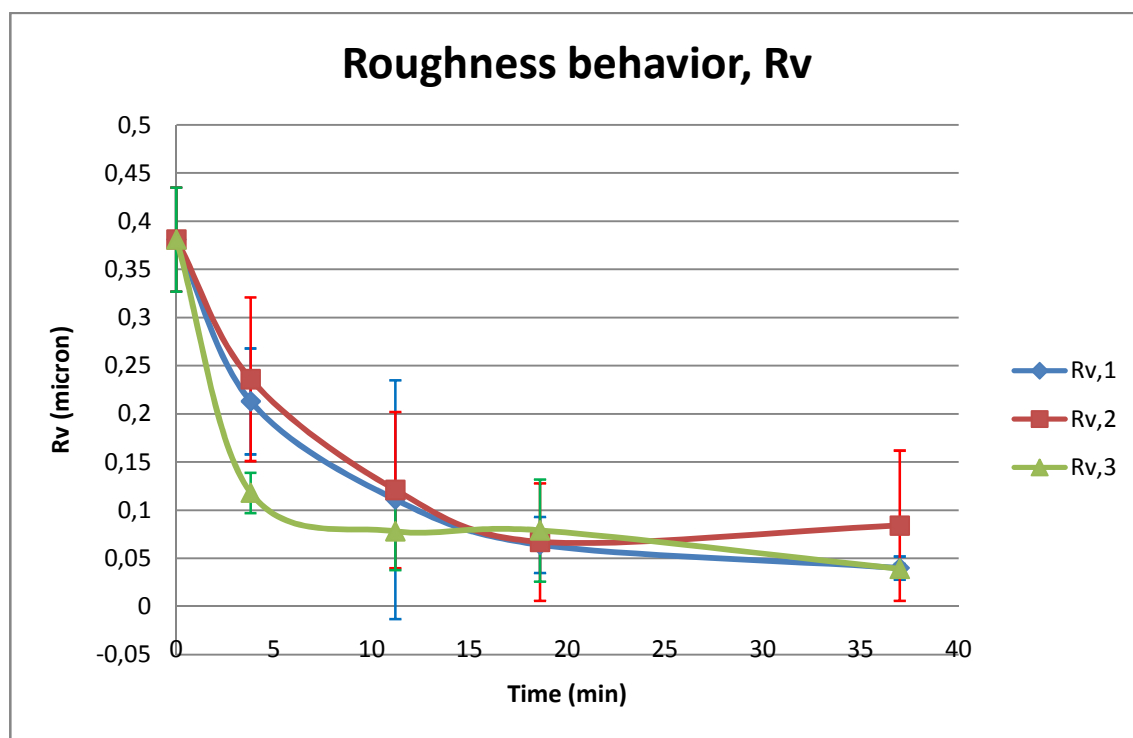


**FIGURE 12.22.** The roughness behavior for the three repetitions, employing  $P=900\text{g}$ ,  $F=1.167\text{ mm/s}$ ;  $f=33.33\text{ 1/s}$ .



<b>Sample 10</b>							
<b>Pressure=900g; Feed rate=0.667 mm/s; Frequency=58.33 1/s</b>							
<b>PASSES</b>	<b>TIME (min)</b>	<b>First repetition</b>		<b>Second repetition</b>		<b>Third repetition</b>	
		$R_{v,avg}$ ( $\mu\text{m}$ )	<b>Std</b>	$R_{v,avg}$ ( $\mu\text{m}$ )	<b>Std</b>	$R_{v,avg}$ ( $\mu\text{m}$ )	<b>Std</b>
0	0	0.423	0.043	0.423	0.043	0.423	0.043
6	2.099	0.148	0.027	0.278	0.063	0.242	0.027
18	6.297	0.076	0.021	0.077	0.012	0.118	0.047
30	10.494	0.037	0.005	0.043	0.013	0.044	0.007
60	20.99	0.05	0.008	0.048	0.014	0.038	0.007

**TABLE 12.28.** Experimental  $R_a$  results.

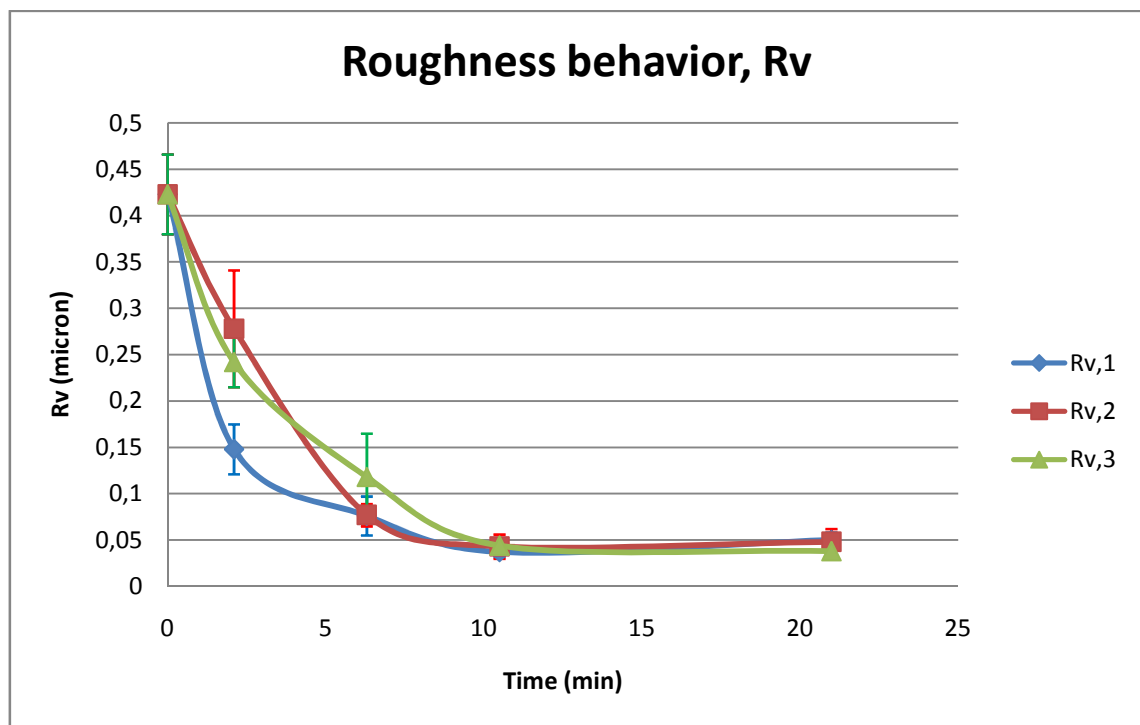


**FIGURE 12.23.** The roughness behavior for the three repetitions, employing  $P=900\text{g}$ ,  $F=0.667\text{ mm/s}$ ;  $f=58.33\text{ 1/s}$ .

<b>Sample 11</b>							
<b>Pressure=500g; Feed rate=1.167 mm/s; Frequency=58.33 1/s</b>							
<b>PASSES</b>	<b>TIME (min)</b>	<b>First repetition</b>		<b>Second repetition</b>		<b>Third repetition</b>	
		$R_{v,avg}$ ( $\mu\text{m}$ )	<b>Std</b>	$R_{v,avg}$ ( $\mu\text{m}$ )	<b>Std</b>	$R_{v,avg}$ ( $\mu\text{m}$ )	<b>Std</b>
0	0	0.427	0.081	0.427	0.081	0.427	0.081
11	2.199	0.137	0.055	0.174	0.034	0.253	0.051
32	6.398	0.068	0.002	0.051	0.009	0.089	0.039
53	10.597	0.051	0.011	0.048	0.004	0.062	0.015
105	20.994	0.043	0.002	0.067	0.047	0.049	0.006

**TABLE 12.29.** Experimental  $R_a$  results.

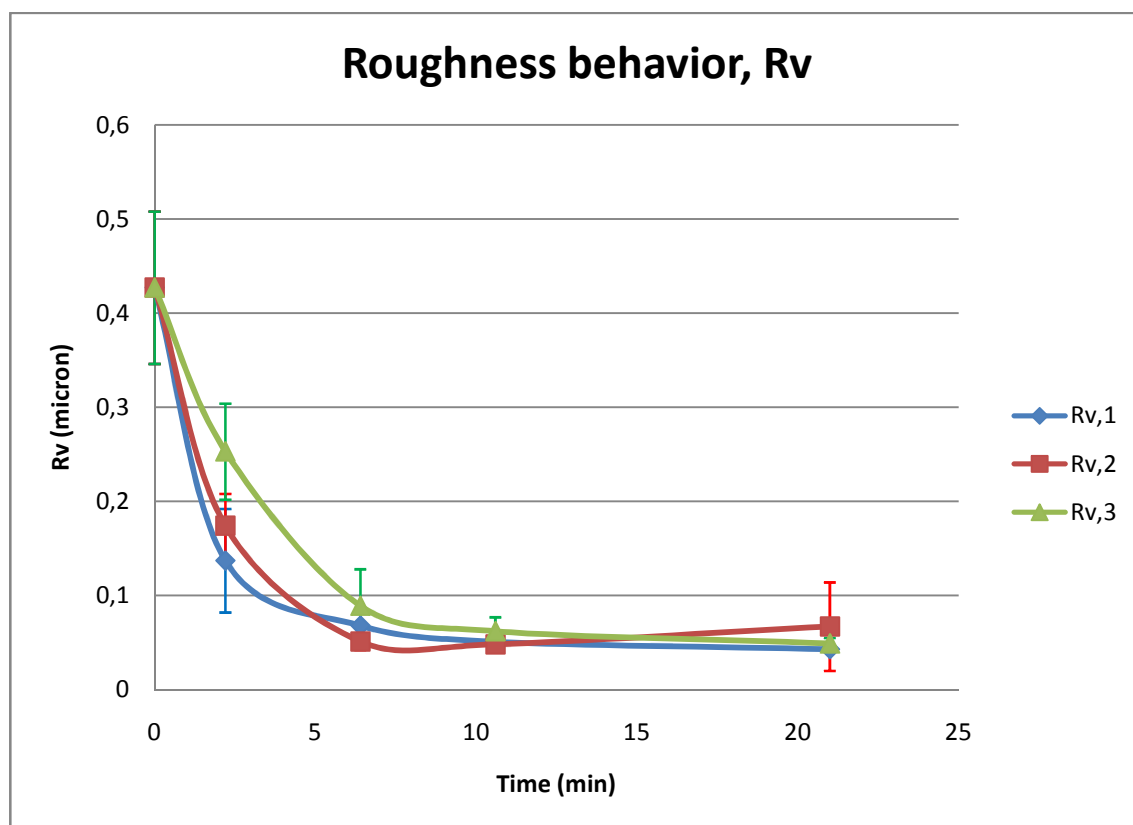


**FIGURE 12.24.** The roughness behavior for the three repetitions, employing  $P=500\text{g}$ ,  $F=1.167\text{ mm/s}$ ;  $f=58.33\text{ 1/s}$ .

As we can see in the previous graphs and tables and as it was previously supposed, the depth of the valley situated in the polishing areas seems to affect the arithmetical

value of the roughness. In fact, the  $R_v$  curves seem to have a trend very similar to the  $R_a$  curves. For much of them (exactly for the samples 0, 3, 5, 6, 9, 10, and 11), the trend is practically the same. In particular, for the samples 0, 2, and 6 the presence of a relative high value for the depth of valleys determines a relative local increment of roughness that locally modifies the roughness behavior which shows a hill. In other hands, rather than following the normal decrease shown for the most of the samples, in same case the roughness shows a brief climb to then returns back to descend. This is clearly shown in the *figures 12.1, 12.3 and 12.7*, where these climbs are present, and the same trend occurs in the *figures 12.13, 12.15, and 12.19*, where the  $R_v$  curves are figured.

Moreover, in the *figures 12.17, 12.18, and 12.20*, corresponding to the combinations of parameters 4, 5, and 7 respectively, the  $R_v$  curves do not show that flat trend typical for the roughness behavior when the final roughness value is more or less reached. This means that for those samples more time is required to reach it, and then the final values measured for them have not been the final values that they can reach. In other hands, more polishing is required to obtain the right results. This is another point of strength regarding that the results related to the three samples in question have been penalized by the three factors introduced in the previous subchapter, that is: low pressure and then low material removal, deep scratches, and the employed method to stop the polishing process in a particular polished area.

#### 12.6.4. Average maximum height of the profile ( $R_z$ ) analysis

To have the final verification that the presence of the scratches have clearly affected the experimental tests, the  $R_z$  behavior is now analyzed. As the two previous analysis the average results of the  $R_z$  values and their standard deviations will be listed below for each combination of parameters. What of interest here is to understand how much the valleys affect the process, or if the peaks can influence the process as well.

<b>Sample 0</b>							
<b>Pressure=500 g; Feed rate=0.667 mm/s; Frequency=33.33 1/s</b>							
<b>PASSES</b>	<b>TIME</b>	<b>First repetition</b>		<b>Second repetition</b>		<b>Third repetition</b>	
		$R_{z,avg}$ ( $\mu\text{m}$ )	<b>Std</b>	$R_{z,avg}$ ( $\mu\text{m}$ )	<b>Std</b>	$R_{z,avg}$ ( $\mu\text{m}$ )	<b>Std</b>
0	0	0.449	0.066	0.449	0.066	0.449	0.066
11	3.023	0.18	0.046	0.175	0.037	0.25	0.031
32	8.796	0.084	0.009	0.145	0.082	0.125	0.066
53	14.568	0.116	0.028	0.094	0.021	0.129	0.047
105	28.861	0.102	0.023	0.092	0.004	0.102	0.044

TABLE 12.30. Experimental  $R_a$  results.

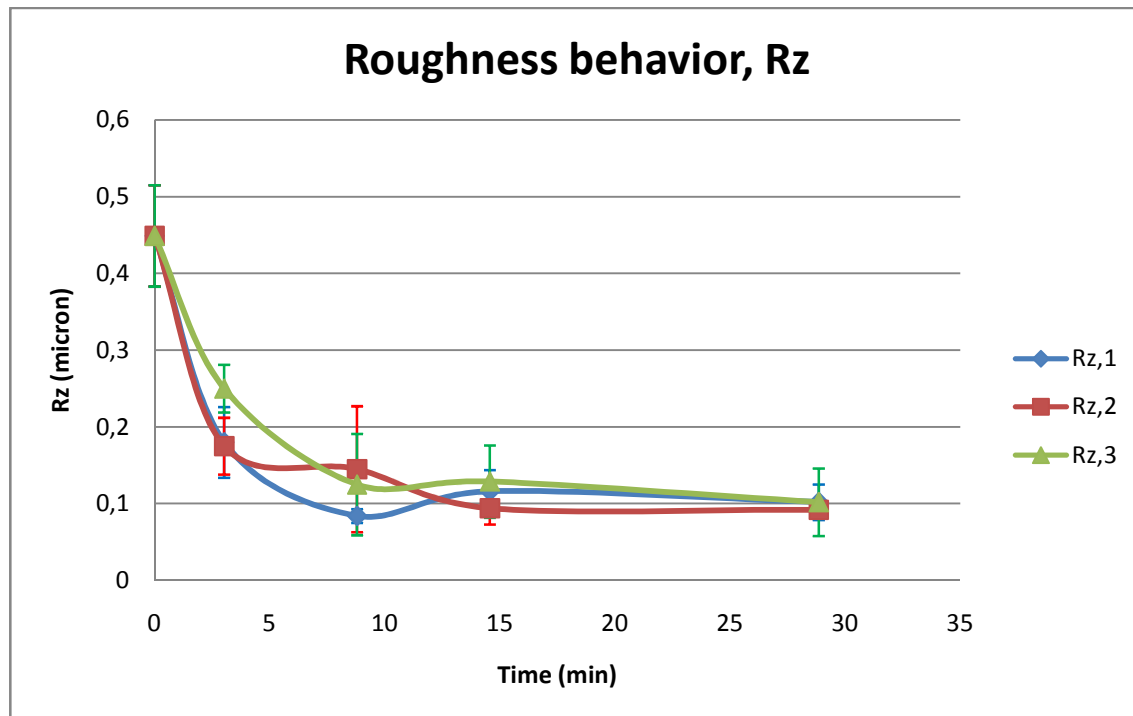
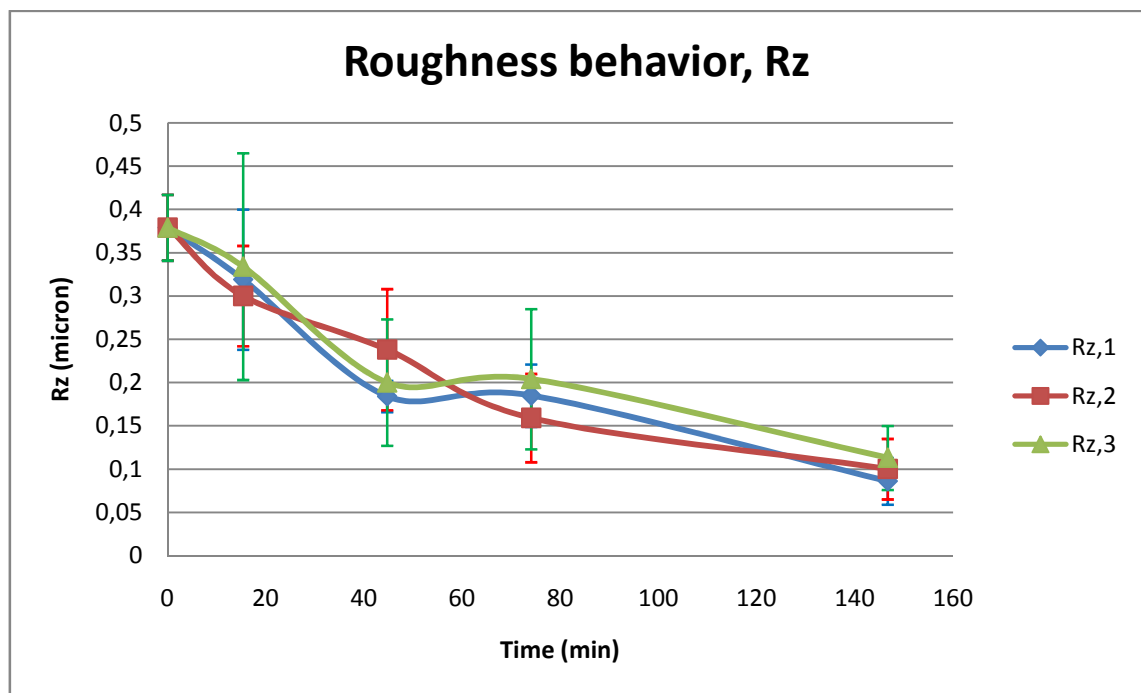


FIGURE 12.25. The roughness behavior for the three repetitions, employing  $P=500\text{g}$ ,  $F=0.667\text{ mm/s}$ ;  $f=33.33\text{ 1/s}$ .

<b>Sample 1</b>							
<b>Pressure=900 g; Feed rate=0.167 mm/s; Frequency=8.33 1/s</b>							
<b>PASSES</b>	<b>TIME</b>	<b>First repetition</b>		<b>Second repetition</b>		<b>Third repetition</b>	
		$R_{z,avg}$ ( $\mu m$ )	<b>Std</b>	$R_{z,avg}$ ( $\mu m$ )	<b>Std</b>	$R_{z,avg}$ ( $\mu m$ )	<b>Std</b>
0	0	0.379	0.038	0.379	0.038	0.379	0.038
11	15.369	0.319	0.081	0.3	0.058	0.334	0.131
32	44.711	0.184	0.018	0.238	0.07	0.2	0.073
53	74.052	0.185	0.036	0.159	0.051	0.204	0.081
105	146.707	0.086	0.027	0.1	0.035	0.113	0.037

**TABLE 12.31.** Experimental  $R_a$  results.



**FIGURE 12.26.** The roughness behavior for the three repetitions, employing  $P=900g$ ,  $F=0.167$  mm/s;  $f=8.33$  1/s.

<b>Sample 2</b>							
<b>Pressure=900 g; Feed rate=1.167 mm/s; Frequency=8.33 1/s</b>							
<b>PASSES</b>	<b>TIME</b>	<b>First repetition</b>		<b>Second repetition</b>		<b>Third repetition</b>	
		$R_{z,avg}$ ( $\mu\text{m}$ )	<b>Std</b>	$R_{z,avg}$ ( $\mu\text{m}$ )	<b>Std</b>	$R_{z,avg}$ ( $\mu\text{m}$ )	<b>Std</b>
0	0	0.982	0.233	0.982	0.233	0.982	0.233
83	16.595	0.42	0.057	0.369	0.17	0.582	0.137
265	52.985	0.432	0.176	0.248	0.084	0.43	0.182
441	88.175	0.56	0.257	0.164	0.097	0.199	0.112
882	176.35	0.271	0.185	0.087	0.033	0.194	0.079

**TABLE 12.32.** Experimental  $R_a$  results.

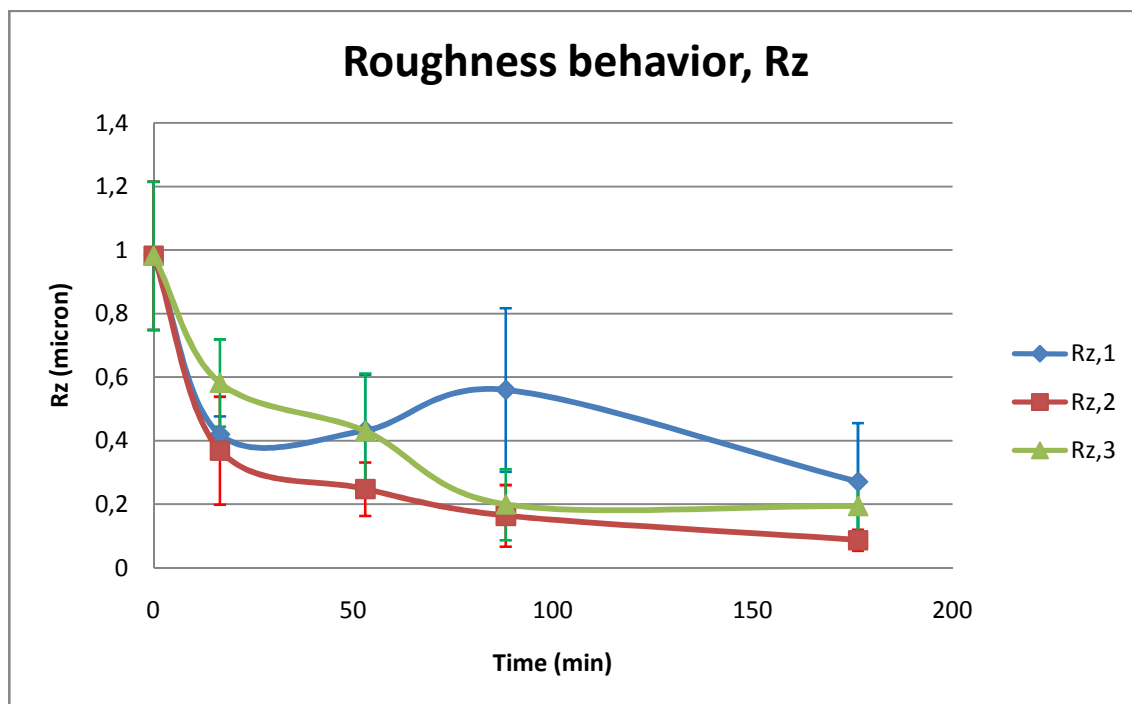


**FIGURE 12.27.** The roughness behavior for the three repetitions, employing  $P=900\text{g}$ ,  $F=1.167\text{ mm/s}$ ;  $f=8.33\text{ 1/s}$ .

<b>Sample 3</b>							
<b>Pressure=900 g; Feed rate=1.167 mm/s; Frequency=58.33 1/s</b>							
<b>PASSES</b>	<b>TIME</b>	<b>First repetition</b>		<b>Second repetition</b>		<b>Third repetition</b>	
		$R_{z,avg}$ ( $\mu\text{m}$ )	<b>Std</b>	$R_{z,avg}$ ( $\mu\text{m}$ )	<b>Std</b>	$R_{z,avg}$ ( $\mu\text{m}$ )	<b>Std</b>
0	0	1.046	0.16	1.046	0.16	1.046	0.16
15	2.999	0.529	0.208	0.359	0.154	0.424	0.077
45	8.997	0.269	0.178	0.247	0.121	0.296	0.189
74	14.796	0.086	0.027	0.164	0.123	0.176	0.107
147	29.392	0.098	0.02	0.088	0.03	0.109	0.04

**TABLE 12.33.** Experimental  $R_a$  results.

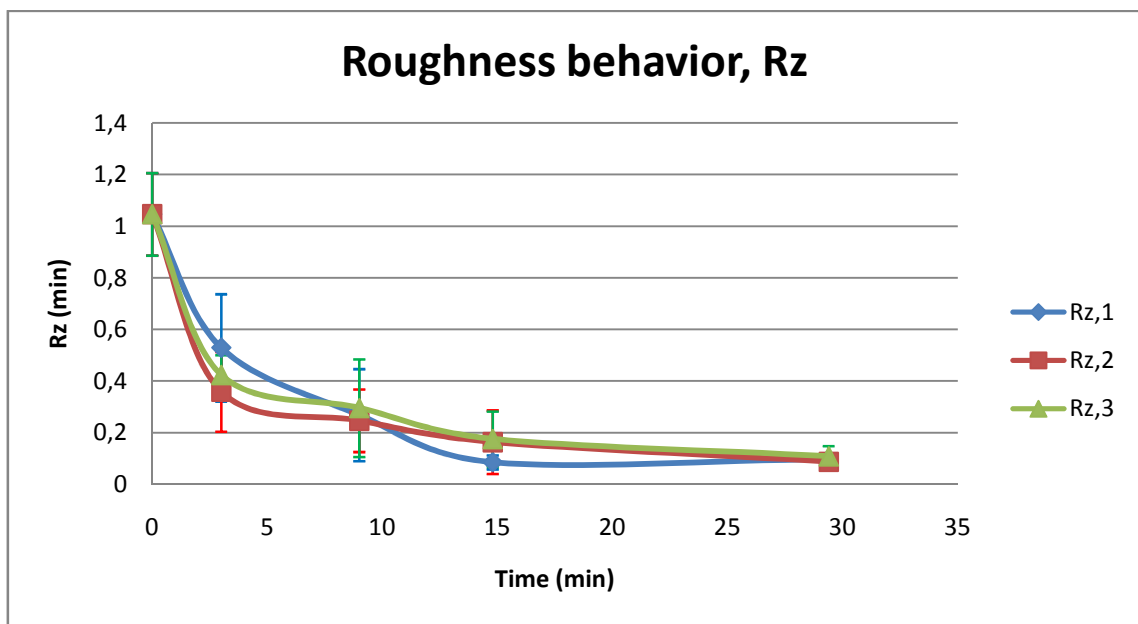


**FIGURE 12.28.** The roughness behavior for the three repetitions, employing  $P=900\text{g}$ ,  $F=1.167\text{ mm/s}$ ;  $f=58.33\text{ 1/s}$ .

<b>Sample 4</b>							
<b>Pressure=100 g; Feed rate=1.167 mm/s; Frequency=8.33 1/s</b>							
<b>PASSES</b>	<b>TIME</b>	<b>First repetition</b>		<b>Second repetition</b>		<b>Third repetition</b>	
		$R_{z,avg}$ ( $\mu\text{m}$ )	<b>Std</b>	$R_{z,avg}$ ( $\mu\text{m}$ )	<b>Std</b>	$R_{z,avg}$ ( $\mu\text{m}$ )	<b>Std</b>
0	0	1.691	0.174	1.691	0.174	1.691	0.174
133	26.592	1.353	0.308	1.364	0.234	1.352	0.08
397	79.377	1.132	0.109	1.325	0.044	0.99	0.255
662	132.362	0.855	0.113	1.16	0.196	0.868	0.127
1323	264.524	0.697	0.093	0.495	0.085	0.464	0.052

**TABLE 12.34.** Experimental  $R_a$  results.

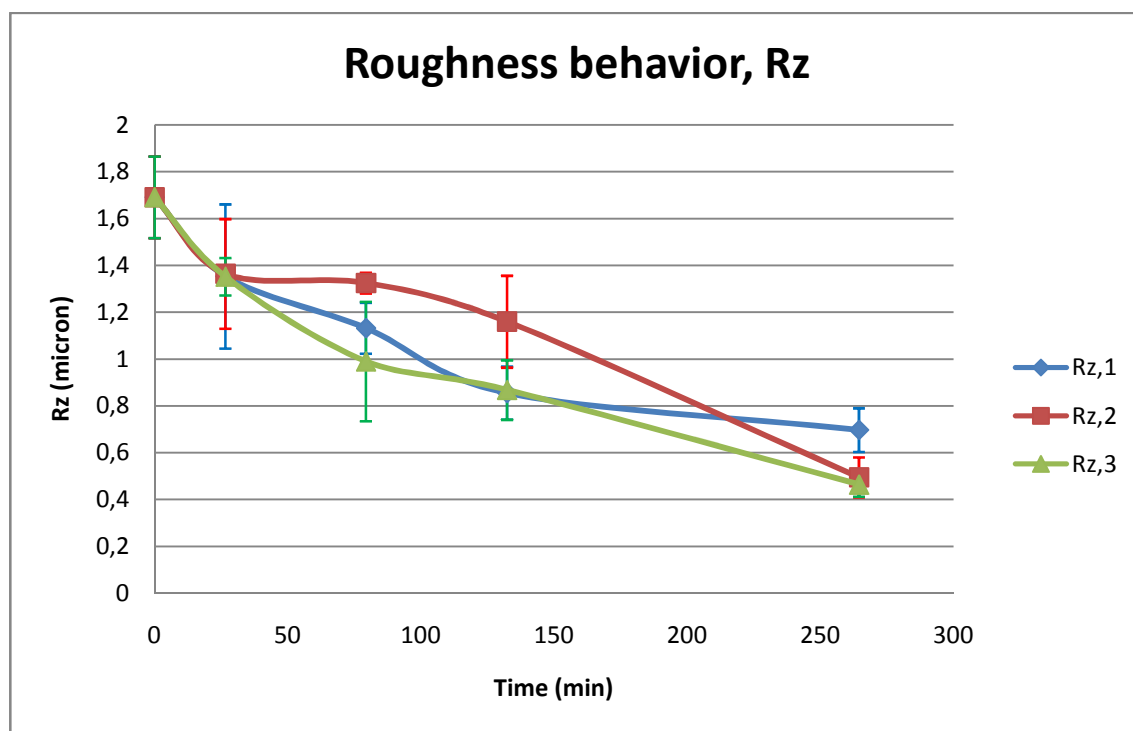


**FIGURE 12.29.** The roughness behavior for the three repetitions, employing  $P=100\text{g}$ ,  $F=1.167\text{ mm/s}$ ;  $f=8.33\text{ 1/s}$ .



<b>Sample 5</b>							
<b>Pressure=100 g; Feed rate=1.167 mm/s; Frequency=58.33 1/s</b>							
<b>PASSES</b>	<b>TIME</b>	<b>First repetition</b>		<b>Second repetition</b>		<b>Third repetition</b>	
		$R_{z,avg}$ ( $\mu m$ )	<b>Std</b>	$R_{z,avg}$ ( $\mu m$ )	<b>Std</b>	$R_{z,avg}$ ( $\mu m$ )	<b>Std</b>
0	0	1.877	0.215	1.877	0.215	1.877	0.215
47	9.397	1.192	0.045	1.31	0.088	1.356	0.132
139	27.792	0.993	0.165	0.985	0.05	1.084	0.101
231	46.187	0.817	0.095	0.908	0.114	0.868	0.19
462	92.374	0.721	0.195	0.655	0.091	0.416	0.111

**TABLE 12.35.** Experimental  $R_a$  results.

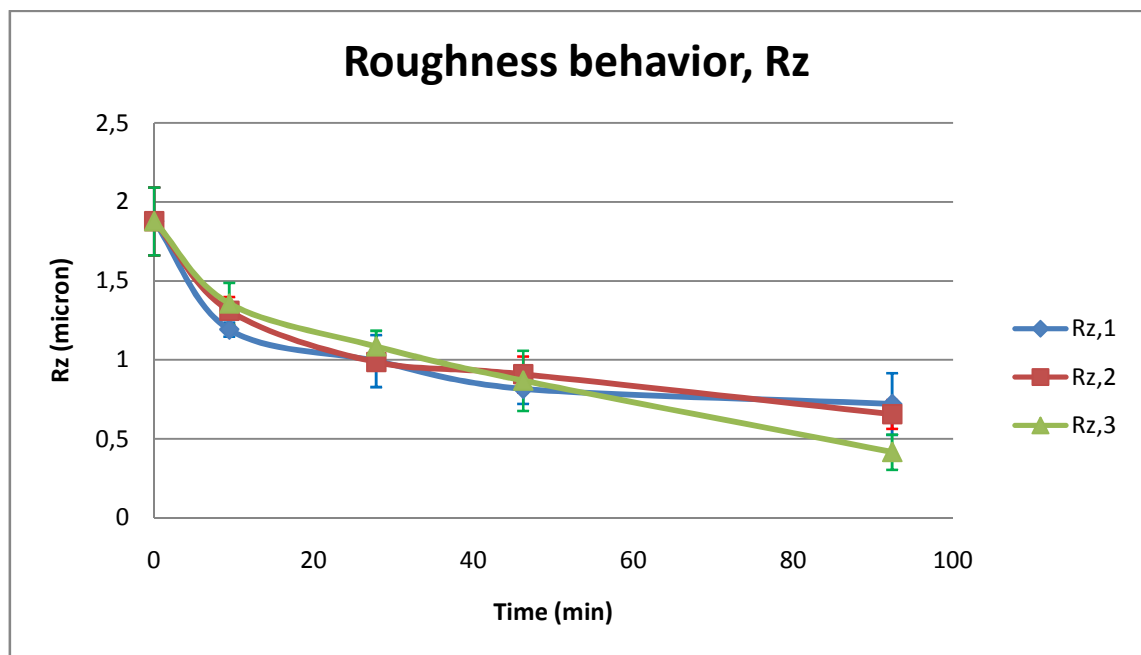


**FIGURE 12.30.** The roughness behavior for the three repetitions, employing  $P=100g$ ,  $F=1.167$  mm/s;  $f=58.33$  1/s.

<b>Sample 6</b>							
<b>Pressure=100 g; Feed rate=0.167 mm/s; Frequency=8.33 1/s</b>							
<b>PASSES</b>	<b>TIME</b>	<b>First repetition</b>		<b>Second repetition</b>		<b>Third repetition</b>	
		$R_{z,avg}$ ( $\mu\text{m}$ )	<b>Std</b>	$R_{z,avg}$ ( $\mu\text{m}$ )	<b>Std</b>	$R_{z,avg}$ ( $\mu\text{m}$ )	<b>Std</b>
0	0	0.427	0.046	0.427	0.046	0.427	0.046
11	15.369	0.403	0.061	0.381	0.09	0.364	0.056
32	44.711	0.314	0.136	0.254	0.021	0.247	0.066
53	74.052	0.23	0.078	0.262	0.066	0.35	0.056
105	146.707	0.145	0.071	0.17	0.026	0.308	0.078

**TABLE 12.36.** Experimental  $R_a$  results.

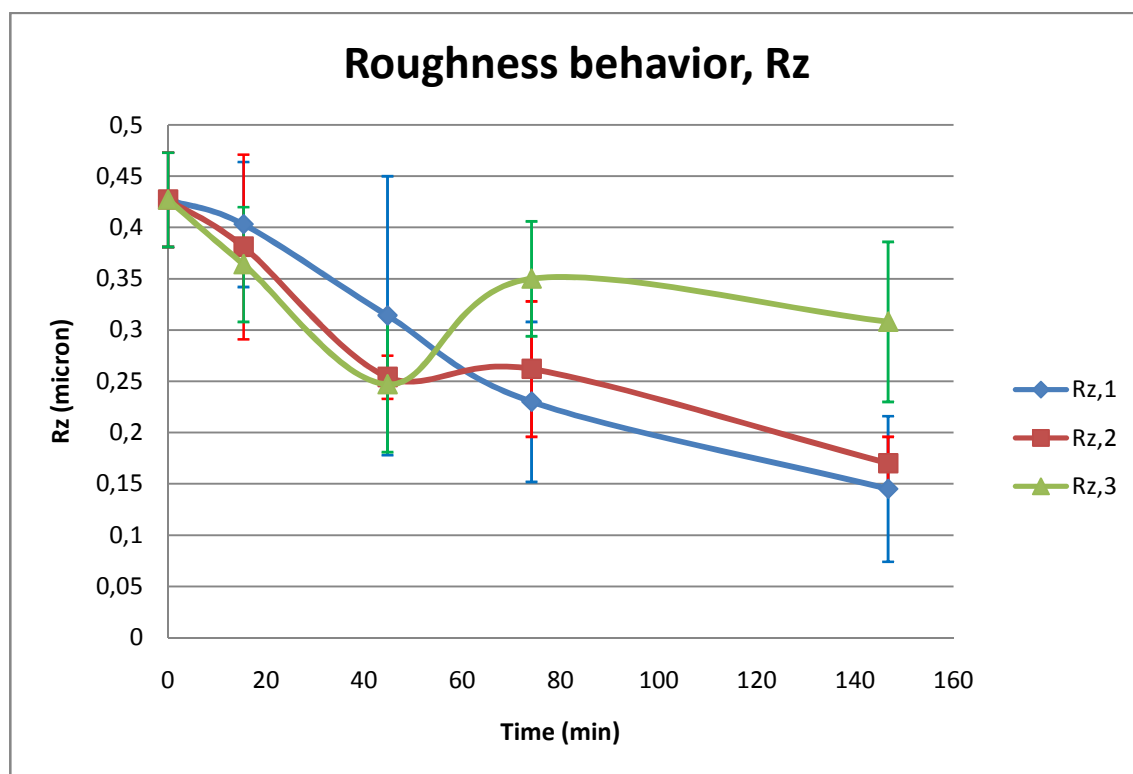


**FIGURE 12.31.** The roughness behavior for the three repetitions, employing  $P=100$  g,  $F=0.167$  mm/s;  $f=8.33$  1/s.

<b>Sample 7</b>							
<b>Pressure=100 g; Feed rate=0.167 mm/s; Frequency=58.33 1/s</b>							
<b>PASSES</b>	<b>TIME</b>	<b>First repetition</b>		<b>Second repetition</b>		<b>Third repetition</b>	
		$R_{z,avg}$ ( $\mu m$ )	<b>Std</b>	$R_{z,avg}$ ( $\mu m$ )	<b>Std</b>	$R_{z,avg}$ ( $\mu m$ )	<b>Std</b>
0	0	1.62	0.169	1.62	0.169	1.62	0.169
7	9.780	1.035	0.197	1.097	0.191	1.21	0.163
19	26.547	0.854	0.076	0.76	0.105	0.727	0.077
32	44.711	0.867	0.205	0.722	0.148	0.791	0.143
63	88.024	0.513	0.089	0.475	0.251	0.614	0.123

**TABLE 12.37.** Experimental  $R_a$  results.

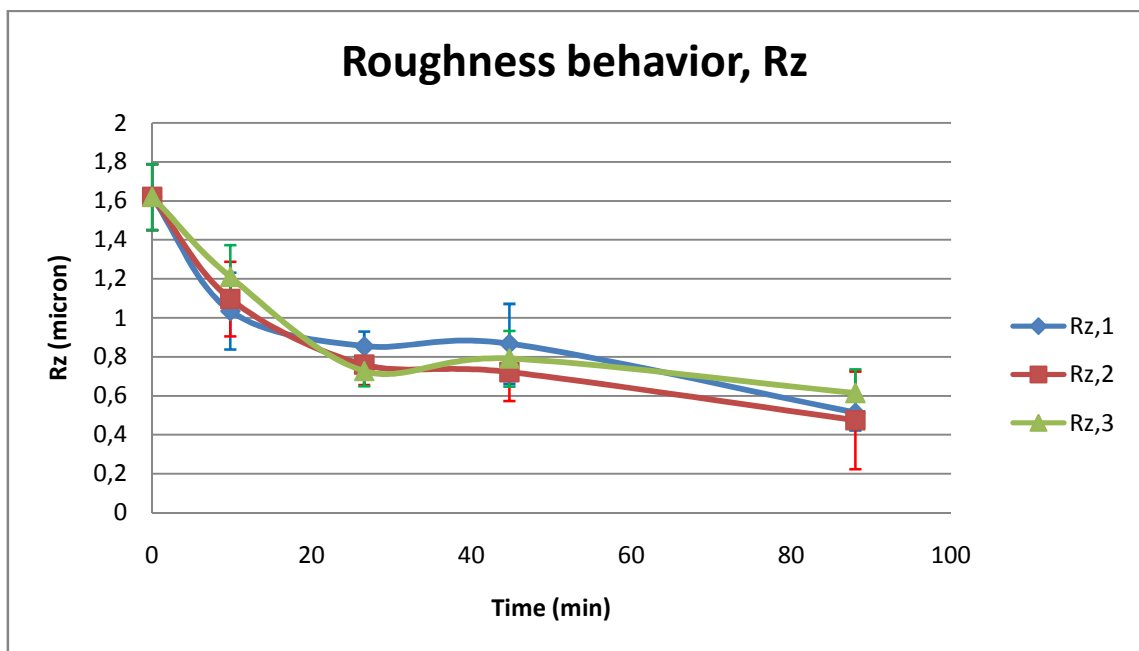


**FIGURE 12.32.** The roughness behavior for the three repetitions, employing  $P=100g$ ,  $F=0.167$  mm/s;  $f=58.33$  1/s.

<b>Sample 8</b>							
<b>Pressure=900 g; Feed rate=0.167 mm/s; Frequency=58.33 1/s</b>							
<b>PASSES</b>	<b>TIME</b>	<b>First repetition</b>		<b>Second repetition</b>		<b>Third repetition</b>	
		$R_{z,avg}$ ( $\mu\text{m}$ )	<b>Std</b>	$R_{z,avg}$ ( $\mu\text{m}$ )	<b>Std</b>	$R_{z,avg}$ ( $\mu\text{m}$ )	<b>Std</b>
0	0	0.403	0.048	0.403	0.048	0.403	0.048
2	2.794	0.165	0.028	0.117	0.024	0.155	0.069
5	6.986	0.12	0.058	0.09	0.01	0.224	0.228
8	11.178	0.09	0.023	0.168	0.138	0.117	0.089
15	20.958	0.118	0.009	0.148	0.131	0.142	0.109

**TABLE 12.38.** Experimental  $R_a$  results.

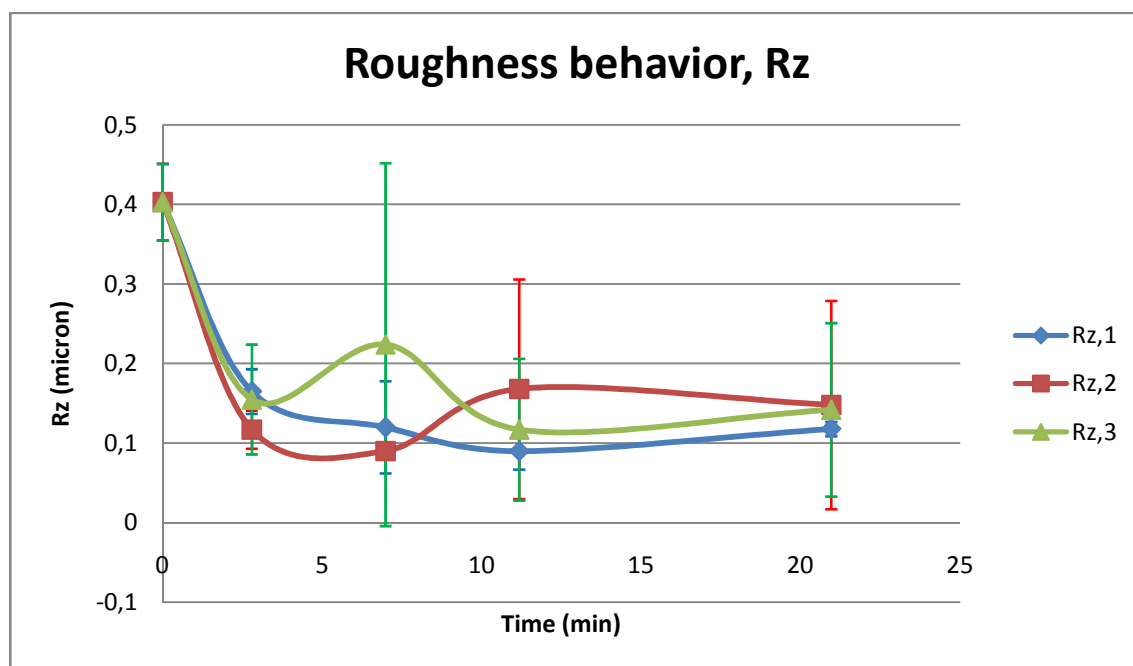


**FIGURE 12.33.** The roughness behavior for the three repetitions, employing  $P=900\text{g}$ ,  $F=0.167\text{ mm/s}$ ;  $f=58.33\text{ 1/s}$ .

<b>Sample 9</b>							
<b>Pressure=900 g; Feed rate=1.167 mm/s; Frequency=33.33 1/s</b>							
<b>PASSES</b>	<b>TIME</b>	<b>First repetition</b>		<b>Second repetition</b>		<b>Third repetition</b>	
		$R_{z,avg}$ ( $\mu m$ )	<b>Std</b>	$R_{z,avg}$ ( $\mu m$ )	<b>Std</b>	$R_{z,avg}$ ( $\mu m$ )	<b>Std</b>
0	0	0.555	0.066	0.555	0.066	0.555	0.066
19	3.799	0.291	0.071	0.312	0.099	0.181	0.022
56	11.197	0.158	0.128	0.177	0.091	0.135	0.049
93	18.595	0.117	0.035	0.122	0.076	0.121	0.054
185	36.989	0.095	0.03	0.133	0.081	0.083	0.007

**TABLE 12.39.** Experimental  $R_a$  results.

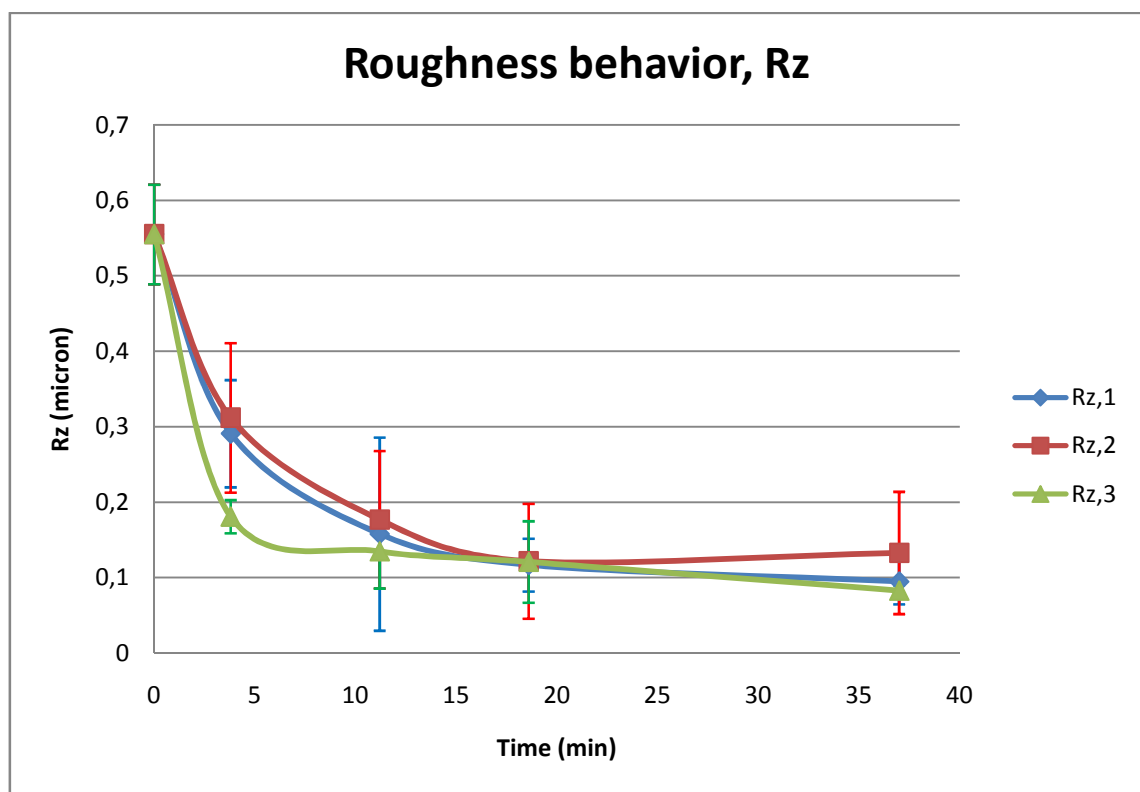


**FIGURE 12.34.** The roughness behavior for the three repetitions, employing  $P=900g$ ,  $F=1.167$  mm/s;  $f=33.33$  1/s.

<b>Sample 10</b>							
<b>Pressure=900g; Feed rate=0.667 mm/s; Frequency=58.33 1/s</b>							
<b>PASSES</b>	<b>TIME</b>	<b>First repetition</b>		<b>Second repetition</b>		<b>Third repetition</b>	
		$R_{z,avg}$ ( $\mu\text{m}$ )	<b>Std</b>	$R_{z,avg}$ ( $\mu\text{m}$ )	<b>Std</b>	$R_{z,avg}$ ( $\mu\text{m}$ )	<b>Std</b>
0	0	0.588	0.048	0.588	0.048	0.588	0.048
6	2.099	0.234	0.027	0.383	0.074	0.337	0.03
18	6.297	0.151	0.035	0.14	0.015	0.199	0.069
30	10.495	0.081	0.014	0.092	0.019	0.096	0.015
60	20.99	0.121	0.025	0.122	0.012	0.085	0.007

**TABLE 12.40.** Experimental  $R_a$  results.

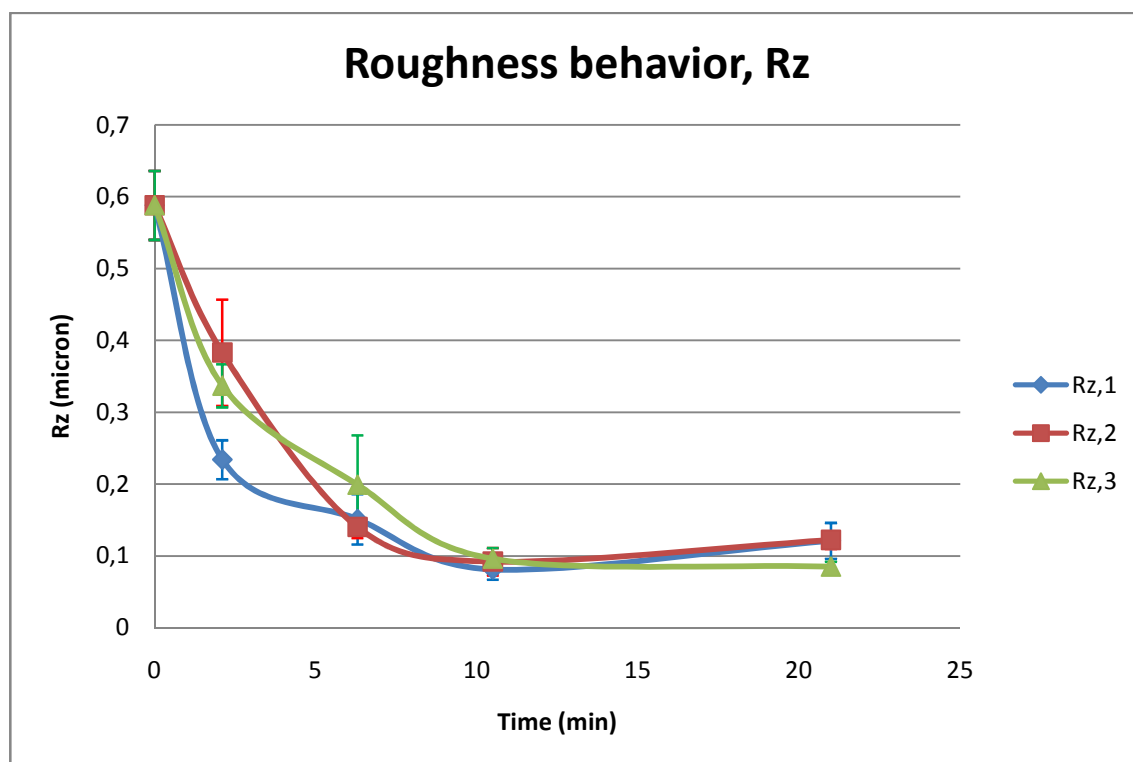


**FIGURE 12.35.** The roughness behavior for the three repetitions, employing  $P=900\text{g}$ ,  $F=0.667\text{ mm/s}$ ;  $f=3500\text{ 1/s}$ .

<b>Sample 11</b>							
<b>Pressure=500 g; Feed rate=1.167 mm/s; Frequency=58.33 1/s</b>							
<b>PASSES</b>	<b>TIME</b>	<b>First repetition</b>		<b>Second repetition</b>		<b>Third repetition</b>	
		$R_{z,avg}$ ( $\mu m$ )	<b>Std</b>	$R_{z,avg}$ ( $\mu m$ )	<b>Std</b>	$R_{z,avg}$ ( $\mu m$ )	<b>Std</b>
0	0	0.583	0.086	0.583	0.086	0.583	0.086
11	2.199	0.209	0.061	0.25	0.042	0.336	0.051
32	6.398	0.137	0.006	0.11	0.015	0.149	0.043
53	10.597	0.122	0.009	0.122	0.007	0.12	0.015
105	20.994	0.104	0.013	0.132	0.05	0.112	0.01

**TABLE 12.41.** Experimental  $R_a$  results.

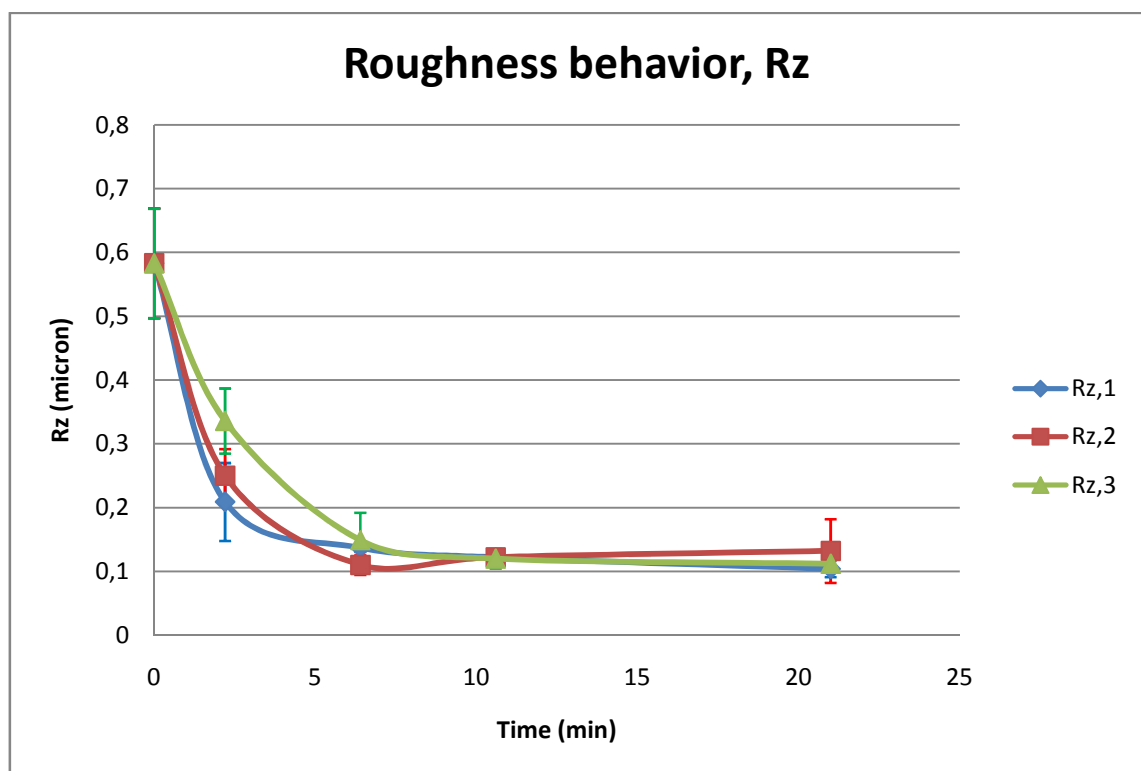


**FIGURE 12.36.** The roughness behavior for the three repetitions, employing  $P=500g$ ,  $F=1.167$  mm/s;  $f=58.33$  1/s.

From these results, it clearly appears that the  $R_z$  curves and  $R_v$  curves have practically the same trend for all the samples. In particular, the behavior is very similar and the  $R_z$  curves respect all the particular features (like the hills explained in the previous

subchapter) present in the  $R_v$  curves. It means that we have the final confirmation that the depth of the valley is the most important parameters which affects the measured roughness behavior in this analyzed case. In fact, the  $R_z$  parameter takes into account both the presence of valley and of peaks. But in this case, since the trend between the parameter which represent the presence of valley ( $R_v$ ) and  $R_z$  does not change, the height of the peaks do not heavily affects the roughness behavior as the presence of the valleys.

#### 12.6.5. Conclusion

Regarding this first analysis, some conclusions can be formulated. Firstly, the final reached roughness values seem to be very low relative to the technical data obtained for that typology of employed paste. Nevertheless, it is true that the Hommel Stylus is not the correct measurement instrument to measure roughness values so fine. In fact, the mechanical noise effect of that machine is around the 10 nanometers. This means that if the real value of the polished area is researched, another kind of instrument has to be used to be more precise. Anyway, Hommel is enough precise to identify if a change in the roughness condition during the experimental tests is happened or not, and this is what has happened.

Secondly, in this case since the samples were ground before the experimental tests, the most important value which determine the roughness behavior of the workpiece surface is the depth of the valley. More the valleys are depth and more the required timing to reach the final value will be long. This situation is worse if low down pressure are applied, because the corresponding amount of material removal will be very small and consequently less material will be got out. Furthermore, the influence of the valley might be so high to modify the normal typical descending trend of the roughness behavior (some demonstrations are the presence of hills in the roughness curves).

Regarding the employed method to stop the process in a specific polished area (called “stopping” method as well), overall it seems to work well, but it does not have any protection against the deep valleys. In fact, they can procure moments of stalemate which might wrongly indicate to have reached the final roughness value. A good solution could be to change this method or change the measurement instrument employed to determine the  $T_4$ .



The obtained roughness behavior results have been discussed and represented by graphs and tables. In particular, the trends of  $R_a$ ,  $R_v$ , and  $R_z$  have been analyzed and compared.

In the next subchapter, the DOE analysis is introduced, here the time to reach the final roughness is analyzed and the effects of the polishing parameters is explored.

## 12.3. DOE analysis

### 12.6.1. Introduction

In this subchapter the effects of the polishing parameters on the required time to reach the final roughness value are analyzed. The main effects of each parameter and the interactions between them on the time are explored to understand how and which parameters mainly affect the polishing process in flat kinematics conditions. Moreover, the suitable setting of parameters to reach quickly a good surface condition is detected.

### 12.6.2. Preliminary regression model

Before starting with the DOE analysis, it has been required to “adjust” the roughness behavior of the twelve combinations of parameters, so that they had the same initial and final roughness value. It is noteworthy, that this operation has been necessary because the only variable in this analysis had to be the required time to reach the final roughness value during the polishing process, and to do this the starting and final point (of the roughness in this case) had to be the same.

Therefore, the first step has been to find a regression model which well fit the detected roughness behavior for each sample. To perform at this aim, a regression model research in the literature has been done and a sequence of regression models has been tested. In the end the best model which well fit the roughness curves has been:

$$y = A + B \times \log(x)$$

**FORMULA 12.1.** *Employed regression model to fit the experimental data.*

Where the  $y$  variable represents the roughness value (micron) and the  $x$  variable means the time (min). The roughness evaluation estimated by this model is shown with an example below:

<b>Time (min)</b>	<b>Experimental data</b>			<b>Model prediction (<math>\mu m</math>)</b>
	<b>First repetition (<math>\mu m</math>)</b>	<b>Second repetition (<math>\mu m</math>)</b>	<b>Third repetition (<math>\mu m</math>)</b>	
<b>0</b>	0.045	0.045	0.045	<b><u>0.045</u></b>
<b>15.369</b>	0.039	0.035	0.04	<b><u>0.038</u></b>
<b>44.711</b>	0.023	0.024	0.026	<b><u>0.029</u></b>
<b>74.052</b>	0.022	0.022	0.031	<b><u>0.024</u></b>
<b>146.707</b>	0.014	0.016	0.025	<b><u>0.018</u></b>

**TABLE 12.42.** Comparison between the experimental measurements made for the sample 6 and the prediction of the regression model relative the corresponding combination of parameters.

To find out the A and B coefficient for each sample, the curve described by the model in the *equation 12.1* has been passed for two timing value ( $T_i$ ) which permitted to estimate the average values of the roughness for each sample with an estimating error smaller than 20%. The best pair of timing values has been detected to be  $T_1$  and  $T_4$ . With these two points, only three on forty-eight evaluations have been found to have an error bigger than 20%. But, since these measurements were only the 6% of the total, this model has been employed in this analysis. The only problem with this model is that it does not work well if we want to estimate roughness with higher values then that one corresponding to  $T_1$ . That is, a good prediction is obtained for the points starting from  $T_1$ , but for the points before this value the roughness behavior is not well fitted. This is because there is the presence of the logarithm in the structure of the model equation and it affects the results for time values close to zero. For this reason, for all the samples, the starting roughness has been supposed to be equal to the starting measured roughness, and the time required to pass from  $T_0$  to  $T_1$  has been considered equal to the experimental one.

This assumption is important, because it influences the choice regarding the common starting and final roughness value for all the samples. In fact, if that regression model is employed, it is possible to obtain a good roughness evaluation only if the roughness curve decreases and does not increase from  $T_1$ . This means that, for reference point, the lowest starting roughness value between the available twelve has to be chosen as common value. A brief analysis of this has brought to use as common starting roughness value of  $0.05 \mu\text{m}$ . It is noteworthy that there were in the made measurements before the experiments some samples with starting roughness lower than  $0.05 \mu\text{m}$ , but the level of the detected value for the standard deviation permitted us to use that value of 50 nanometers in this case as well.

Then, once the common initial roughness has been decided, the second and last point before starting with the DOE analysis has been to decide the common final roughness value. From the observations of the data, it has been decided to be  $0.015 \mu\text{m}$ . Therefore, once established the common initial and final roughness for all the samples, the time required to reach the final  $0.015 \mu\text{m}$  from the starting  $0.05 \mu\text{m}$  has been calculated, and the DOE analysis has been started. It is necessary to say, that for the sample 4, 5, and 7, where the final roughness was higher than  $0.015 \mu\text{m}$ , the time required to reach that value starting from  $0.05 \mu\text{m}$  has been detected completely with the model. In this choice, we were conscious that we were estimating some values outside the range of evaluation of the model (that is we were outside the range  $0.107 \mu\text{m}/0.055 \mu\text{m}$  employed for example to compute the model for the sample 7), but to obtain a first indication of the influence of the parameter on the polishing process, it has been necessary to have those data which were not available from the test. The reasons of this acting have been two: the first one is that these three samples were not ground good as the others, and a new grinding process on them has been impossible to do for the proximity of the experimental tests, and the second one is that the presence of deeper scratches on the surface of these sample has caused a very low descend of the roughness curve to reach the real final roughness value, “deceiving” the employed stopping method explained in the chapter ten, so that the detected roughness at the  $T_4$  has been higher. In this case, anyway, the presence of these scratched would have badly affected the results for the DOE analysis in the same way, because a very big final time would have been required, employing pressure of 100 g, to reach the final roughness value common to the others. For this reason, the analysis conducted in this chapter regarding the DOE, have to be interpreted as a starting indications of the influence of the polishing parameters on the process, verifying these in the next future with new tests.

The results from this computation have been:

	<i>Pressure (g)</i>	<i>FeedRate (mm/s)</i>	<i>Frequency. (1/s)</i>	<i>Required time from 0.05<math>\mu</math>m to 0.015<math>\mu</math>m (min)</i>
<b>Sample01</b>	900	0.167	8.33	83.464
<b>Sample02</b>	900	1.167	8.33	175.639
<b>Sample03</b>	900	1.167	58.33	16.499
<b>Sample04</b>	100	1.167	8.33	299.992
<b>Sample05</b>	100	1.167	58.33	129.929
<b>Sample06</b>	100	0.167	8.33	205.788
<b>Sample07</b>	100	0.167	58.33	148.816
<b>Sample08</b>	900	0.167	58.33	0.373
<b>Sample00</b>	500	0.667	33.33	7.046
<b>Sample09</b>	900	1.167	33.33	15.414
<b>Sample10</b>	900	0.667	58.33	15.441
<b>Sample11</b>	500	1.167	58.33	16.754

**TABLE 12.43.** Time required to reach the final roughness of 0.015  $\mu$ m, starting from a initial value of 0.05  $\mu$ m.

Now the DOE analysis is introduced and it is explained step by step. The overall work has been divided in three: in the first part a normal full factorial is analyzed, then in the second one the effect of the central point is added, and finally in the third one all the combinations of parameters (including the samples 9, 10, and 11) are taken into account and analyzed. This simple structure will permit us to better understand how the polishing parameters affect the polishing process. It is noteworthy also that if in this following papers the term “oscillation” is employed, it means only the frequency of the pad. The word “oscillation” is sometime employed here because it is the term employed by STRECON to describe the frequency of the polishing pad.

### 12.6.3. Analysis of the full factorial design (3 factors and 2 levels each)

The first step of our analysis has been to verify how the eight combinations of parameters, provided by a normal full factorial design with three parameters and two levels each, have affected the final required time to reach the common final roughness value. This means that, in this subchapter, only the samples from 1 to 8 are analyzed, whereas the samples 0, 9, 10, and 11 are not taken into account now.

The employed analysis tool in this case has been MINITAB, a program which is capable to process the starting data of a full factorial design and to provide us graphs, coefficients, and curves to understand how the parameters and the interactions between them have affected the process. For this reason, the eight combinations of parameters and the corresponding results have been put into the program which has given us the following results that now we introduce.

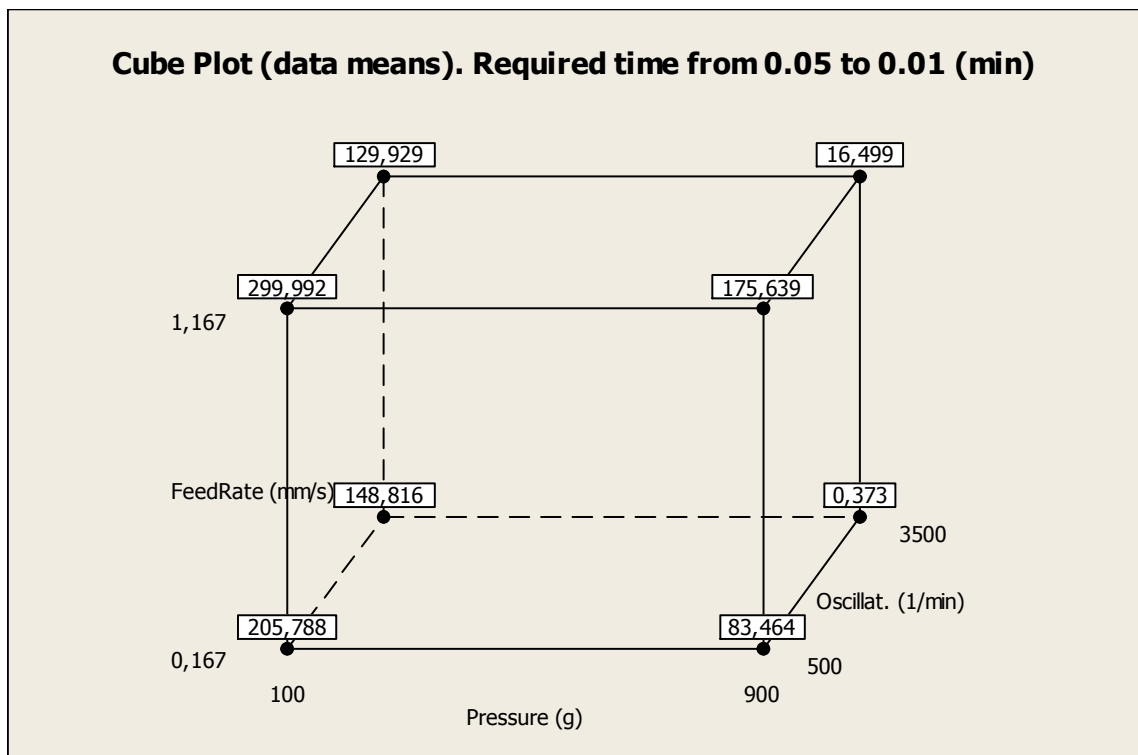


**FIGURE 12.37.** MINITAB cub plot, where the required time to reach the final roughness is plotted for every combination of parameters.

The first operation to do in this analysis is to see how each parameter (down pressure, feed rate, and oscillations) has affected the process. For this reason, firstly, the main effects of each polishing parameter have been detected.

The first polishing parameter to be analyzed has been the pressure. The main effect of the pressure is shown in the figure below:

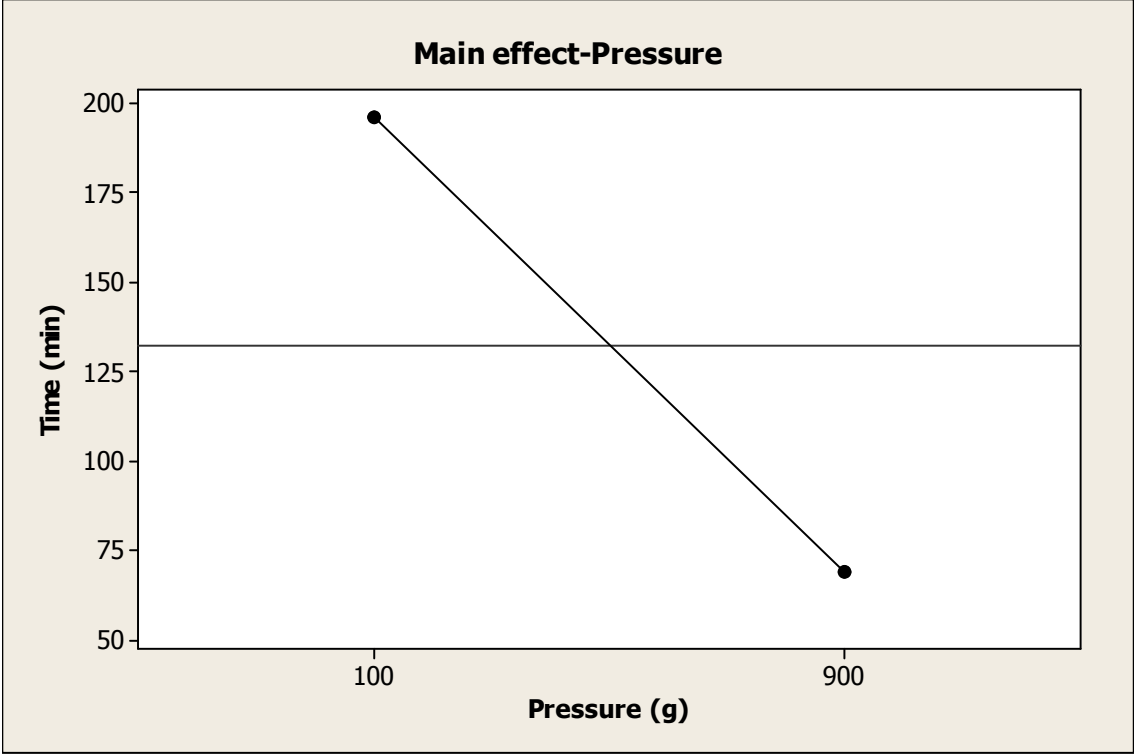
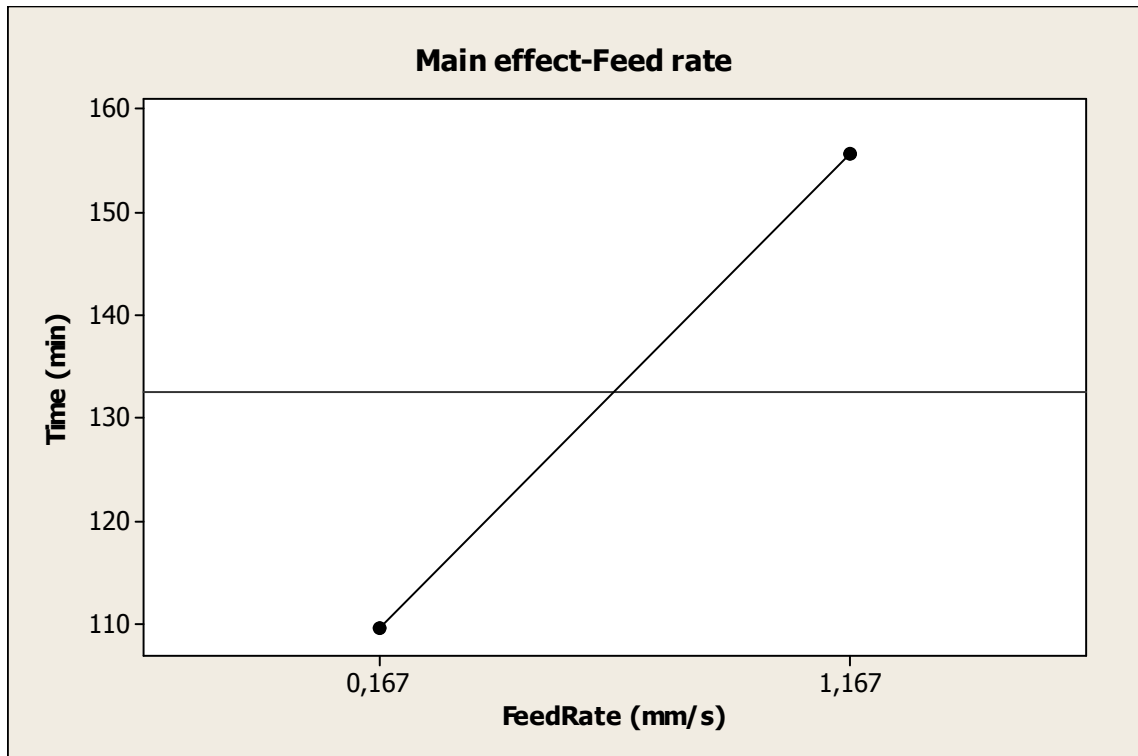


FIGURE 12.38. Main effect of the pressure.

As it can be seen in the *figure 12.38*, an increment of the pressure reduces the time to reach the final roughness, passing from a mean value of 196.131 min when the applied down pressure is equal to 100 g, to a mean value of 68.994 min when the pressure is 900 g. This indicates an important reduction in process timing to reach the final roughness value. But this is only an indication of the single effect of the pressure on the process. To have deeper and strong conclusions regarding the role of the pressure, the interaction between pressure and feed rate, and between pressure and frequency have to be analyzed to understand how and how much these interactions affect the process.

The second parameter to be singly analyzed has been the feed rate. Its main effect is shown below:



**FIGURE 12.39.** Main effect of the feed rate.

From the graph above, it can be seen that the feed rate influence on the process is opposite to the previous pressure influence. In fact, if before an increase in pressure determined a decrease of the polishing time, now an increment of the feed rate brings to get worse results. In fact, the timing value passes from 109.61 min for feed rate equal to 0.167 mm/s, to 155.515 min for 1.167 mm/s. Therefore, the feed rate seems to get worse results when it is increased, but, as for the pressure, also here the interactions feed rate-pressure and feed rate-frequency have to be analyzed to have an overview of how the feed rate affects the process.

The last parameter to be analyzed has been the oscillation main effect (with oscillation is indicated the frequency of the pad):

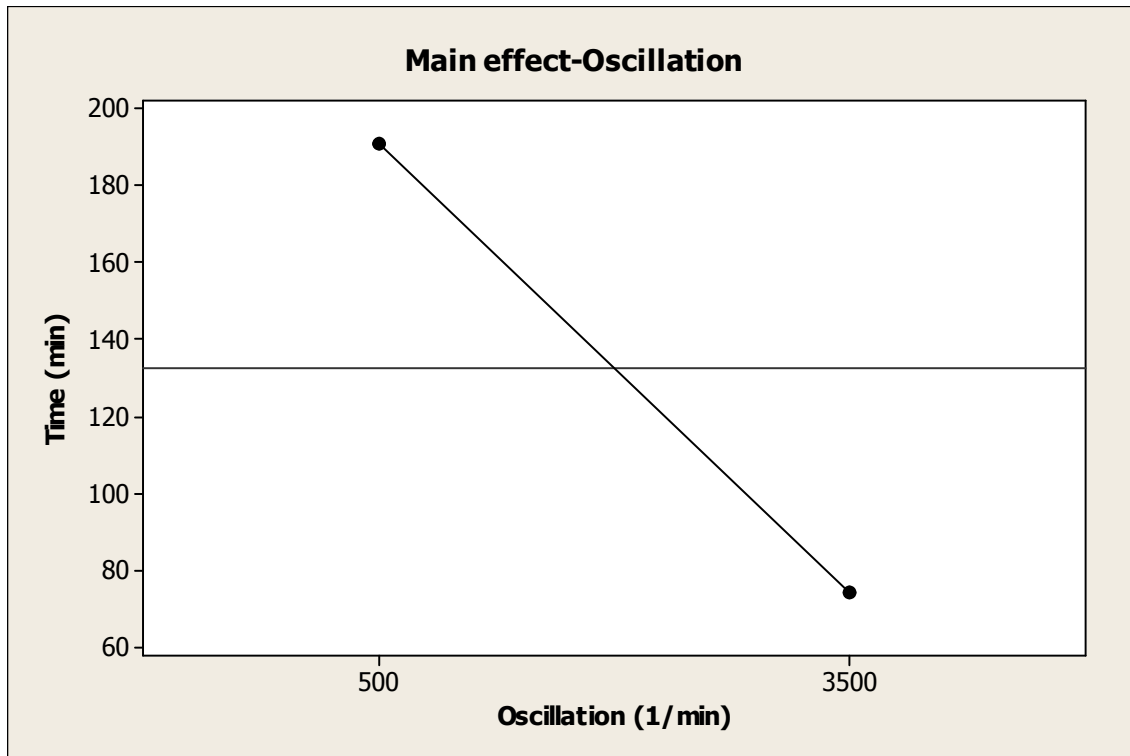


**FIGURE 12.40.** Main effect of the oscillation.

What we see now in the graph above is that the influence of the oscillation seems to have a trend very similar to the pressure influence. In fact, with an increment from 500 1/min to 3500 1/min, the polishing time decreases from 191.221 min to 73.904 min. This variation, as that determined from the pressure, seems to be very big and important in the process relative to the variation caused by the feed rate. But no certain conclusions can be formulated without considering the interactions related with it.

In fact, to understand better how the polishing time varies with the parameters, the interactions between them have to be analyzed. Therefore, the four interaction parameters (pressure-feed rate, pressure-oscillation, oscillation-feed rate, and pressure-feed rate-oscillation) are now introduced and analyzed.

To better understand the interactions between the parameters and how they can affect the process, two graphs for each considered interaction are shown. The first one is related to the linear curves previously shown for each parameter, whereas the second one is related to the variation in the response that the interaction can cause when it is varied from the lower to the higher level (it is noteworthy that if this last curve appears flat, it means that the considered parameter or interaction does not affect the process).



Anyway, every consideration relative this argument is done in the following pages, when the slopes of the curves will be taken into account).

The first interaction which was considered has been the pressure-feed rate. As it has been previously described, two graphs regarding this interaction are now shown:

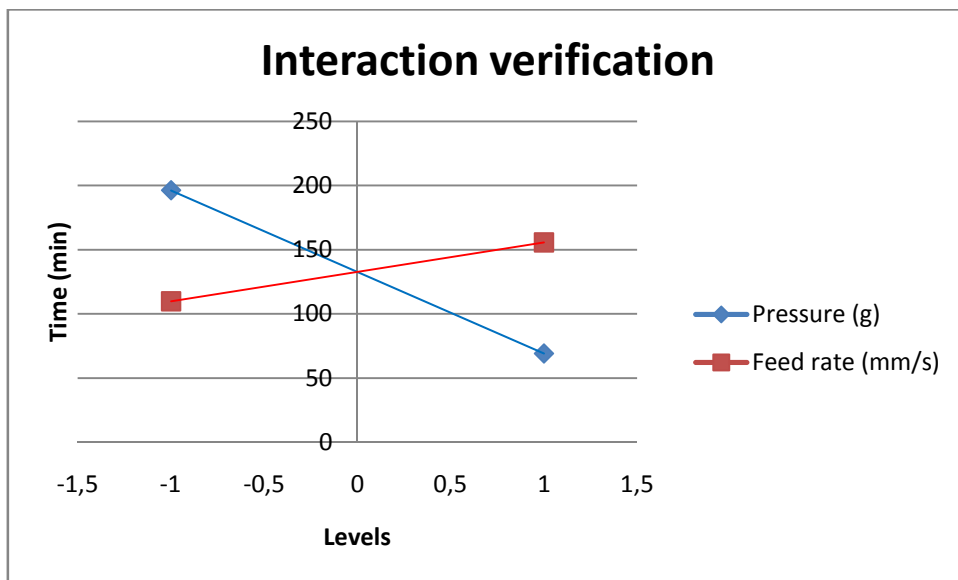


**FIGURE 12.41.** Verification of the interaction between the two interested parameters.

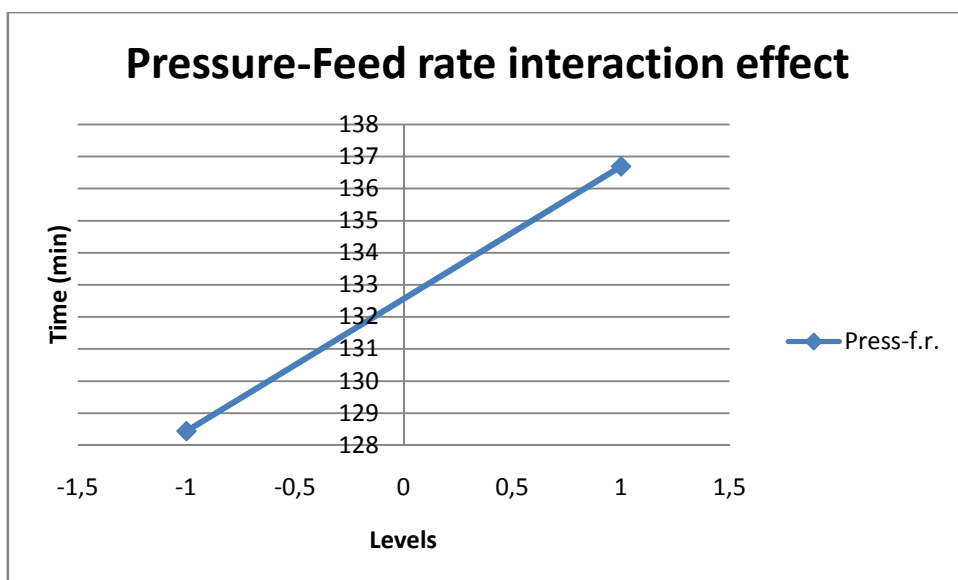


**FIGURE 12.42.** Effect of the interaction on the polishing process regarding the required time.

From the *figure 12.41*, the interaction between the two parameters clearly appears. In fact, the intersection between the two lines, representing the main effect of pressure and feed rate respectively, determines that the two polishing parameter interact each other. This means due to the variation of one of this two, the effect of the other one on the process can be modified compared to the previous one corresponding to the main effect. To understand how much this interaction is important for the process compared to the main effect, the analysis of the slopes of the linear curves and the Pareto chart are required. These data are introduced and analyzed after having shown all the interactions between the parameters.

In the *figure 12.43*, the effect of the variation of the parameter pressure-feed rate is shown. As it can be seen, an increment of this interaction parameter get an aggravation of the final polishing time required to reach the final roughness value.

The second analyzed interaction has been the Pressure-Oscillation.

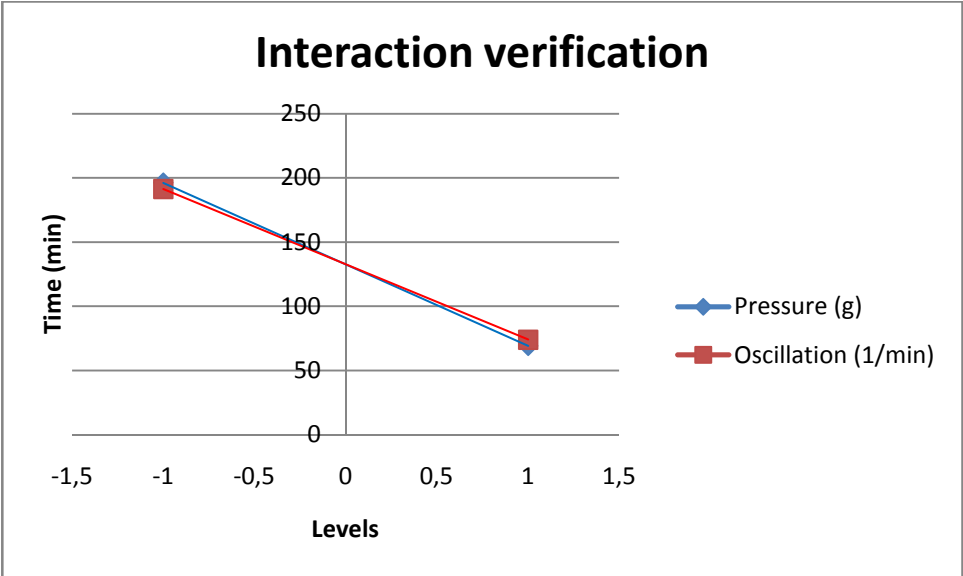


**FIGURE 12.43.** Verification of the interaction between the two interested parameters.

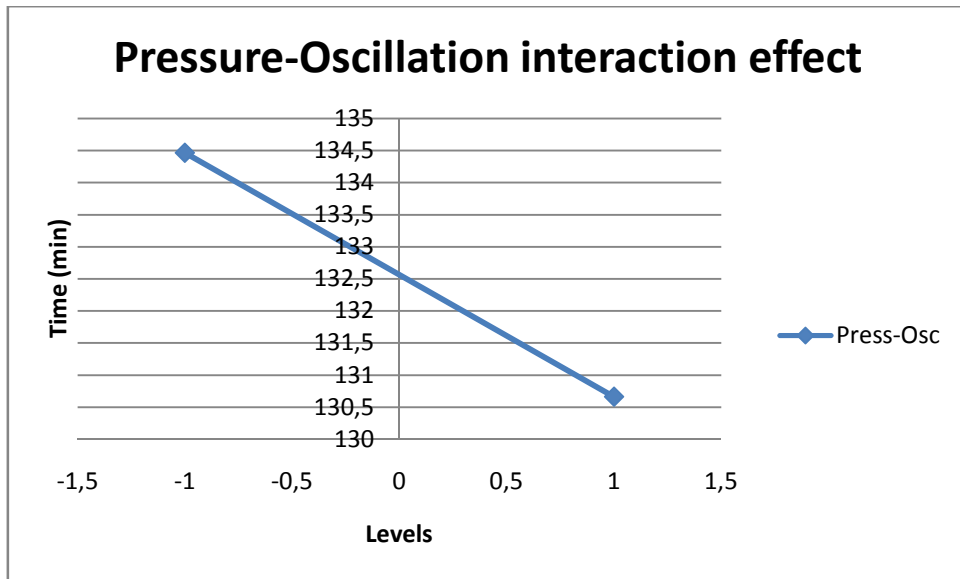


**FIGURE 12.44.** Effect of the interaction on the polishing process regarding the required time.

From the *figure 12.43*, it can be seen that, in opposition with the *figure 12.41*, the intersection between the two linear curves is not so clear, in fact they are almost parallel. This means that the interaction between these two polishing parameters into the considered range values of parameters is very small.

The last interaction parameter has been the Feed rate-Oscillation. The corresponding graphs are shown below:

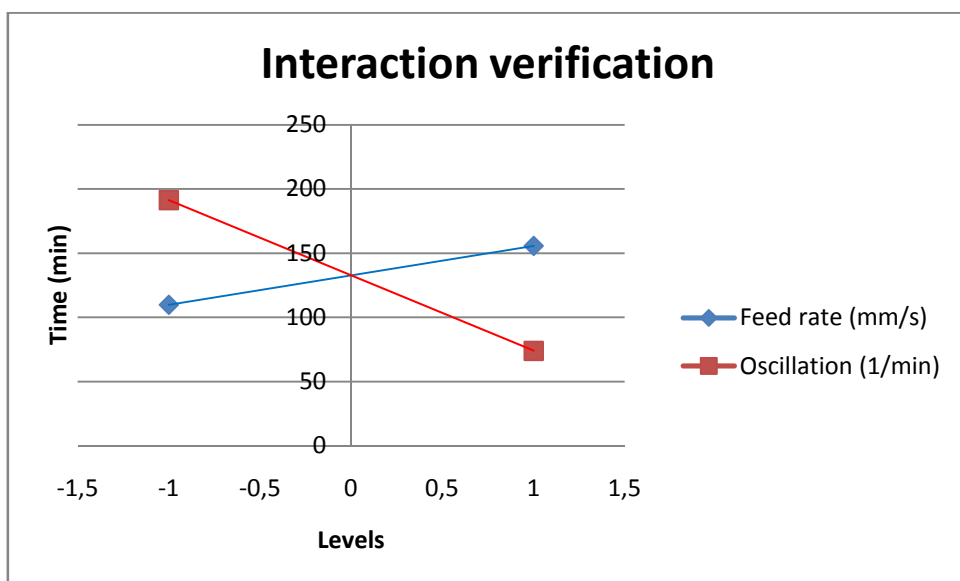


**FIGURE 12.45.** Verification of the interaction between the two interested parameters.

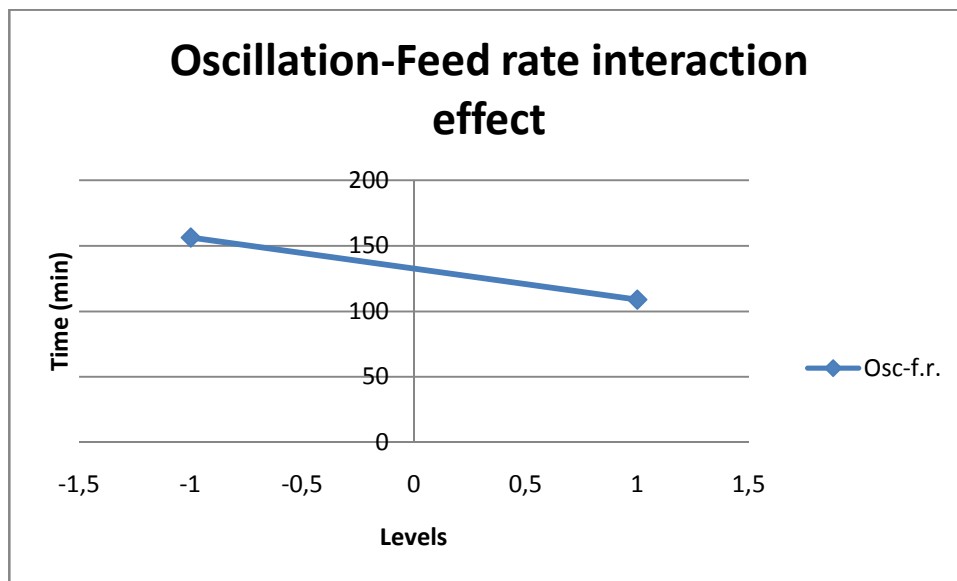


**FIGURE 12.46.** Effect of the interaction on the polishing process regarding the required time.

In the figure 12.45, as it was happened for the figure 12.41 where the pressure-feed rate interaction was analyzed, it can be seen that an interaction between the oscillation and the feed rate exists. Nevertheless, this interaction was expected, since these two parameters are related together with the velocity of the pad. In other hands, they are the two variables which describe the movement of the polishing pad itself.

From these results, it is clear that all the three considered parameters affect the process, regarding the final required time to reach the supposed final roughness value. In particular, pressure and oscillation seem to have a good influence if they are employed in their highest levels. The feed rate seems to be good for the process if it is kept to low velocity, moreover it seems to strongly interact with the other two.

To understand now how much the analyzed parameters and their corresponding interactions affect the process, that is, to understand which is the magnitude of each of them on the variation of the final process time, a deeper analysis is required.

This analysis consists in interpreting the Pareto chart and the interaction plots provided by MINITAB. These last plots are different from the previous ones, where the variation of the response has been shown as function of only one parameter. In fact, here the response is represented as function of two parameters, one kept constant and the other varied. In this way, the interaction between the two parameters is more clearly shown.

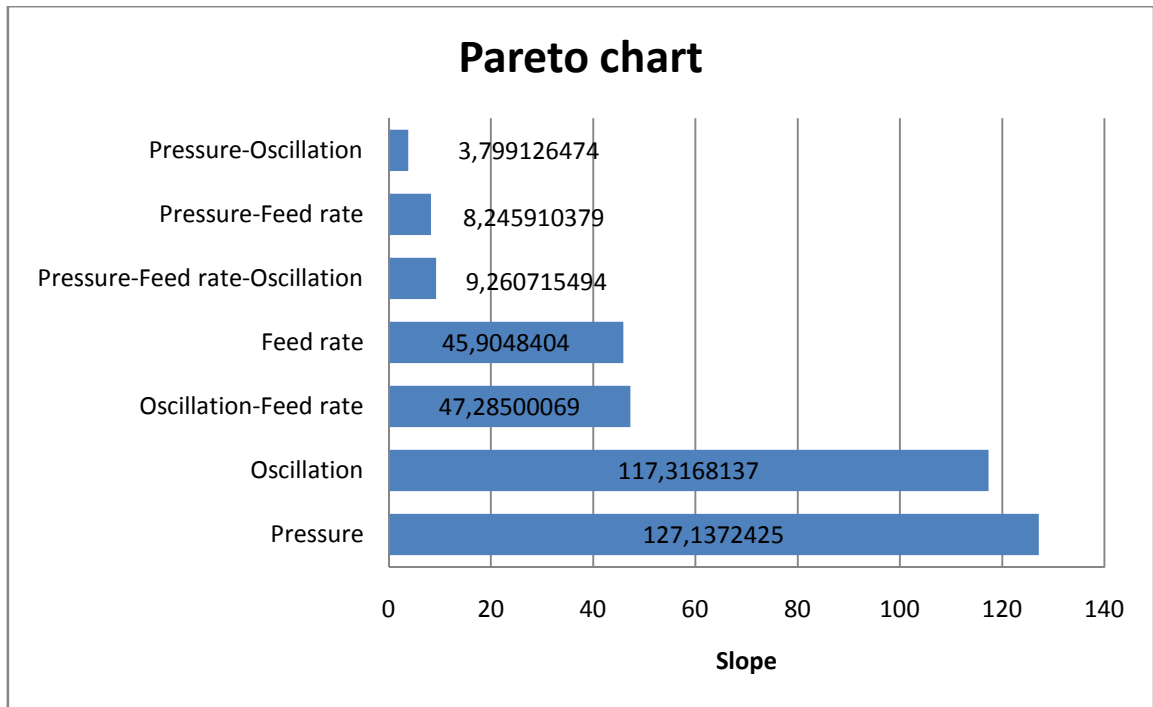


FIGURE 12.47. Pareto chart of the considered polishing parameter and their interactions.

<b>PARAMETERS</b>	<b>MAXIMUM VALUE</b>	<b>MINIMUM VALUE</b>	<b>SLOPE OF THE LINEAR CURVE</b>
<b>Pressure [g]</b>	196.131	68.99379	-127.137
<b>Oscillation [1/min]</b>	191.2208	73.90401	-117.317
<b>Oscillation-Feed rate</b>	156.2049	108.9199	-47.285
<b>Feed rate [mm/s]</b>	109.61	155.5148	45.90484
<b>Pressure-Feed rate-Oscillation</b>	127.9321	137.1928	9.260715
<b>Pressure-Feed rate</b>	128.4395	136.6854	8.24591
<b>Pressure-Oscillation</b>	134.462	130.6628	-3.79913

TABLE 12.44. Table of the slopes.

The Pareto chart is a powerful instrument of analysis because underlines which parameters have more importance during the process. That is, it shows the magnitude of each parameter and gives us an indication on which parameters more strongly affect the process. From this analysis we can see that the influences of pressure and oscillation (that is frequency of the pad) on the final polishing time are more important than the feed rate or the all interactions between the parameters. In fact, the effects of pressure and oscillation are equal to 127.1 and 117.3 respectively, and they are three times bigger than the effect of oscillation-feed rate and feed rate itself which are 47.3 and 45.9 respectively.

Regarding the pressure-feed rate interaction, its magnitude is very low (three orders of magnitude smaller than pressure and oscillation). This means it is true that pressure and feed rate interact together, but their effect on the process is negligible compared to the first two.

The same consideration is true for the interaction pressure-oscillation, whereas for the oscillation-feed rate parameter the conclusions are different. In fact, in this case, this parameter (if oscillation-feed rate is seen as a parameters) is the third one for importance to affect the process. This means that more attention has to be posed in this interaction. Also its effect is bigger than the effect of the feed rate itself.

To better understand and see what has been previously affirmed, the MINITAB interaction plots are introduced.

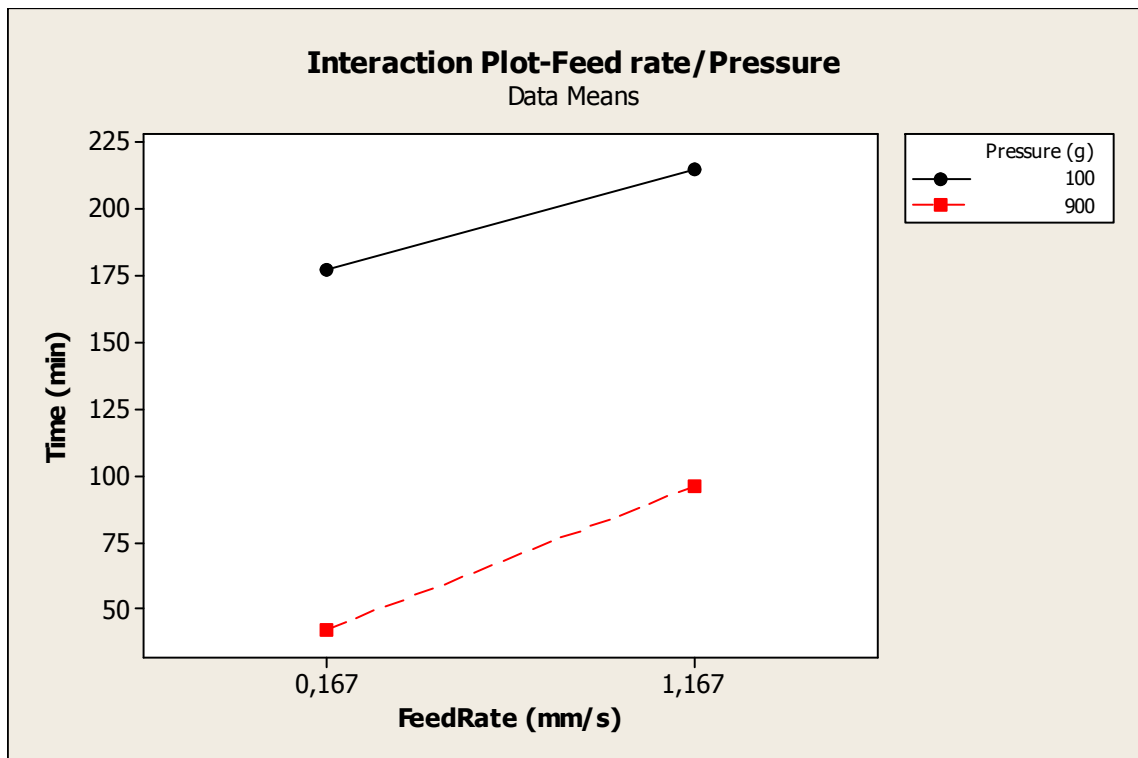


**FIGURE 12.48.** Interaction plot: Feed rate/Pressure.

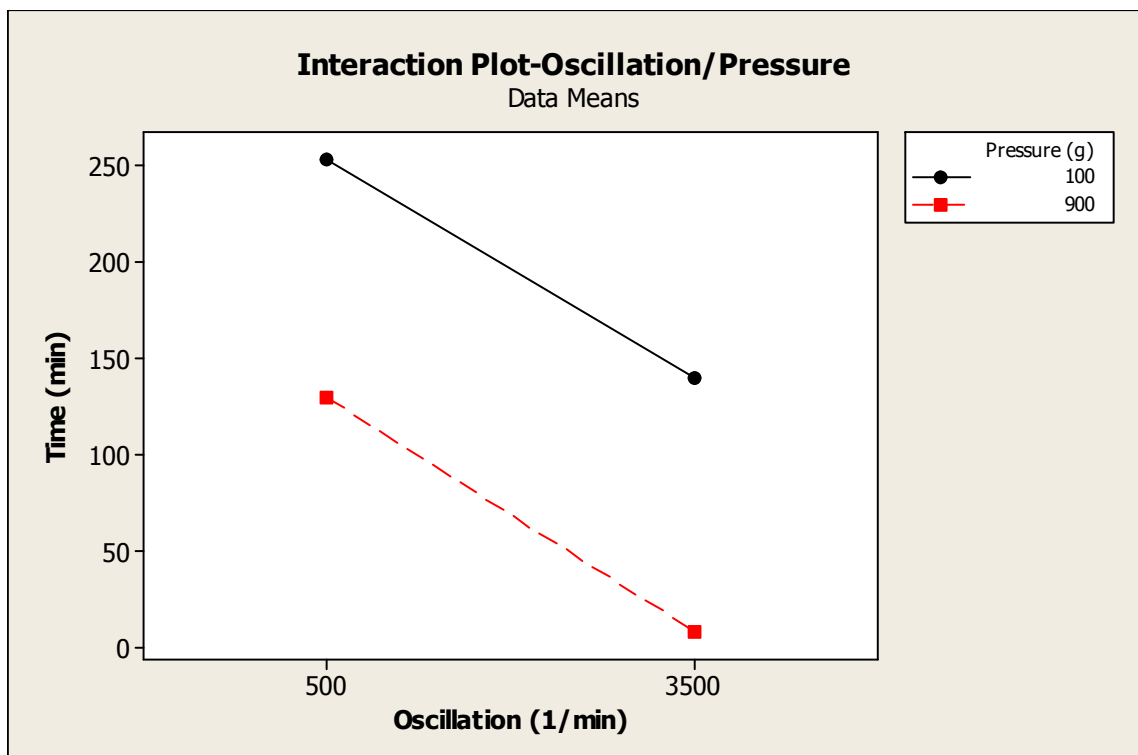


**FIGURE 12.49.** Interaction plot: Oscillation/Pressure.

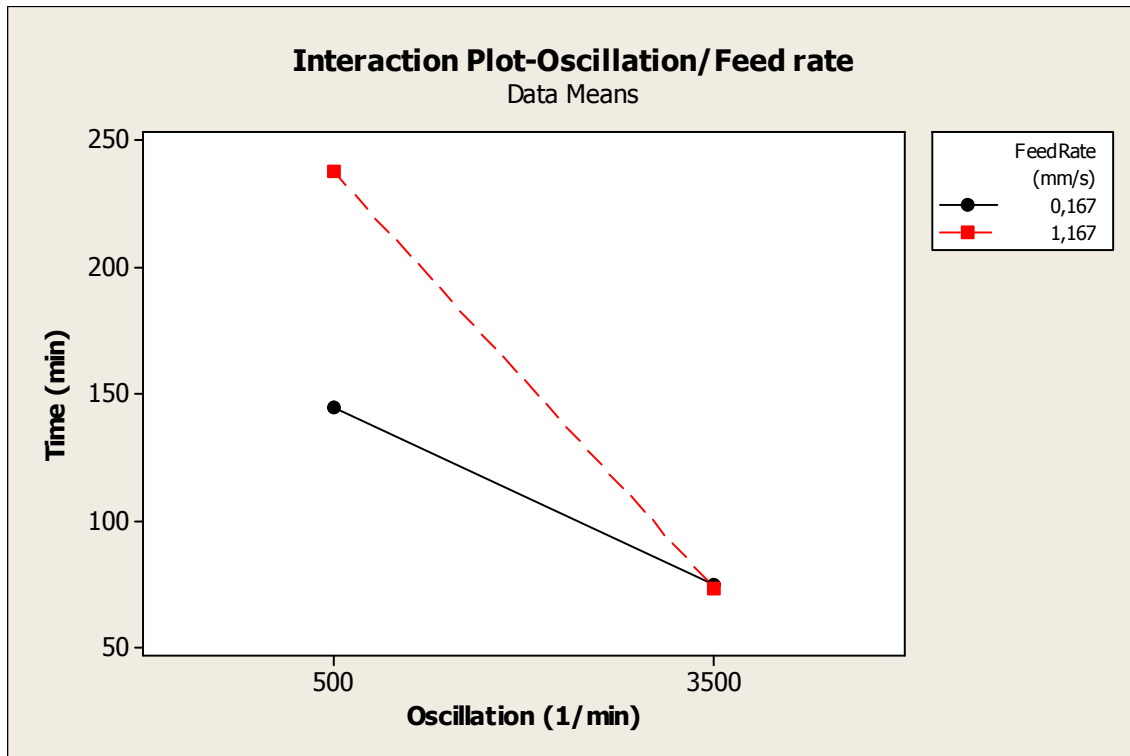


FIGURE 12.50. Interaction plot: Oscillation/Feed rate.

The three graphs shown above clarify what has been said previously. In the first one (*figure 12.48*) the curves are not parallel, but their slope is not so different each other. This means that it is true to say that there is an interaction between these two parameters (as it has been confirmed by the *figure 12.41*), but it is very low (as it has been confirmed by the Pareto chart). This means that the employment of high level of pressure conduce always to better response compared with the low pressure level. Whereas, if the feed rate increases, the polishing time required to reach the supposed final roughness value increases more or less of the same amount in the two cases.

Regarding the *figure 12.49*, the previous formulated consideration for the interaction pressure-feed rate are true again. In fact, in this case the two slopes of the curves are even closer than *figure 12.48*. This fact is underlined by the Pareto chart where the effect related to this interaction is the lowest. This means that when a high pressure is employed, a shorter polishing time is always obtained, and the same consideration is true for the oscillation.

In the *figure 12.50*, the effect of the interaction between oscillation and feed rate is clearly shown. In fact, the two slopes are evidently different each other, and the



intersection happens when the highest level for the oscillation is reached. This is a confirmation of the fact that the oscillation strongly affects the process. In fact, if high value of that are employed, low polishing time will be obtained for every value of the feed rate included between 0.167 mm/s and 1.167 mm/s. Moreover, for oscillation of 3500 m/s it appears better to use high feed rate rather than low, because the final required time is lower. Then this interaction has to be taken into account in the process, in particular because for low oscillation the polishing time, when high feed rate are employed, strongly increase.

These concepts are reaffirmed and confirmed by the surface plots and contour plots shown below:

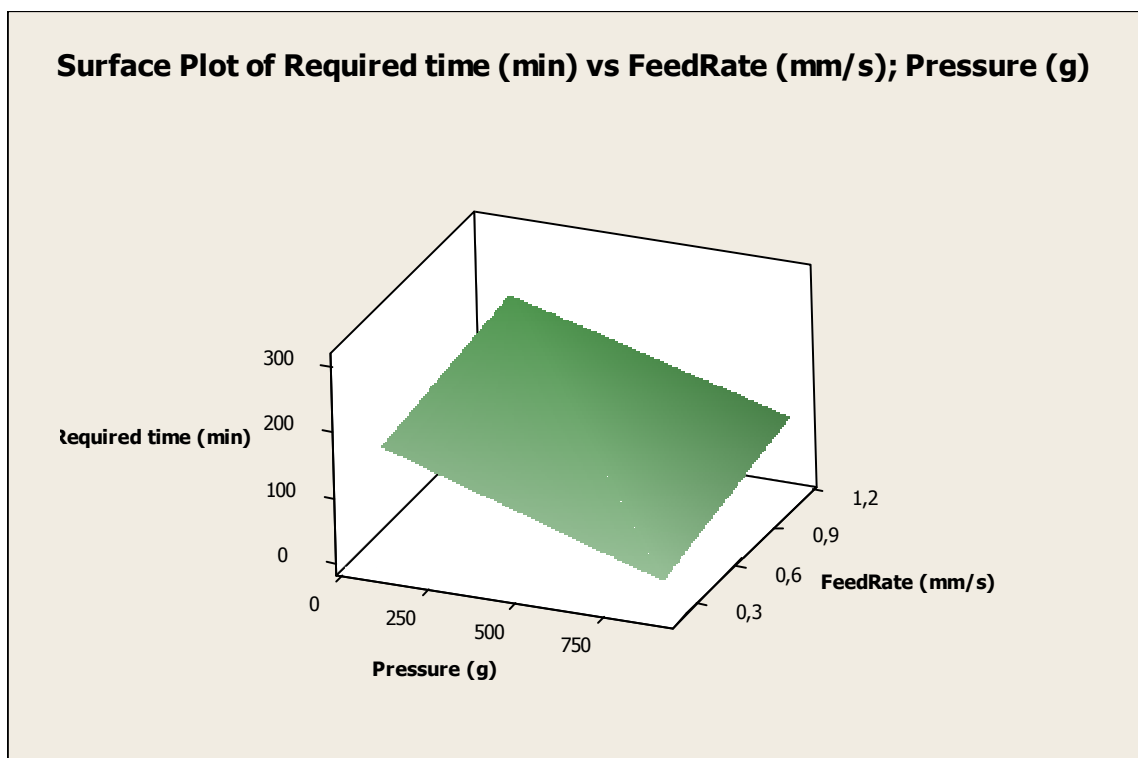


**FIGURE 12.51.** Surface plot: Feed rate/Pressure.

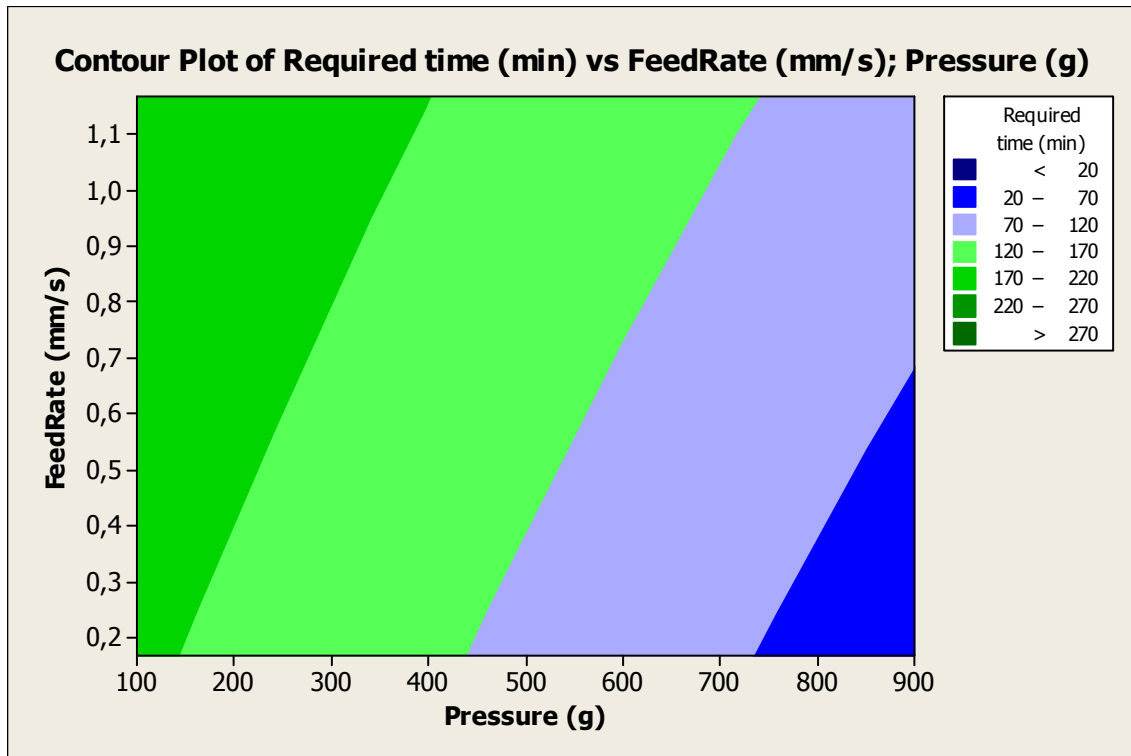


FIGURE 12.52. Contour plot: Feed rate/Pressure.

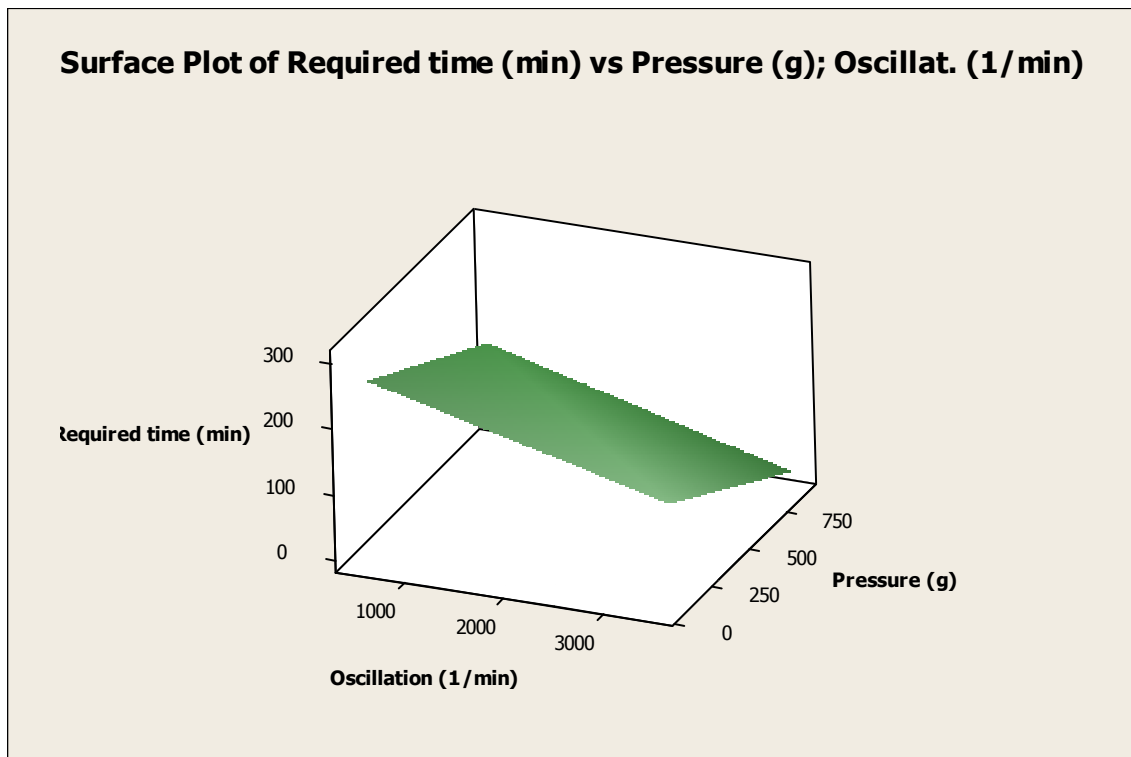
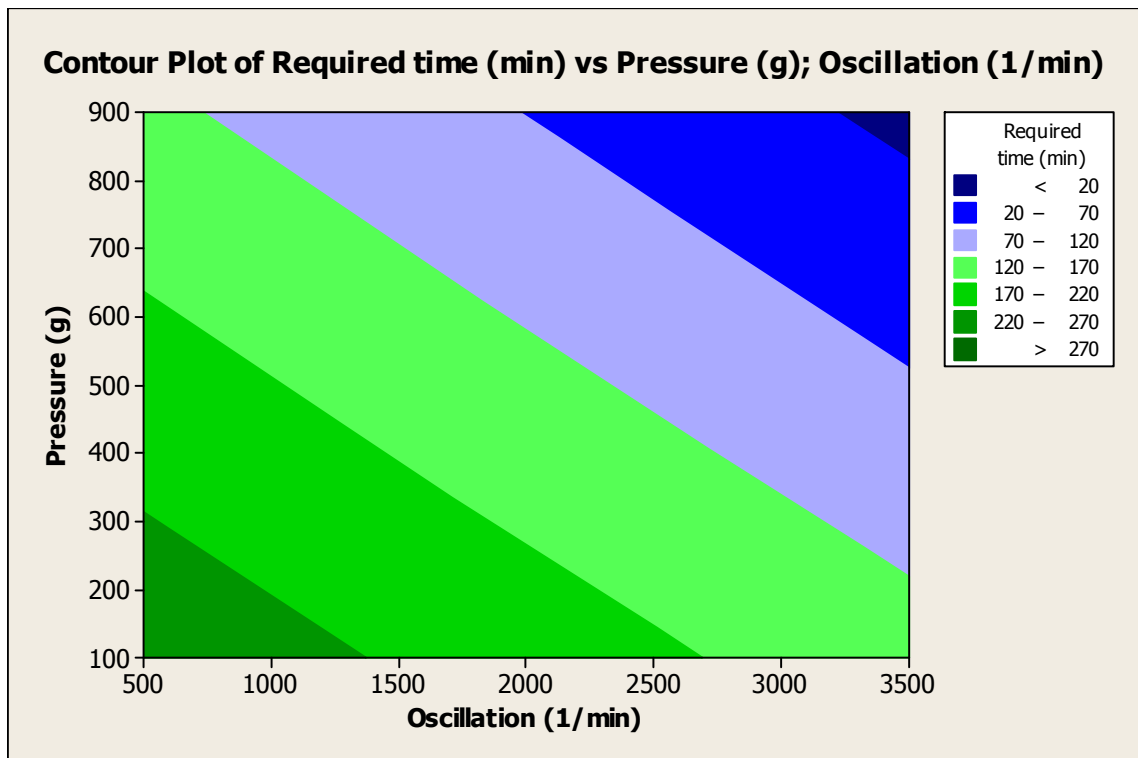
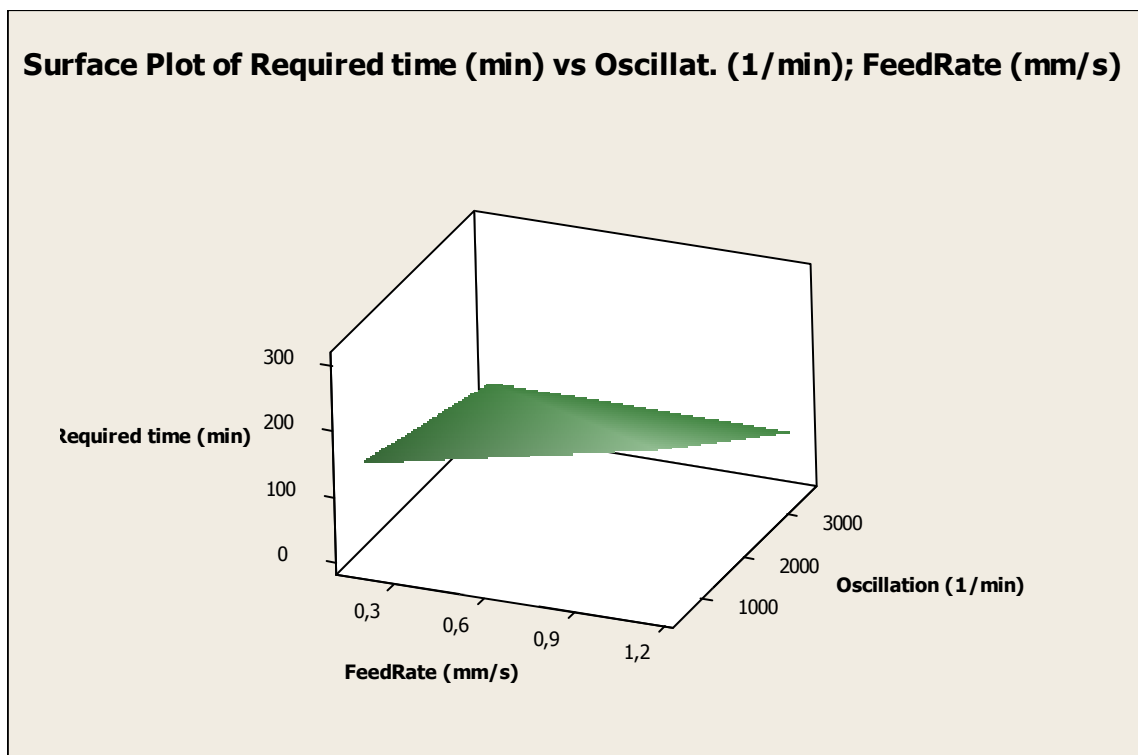


FIGURE 12.53. Surface plot: Pressure/Oscillation.



**FIGURE 12.54.** Contour plot: Pressure/Oscillation.



**FIGURE 12.55.** Surface plot: Oscillation/Feed rate.

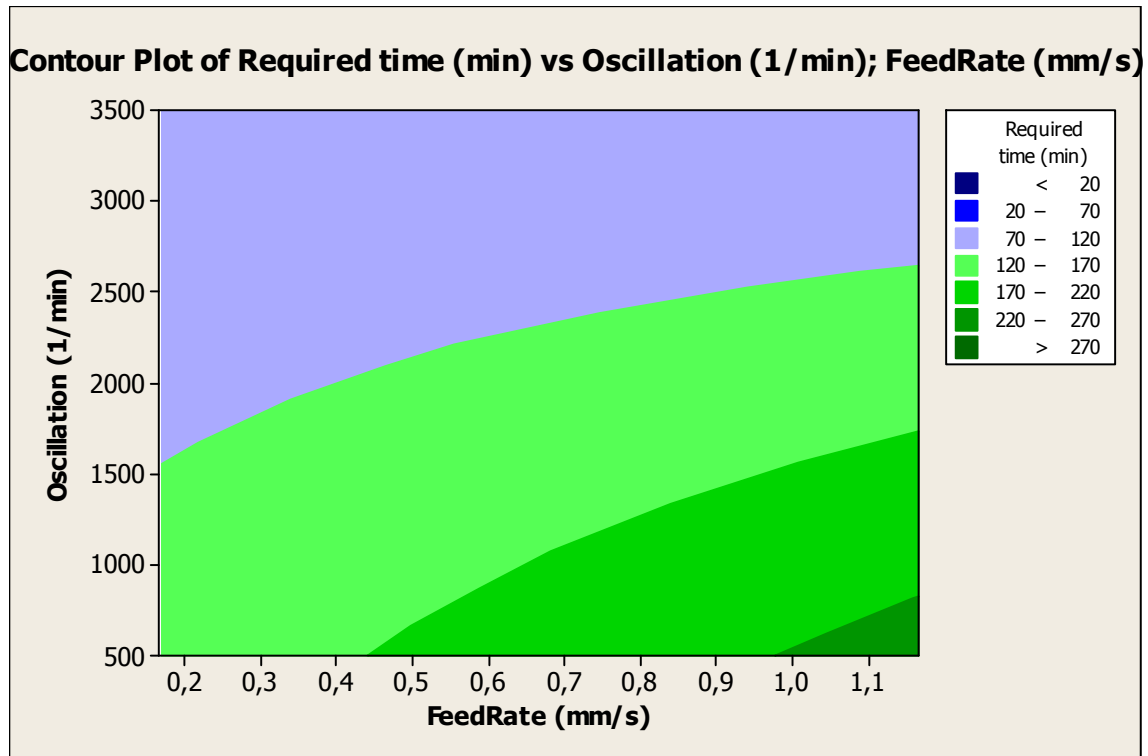


**FIGURE 12.56.** Contour plot: Oscillation/Feed rate.

#### 12.6.4. Conclusion regarding the full factorial analysis

After this first DOE analysis some considerations can be formulated.

Regarding the polishing parameters (down pressure, feed rate, and oscillation), if taken singly, they strongly affect the process, but not in the same way. In fact, pressure and oscillation are the two most important parameters of the process (as it is indicated in the Pareto chart, *figure 12.47*) and an increment of them brings to an evident reduction of the required time to reach the final roughness. Their effects on the process is largely bigger than all the others (three times bigger than the fourth most important parameter in the Pareto chart) and their strong influence is shown from the interaction plots provided by MINITAB (*figures 12.48, 12.49, and 12.50*). Regarding the feed rate instead, it does not affect the process as the first two parameters previously introduced, but it is anyway the fourth most important parameters in the process. Moreover, its influence on the process is opposite to those shown by pressure and oscillation. This means that it cannot be neglected from the process. In fact, if low or quite low levels of pressure and oscillation are employed during the process, the required final time to reached the wanted final roughness, strongly increases with an increment of the feed rate. Whereas, for high values of pressure and oscillation its effect on the process is more or less covered (this is indicated in the *figures 12.48 and 12.50*).

Regarding the interaction between the parameters, the only one worthy of note is the oscillation-feed rate interaction. As we can see from the Pareto chart (*figure 12.47*), and from the corresponding interaction plot (*figure 12.50*) it is important for the process. In fact, if the oscillation is decreased, and in particular high feed rate are employed in the process, the increment of the required time to reach the final process can reach the 164.602 minutes (in fact, the maximum time value when the lowest oscillation and the highest feed rate are employing is equal to 237.816 minutes, whereas the minimum is 73.214 minutes). The increment is smaller when a low feed rate is employed, only 70.032 minutes (where in this case the maximum value for the time is 144.626 minutes and the minimum 74.594 minutes), that means more of 2.5 times smaller than the previous one. Anyway, these increments of the value of the required time indicate that the process employing these combinations of parameters is ineffective.

Therefore, from this analysis it clearly appears that the employment of high levels for pressure and oscillation with low value for the feed rate implies the shortest polishing time to reach the desired final roughness value. In fact, if the *figure 12.37* is analyzed, where all the experimental results obtained from the tests are listed, it can be seen that for a combination of parameters equal to pressure=900 g, feed rate=0.167, and oscillation=3500 1/min, the shortest time is obtained. Anyway, it is correct to remember that this data are only an indication of the influence which these analyzed parameters have on the process. Additional tests are required to verify these considerations.

#### 12.6.5. DOE analysis adding the central point

What we have seen in the previously DOE analysis of a full factorial design with three parameters and two levels each, is that the parameters which strongly affect the process in terms of polishing required time to reach the final roughness value of 0.015  $\mu\text{m}$  from a starting roughness of 0.05  $\mu\text{m}$  are (in order to magnitude): pressure, oscillation, oscillation-feed rate, and feed rate. The other two remaining interactions (pressure-feed rate and pressure-oscillation) are neglected for the chosen intervals of the parameters, since their effects on the process are too low compared with the others.

We have explained how these parameters affect the process and which combination of parameter is the best between the eight available.

Nevertheless, we do not know anything about how the response of the model varies if some different values are chosen during the process. In other hands, we do not know if

the variation of the response, between the two threshold levels employing for each parameter, is linear or it has another shape, when a change in the parameters happens.

To better understand this, a central point has been added to the experiments made in STRECON and in this subchapter the results related to it will be discussed.

To be precise, what we was looking for with the central point has been to detect if the best combination of parameters were that provided by the first DOE analysis without central point (that is, it is corresponding to pressure=900 g, feed rate=0.167, and oscillation=3500 1/min) or if the optimum was situated into the chosen intervals for the polishing parameters. That is, after this new analysis which completes the previous one, we are not able to exactly detect the optimum value to obtain the shortest polishing time in absolute, but we have a first indication on how the response of the model varies, providing if the variation is linear or not (this is the information that we have wanted to understand from the central point).

To do that, the sample 0 (pressure=500 g, feed rate=0.667 mm/s, and oscillation=2000 1/min) has been added into the experimental planning, and now its results are compared with the previous ones obtained by the full factorial analysis.

Obviously, for the main effects (*figure 12.57*) related to the three polishing parameters (pressure, feed rate, and oscillation), nothing changes in this case, but the previous formulated considerations in the full factorial analysis are here even true. In fact the results do not change. The same considerations are true for the interaction plots (*figure 12.58*, Pareto chart included). But what is of interest here is to see the position of the timing response related to the central point (red point in the *figure 12.57*).

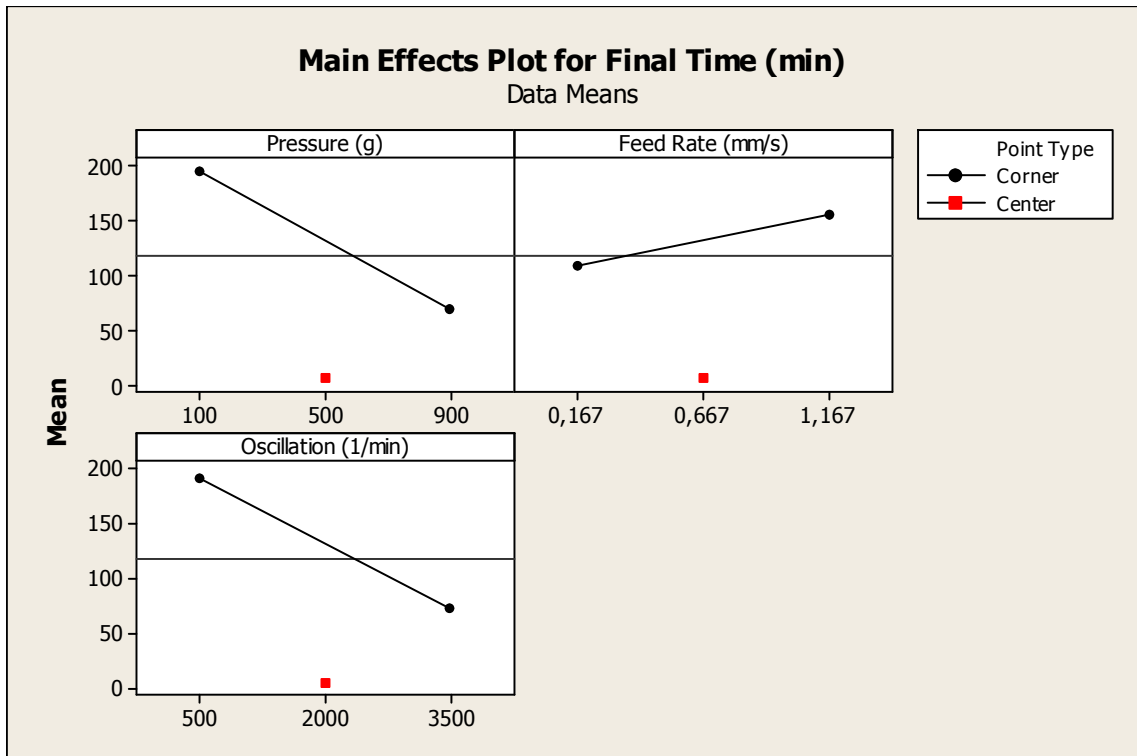


**FIGURE 12.57.** Main effects plot.

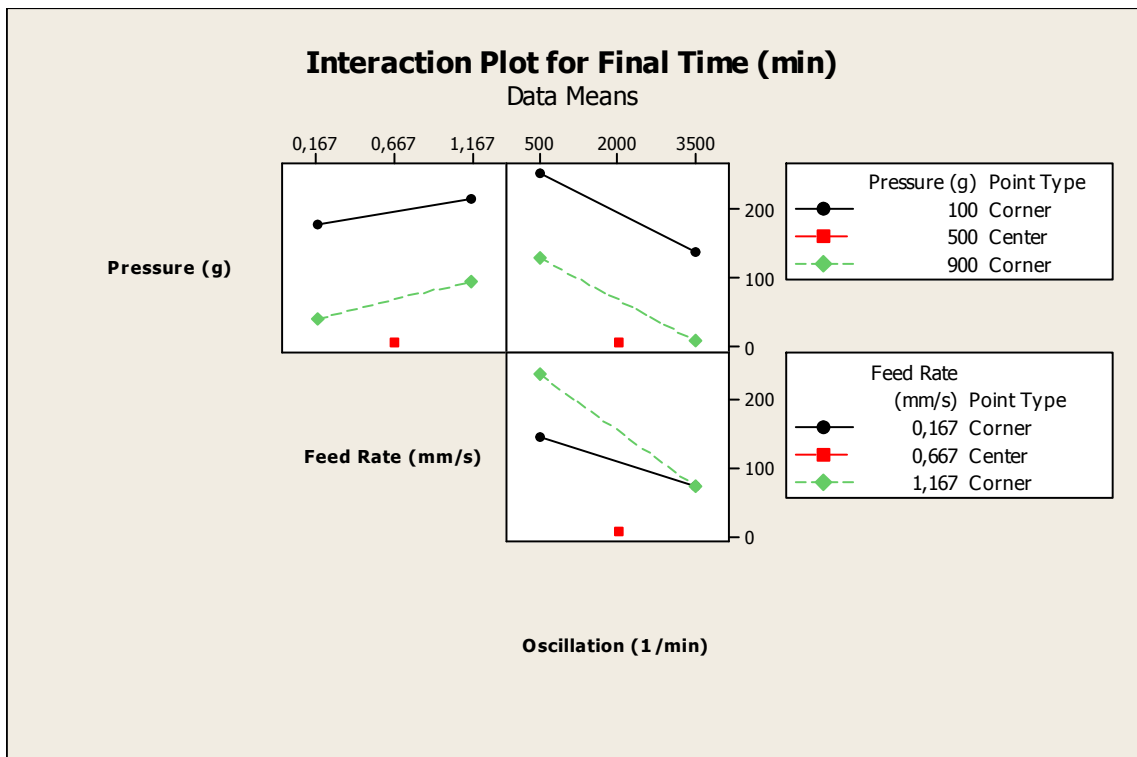


**FIGURE 12.58.** Interaction plot.

In fact, in these graphs, we can see that the polishing time value of the central point does not stay on the line representing the main effects, neither close to it, but it is situated very far from it. This result can be noted in the interaction plots too, where the red point representing the central combination of parameters (figure 12.58). As it can be seen, it is always under the linear curves.

This means that the variation of the time response is not linear with the variation of the parameters. In fact, to be linear, it should stay at least close to the designed lines. But this does not happen.

Moreover, this concept is more clear when the surface plots and the contour plots are analyzed in this case.

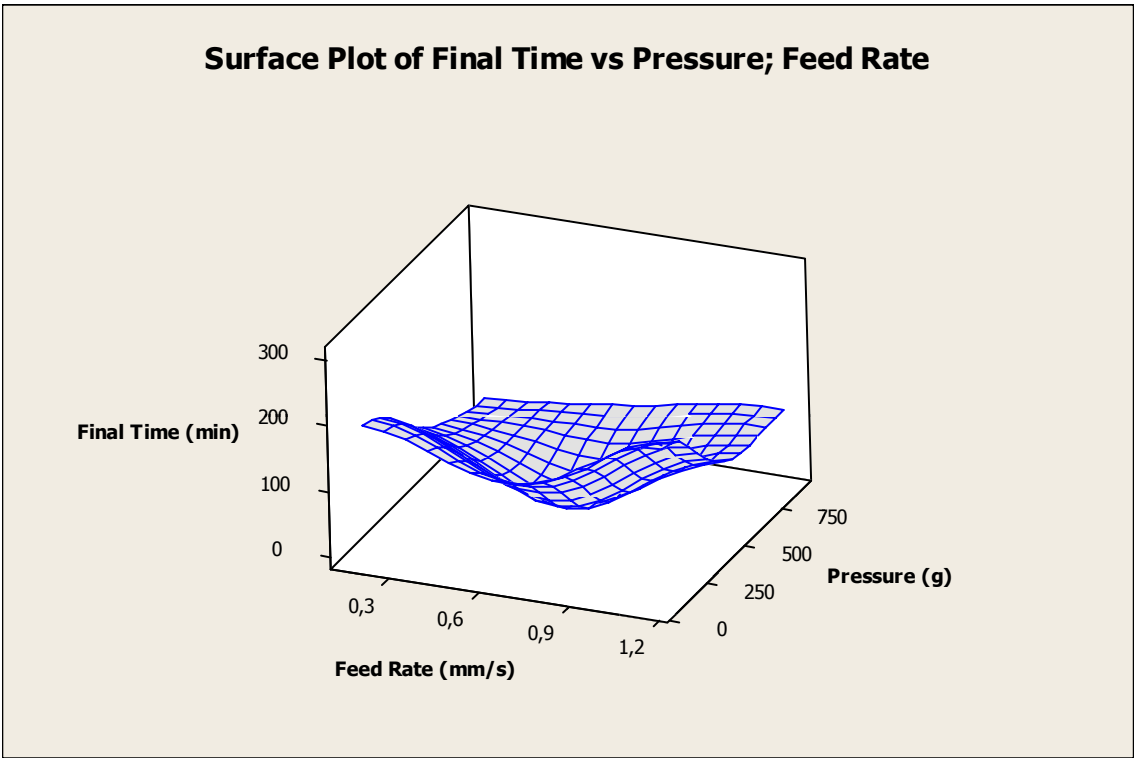
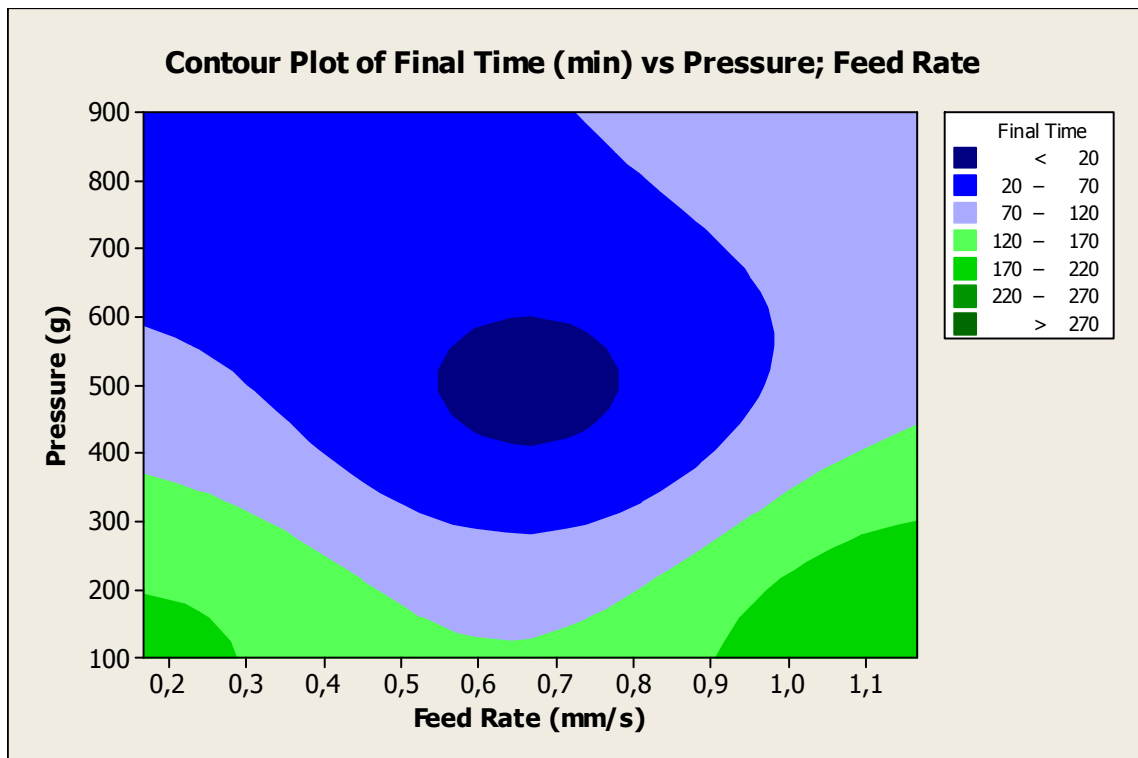
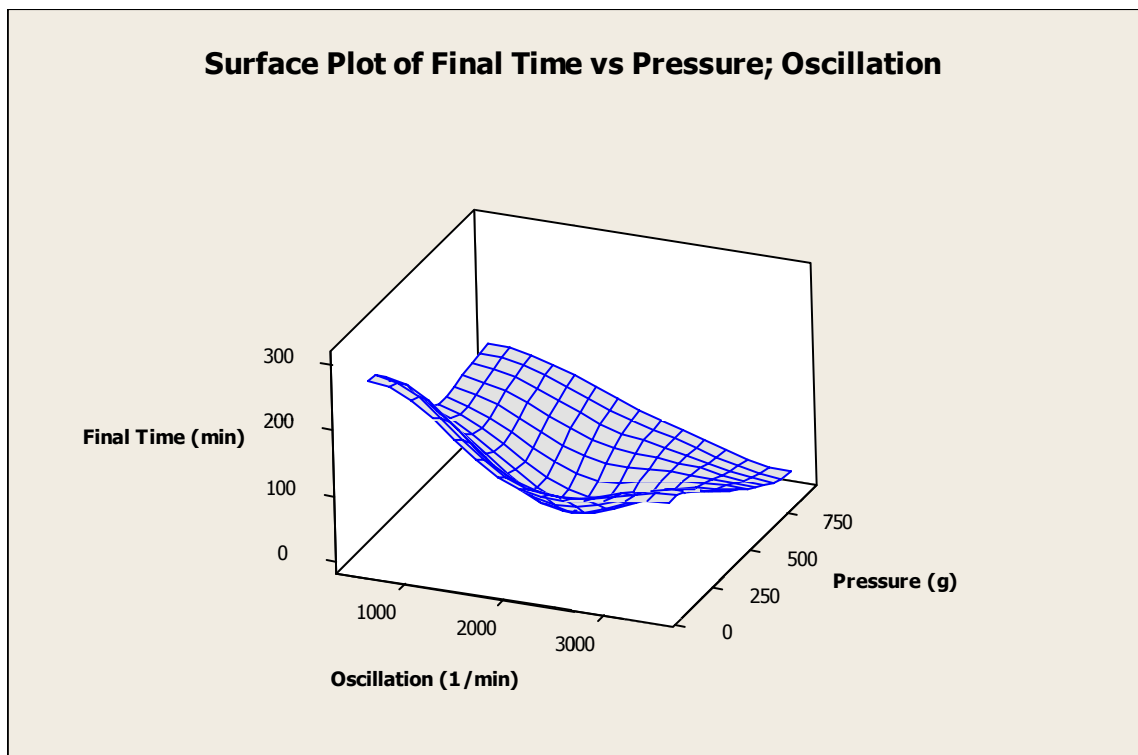


FIGURE 12.59. Surface plot.





**FIGURE 12.60.** Contour plot.



**FIGURE 12.61.** Surface plot.

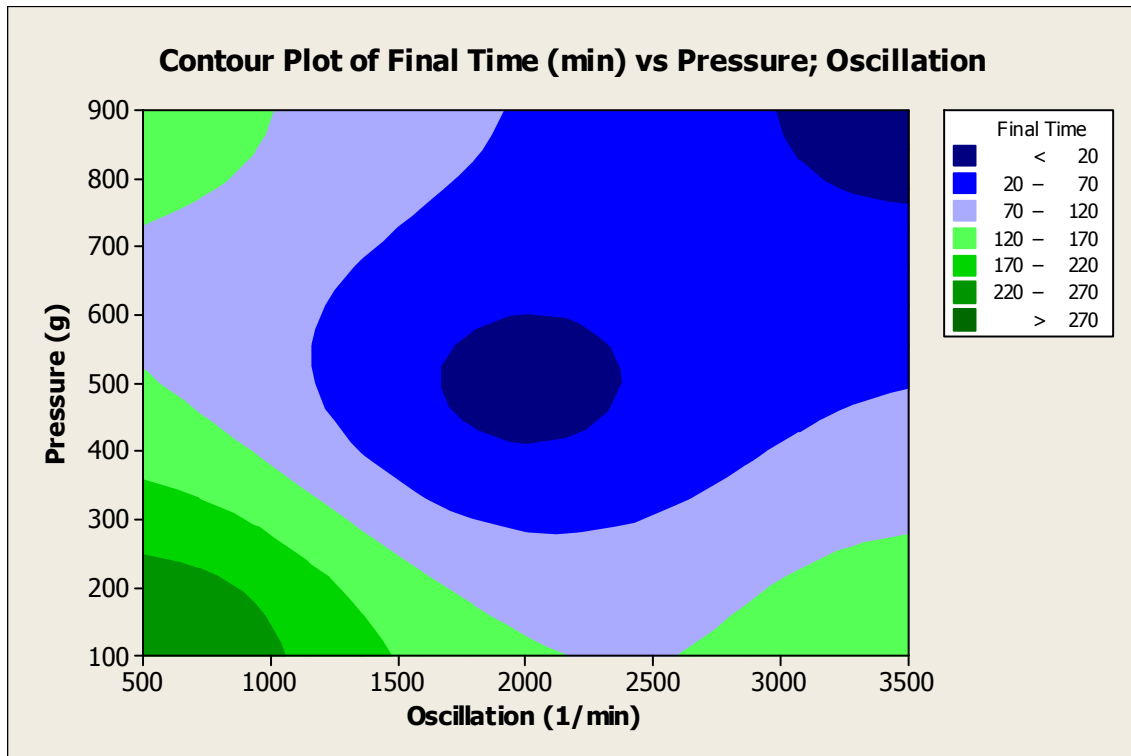


FIGURE 12.62. Contour plot.

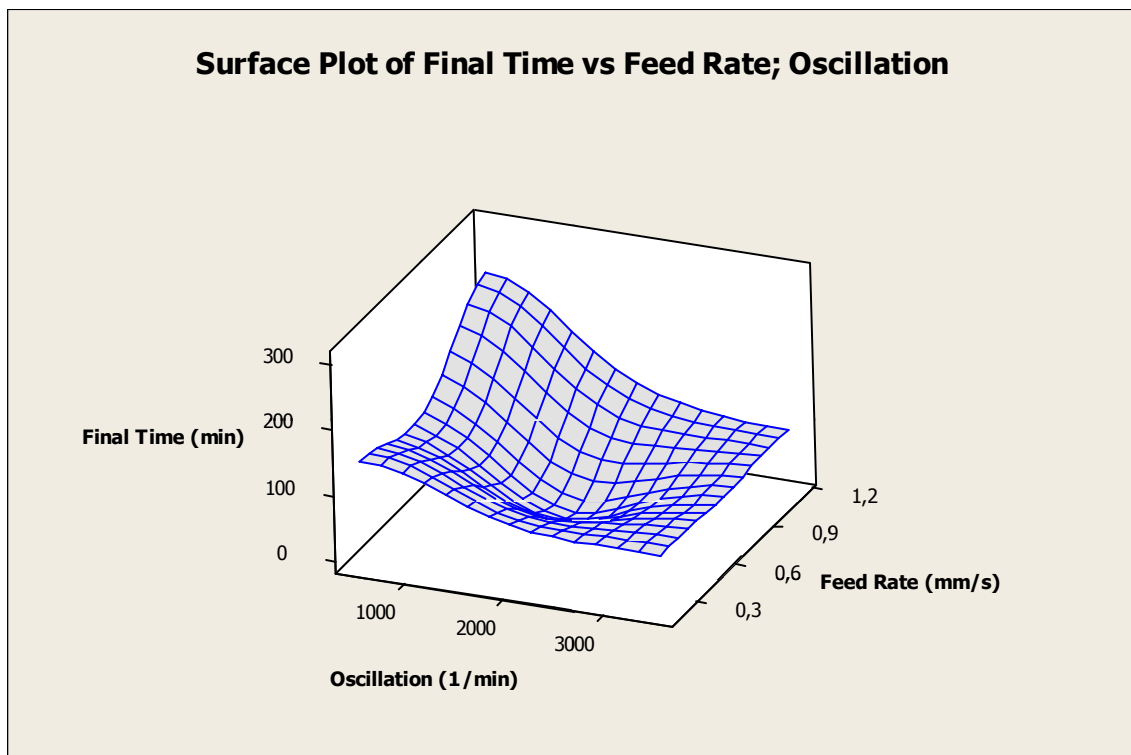
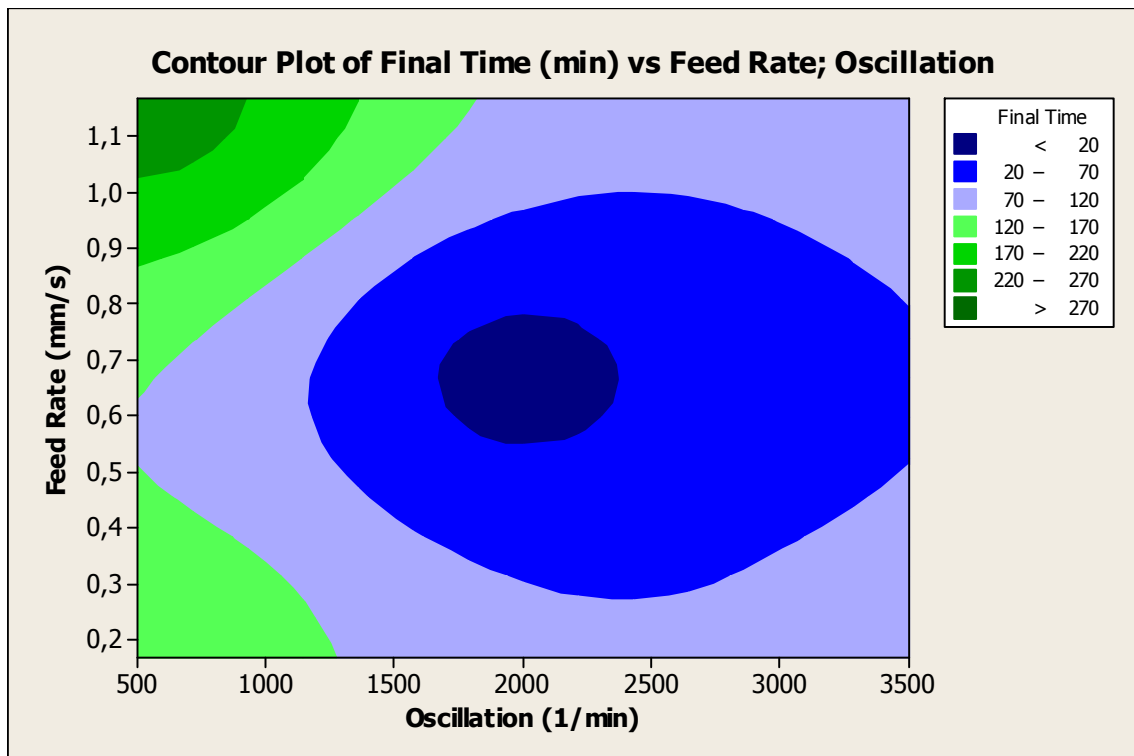


FIGURE 12.63. Surface plot.



**FIGURE 12.64.** Contour plot.

As it is shown in the *figures 12.59, 12.60, 12.61, 12.62, 12.63, and 12.64*, these graphs are very different compared with those obtain from a simple full factorial analysis. In fact, a low final polishing time is reached by the central point too and this modifies the shape of the plots. In fact, the previous full factorial assumed a linear variation of the response with the parameters, but this indeed does not happen and it is confirmed by the central point results. This means more tests will have to be run to understand what happens in that zone and how the response changes there. In fact, after having verified with the previous analysis (full factorial analysis) that the employment of low level for pressure and oscillation and high values for feed rate is not advantageous to obtain a fast polishing process, it will be interesting to understand how the time variation behaves to reach those high value, or if there are some zones where the response remains constant independently from the parameters employed. In this way the real optimum point or a stable region where the final polishing time does not significantly change can be detected.

This information can be found for example planning a full factorial design with three parameters with three levels. In fact, with this DOE design more information about how the analyzed response of the process varies, can be obtained and a optimal region can be detected. Also with this analysis it will be possible to confirm or not if the region

determined by low values for the pressure and oscillation parameters, but with high levels for the feed rate, is so disadvantageous for the polishing process.

In other hands, this full factorial with central value analysis has been useful to understand how to planning the next experiments with the aim to detect response zones of particular interest for the process.

#### 12.6.6. Analysis deriving by all the parameter combinations employed in these experimental tests

After having determined which are the most important parameters which affect the polishing process, how their interactions affect the required time to reach the final roughness, and after having detected that the variation of the model response is not linear with the variation of the parameters, three more tests has been run with the other nine, to take some more information about the process, in particular in the zone where the values of the parameters are medium-high.

The chosen polishing parameters for these three sample were:

- Pressure=900 g; feed rate=1.167 mm/s; oscillation=2000 1/min, for the sample 9;
- Pressure=900 g; feed rate=0.667 mm/s; oscillation=3500 1/min, for the sample 10;
- Pressure=500 g; feed rate=1.167 mm/s; oscillation=3500 1/min, for the sample 11.

This choice of parameters has been done because from the literature and from the experience of the STRECON operators more material removal is expected employing high values of pressure, feed rate, and oscillation, so that the final roughness value was supposed to be reach faster. It is noteworthy that this choice and considerations were done before to get some information from the DOE analysis and therefore before understanding how pressure, feed rate, oscillation, and their corresponding interactions affected the process. This means that this choice was only a consequence of theoretical assumptions and not of empirical considerations.

Anyway, as it has been previously done, some graphs are shown below and then discussed.

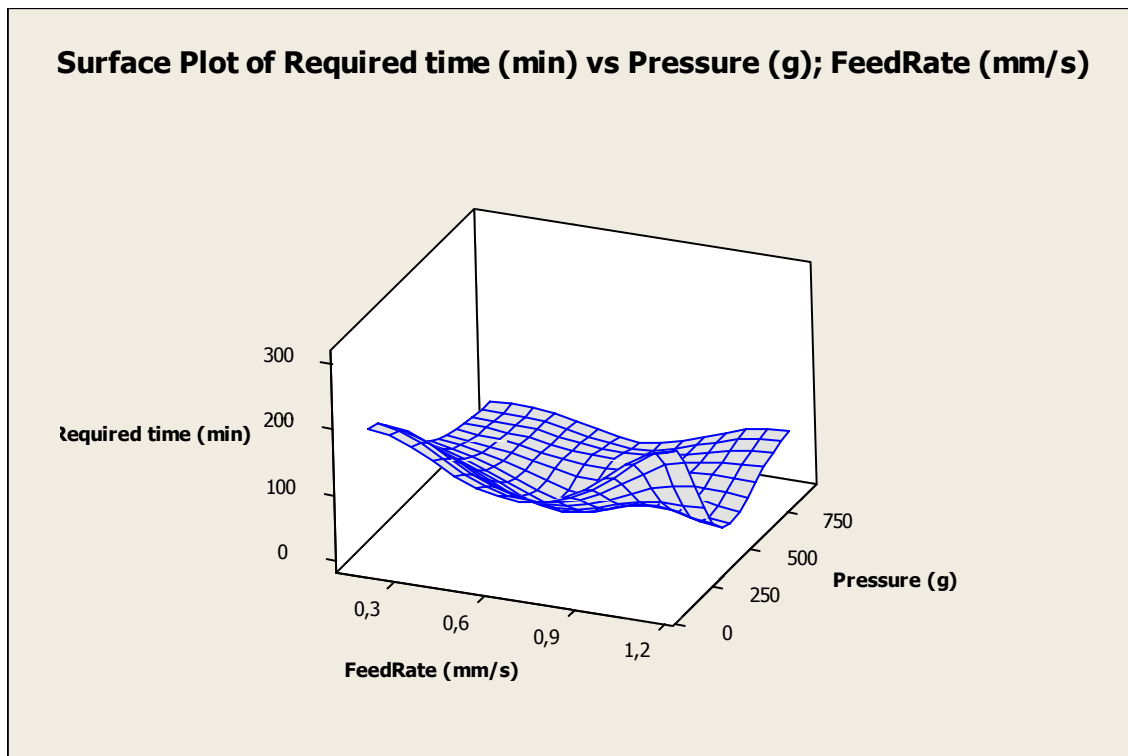


FIGURE 12.65. Surface plot.

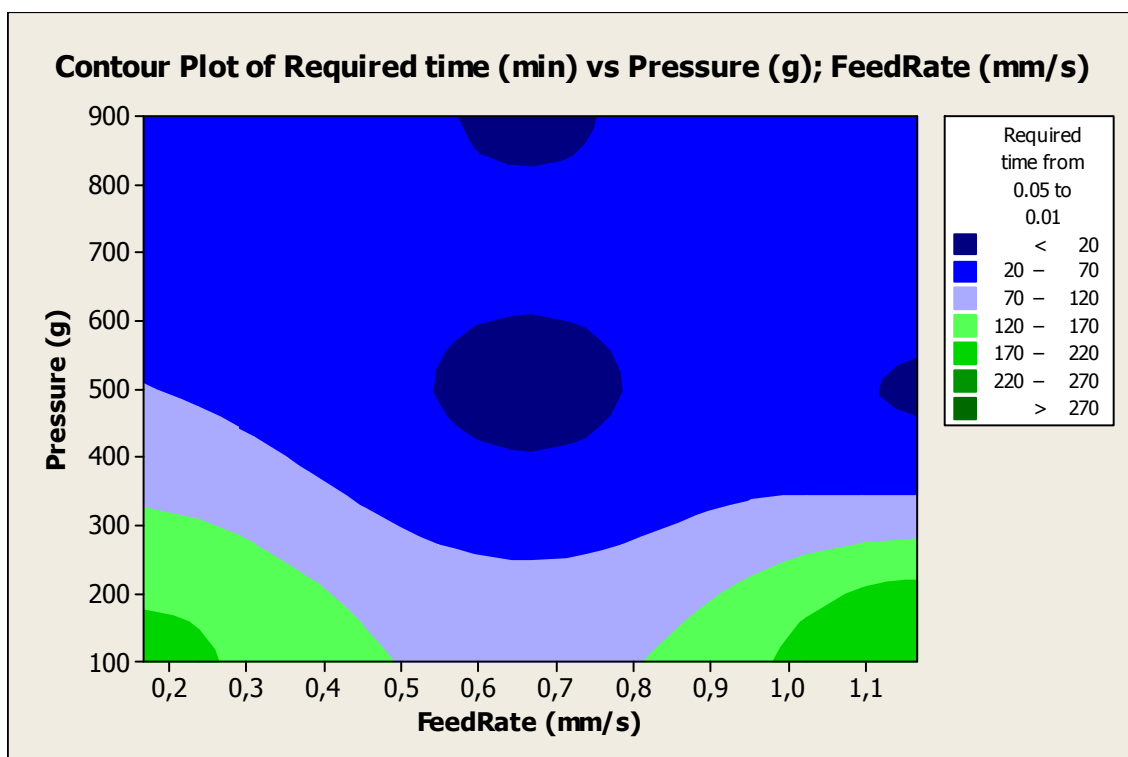


FIGURE 12.66. Contour plot.

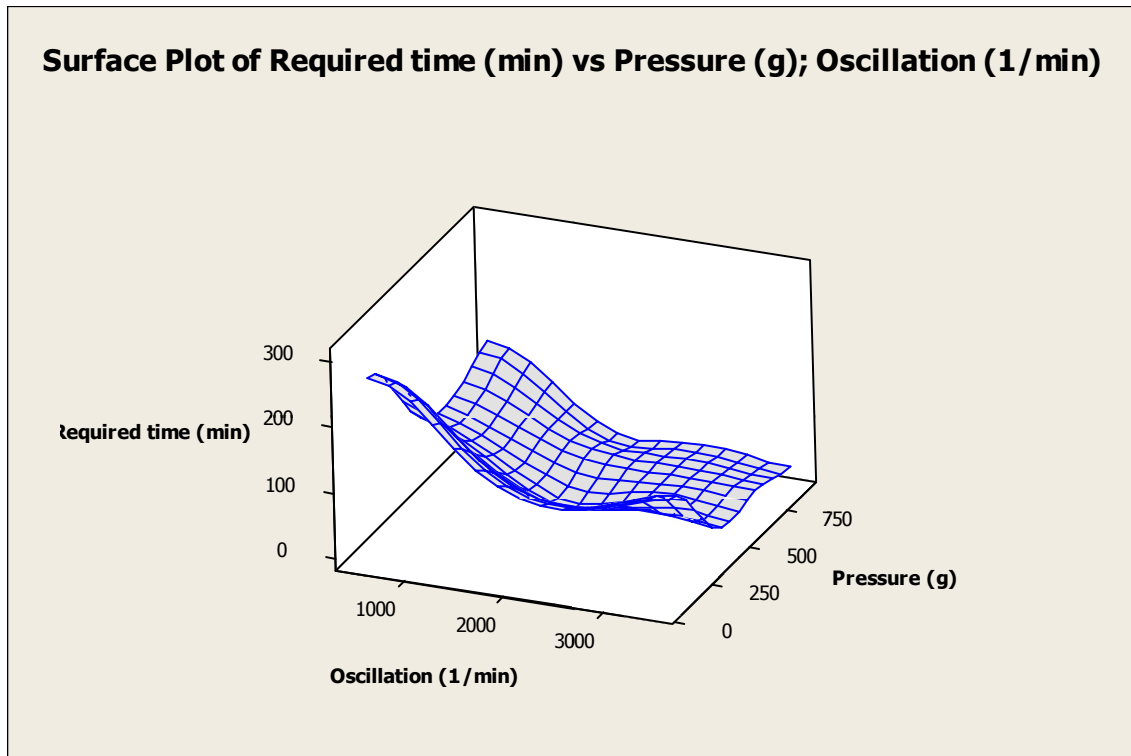


FIGURE 12.67. Surface plot.

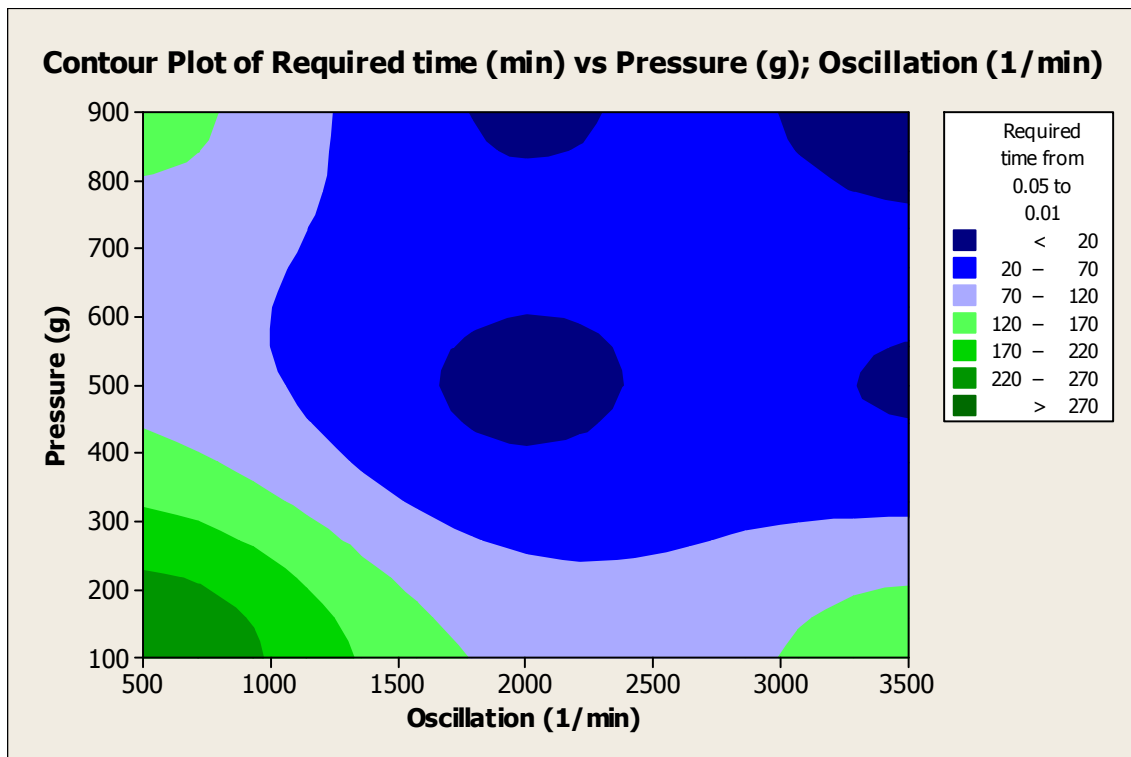


FIGURE 12.68. Contour plot.

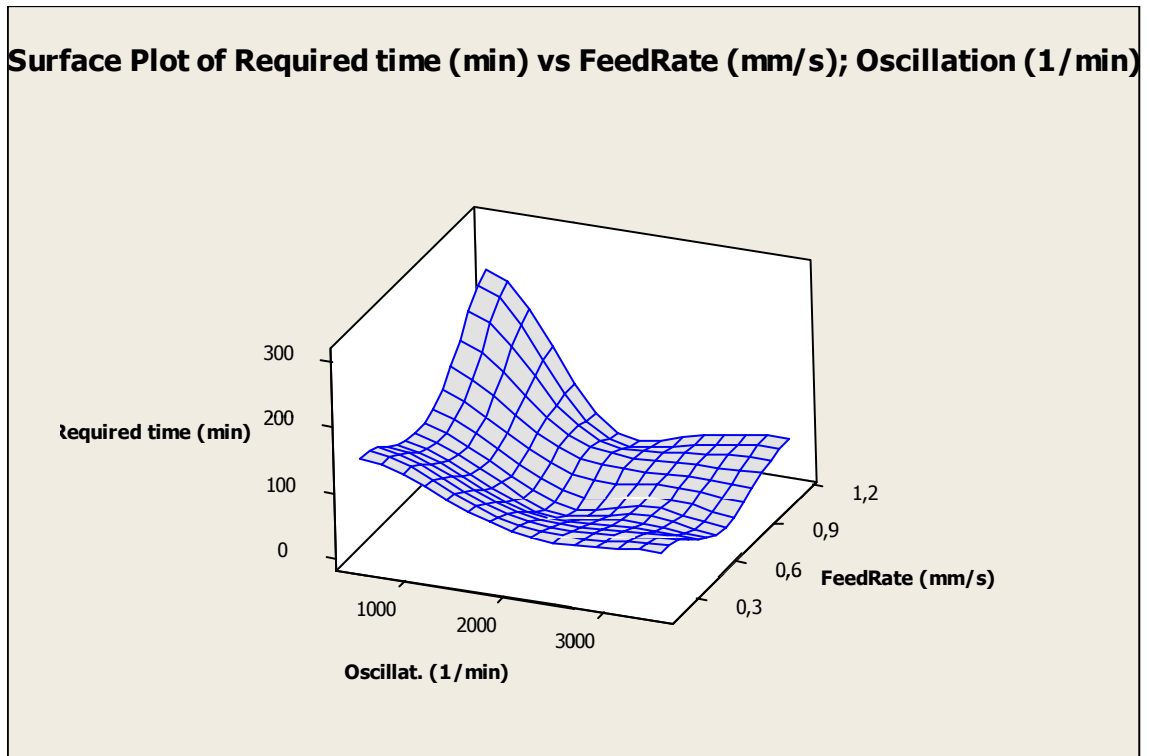


FIGURE 12.69. Surface plot.

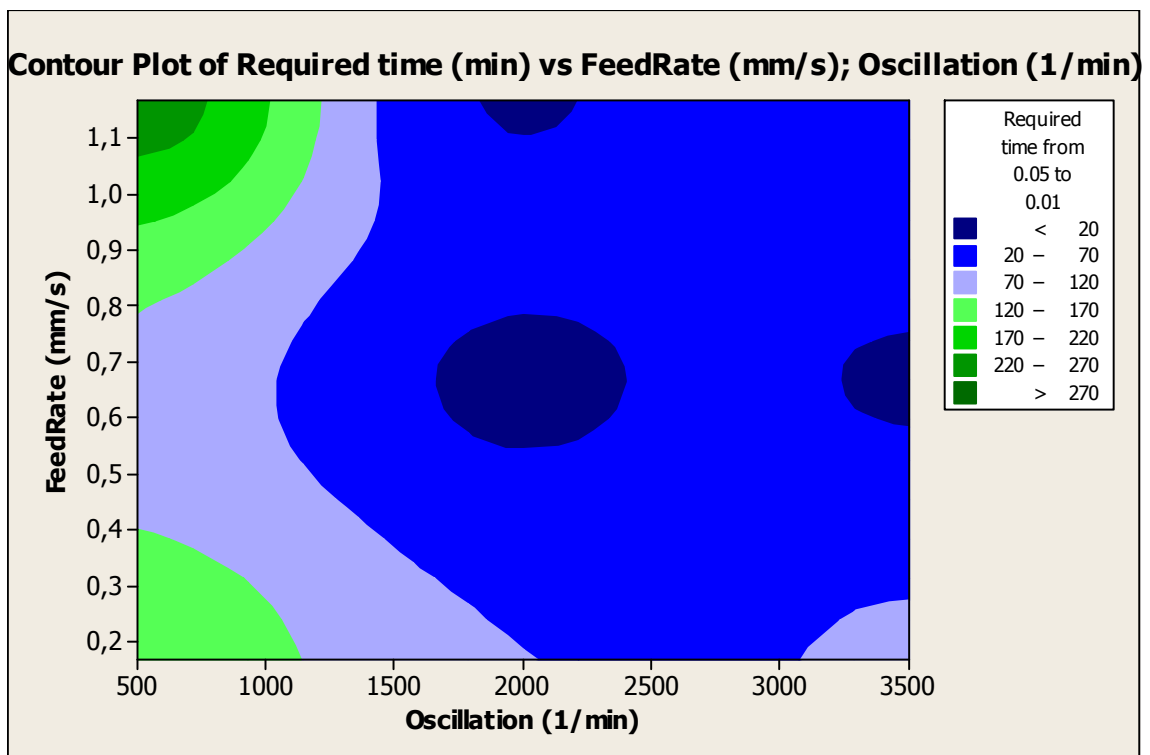


FIGURE 12.70. Contour plot.

Only the surface and contour plots have been reported above, because this last analysis is not a complete analysis which takes into account all the possible combination of factors (in fact this is an incomplete full factorial with three factors and three levels each, but it is not to confuse with a fractional factorial too, because for example a  $3^2$  fractional factorial will require only nine combinations of parameters), but it has to be interpreted as an indication where the optimum machining zone could be situated and how new experimental tests could be done. In other hands, it can be seen from the graphs that good results in terms of time have been obtained from these last three tests as well. In fact, results more or less similar have been obtained: 15.41 minutes for the sample 9, 15.44 minutes for the sample 10, and 16.75 minutes for the sample 11. This could bring to think that a stable zone where the response of the model does not change exists, and that it could be a confirmation of the fact that high values of pressure and oscillation are capable to cover the bad effect of the feed rate. Anyway, it is true that the obtained values for this combinations of parameters are however higher than the results obtained by the sample 0 (7.05 minutes) and 8 (0.37 minutes). Nevertheless, it is noteworthy to underline again that to be sure that this stable zone exists, and to understand the shape of the model response with the variation of the parameters, is necessary to run with new tests which permit us to detect and affirm this initial indications. What we can say with these results is that a non-linear behavior of the model response (time) is clearly individuated and this is confirmed both by the central point and by these last three samples.

#### **12.4. Correlation between the roughness behavior and the number of strokes made by the pad during the process**

One of the aim of the experimental planning has been to understand if the roughness behavior could depend on the number of strokes of the pad rather than on the time. That is, the choice of the levels of the parameters has been done to correlate feed rate and oscillation so that the wavelength of the journey of the pad was always the same. It is important to remember, in fact, that the movement of the pad during the polishing process is sinusoidal, this means that it has a certain amplitude, period, and wavelength. If a combination of parameters is chosen so that the wavelength remains the same during the journey of the pad and if the roughness behavior is demonstrated to depend on the journey itself and not on the time, it will possible to demonstrate that the roughness behavior is indeed determined by the strokes of the pad (here with stroke is indicated the sinusoidal way which the pad makes inside the wavelength).



As explained in the chapter six, it is required, before deciding which parameter values to use in the process, to establish a reference point from that the reference wavelength is extracted. As reference point has been decided to consider the usual parameter combination employed by STRECON, that is feed rate=1 mm/s and oscillation=3000 1/min. From this relation, the resulting wavelength is equal to 20  $\mu\text{m}$ .

Now, from this reference wavelength of 20  $\mu\text{m}$ , two pairs of parameters have been chosen and that is feed rate=1.167 mm/s; oscillation=3500 1/min and feed rate=1 mm/s; oscillation=500 1/min. this choice has permitted us to detect if there was a effective dependence of the roughness on the number of strokes made during the polishing process.

If this dependence happens, the final roughness value will be reached after the same number of strokes, independently therefore from the time.

To see if this fact really happens, the previous experimental results presented in the DOE analysis in terms of time are now converted in number of strokes. The operation is easy and intuitive, in fact it is necessary only to multiply the employed level of oscillation by the corresponding final time for each combination of parameters.

The overall number to reach the final roughness value of  $0.015 \mu\text{m}$ , starting from a initial roughness value of  $0.05 \mu\text{m}$  are listed in the table below:

	<b>Pressure (g)</b>	<b>FeedRate (mm/s)</b>	<b>Oscillation (1/min)</b>	<b>Required number of strokes from <math>0.05\mu\text{m}</math> to <math>0.015\mu\text{m}</math></b>
<b>Sample01</b>	900	0.167	500	41732.122
<b>Sample02</b>	900	1.167	500	87819.64
<b>Sample03</b>	900	1.167	3500	57746.688
<b>Sample04</b>	100	1.167	500	149996.100
<b>Sample05</b>	100	1.167	3500	454750.789
<b>Sample06</b>	100	0.167	500	102893.777
<b>Sample07</b>	100	0.167	3500	520854.540
<b>Sample08</b>	900	0.167	3500	1304.059
<b>Sample00</b>	500	0.667	2000	14091.655
<b>Sample09</b>	900	1.167	2000	30828.105
<b>Sample10</b>	900	0.667	3500	54042.684
<b>Sample11</b>	500	1.167	3500	58638.602

**TABLE 12.45.** Number of strokes required to reach a final roughness of  $0.015 \mu\text{m}$  from a starting roughness of  $0.05 \mu\text{m}$ .

Nevertheless, it clearly appears from the data that there is not correlation between the reached final roughness value and the number of strokes of the pad. In fact, if the samples 1 and 3 are taken into account, it can be seen that for the first one the number of strokes required to reach the final roughness is smaller than for the second one (41732.122 strokes, against 57746.688strokes respectively). The same situation is verified for the samples 5 and 6 (454750.789 strokes and 102893.777strokes respectively). The cause of this differenceson the final roughness values listed in the table above cannot be attributed to the pressure, because in the two considered pairs of samples it is kept constant (otherwise the comparison would not make sense).

Anyway, before presenting the MRR results, the regression model introduced by the *formula 12.1* to describe the roughness behavior will be generalized and the verification of the previous conclusion can be done.

## 12.5. Fitting of the preliminary regression model

In this subchapter the preliminary regression model employed to lead all the initial and final roughness of the samples to a common value will be generalized to verify its accuracy.

Indeed, some verifications regarding this aim have been done in the two previous subchapters, when for all the combinations of parameters the empirical estimation of the model has been performed for all the experimental points describing the roughness behavior for the particular sample. Anyway a generalization of this model is required to understand the goodness of the model itself.

Also, this fitting of the preliminary model will be valid both to confirm that it predicts well the examined roughness behavior (with the relative considerations on the dependence of the roughness on the number of strokes), and to give a first empirical model which will be subsequently compared with the empirical model provided by MATLAB program. The first model which will be fitted is related to the required time to reach the final roughness value (0.015  $\mu\text{m}$ ), whereas that other one correlated with the number of strokes will be introduced as second.

To start with this purpose, the employed preliminary regression model is reported below again:

$$y = A + B \times \log(x)$$

**FORMULA 12.2.** *Preliminary regression model.*

The first step required to generalize this model, is to write the two coefficients A and B as functions of the polishing parameters employed during the process, that is this two coefficients have to depends on pressure, feed rate, and oscillation. It is noteworthy however that the values of A and B for each samples depend on the made choice to pass the model on the time points  $T_1$  and  $T_4$ .

$$A = f(P, f.r., Osc.)$$

**FORMULA 12.3.**

$$B = f(P, f.r., Osc.)$$

**FORMULA 12.4.**

To do that, the twenty-four values found out from the estimation of the roughness behavior have to be considered. They are listed in the table below:

<b>SAMPLE</b>	<b>PRESSURE (g)</b>	<b>FEED RATE (mm/s)</b>	<b>OSCILLATION (1/min)</b>	<b>A</b>	<b>B</b>
<i>Sample01</i>	900	0.167	500	0.046	-0.016
<i>Sample02</i>	900	1.167	500	0.048	0.015
<i>Sample03</i>	900	1.167	3500	0.035	0.016
<i>Sample04</i>	100	1.167	500	0.256	0.089
<i>Sample05</i>	100	1.167	3500	0.201	0.081
<i>Sample06</i>	100	0.167	500	0.062	-0.020
<i>Sample07</i>	100	0.167	3500	0.176	0.069
<i>Sample08</i>	900	0.167	3500	0.014	0.002
<i>Sample00</i>	500	0.667	2000	0.022	-0.008
<i>Sample09</i>	900	1.167	2000	0.031	0.013
<i>Sample10</i>	900	0.667	3500	0.033	-0.015
<i>Sample11</i>	500	1.167	3500	0.027	-0.010

**TABLE 12.46.** Coefficients A and B employed to make the DOE analysis considering the required time.

Now, with the help of the regression program built by Roman Wechsler in MATLAB, a function providing the two coefficients A and B expressed as function of the process parameter employed during the experiments can be formulated.

It is noteworthy that, since the values of the A and B coefficients are twelve for each, maximum a quadratic equation can be taken into account to accurately describe them.

Therefore, the required equation will have a structure like this shown below:

$$A = a + bx_1 + cx_2 + dx_3 + ex_1x_2 + fx_1x_3 + gx_2x_3 + hx_1^2 + ix_2^2 + lx_3^2$$

**FORMULA 12.5.**

$$B = a' + b'x_1 + c'x_2 + d'x_3 + e'x_1x_2 + f'x_1x_3 + g'x_2x_3 + h'x_1^2 + i'x_2^2 + l'x_3^2$$

**FORMULA 12.6.**

As it can be seen from the *equations 12.5 and 12.6*, ten coefficients are required for each estimation. The task to compute them has been carried out by the MATLAB program when the data shown in the *table 12.46* were entered.

If for  $x_1$  is considered the feed rate, for  $x_2$  the pressure, and for  $x_3$  the oscillation, the values for the coefficients of the quadratic equation are:

<b>COEFFICIENTS FOR A</b>	<b>VALUE</b>
<i>a</i>	$0.998 \cdot 10^{(-1)}$
<i>b</i>	0.232
<i>c</i>	$-0.596 \cdot 10^{(-3)}$
<i>d</i>	$0.148 \cdot 10^{(-4)}$
<i>e</i>	$-0.123 \cdot 10^{(-3)}$
<i>f</i>	$-0.251 \cdot 10^{(-4)}$
<i>g</i>	$-0.221 \cdot 10^{(-7)}$
<i>h</i>	$-0.453 \cdot 10^{(-1)}$
<i>i</i>	$0.548 \cdot 10^{(-6)}$
<i>l</i>	$0.346 \cdot 10^{(-8)}$

**TABLE 12.47.** Values of the coefficients for the equation employed to evaluate A.

<b>COEFFICIENTS FOR B</b>	<b>VALUE</b>
$a'$	-0.033
$b'$	-0.096
$c'$	$2.463 \cdot 10^{(-4)}$
$d'$	$1.062 \cdot 10^{(-5)}$
$e'$	$4.278 \cdot 10^{(-5)}$
$f'$	$7.025 \cdot 10^{(-6)}$
$g'$	$1.105 \cdot 10^{(-8)}$
$h'$	0.028
$i'$	$2.309 \cdot 10^{(-7)}$
$l'$	$4.478 \cdot 10^{(-10)}$

**TABLE 12.48.** Values of the coefficients for the equation employed to evaluate B.

The regression of these coefficient is done employing the least squares regression. After having found out the values of the coefficients for the *equations* 12.5 and 12.6, the fitting of the preliminary regression model is done. In fact, now we are able to write it in a generalized form shown below:

$$y = A(P, F. r., Osc) + B(P, F. r., Osc) \times \log (x)$$

**FORMULA 7.** Generalization of the preliminary empirical model for the roughness on the time.

Where x indicates the time variable.

To see if this new model describes well the experimental data, a tables is listed below, where the comparison between the estimations of the model and five experimental results are compared:

<b>Pressure (g)</b>	<b>Feed rate (mm/s)</b>	<b>Oscillation (1/min)</b>	<b>Time (min)</b>	<b>Experimental data (<math>\mu\text{m}</math>)</b>	<b>Prediction (<math>\mu\text{m}</math>)</b>
500	0.667	2000	3.023	0.017 0.016 0.021	<b>0.017</b>
100	1.167	500	132.362	0.074 0.083 0.085	<b>0.062</b>
900	1.167	3500	2.999	0.03 0.021 0.03	<b>0.006</b>
100	0.167	3500	26.547	0.093 0.07 0.064	<b>0.068</b>
900	1.167	500	52.985	0.023 0.014 0.024	<b>0.030</b>
900	0.167	3500	11.178	0.012 0.01 0.009	<b>0.025</b>
900	0.667	3500	6.297	0.015 0.015 0.016	<b>0,021</b>

**TABLE 12.49.** Comparison of the predictions of the model with the experimental results.

The three values reported on the experimental data column for each parameter combination are related to the three made repetition for each polished area. As it can be seen from the table above, the model predicts quite well the roughness behavior

shown during the polishing process. The only wrong predictions are related to the sample 3 (pressure=900 g, feed rate=1.167 mm/s, and oscillation=3500 1/min) and 8 (pressure=900 g, feed rate=0.167 mm/s, and oscillation=3500 1/min).

Now the same fitting operation is done, but this time our interested variable is the number of strokes required to reach the final roughness.

The form of the preliminary regression model remains the same of the *equation 12.2*, but this time new A and B coefficients have to be calculated. The same method followed for the previous preliminary model is employed as well.

Firstly the A and B coefficient found out from the combinations of parameters are listed below:

<b>SAMPLE</b>	<b>PRESSURE (g)</b>	<b>FEED RATE (mm/s)</b>	<b>OSCILLATION (1/min)</b>	<b>A</b>	<b>B</b>
<b>Sample01</b>	900	0.167	500	0.090	-0.016
<b>Sample02</b>	900	1.167	500	0.087	-0.015
<b>Sample03</b>	900	1.167	3500	0.092	-0.016
<b>Sample04</b>	100	1.167	500	0.497	-0.089
<b>Sample05</b>	100	1.167	3500	0.487	-0.081
<b>Sample06</b>	100	0.167	500	0.117	-0.020
<b>Sample07</b>	100	0.167	3500	0.422	-0.069
<b>Sample08</b>	900	0.167	3500	0.022	-0.002
<b>Sample00</b>	500	0.667	2000	0.049	-0.008
<b>Sample09</b>	900	1.167	2000	0.074	-0.013
<b>Sample10</b>	900	0.667	3500	0.086	-0.015
<b>Sample11</b>	500	1.167	3500	0.064	-0.010

**TABLE 12.50.** Coefficients A and B employed to make consideration about the required strokes for the final roughness.

Now, these values have been entered in the MATLAB program to found out the coefficients required to the quadratic model for estimating A and B as functions of



pressure, feed rate, and oscillation (the form of these new quadratic equations are the same shown in *equations 12.5* and *12.6*).

The results are listed below:

<b>COFFICIENTS FOR A</b>	<b>VALUE</b>
<i>a</i>	0.185
<i>b</i>	0.535
<i>c</i>	-0.001
<i>d</i>	$7.360 \cdot 10^{-5}$
<i>e</i>	$-2.389 \cdot 10^{-4}$
<i>f</i>	$-4.083 \cdot 10^{-5}$
<i>g</i>	$-7.543 \cdot 10^{-8}$
<i>h</i>	-0.156
<i>i</i>	$1.348 \cdot 10^{-6}$
<i>l</i>	$2.423 \cdot 10^{-9}$

**TABLE 12.51.** Values of the coefficients for the equation employed to evaluate A.

<b>COEFFICIENTS FOR B</b>	<b>VALUE</b>
<i>a'</i>	-0.033
<i>b'</i>	-0.096
<i>c'</i>	$2.463 \cdot 10^{-5}$
<i>d'</i>	$-1.062 \cdot 10^{-5}$
<i>e'</i>	$4.278 \cdot 10^{-5}$
<i>f'</i>	$7.025 \cdot 10^{-6}$
<i>g'</i>	$1.105 \cdot 10^{-8}$
<i>h'</i>	0.028
<i>i'</i>	$-2.309 \cdot 10^{-7}$
<i>l'</i>	$-4.478 \cdot 10^{-10}$

**TABLE 12.52.** Values of the coefficients for the equation employed to evaluate B.

With this coefficients, the model can now be written as:

$$y = A(P, f.r., Osc) + B(P, f.r., Osc) \times \log(x)$$

**FORMULA 8.** Generalization of the preliminary empirical model for the roughness on the number of strokes.

As done for the time variable, now the prediction of the model are compared with the experimental results obtained by the tests.

<b>Pressure (g)</b>	<b>Feed rate (mm/s)</b>	<b>Oscillation (1/min)</b>	<b>Strokes</b>	<b>Experimental data (<math>\mu\text{m}</math>)</b>	<b>Prediction (<math>\mu\text{m}</math>)</b>
500	0.667	2000	6046.98	0.017 0.016 0.021	0.027
100	1.167	500	66181.1	0.074 0.083 0.085	0.064
100	0.167	3500	92914.2	0.093 0.07 0.064	0.077
900	1.167	500	26492.4	0.023 0.014 0.024	0.052
900	0.667	3500	22039	0.015 0.015 0.016	0.046

**TABLE 12.53.** Comparison of the predictions of the model with the experimental results.

As it appears from the *table 12.53*, when the preliminary regression model takes into account the number of strokes, it does not work well. In fact, almost all the prediction shown in the table are far from the experimental results. This means that if it is required

to describe the roughness behavior as a function of the strokes, another model has to be employed or another equation for the A and B coefficient which estimates better their values has to be found, for example using an equation with a degree bigger than the second (this was impossible in this case because the A and B values were only twelve).

Regarding the verification if the roughness behavior is related to the number of strokes or not, it can be done now employing this model. Two combinations of parameters can be assumed, but they must to have the same pressure, because otherwise it would affect the roughness behavior. The assumed values for feed rate and oscillation have to bring the wavelength of the pad motion. An example of these combinations are: pressure=100 g, feed rate=1.167 mm/s, oscillation=3500 1/min; and pressure=100 g; feed rate=0.167 mm/s; oscillation=500 1/min. If the relation exists, the reached roughness after a certain number of strokes should be more or less the same. The chosen number of strokes in this case has been 20000, but the results obtained by the two combinations of parameters have been different. In fact, for the first one, the roughness value corresponding to 20000 strokes has been 0.15  $\mu\text{m}$ , whereas for the second one 0.042  $\mu\text{m}$ .

Anyway, to have confirmation of this fact, another regression model which better fit the roughness behavior as a function of the number of the strokes should be tested.

## **12.6. Creation of an empirical regression model using the experimental results**

### 12.6.1. Formulation of the empirical model

In this chapter an empirical regression model to describe the roughness behavior is provided. Indeed, a quite good regression model which predicts the roughness as a function of the time has been shown in the chapter before. That one, however, has been proposed because to do the DOE analysis and to understand how the employed parameters affect the polishing process, it was required to have a common value for the initial and final roughness, so that only the required time to finish the process had to be the investigated variable.

Now instead it is required to find out an empirical model employing only the experimental data obtained from the tests. To do this purpose, we have used

theMATLAB program (created by Roman Wechsler) which is cable to provide us a regression model starting by the experimental data (see chapter four).

Therefore, firstly the database where the experimental data are listed have to be created and entered in the program. Then, a regression model has to be chosen from the available into the program.

Before to do that, an issue has to be solved. In fact, an important problem is that the samples do not have all the same starting roughness and this implies some considerations. In fact, we do not have any information on how the roughness behavior is forthose samples, which have starting roughness near 50 nm, when an higher roughness has to be evaluated. That is, we do not know how many minutes are required for those samples (and therefore for that combination of polishing parameters) to reach the same starting roughness value (50 nm) when their initial roughness is for example 193 nm(that is the starting roughness for the sample 5 for example).

Therefore it has been required to understand how dealing with the experimental data so to obtain a reliable empirical model.

The first consideration has been that it is not possible to pull forward the roughness curve with lower starting values assuming that they do not start at the time zero but after some minutes (*figure 12.71*). That is, it is not possible to determine with the available data after how many minutes it is appropriate to collocate in the graph roughness-time the curves which start with values minor than 0.193  $\mu\text{m}$  (this value is reported because it is the highest starting roughness measured before the tests).

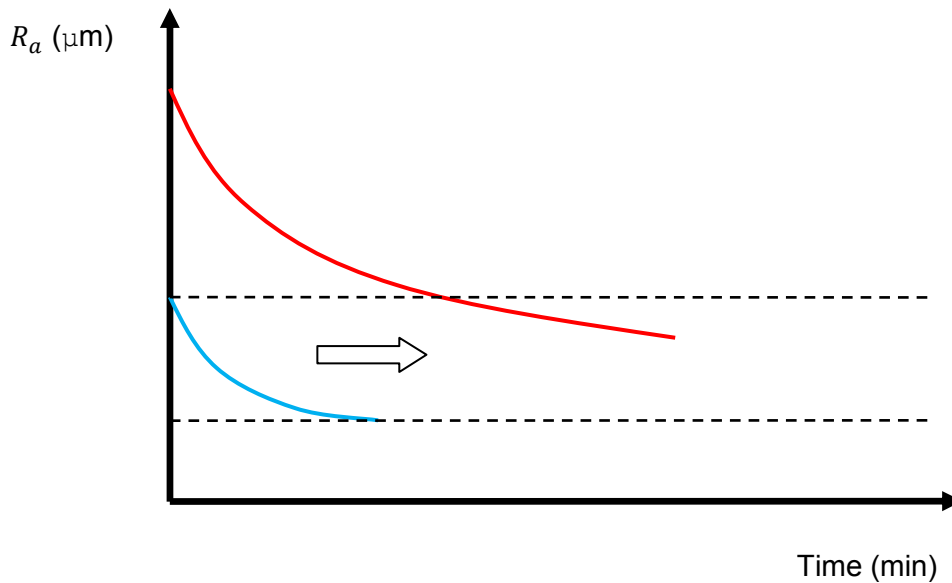


**FIGURE 12.71.** Shifting of the roughness curve with a small starting value to another different position from the time zero.

In fact, to be able to do that, the behavior of the roughness curves over their starting value should be known. But we do not have this information because, firstly, one of the aims of this thesis is to detect a reliable empirical model which predict this behavior, and, secondly, the previous preliminary regression model cannot help us in this case because being present the logarithm inside that model, it is not capable to reliably predict the roughness values for timing values bigger than  $T_1$  (this is because the employed points to find out the A and B coefficients for each combination of parameters have been  $T_1$  and  $T_4$ ).

Therefore, this way cannot be covered, because we are not able to detected the correct position of the roughness curves on the graph roughness-time.

If we cannot shift the curves starting from low value, we can instead move the curves with high roughness value and suppose that they starts from a lower value (*figure 12.72*).

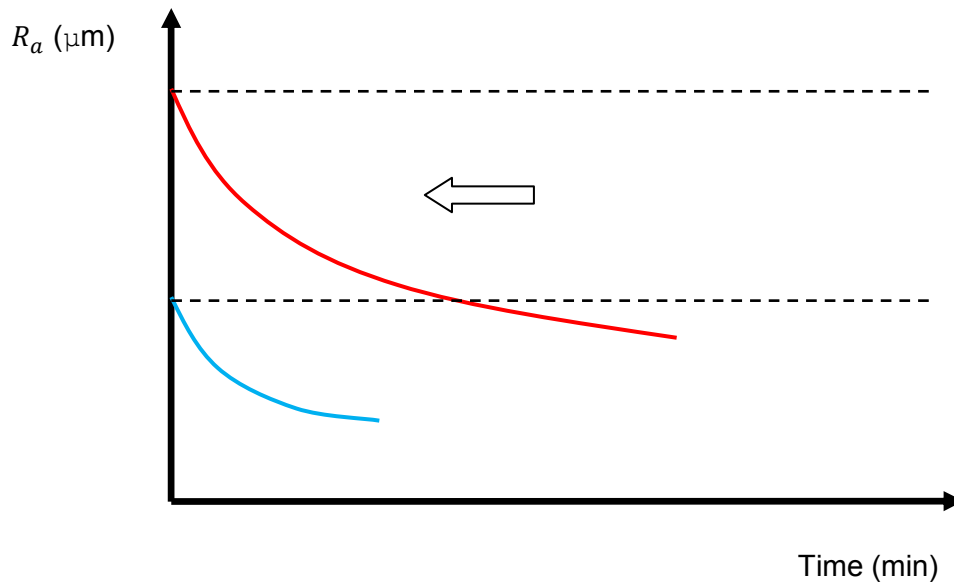


**FIGURE 12.72.** Shifting backward of the roughness curve with a high starting value.

This idea could be similar to that used to analyze the DOE results, but this time only the experimental data are employed to do this operation and no preliminary regression models are employed. This implies that not all the experimental results can be employed. This because some samples do not show a roughness value common for all, or because the roughness measurements done in correspondence to  $T_1$ ,  $T_2$ ,  $T_3$  and  $T_4$  cannot be used because they are or too high or too low. For example, the information related to the sample 1 cannot be used, because the starting roughness is too low ( $0.035 \mu\text{m}$ ) to be related with the others.

As it has been done in the DOE analysis, the common chosen value from which to start all the curves has been  $0.05 \mu\text{m}$ , because it is clearly the value most present in all the made measurement. Indeed, this time, this number is not considered like an absolute value, but it has to be seen as a small range of value. That is, to not modify the experimental results obtained from the test it has been considered that all the curves (or piece of curve) showing a roughness value included between  $(0.05 \pm 0.008) \mu\text{m}$ , started from the time zero. This fact has been done to not introduce any affection to the experimental data.

This means that data coming from the samples 0, 6, 8, 9, 10, are completed included in the database required by the program to build the regression model, whereas the data

from the samples 5 and 6 are not completely included and the data of the sample 1, 2, 3, and 4 are excluded.

In fact, regarding the sample 1 (as it has been previously said), the starting roughness is to low compared with the other to be included in the database (*table 12.54*).

<b>PASSES</b>	<b>TIME (min)</b>	<b>Ra,1 (<math>\mu\text{m}</math>)</b>	<b>Ra,2 (<math>\mu\text{m}</math>)</b>	<b>Ra,3 (<math>\mu\text{m}</math>)</b>
<b>0</b>	<b>0</b>	<b>0.035</b>	<b>0.035</b>	<b>0.035</b>
<b>11</b>	<b>15.369</b>	<b>0.027</b>	<b>0.026</b>	<b>0.029</b>
<b>32</b>	<b>44.710</b>	<b>0.019</b>	<b>0.018</b>	<b>0.021</b>
<b>53</b>	<b>74.052</b>	<b>0.016</b>	<b>0.016</b>	<b>0.018</b>
<b>105</b>	<b>146.707</b>	<b>0.01</b>	<b>0.011</b>	<b>0.013</b>

**TABLE 12.44.** Roughness measurements corresponding to the four intervals of time. For each measurement, three repetitions have been done. (sample 1).

Regarding the samples 2, 3, and 4, they have starting roughness higher than  $0.05 \mu\text{m}$ , but they do not have some coupling points which can be used. To better explain this, the table showing the measurement results for the sample 2 is showed below:

<b>PASSES</b>	<b>TIME (min)</b>	<b>Ra,1 (<math>\mu\text{m}</math>)</b>	<b>Ra,2 (<math>\mu\text{m}</math>)</b>	<b>Ra,3 (<math>\mu\text{m}</math>)</b>
<b>0</b>	<b>0</b>	<b>0.08</b>	<b>0.08</b>	<b>0.08</b>
<b>83</b>	<b>16.595</b>	<b>0.027</b>	<b>0.025</b>	<b>0.037</b>
<b>265</b>	<b>52.985</b>	<b>0.023</b>	<b>0.014</b>	<b>0.024</b>
<b>441</b>	<b>88.175</b>	<b>0.034</b>	<b>0.012</b>	<b>0.014</b>
<b>882</b>	<b>176.349</b>	<b>0.022</b>	<b>0.009</b>	<b>0.015</b>

**TABLE 12.44.** Roughness measurements corresponding to the four intervals of time. (sample 2).

From the *table 12.44*, the roughness value of  $0.05 \mu\text{m}$  never appears. This fact has not permitted us to use the information related to this combination of parameters, because we have not been able to collocated the corresponding roughness curve on the graph roughness-time. The same considerations are true for the samples 3 and 4.

Finally, regarding the samples 5 and 7, not all the data coming from the experiment could be employed in the database, but only a part. In fact, since their starting roughness were very high, the first two measurements corresponding to the time  $T_1$  and  $T_2$  could not be included, because the roughness value was still too high. For this reason only the value corresponding to the time intervals  $T_3$  and  $T_4$  have been employed and put in the database (this is not true for the third repetition because for both the observed roughness was still high to be taken into account). Anyway, to understand better this choice, the measurement results for these two samples are shown below:

<b>PASSES</b>	<b>TIME (min)</b>	<b>Ra,1 (<math>\mu\text{m}</math>)</b>	<b>Ra,2 (<math>\mu\text{m}</math>)</b>	<b>Ra,3 (<math>\mu\text{m}</math>)</b>
<b>0</b>	<b>0</b>	<b>0.193</b>	<b>0.193</b>	<b>0.193</b>
<b>47</b>	<b>9.397</b>	<b>0.112</b>	<b>0.13</b>	<b>0.127</b>
<b>139</b>	<b>27.792</b>	<b>0.072</b>	<b>0.077</b>	<b>0.09</b>
<b>231</b>	<b>46.19</b>	<b>0.059</b>	<b>0.056</b>	<b>0.074</b>
<b>462</b>	<b>92.374</b>	<b>0.034</b>	<b>0.044</b>	<b>0.05</b>

**TABLE 12.45.** Roughness measurements corresponding to the four intervals of time. (sample 5).

<b>PASSES</b>	<b>TIME (min)</b>	<b>Ra,1 (<math>\mu\text{m}</math>)</b>	<b>Ra,2 (<math>\mu\text{m}</math>)</b>	<b>Ra,3 (<math>\mu\text{m}</math>)</b>
<b>0</b>	<b>0</b>	<b>0.045</b>	<b>0.045</b>	<b>0.045</b>
<b>11</b>	<b>15.369</b>	<b>0.039</b>	<b>0.035</b>	<b>0.04</b>
<b>32</b>	<b>44.711</b>	<b>0.023</b>	<b>0.024</b>	<b>0.026</b>
<b>53</b>	<b>74.052</b>	<b>0.022</b>	<b>0.022</b>	<b>0.031</b>
<b>105</b>	<b>146.707</b>	<b>0.014</b>	<b>0.016</b>	<b>0.025</b>

**TABLE 12.46.** Roughness measurements corresponding to the four intervals of time. (sample 7).

As it can be seen from the *tables 12.45 and 12.46*, the only coupling points are provided by the first and second repetition for the  $T_3$  and  $T_4$ .

Therefore, after having introduced the made choices regarding the experimental data, and after having justified them, the database required to the program can now be filled. The database has to contain all the process parameters (pressure, feed rate,



oscillation, time or passes) resulting useful for the regression model, with the corresponding roughness value. That is the database has to be like the table below:

<b>Passes</b>	<b>Time (min)</b>	<b>Pressure (g)</b>	<b>Feed rate (mm/s)</b>	<b>Oscillation (1/min)</b>	<b>Roughness (<math>\mu\text{m}</math>)</b>
0	0	500	0.667	2000	0.045
11	3.023	500	0.667	2000	0.017
32	8.796	500	0.667	2000	0.011
...	...	...	...	...	...
0	0	900	0.167	500	0.035
11	15.369	900	0.167	500	0.027
...	...	...	...	...	...

**TABLE 12.47.** Required database for the regression model.

Once having entered the database into the program, and after having indicated to the program what are the variables (pressure, feed rate, oscillation, time or passes) and the response (roughness), the form of the regression model has to be chosen. The predefined regression models implemented into the program are four: linear, interaction, quadratic, and pure-quadratic. Since the first two models (linear and interaction) seem to be not adapt to describe the roughness and the pure-quadratic takes into account only the factors of seconds degree, the most adapt to fit the roughness behavior has been seemed to be the quadratic function.

This means that the form of our model has been equal to:

$$y = a + bx_1 + cx_2 + dx_3 + ex_4 + fx_1x_2 + gx_1x_3 + hx_1x_4 + ix_2x_3 + lx_2x_4 + mx_3x_4 + nx_1^2 + ox_2^2 + px_3^2 + qx_4^2$$

**FORMULA 12.9.** Quadratic regression model.

The coefficients required by the model are fifteen and they are all estimated by the program using the experimental data contained in the database previously entered.

In our case, the coefficients are:

<b>Coefficient of regression model</b>	<b>Value</b>
<i>a</i>	$0.489 \cdot 10^{(-1)}$
<i>b</i>	0
<i>c</i>	$-5.09 \cdot 10^{(-5)}$
<i>d</i>	$-8.85 \cdot 10^{(-7)}$
<i>e</i>	$-0.0005.3 \cdot 10^{(-4)}$
<i>f</i>	$2.64 \cdot 10^{(-5)}$
<i>g</i>	$-6.73 \cdot 10^{(-7)}$
<i>h</i>	$-3.4 \cdot 10^{(-4)}$
<i>i</i>	$-1.07 \cdot 10^{(-8)}$
<i>l</i>	$1.17 \cdot 10^{(-7)}$
<i>m</i>	$7.59 \cdot 10^{(-8)}$
<i>n</i>	0.003
<i>o</i>	$3.70 \cdot 10^{(-8)}$
<i>p</i>	$1.06 \cdot 10^{(-9)}$
<i>q</i>	$2.59 \cdot 10^{(-6)}$

**TABLE 12.48.** Coefficient employed in the regression model.

After having found out the coefficient correlated with the regression model of *equation 12.9*, the verification of the model itself has been carried out. In this verification, all the combination of parameters have been tested. Overall, the regression model fits well almost all the samples. It works well in estimating the roughness behavior of the samples 0, 1, 3, 6, and 9, whereas for the sample 10 and 11 it works quite good.

<b>SAMPLE 1</b>				
<i>Pressure=900 g; Feed rate=0.167 mm/s; Oscillation= 500 (1/min)</i>				
<b>PASSES</b>	<b>REPETITION 1</b>	<b>REPETITION 2</b>	<b>REPETITION 3</b>	<b>PREDICTION</b>
0	0.035	0.035	0.035	0.032
11	0.027	0.026	0.029	0.027
32	0.019	0.018	0.021	0.020
53	0.016	0.016	0.018	0.016
105	0.01	0.011	0.013	0.014

**TABLE 12.49.** Comparison between the prediction of the regression model and the experimental data (sample 1).

<b>SAMPLE 6</b>				
<i>Pressure=100 g; Feed rate=0.167 mm/s; Oscillation= 500 (1/min)</i>				
<b>PASSES</b>	<b>REPETITION 1</b>	<b>REPETITION 2</b>	<b>REPETITION 3</b>	<b>PREDICTION</b>
0	0.045	0.045	0.045	0.044
11	0.039	0.035	0.04	0.038
32	0.023	0.024	0.026	0.029
53	0.022	0.022	0.031	0.023
105	0.014	0.016	0.025	0.016

**TABLE 12.50.** Comparison between the prediction of the regression model and the experimental data (sample 6).

<b>SAMPLE 10</b>				
<i>Pressure=900g; Feed rate=0.667 mm/s; Oscillation= 3500 (1/min)</i>				
<b>PASSES</b>	<b>REPETITION 1</b>	<b>REPETITION 2</b>	<b>REPETITION 3</b>	<b>PREDICTION</b>
0	0.056	0.056	0.056	0.025
6	0.024	0.032	0.029	0.023
18	0.015	0.015	0.016	0.019
30	0.01	0.011	0.013	0.016
60	0.015	0.015	0.01	0.011

**TABLE 12.51.** Comparison between the prediction of the regression model and the experimental data (sample 10).

<b>SAMPLE 11</b>				
<i>Pressure=500 g; Feed rate=1.167 mm/s; Oscillation= 3500 (1/min)</i>				
<b>PASSES</b>	<b>REPETITION 1</b>	<b>REPETITION 2</b>	<b>REPETITION 3</b>	<b>PREDICTION</b>
0	0.055	0.055	0.055	0.040
11	0.021	0.023	0.028	0.034
32	0.016	0.015	0.017	0.024
53	0.015	0.015	0.014	0.016
105	0.014	0.013	0.015	0.006

**TABLE 12.52.** Comparison between the prediction of the regression model and the experimental data (sample 11).

As it can be seen from the table above, the model fits very well the first two samples (sample 1 and 6), whereas regarding the last two (samples 10 and 11) the predictions are not good as the first one but they are not so far from the roughness behavior detected.

Otherwise, for the samples 2, 4, 5, 7, and 8 the predictions are not good. For the samples 5 and 7, the prediction is quite good only in the end of their roughness curves. And this was expected, since the experimental data regarding this part of the curve have been entered in the database. For the samples 2 and 4 the predictions are very far from the real behavior of the roughness as it can be seen from the *table 12.53*:

<b>SAMPLE 4</b>				
<i>Pressure=100 g; Feed rate=1.167 mm/s; Oscillation= 500 (1/min)</i>				
<b>PASSES</b>	<b>REPETITION 1</b>	<b>REPETITION 2</b>	<b>REPETITION 3</b>	<b>PREDICTION</b>
0	0.192	0.192	0.192	0.050
133	0.129	0.123	0.135	-0.021
397	0.112	0.104	0.09	0.110
662	0.074	0.083	0.085	0.604
1323	0.053	0.025	0.043	3.418

**TABLE 12.51.** Comparison between the prediction of the regression model and the experimental data (sample 4).

It can be seen as the model does not work well in this case. The reasons are essentially two: the lack of experimental data for roughness values lower than  $0.05 \mu\text{m}$  when a combination of parameters as that one used in sample four is employed; and the fact that all the considered curves start with initial roughness near the  $0.05 \mu\text{m}$ , whereas for sample 4 that value is more or less equal to the reached final value for that tests. This means that to verify completely the veracity of this model, it is necessary to extend the database with new experimental tests.

12.6.2. Comparison between two empirical regression model created from the same experimental data but with different starting considerations

It is interesting now to see if the initial considerations related the value of the starting roughness have positively affect the regression model or it could be built without this precaution. To do that, a new regression model has been created, where this time all the data have been put inside the database, and the obtained results have been compared with the previous ones provided by the first empirical model.

To create the new empirical model, the same previous procedure has been followed.

This time the coefficients of the quadratic equation for the regression model are equal to:

<b>Coefficient of regression model</b>	<b>Value</b>
<i>a</i>	0.047
<i>b</i>	0.193
<i>c</i>	$-3.1 \cdot 10^{-4}$
<i>d</i>	$-1.29 \cdot 10^{-6}$
<i>e</i>	$-3 \cdot 10^{-4}$
<i>f</i>	$-9.98 \cdot 10^{-5}$
<i>g</i>	$-1.30 \cdot 10^{-5}$
<i>h</i>	$7.72 \cdot 10^{-5}$
<i>i</i>	$-1.11 \cdot 10^{-8}$
<i>l</i>	$8.86 \cdot 10^{-8}$
<i>m</i>	$-3.08 \cdot 10^{-8}$
<i>n</i>	-0.042
<i>o</i>	$3.08 \cdot 10^{-7}$
<i>p</i>	$3.06 \cdot 10^{-9}$
<i>q</i>	$9.73 \cdot 10^{-8}$

**TABLE 12.52.** Coefficient employed in the new regression model.

With these coefficients the new regression model can be built, and its predictions will be now compared with the previous one:

<b>SAMPLE 1</b>					
<i>Pressure=900 g; Feed rate=0.167 mm/s; Oscillation= 500 (1/min)</i>					
<b>PASSES</b>	<b>REPETITION 1</b>	<b>REPETITION 2</b>	<b>REPETITION 3</b>	<b>NEW PREDICTION</b>	<b>PREVIOUSLY PREDICTION</b>
0	0.035	0.035	0.035	0.026	0.032
11	0.027	0.026	0.029	0.024	0.027
32	0.019	0.018	0.021	0.019	0.020
53	0.016	0.016	0.018	0.015	0.016
105	0.01	0.011	0.013	0.004	0.014

**TABLE 12.53.** Comparison between the experimental data and the two predictions (sample 1).

<b>SAMPLE 6</b>					
<i>Pressure=100 g; Feed rate=0.167 mm/s; Oscillation= 500 (1/min)</i>					
<b>PASSES</b>	<b>REPETITION 1</b>	<b>REPETITION 2</b>	<b>REPETITION 3</b>	<b>NEW PREDICTION</b>	<b>PREVIOUSLY PREDICTION</b>
0	0.045	0.045	0.045	0.047	0.044
11	0.039	0.035	0.04	0.044	0.038
32	0.023	0.024	0.026	0.038	0.029
53	0.022	0.022	0.031	0.032	0.023
105	0.014	0.016	0.025	0.017	0.016

**TABLE 12.54.** Comparison between the experimental data and the two predictions (sample 6).

<b>SAMPLE 9</b>					
<i>Pressure=900 g; Feed rate=1.167 mm/s; Oscillation= 2000 (1/min)</i>					
<b>PASSES</b>	<b>REPETITION 1</b>	<b>REPETITION 2</b>	<b>REPETITION 3</b>	<b>NEW PREDICTION</b>	<b>PREVIOUSLY PREDICTION</b>
0	0.054	0.054	0.054	0.039	0.046
3.798915	0.024	0.025	0.02	0.035	0.035
11.1968	0.012	0.017	0.015	0.028	0.017
18.59469	0.013	0.013	0.011	0.022	0.007
36.98943	0.01	0.011	0.009	0.006	0.011

**TABLE 12.55.** Comparison between the experimental data and the two predictions (sample 9).

As it can be seen from the two table above (*table 12.53,12.54, and 12.55*) the two models are not so different each other. But anyway, it evidently appears from the *table 12.55* that the considerations done in the beginning of this subchapter have brought to an empirical model that fits better the roughness behavior compared with the new one where all the sample with different starting roughness have been considered starting together at the time zero. In fact, the great dispersion of the data in this last case affects the empirical model, bringing to worse results.

### 12.6.3. Roughness behavior evaluation of the empirical model

Premising that the regression model where all the starting roughness values of the samples have been considered into the range of  $(0.05 \pm 0.008)$  is a model that has to be improved, expanding its database with new data related to the missing information coming from the test (for example the sample 4 is not taken into account in the database because its final roughness value is too high), it is now interesting to see how this model estimates the variation of the roughness behavior with the variation of the process parameters. in other hands, a trial of goodness of the regression model is now done. Always with the help of the program, some graphs can be done to see how the regression model predicts the variation of roughness within a range of parameter values. The passes are kept constant and equal to 2000, whereas case by case one of the three polishing parameters (pressure, feed rate, and oscillation) will keep constant and the other two will be free to vary.

The first effect to be seen is how the roughness varies when the oscillation is constant before to 500 1/min and then to 3500 1/min, whereas the other two parameter change in the following intervals: pressure=100/900 g, feed rate=0.1677/1.167 mm/s.



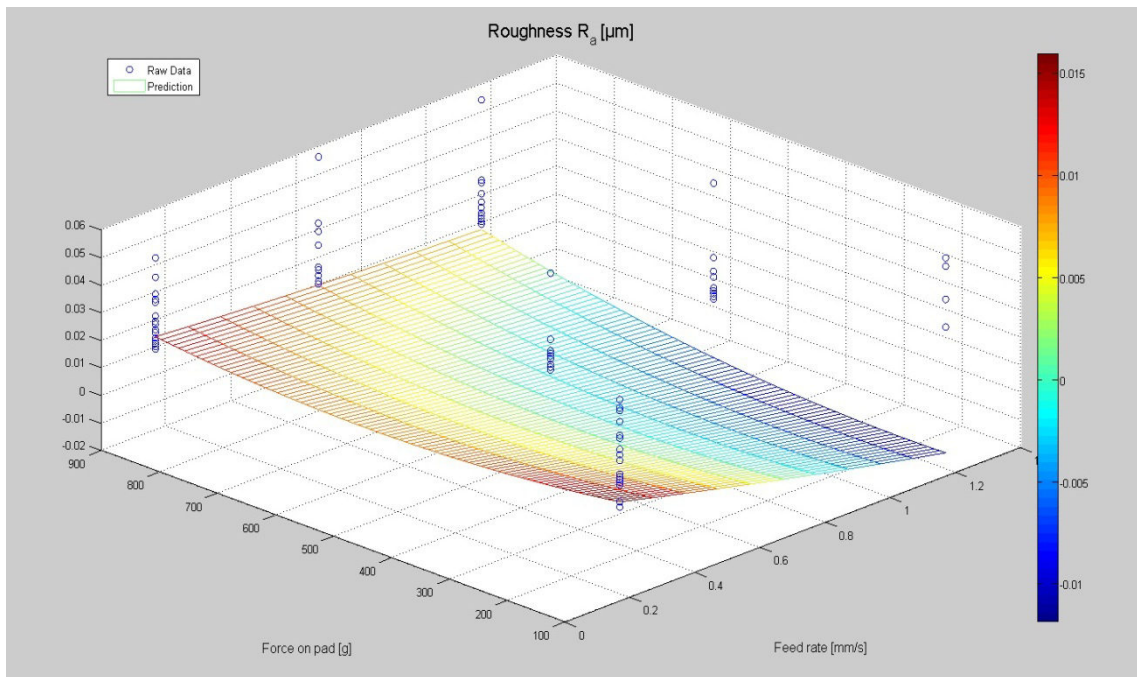


**FIGURE 12.73.** Surface plot of the empirical regression model with passes=2000 and oscillation=500 1/min.

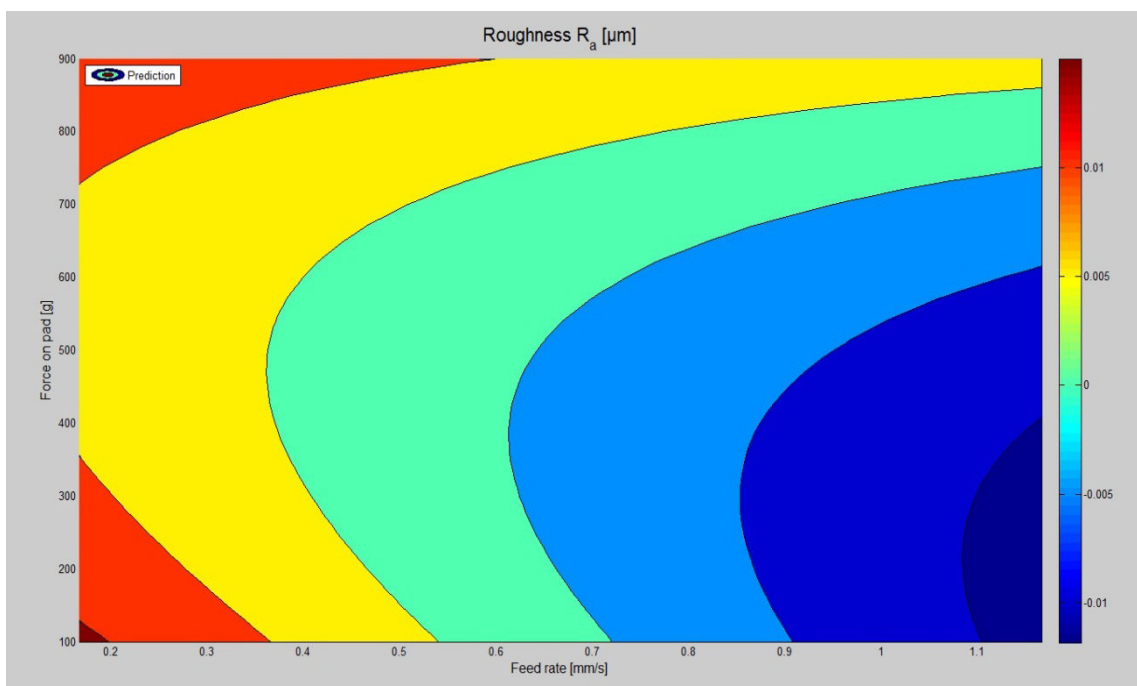


**FIGURE 12.74.** Contour plot of the empirical regression model with passes=2000 and oscillation=500 1/min.

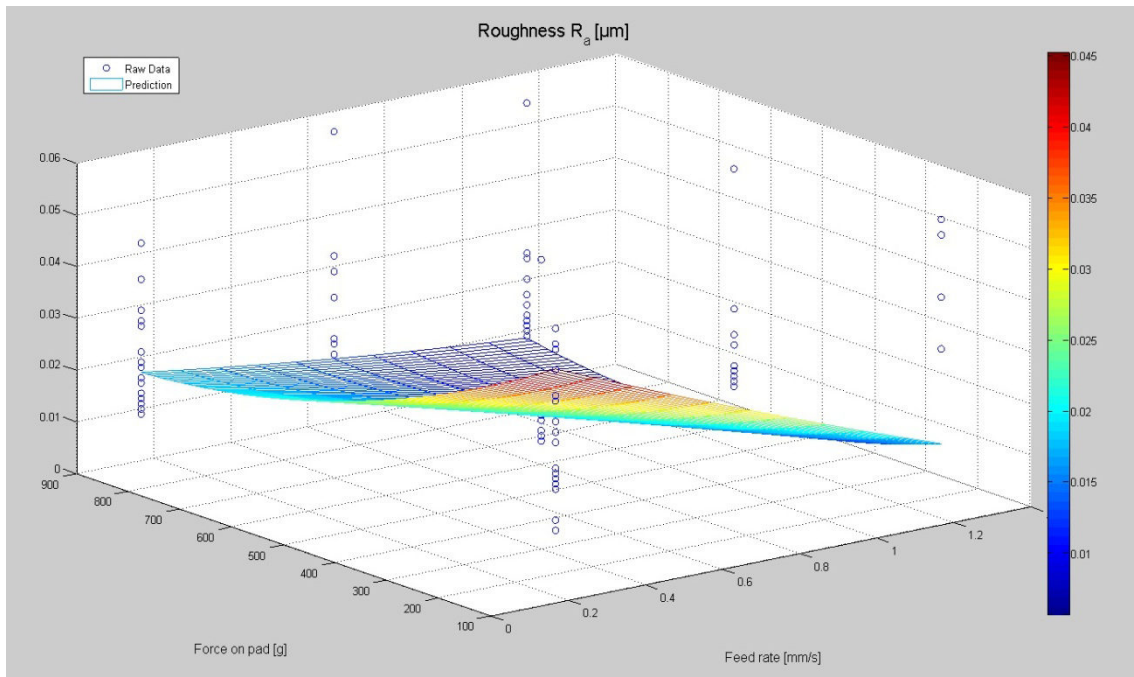


**FIGURE 12.75.** Surface plot of the empirical regression model with passes=2000 and oscillation=3500 1/min

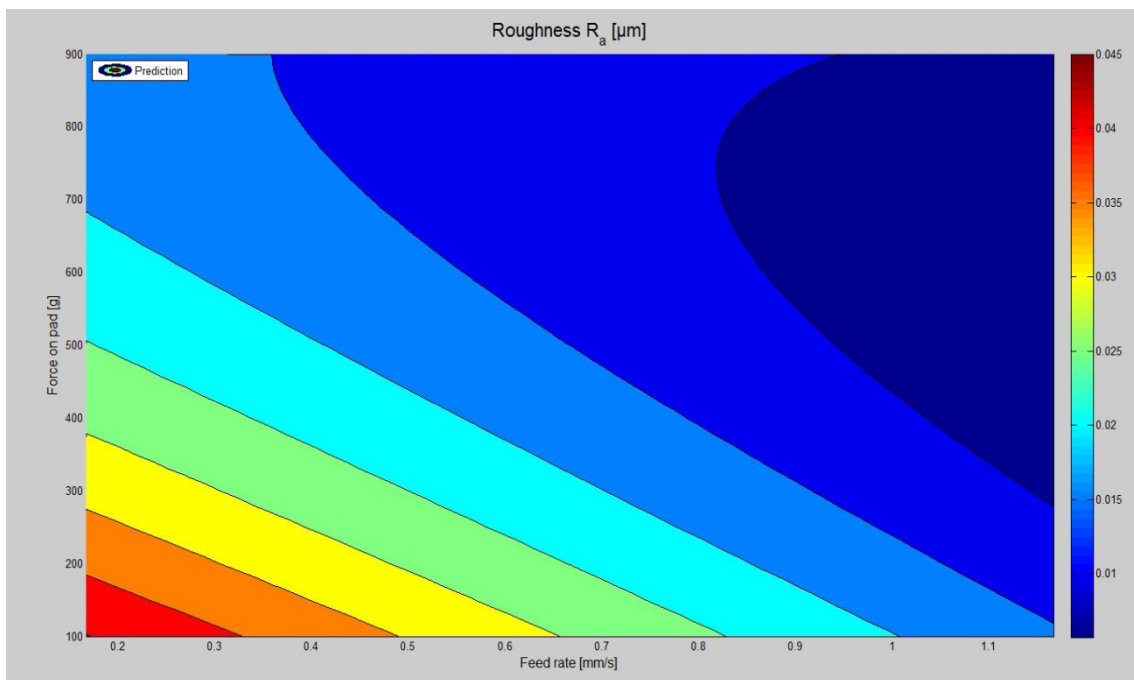


**FIGURE 12.76.** Contour plot of the empirical regression model with passes=2000 and oscillation=3500 1/min

It is noteworthy that these graphs play only a indicative purposed to understand the goodness of the regression model. As it has been said before, this process has to be improved because it requires more data to be more precise. In fact, it can be seen as in the *figure 12.73*, as there is not a good fitting of the experimental data. Also some negative value appears in the graph. This is a trial that to better describe the roughness behavior this model requires more experimental point. Only when more data will be provided, then some deeper consideration on the resulting graphs and on the goodness of the model will can be done. Anyway, for the moment we can only see that the roughness behavior distribution appears very different when the applied oscillation changes. In fact for low oscillation, the better roughness is obtained when the feed rate increase and the pressure decrease. But when the oscillation is high the situation changes, for high pressure the feed rate affects less the final roughness value. After this first two graphs, the influence of the feed rate seems to be the opposite of that detected in the DOE analysis, where high feed rate value required more time to reach the final roughness value.

Other four graphs are now introduced. This time the feed rate will be kept constant (before 0.167 mm/s and then 1.167), whereas the pressure changes between 100/900 g and the oscillation between 500/3500 1/min.

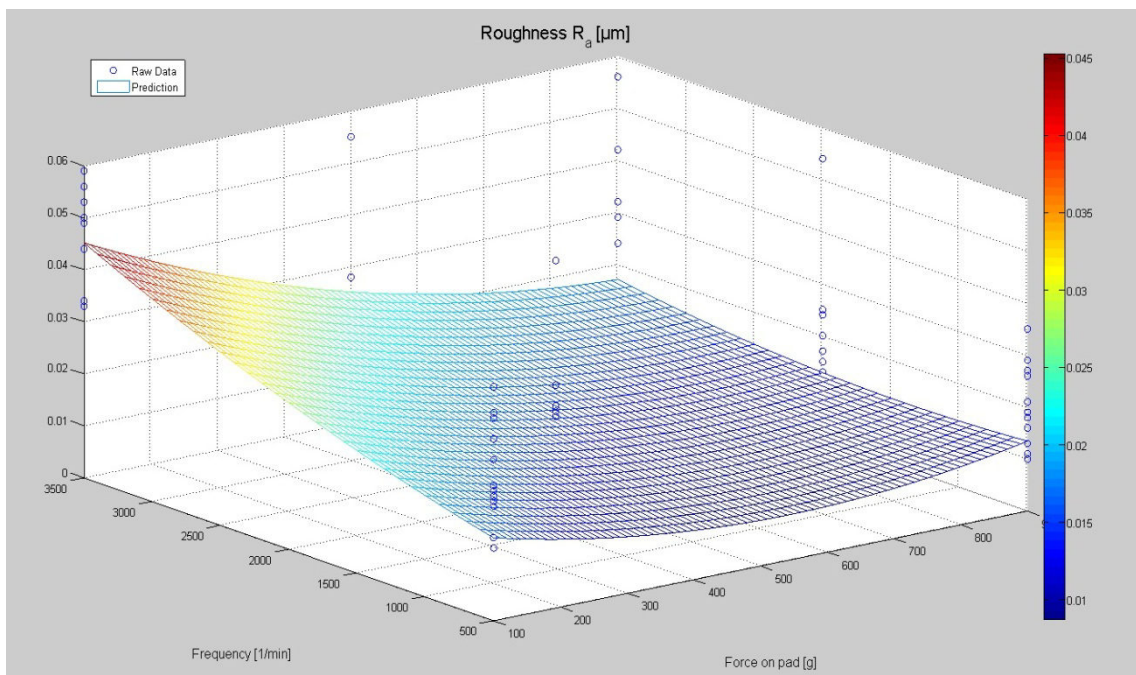


**FIGURE 12.77.** Surface plot of the empirical regression model with passes=2000 and feed rate=0.167 mm/s

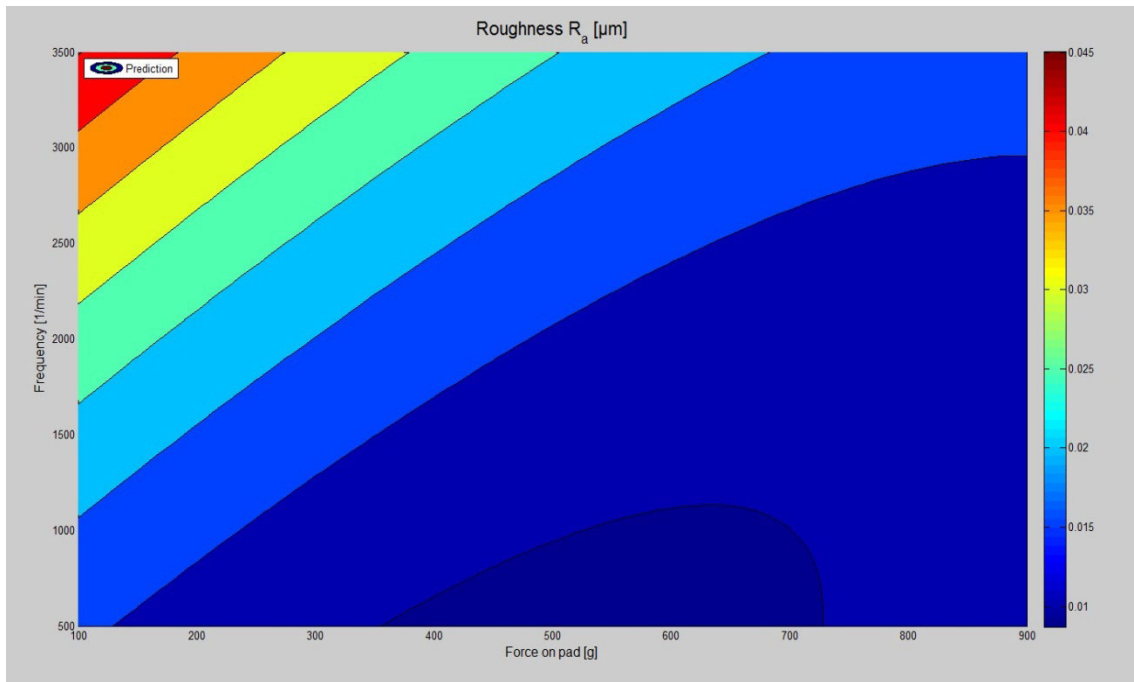


**FIGURE 12.78.** Contour plot of the empirical regression model with passes=2000 and feed rate=0.167 mm/s

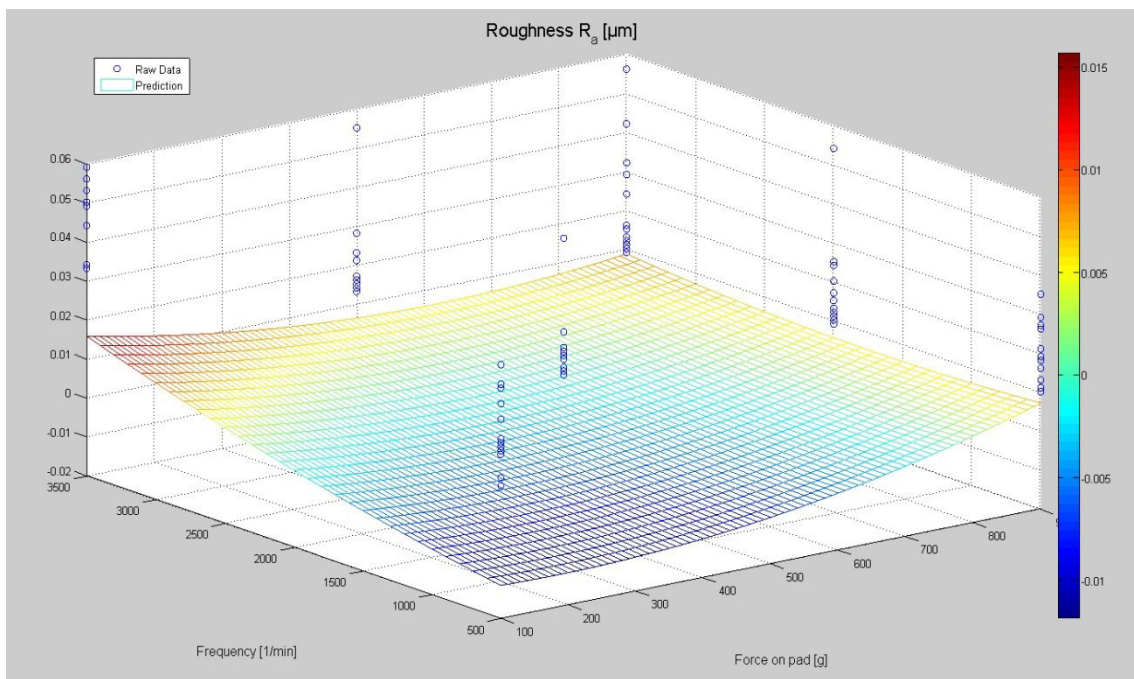


**FIGURE 12.79.** Surface plot of the empirical regression model with passes=2000 and feed rate=1.167 mm/s.

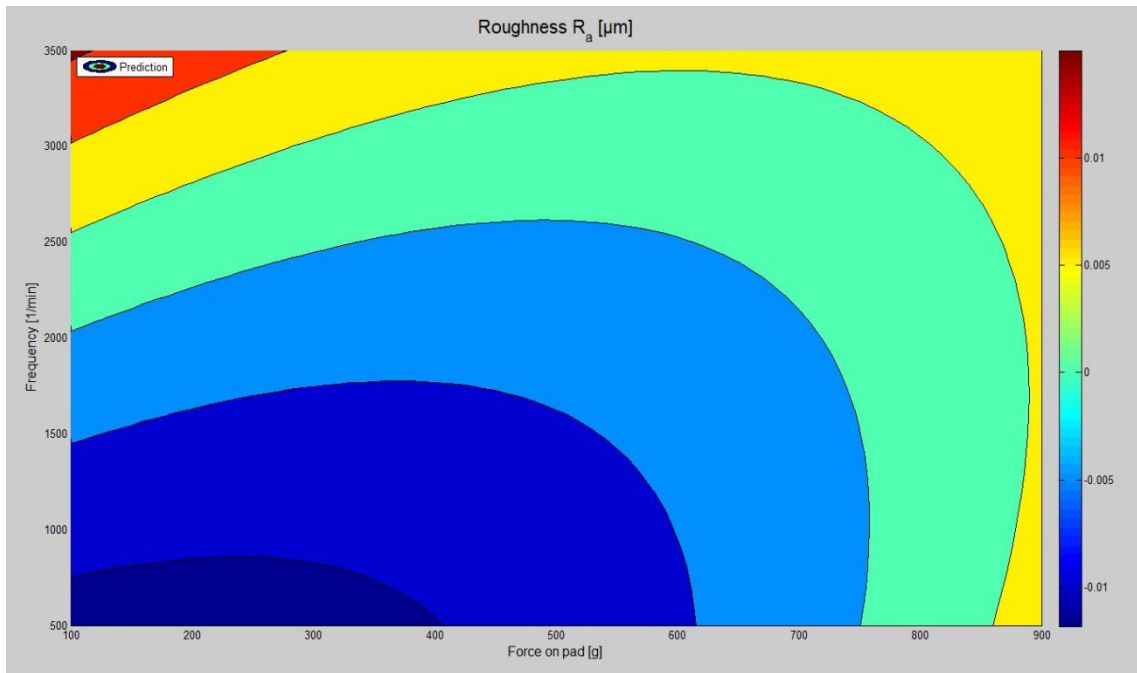


**FIGURE 12.80.** Contour plot of the empirical regression model with passes=2000 and feed rate=1.167 mm/s.

In this graph, it seems that good final roughness values can be always obtained employing low oscillation. Whereas the positive effect of the pressure seems to be bigger when the feed rate is low, but when it increases it seems that good results can be obtained only for middle-low value of the pressure. This result contradicts the DOE observations, where pressure and oscillation play a fundamental role in the polishing process to obtain low roughness value in short time.

The last evaluated graphs are related to the variation of the roughness when the force is kept constant (before 100 g then 900 g) and the feed rate (0.167/1.167 mm/s) and oscillation (500/3500 1/min) change.

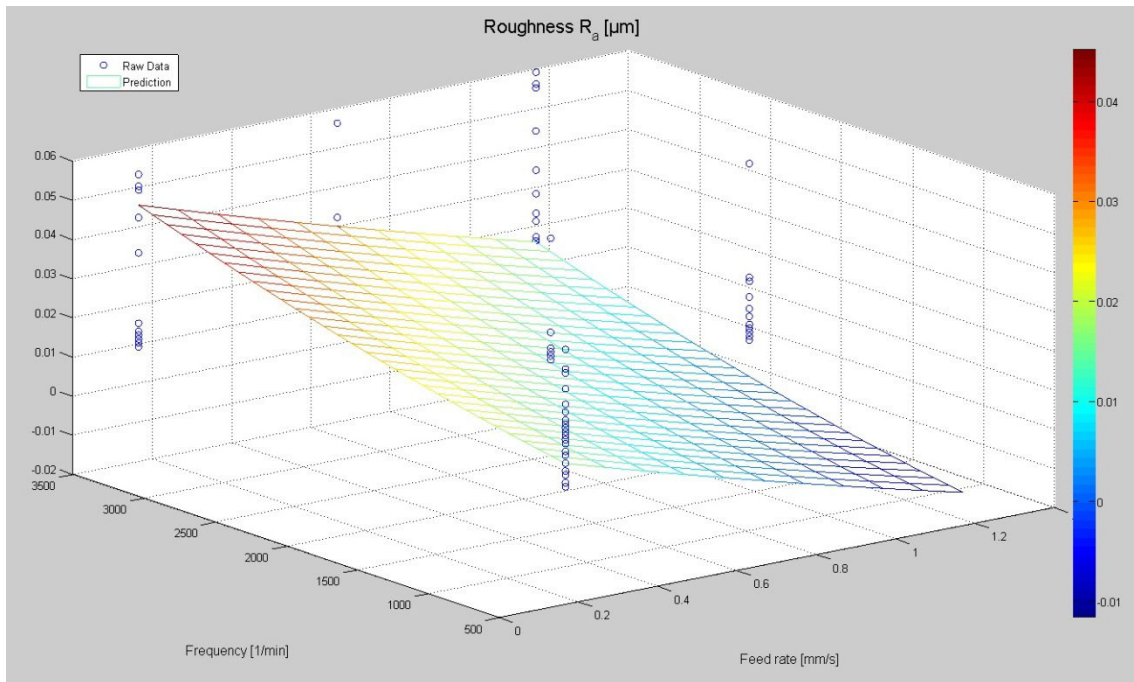


**FIGURE 12.81.** Surface plot of the empirical regression model with passes=2000 and pressure=100 g.

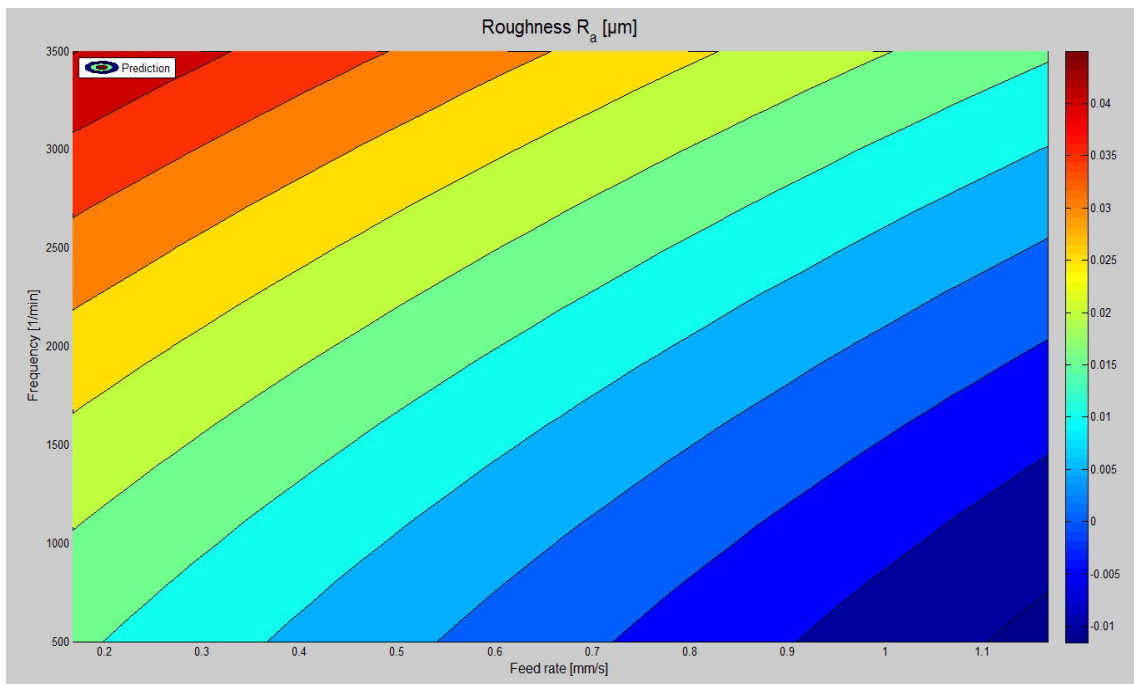


**FIGURE 12.82.** Contour plot of the empirical regression model with passes=2000 and pressure=100 g.

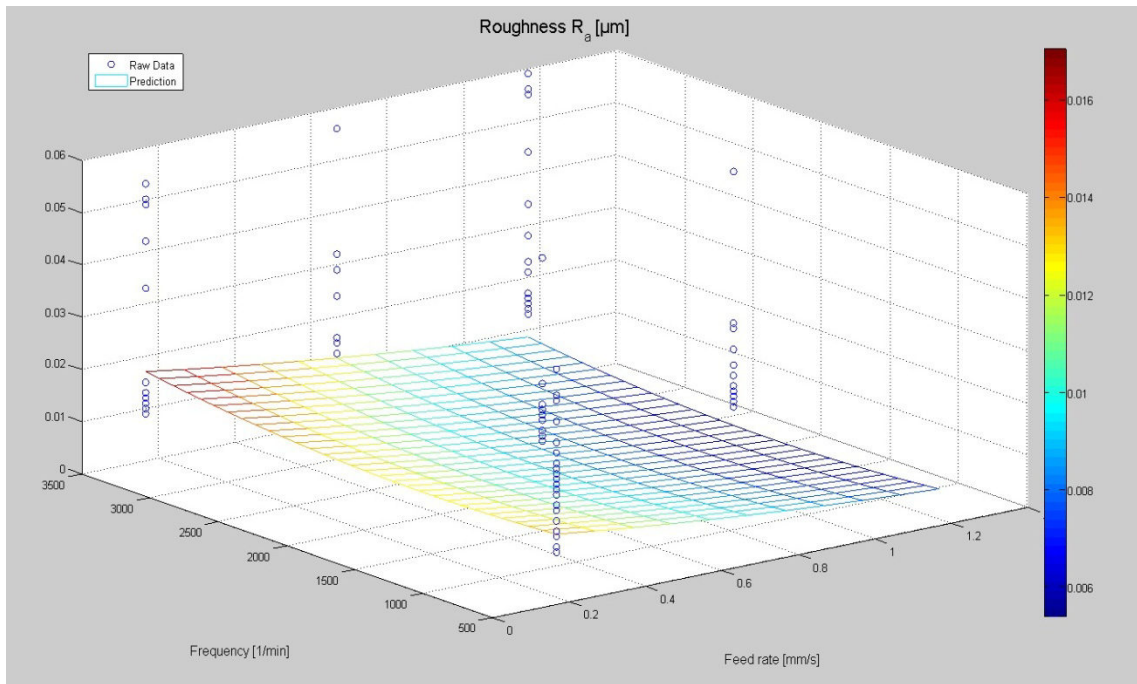


**FIGURE 12.83.** Surface plot of the empirical regression model with passes=2000 and pressure=900 g.

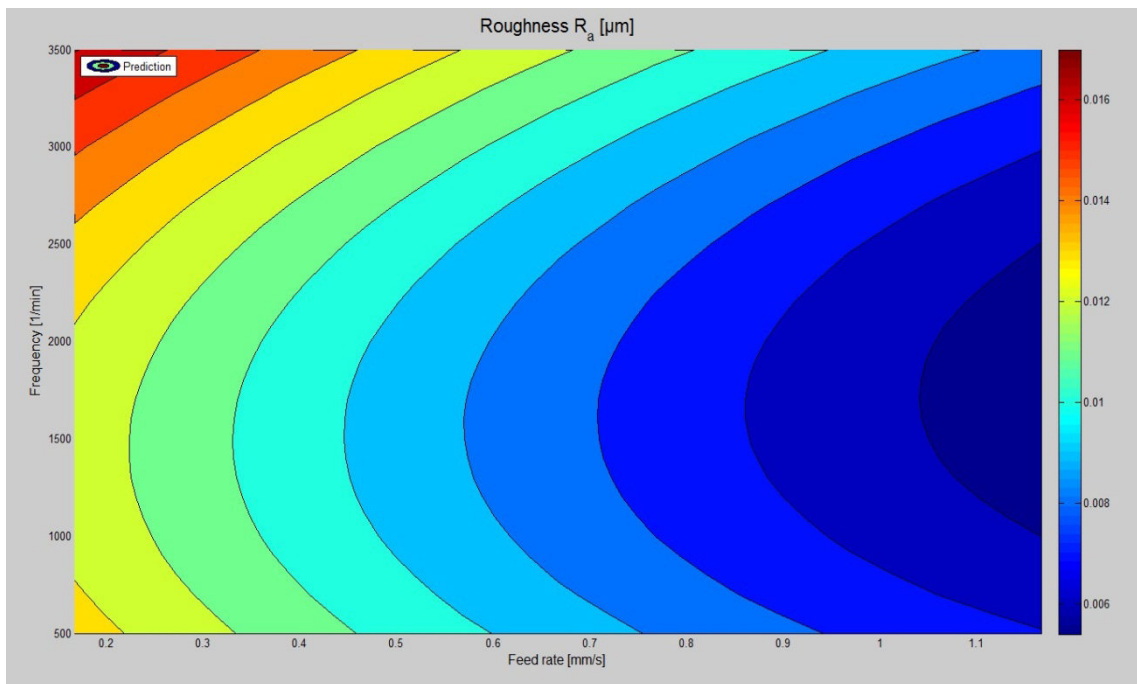


**FIGURE 12.84.** Contour plot of the empirical regression model with passes=2000 and pressure=900 g.

In these figures, it seems once again that with high value for the feed rate the roughness value after 2000 passes is better. This is detected in both the figures, with high or low pressure.

In conclusion therefore this model detects a influence of the feed rate on the polishing process completely different from what has been observed in the DOE analysis. But it is correct to repeat again, that this graphs have been shown only to see how the model predicts the roughness behavior with the variation of the process parameter. Obviously this prediction cannot be reliable, in fact the model does not work well for all the analyzed combination of parameters (the negative values of the roughness is a trial of that), and also its database is not complete because some data are missing. Therefore, to better fit the roughness behavior of the surface, more experimental data are required to complete the database employed by this model and only after that, the model can tested to see if its roughness predictions are good, or if the regression equation employed has to be changed.

#### 12.6.4. Comparison of predictions between the preliminary empirical model and the last empirical model

In the previous subchapters, two empirical regression model have been introduced and described. It is now interesting to compare the two different models and understand which are the main differences among them.

The two regression models are remembered below:

$$y = A(P, f.r., Osc) + B(P, f.r., Osc) \times \log(x)$$

**FORMULA 12.10.** Equation of the empirical preliminary regression model.

$$y = a + bx_1 + cx_2 + dx_3 + ex_4 + fx_1x_2 + gx_1x_3 + hx_1x_4 + ix_2x_3 + lx_2x_4 + mx_3x_4 + nx_1^2 + ox_2^2 + px_3^2 + qx_4^2$$

**FORMULA 12.11.** Equation of the regression model using part of the overall experimental data.



To see what are the difference between them, and to analyze how the prediction are good or not, some experimental results are compared with the two different prediction coming from the two regression models:

<b>SAMPLE 1</b>					
<i>Pressure=900 g; Feed rate=0.167 mm/s; Oscillation= 500 (1/min)</i>					
<b>PASSES</b>	<b>REPETITION 1</b>	<b>REPETITION 2</b>	<b>REPETITION 3</b>	<b>PRELIMINARY MODEL</b>	<b>PREVIOUSLY PREDICTION</b>
0	0.035	0.035	0.035	-	0.032
11	0.027	0.026	0.029	0.014	0.027
32	0.019	0.018	0.021	0.011	0.020
53	0.016	0.016	0.018	0.009	0.016
105	0.01	0.011	0.013	0.007	0.014

**TABLE 12.56.** Comparison between the experimental data and the two predictions (sample 1).

<b>SAMPLE 6</b>					
<i>Pressure=100 g; Feed rate=0.167 mm/s; Oscillation= 500 (1/min)</i>					
<b>PASSES</b>	<b>REPETITION 1</b>	<b>REPETITION 2</b>	<b>REPETITION 3</b>	<b>PRELIMINARY MODEL</b>	<b>PREVIOUSLY PREDICTION</b>
0	0.045	0.045	0.045	-	0.044
11	0.039	0.035	0.04	0.051	0.038
32	0.023	0.024	0.026	0.037	0.029
53	0.022	0.022	0.031	0.031	0.023
105	0.014	0.016	0.025	0.022	0.016

**TABLE 12.57.** Comparison between the experimental data and the two predictions (sample 6).

<b>SAMPLE 9</b>					
<i>Pressure=900 g; Feed rate=1.167 mm/s; Oscillation= 2000 (1/min)</i>					
<b>PASSES</b>	<b>REPETITION 1</b>	<b>REPETITION 2</b>	<b>REPETITION 3</b>	<b>PRELIMINARY MODEL</b>	<b>PREVIOUSLY PREDICTION</b>
0	0.054	0.054	0.054	-	0.046
3.798915	0.024	0.025	0.02	0.024	0.035
11.1968	0.012	0.017	0.015	0.018	0.017
18.59469	0.013	0.013	0.011	0.015	0.007
36.98943	0.01	0.011	0.009	0.010	0.011

**TABLE 12.58.** Comparison between the experimental data and the two predictions (sample 9).

<b>SAMPLE 10</b>					
<i>Pressure=900g; Feed rate=0.667 mm/s; Oscillation= 3500 (1/min)</i>					
<b>PASSES</b>	<b>REPETITION 1</b>	<b>REPETITION 2</b>	<b>REPETITION 3</b>	<b>PRELIMINARY MODEL</b>	<b>PREVIOUSLY PREDICTION</b>
0	0.056	0.056	0.056	-	0.025
6	0.024	0.032	0.029	0.029	0.022558
18	0.015	0.015	0.016	0.022	0.018682
30	0.01	0.011	0.013	0.018	0.016
60	0.015	0.015	0.01	0.014	0.011

**TABLE 12.59.** Comparison between the experimental data and the two predictions (sample 10).

As we can see from the samples above, the two regression models fit quite well the demonstrated roughness behavior. In fact, both are very close to the real obtained roughness value. What we can see is that for the preliminary regression model the roughness prediction are overall less accurate than the regression model found with the help of the MATLAB program. In fact, it can be seen from the table above that only for the sample 9 (*table 12.58*) this model provides more accurate values for the roughness, but in the other three tables, the MATLAB regression model works better. Moreover, for the preliminary regression model it is not possible to determine which value the roughness assumes in the beginning (time zero). This happens due to two reasons: the first one is that the structure of the model (its form) contains the logarithm of the time, and second one is that to evaluate the A and B coefficient of the models for each sample the points  $T_1$  and  $T_4$  have been employed as reference, and this two

considerations imply that the evaluation of the roughness for time minor than  $T_1$  is not possible (in fact the logarithm of zero tends to infinity).

## 12.7. MRR analysis

### 12.7.1. Alignment of the profiles

One of the aim of this thesis is to calculate the amount of material removal that the polishing process in flat conditions causes and validating in this way some theoretical models introduced in the chapter four. In this chapter this aim is discussed, the procedure to calculate the material removal of the process on the polished area is explained and the validation of the models is presented.

The first step to start with this analysis has been to measure the polishing areas with the Hommel Stylus before the machining process, so that some profiles of the interested area have been obtained. As described in the chapter eight, the detected profiles have to include the two grooves which alongside the polishing area, so that some reference points to align the two profiles before and after polishing can be found from these.

The measurements have been three for every polished surface, this means that for a sample with twelve polished area the overall measurements have been thirty-six. It is noteworthy that to include the grooves in the measurement, a overall evaluation length of 15 mm has been employed against the 4.8 mm used to evaluate the roughness value in the surface area.

After having made this initial measurements, the experimental tests have been run, and once finished, a second session of measurements have been done to detect what was changed from the starting profiles.

The profiles, as said, have been detected by using of Hommel Stylus which employs a processing program called SURSAM. Now, in this program the alignment of two profiles is not possible to do, so for this reason all the data were imported and elaborated with EXCEL.

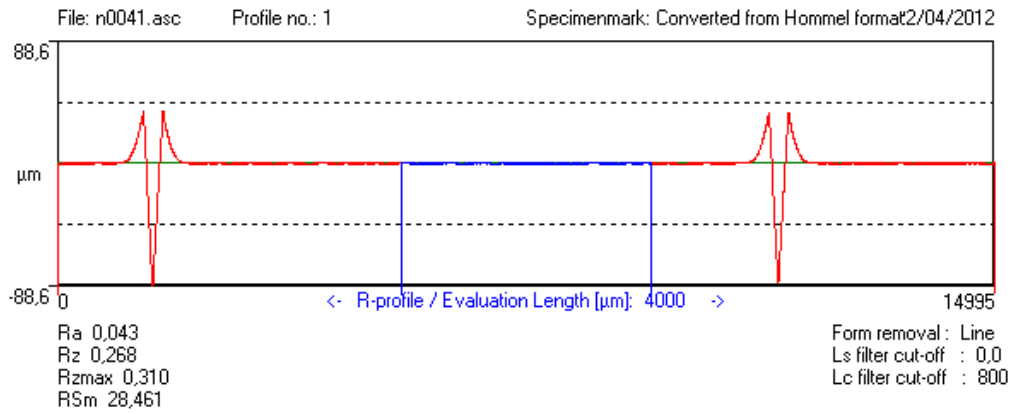


**FIGURE 12.85.** An example of profile measured with Hommel and visualized with Sursam. This profile is the first one for the sample 0, area of first repetition column  $T_4$ .

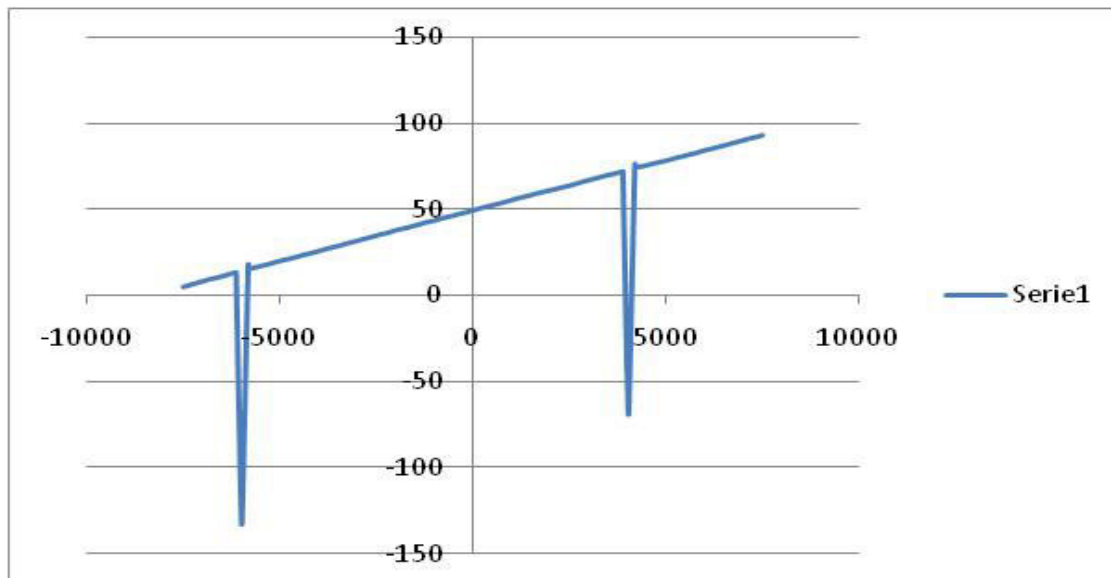


**FIGURE 12.86.** Same profile of figure 85 but elaborated with Excel.

What we can see from the comparison of the two figures show above is that when the same profile is elaborated with Excel, it appears oblique. This because during the measurements of the profile, the sample was not perfectly straight. Anyway, this fact does not bring to particular problem and does not affect the measurement, but before to do the alignment with the corresponding profile measured after the tests, it has

been necessary to report it horizontal. The other observation very important is that the two profiles, one shown by SURSAM (*figure 12.85*) and the other one by EXCEL (*figure 12.86*), do not look like perfectly the same. In fact if the zones of the grooves are observed, they are very different from a picture to another. This can be clearly seen by the figures below:

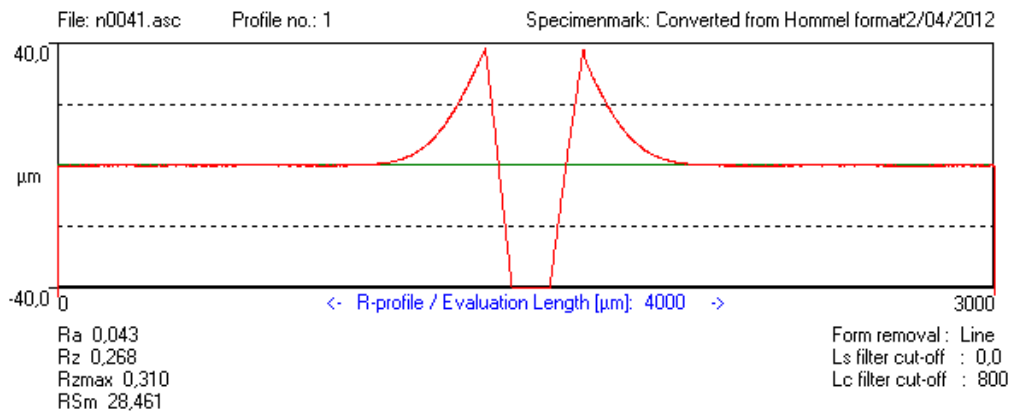


**FIGURE 12.87.** Groove shown by Sursam.

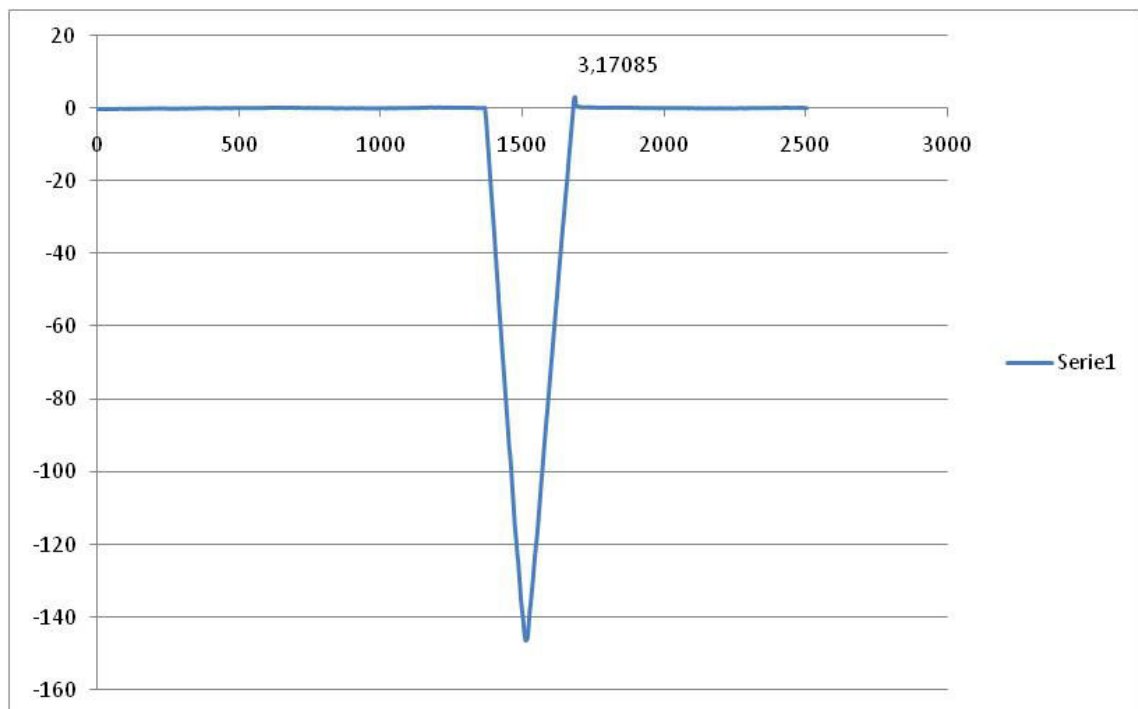


**FIGURE 12.88.** Groove shown by Excel.

From the scale on the left, it appears clear that the Excel profile does not reproduced perfectly the shape of the groove shown in *figure 12.87*. The reason of this diversity is not clear, but probably it is a problem related with the transmission of data from SURSAM to EXCEL. Anyway, this problem appears to be concerning only the grooves zone. In fact, analyzing the other profiles it has been noted that in the zone not in close proximity of the grooves, the Sursam profile was well replaced from the Excel profile. Indeed, the values of some peak heights were not perfectly replaced in EXCEL but difference between them was acceptable to continue with the analysis (see figures 12.89, 12.90 below).

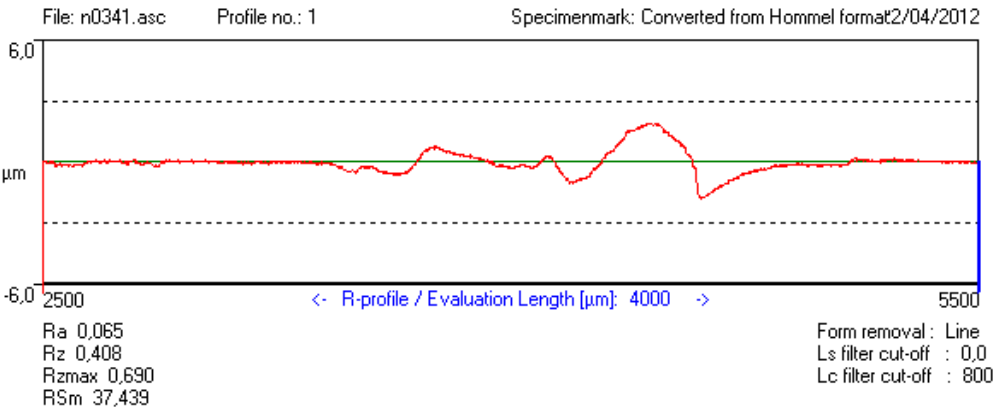


**FIGURE 12.89.** Feature detected in the first profile of sample 3, first repetition of column  $T_4$ .

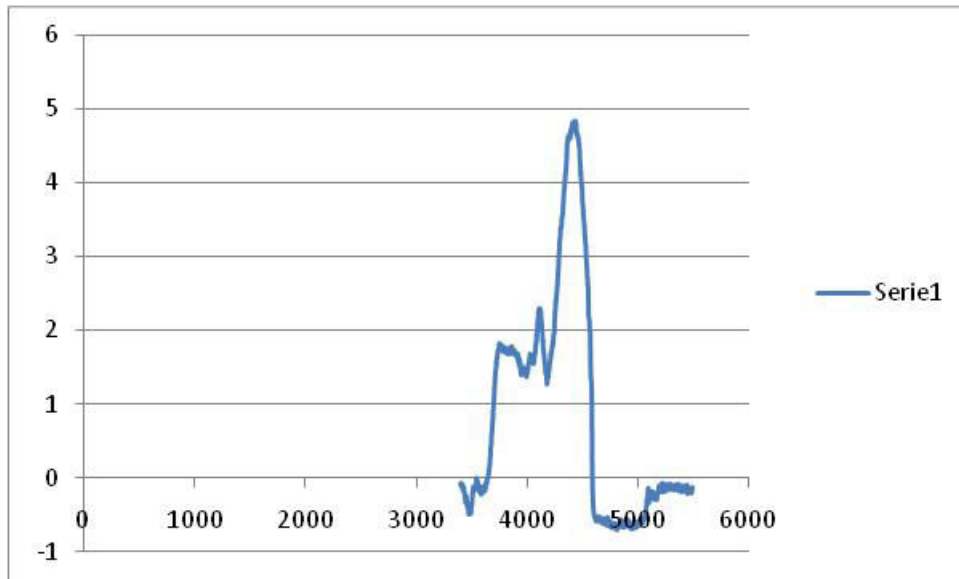


**FIGURE 12.90.** Same feature detected in figure 89, but visualized in Excel.

Anyway, after having verified there were not great difference between the Sursam profile and Excel profile except for the regions without interest for detecting the MRR (that is the grooves), the profiles have been made horizontal with the help of SPIP program, and then they have been aligned in EXCEL.

The alignment of the two corresponding profiles has been done taking as x reference the x corresponding to the deepest point of the first grooves on the left, and as y reference a pairs of values that permitted to overlap the two profiles. One of the results is shown below:

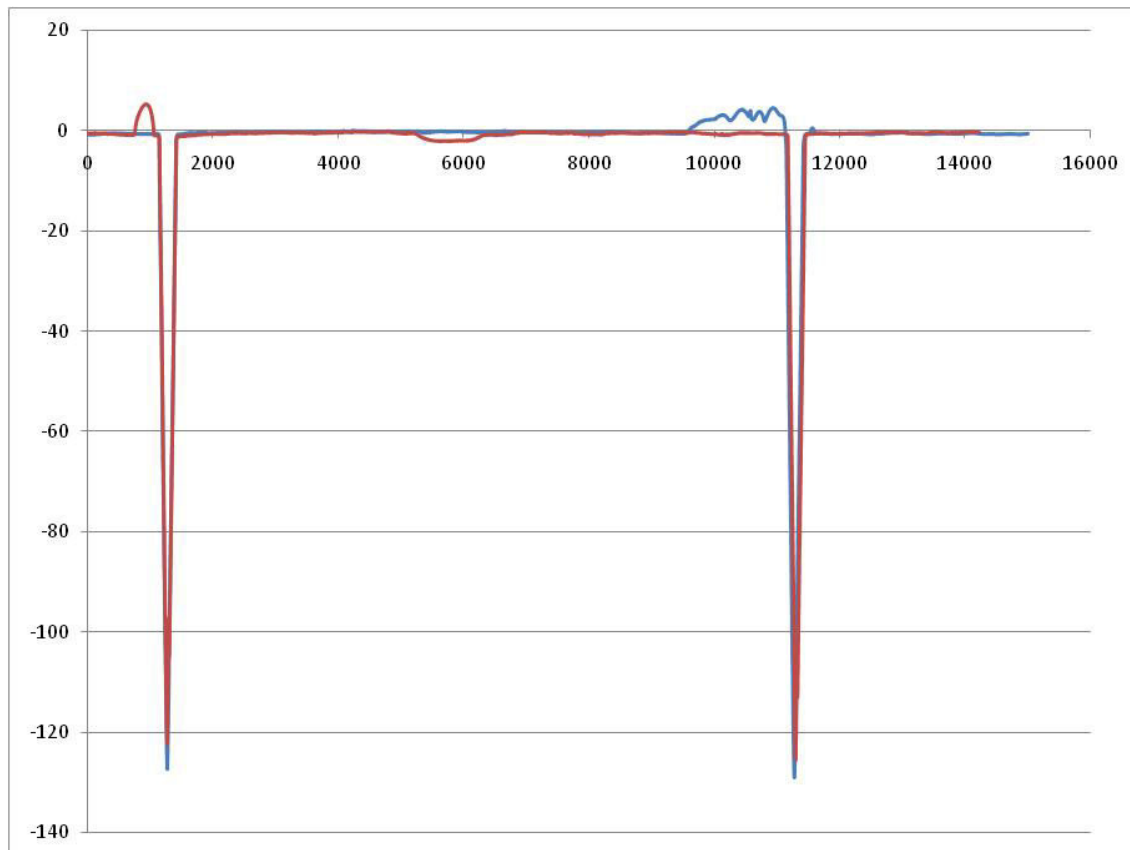


**FIGURE 12.91.** Alignment of two corresponding profiles of the sample 11, second repetition column  $T_4$ .

As it appears from the *figure 12.91* the bad representation of the zone near the grooves is still present, but as explained before it does not affect the area where the material removal is calculated.

Now, not all the made measurements of the profiles have been used, in fact for the  $T_1$ ,  $T_2$ , and  $T_3$  the left track by the pad on the surface was so small that was difficult to detect it. For this reason it has been decided to calculate only the amount of material removal related to the time  $T_4$ .



### 12.7.2. Computation of the experimental amount of material removal caused by the polishing process

After having introduced the alignment of the profiles, the MRR analysis can be begun. The first step to do has been to detect the polished area from the pad. As it can be seen from the *figure 12.91*, the width of the pad track is smaller than expected. In fact, the biggest problem was to make the contact surface of the polishing pad perfectly parallel to the polishing surface of the sample. But no precise tool was available to making that. In fact, even if long time of running-in was dedicated to try to improve the contact surface of the pad, it proved ineffective to render the pad surface in the optimum condition to polish. This means the real contact area between pad and workpiece was effectively smaller, and the real distribution of the pressure was different from the expected. This also means that for each polished surface the contact zone has to be detected every time.

To detect from the graphs the polished zone has been relatively easy for the samples where the employed pressure was bigger than 100 g. In fact, for that samples where the lower level of pressure has been used, no evident difference between the two profiles was detected (*figure 12.92*). For this reason, the calculation of the material removal has been restricted to those samples with a pressure bigger than 100 g, analyzing for them the polished surfaces corresponding to  $T_4$  (that is sample 0, 2, 3, 8, 9, 10, 11, 12. For the sample 1 the material removal has not been possible to computed because the tests regarding it were repeated behind the sample 7, for problems regarding the paste refresh. In this way, no grooves could be used to align the profiles). It is important to underline anyway, that the pressure of 100 g is not used during the polishing process because it is too low. We have choose this value of pressure to understand how the process and therefore the roughness behavior behave in these conditions.

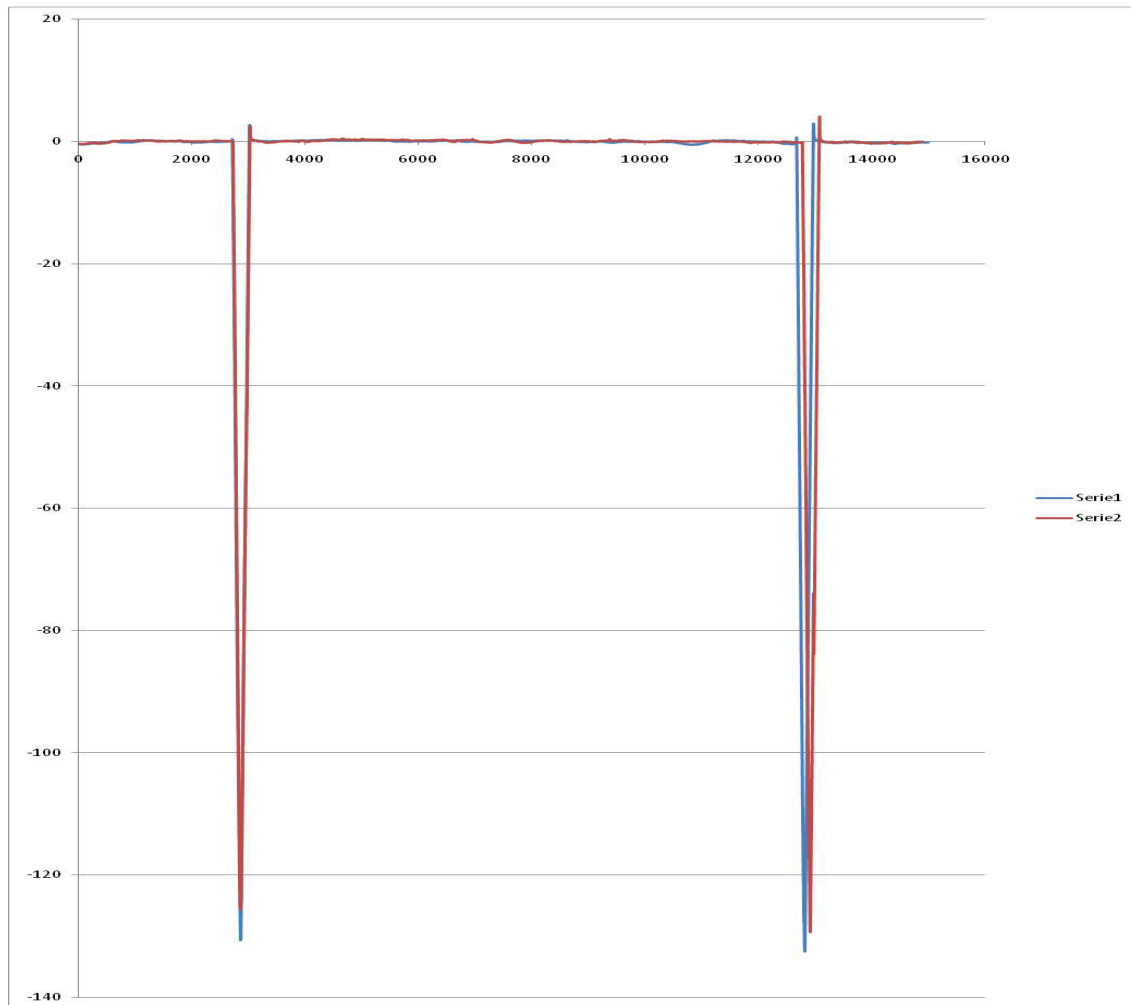


**FIGURE 12.92.** This is a profile measured from the sample 6 employing a pressure of 100 g for the surface corresponding to polishing time  $T_4$ .

What we can see of interest in the figure above again is that the alignment of the profiles along the x direction, using as reference point the groove on the left, did not always imply a perfect correspondence with the other groove on the right. This is because the position of the interested sample at the moment of the measurement could not be perfectly orthogonal with the direction of the Hommel tip. This means that if the travel of the tip is oblique respect to the orthogonal direction to the grooves, the length between the two grooves will result a little more long respect the case where the travel is perfectly straight. Anyway, this fact does not affect the measurements because the difference between the two grooves on the right regards only few microns.

Now the evaluation widths for each considered sample are listed below:

<b>SAMPLE</b>	<b>VALUE (mm)</b>
<b>Sample 00</b>	3.8
<b>Sample 02</b>	3.5
<b>Sample 03</b>	3.2
<b>Sample 08</b>	3.5
<b>Sample 09</b>	3.5
<b>Sample 10</b>	3.8
<b>Sample 11</b>	3.8
<b>Sample12</b>	3.8

**TABLE 12.60.** Evaluation widths employed to calculated the MRR.

The evaluation width have been taken constant for each measurement of the same samples. In other hands, if for the column  $T_4$  there are three polished surfaces with three measurements each, this means that for the nine overall measurements the evaluation width is kept constant. This because the track of the pad is supposed constant at least for the same sample. Moreover, the widths have been chosen so that no strange feature (*figure 12.90*), which could appear in the profile, would affect the measure.

Once detected these evaluation width, the material removal has been calculated subtracting the profile before polishing with that one after the process (that is it was done the difference between the different heights of the profiles) and multiply that result for the distance between two consecutive points of measurement. In other hands, the definition of integral was applied.

After having made this operation, what we have obtained was the amount of material removal for unit of length (in fact the measurements done for the material removal were orthogonal to the direction of the feed rate of the pad, this means that they are orthogonal to the length of the track, see chapter eight). Then for the three MRR measurement corresponding to the same polished area, an arithmetical average was done.

The results are listed below:

<b>SAMPLE</b>	<b>POLISHED AREA</b> <sub>(column, repetition)</sub>	<b>MEAN MATERIAL REMOVAL</b> ( $\mu\text{m}^2$ )
Sample 00	41	2076.826
	42	1547.666
	43	1900.554
Sample 02	41	2905.133
	42	3061.005
	43	2573.666
Sample 03	41	2824.315
	42	3168.745
	43	2858.95
Sample 08	41	2551.439
	42	2521.61
	43	2488.859
Sample 09	41	1760.671
	42	1945.687
	43	1837.259
Sample 10	41	2531.871
	42	2580.272
Sample 11	42	2131.711
	43	2508.545
Sample 12	11	2575.314
	12	2450.555
	21	2371.625
	22	2349.913
	31	2396.716
	32	2174.541

**TABLE 12.61.** Mean value for the material removal resulting for each polished sureface

At this point, it has been necessary to choose the results to enter inside the material removal program to calibrate the models, so that to obtain the exact material removal rate from them. The program provides the exact material removal rate from the theoretical models implemented, employing only one combination of parameters at once. That is, it uses one and no more value of the material removal calculated in the table above with its corresponding combination of parameters (pressure, feed rate, and oscillation) to give an estimation of the material removal rate, as a function of or pressure, or feed rate, or oscillation. For this reason, all the material removal data listed in the *table 12.61* are not required to put into the MRR database. The combinations of parameters chosen to enter inside the MRR database have been: sample 8-42 (pressure=900 g, feed rate=0.167 mm/s; oscillation=3500 1/min), sample 9-43 (pressure=900 g, feed rate=1.167 mm/s; oscillation=2000 1/min), and sample 12-12 (pressure=500 g, feed rate=0.667 mm/s; oscillation=2000 1/min) (see *table 12.61*). With each of these combinations of parameters the MRR given by the three theoretical models will be calculated, whereas with the other remains material removal data coming from the alignment of the profiles, the model verification has been possible.

Before to start with the verification, the parameters and the values which will be used in the three models are listed in the table below:

<b>Yield strength of the workpiece (MPa) [31]</b>	2350
<b>Dilution ratio [27]</b>	0.1
<b>Young modulus pad (GPa) [27]</b>	60
<b>Mean height of the single asperity (<math>\mu\text{m}</math>) [27]</b>	58
<b>Standard deviation of the grain size (<math>\mu\text{m}</math>) [27]</b>	0.015
<b>Density of the diluted slurry (<math>\text{g}/\text{mm}^3</math>) [27]</b>	$1 \cdot 10^{-3}$
<b>Density of abrasive (<math>\text{g}/\text{mm}^3</math>) [27]</b>	$1,08^{-3}$
<b>Size abrasive (<math>\mu\text{m}</math>)</b>	14
<b>Hardness of the pad (MPa) [27]</b>	50
<b>Height of the asperities (mm) [27]</b>	$58 \cdot 10^{-3}$
<b>Radius of single asperities (<math>\mu\text{m}</math>) [27]</b>	100

**TABLE 12.62.** Data employed in the models.

After having introduced this data, the verification of the theoretical MRR models can begin.

### 12.7.3. Comparison between the experimental data and the prediction of the first theoretical model

In the first model, the data related to the sample 8-42, 9-43, and 12-12 are employed one by one to estimate the material removal. This model (as the other two) required to defined one of the three parameters (pressure, feed rate, and oscillation) as a vector, and to keep constant the other two. Then, it has been established to keep constant feed rate to 1.167 mm/s and oscillation to 3500 1/min and to see how the model estimates the MRR as a function of the pressure. The employed range for the pressure has been from 500 g to 900 g. The previous combination of parameter, where the pressure is assumed as a vector, has always been kept constant, so that the three models will be verified for the samples 3 and 11. Now the results obtained putting the samples 8-42, 9-43, and 12-12 one by one inside the first model are shown below:

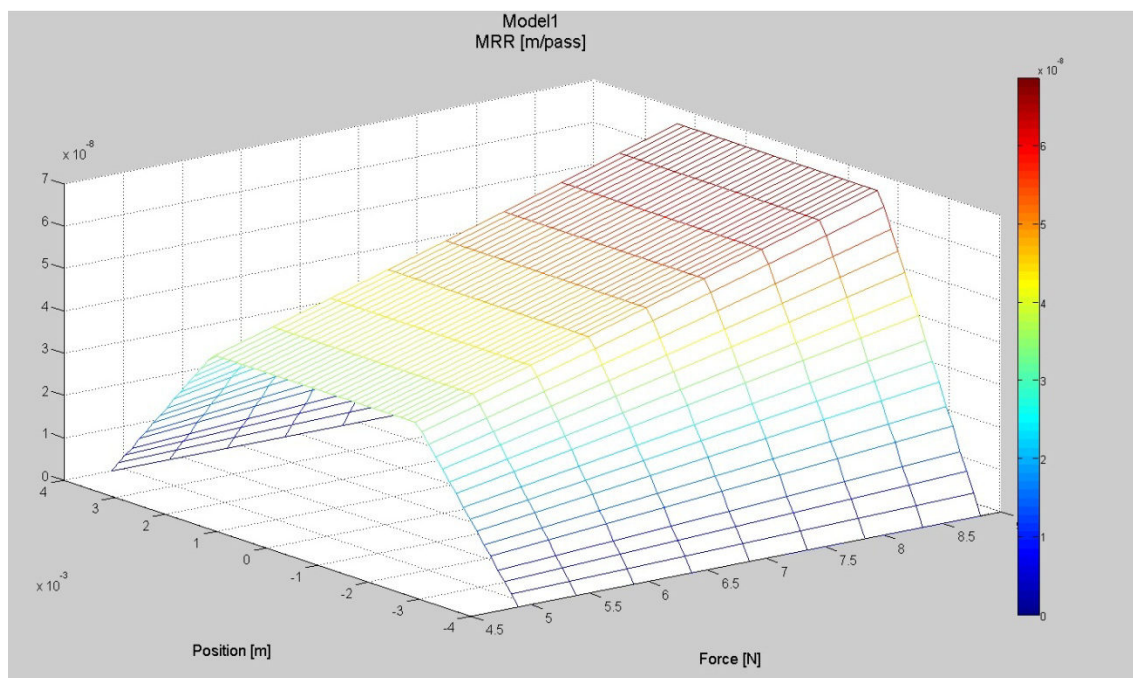


**FIGURE 12.92.** Surface plot of the estimation of the MRR for the first model employing the combination of parameters sample 8-42.

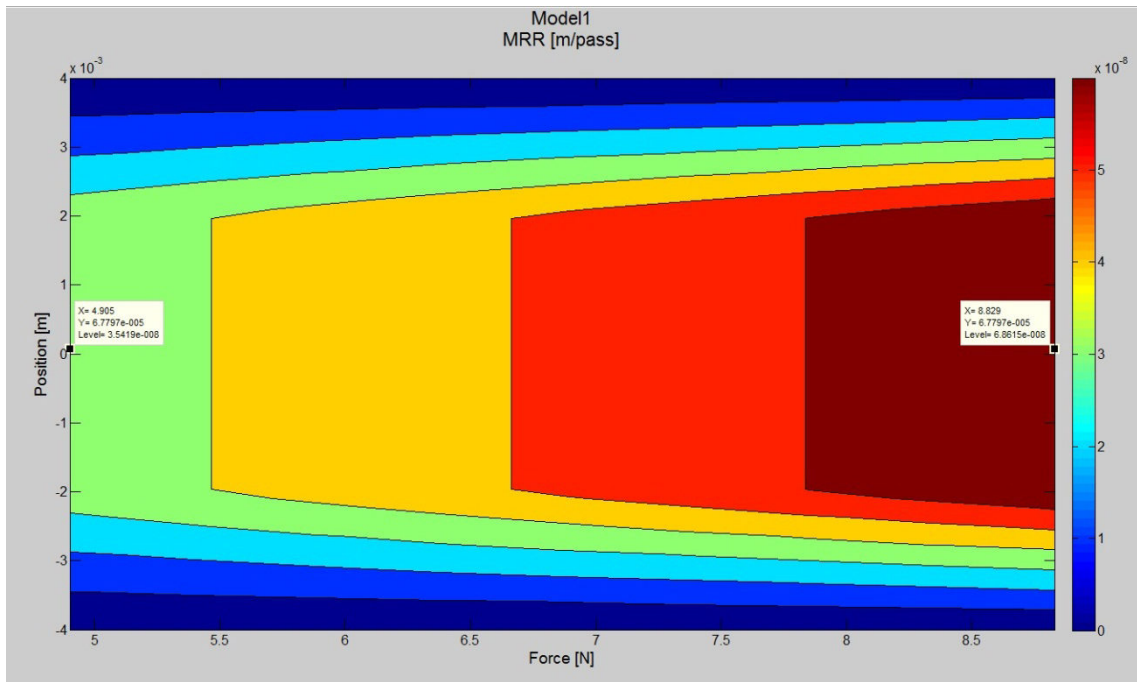


**FIGURE 12.93.** Contour plot of the estimation of the MRR for the first model employing the combination of parameters sample 8-42.

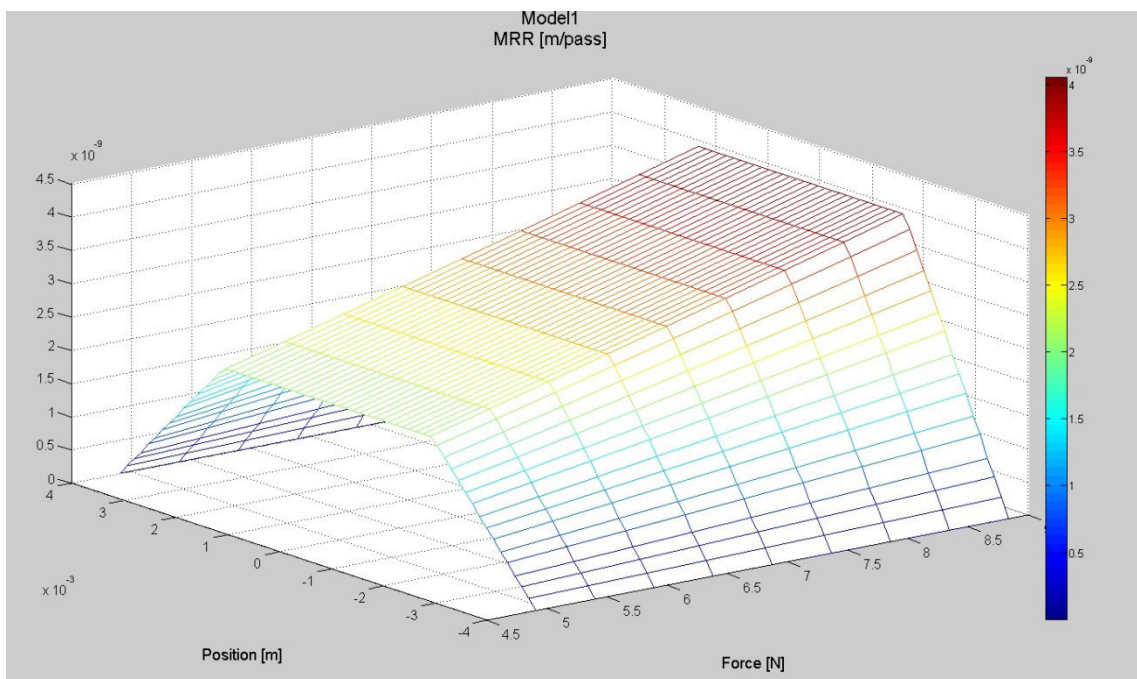


**FIGURE 12.94.** Surface plot of the estimation of the MRR for the first model employing the combination of parameters sample 9-43.

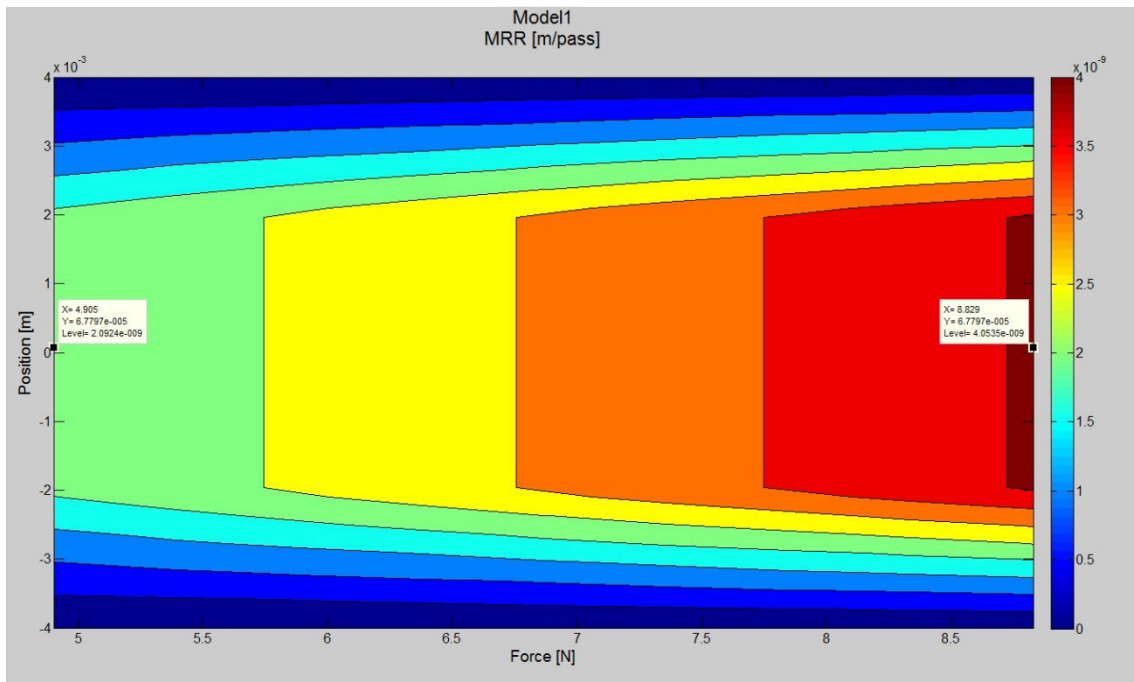


**FIGURE 12.95.** Contour plot of the estimation of the MRR for the first model employing the combination of parameters sample 9-43.

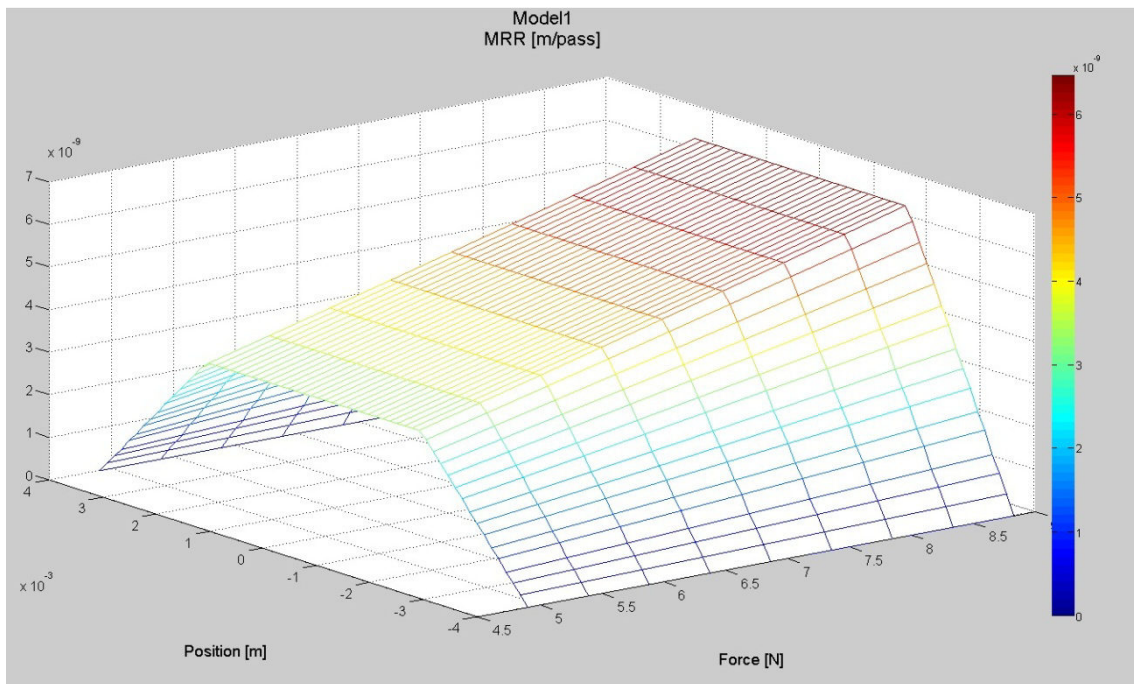


**FIGURE 12.96.** Surface plot of the estimation of the MRR for the first model employing the combination of parameters sample 12-12.



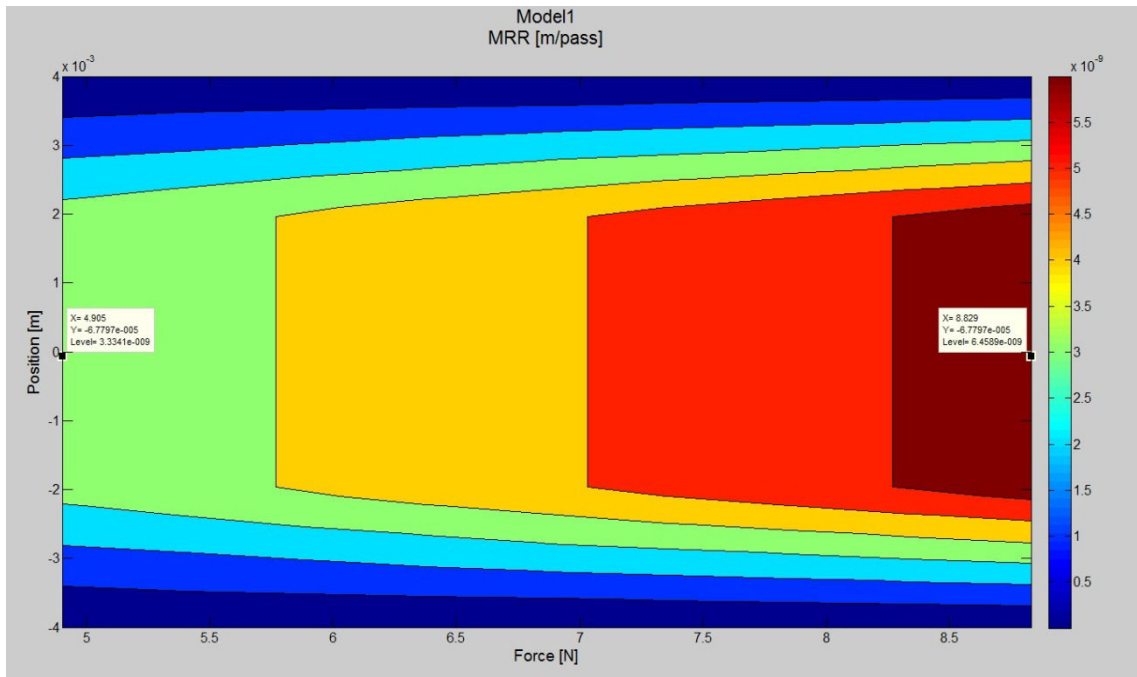


**FIGURE 12.97.** Contour plot of the estimation of the MRR for the first model employing the combination of parameters sample 12-12.

After having shown the graph provided from the program which demonstrate how the material removal rate varies with the force, the results are summarized below:

<b>Pressure (g)</b>	<b>Feed rate (mm/s)</b>	<b>Oscillation (1/min)</b>	<b>First measured MRR (<math>\mu\text{m/pass}</math>)</b>	<b>Second measured MRR (<math>\mu\text{m/pass}</math>)</b>	<b>Third measured MRR (<math>\mu\text{m/pass}</math>)</b>	<b>Prediction first model employing data from 8-42 (<math>\mu\text{m/pass}</math>)</b>
900	1.167	3500	0.009	0.0010	0.009	0.069
500	1.167	3500	/	0.008	0.009	0.035

**TABLE 12.63.** Comparison between the detected MRR and the predictions of the first model.

<b>Pressure (g)</b>	<b>Feed rate (mm/s)</b>	<b>Oscillation (1/min)</b>	<b>First measured MRR (<math>\mu\text{m/pass}</math>)</b>	<b>Second measured MRR (<math>\mu\text{m/pass}</math>)</b>	<b>Third measured MRR (<math>\mu\text{m/pass}</math>)</b>	<b>Prediction first model employing data from 9-43 (<math>\mu\text{m/pass}</math>)</b>
900	1.167	3500	0.009	0.010	0.009	0.004
500	1.167	3500	/	0.008	0.009	0.002

**TABLE 12.64.** Comparison between the detected MRR and the predictions of the first model.

<b>Pressure (g)</b>	<b>Feed rate (mm/s)</b>	<b>Oscillation (1/min)</b>	<b>First measured MRR (<math>\mu\text{m/pass}</math>)</b>	<b>Second measured MRR (<math>\mu\text{m/pass}</math>)</b>	<b>Third measured MRR (<math>\mu\text{m/pass}</math>)</b>	<b>Prediction first model employing data from 12-12 (<math>\mu\text{m/pass}</math>)</b>
900	1.167	3500	0.009	0.010	0.009	0.006
500	1.167	3500	/	0.008	0.009	0.003

**TABLE 12.65.** Comparison between the detected MRR and the predictions of the first model.

#### 12.7.4. Comparison between the experimental data and the prediction of the second model

For the verification of the second model the same procedure followed before in the first model is performed here. The three samples employed by the second model to predict the MRR have always been the sample 8-42, 9-43, and 12-12. For the verification, the oscillation and the feed rate have always been kept constant to the value of 3500 1/min and 1.167 mm/s respectively. The force has always been seen as a vector which changes between 500 g and 900 g. As previously done for the first model, before the graphs provided by the program are shown and then the corresponding predictions for the samples 3 and 11 are listed in comparison with the experimental MRR data.

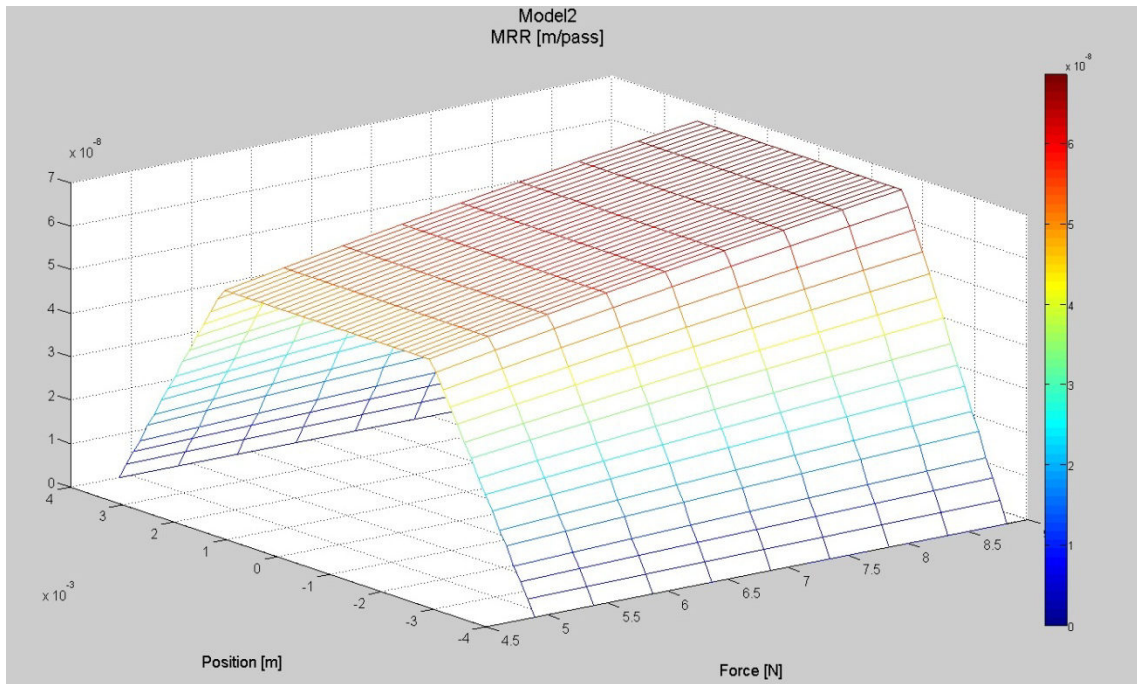


**FIGURE 12.98.** Surface plot of the estimation of the MRR for the second model employing the combination of parameters sample 8-42.

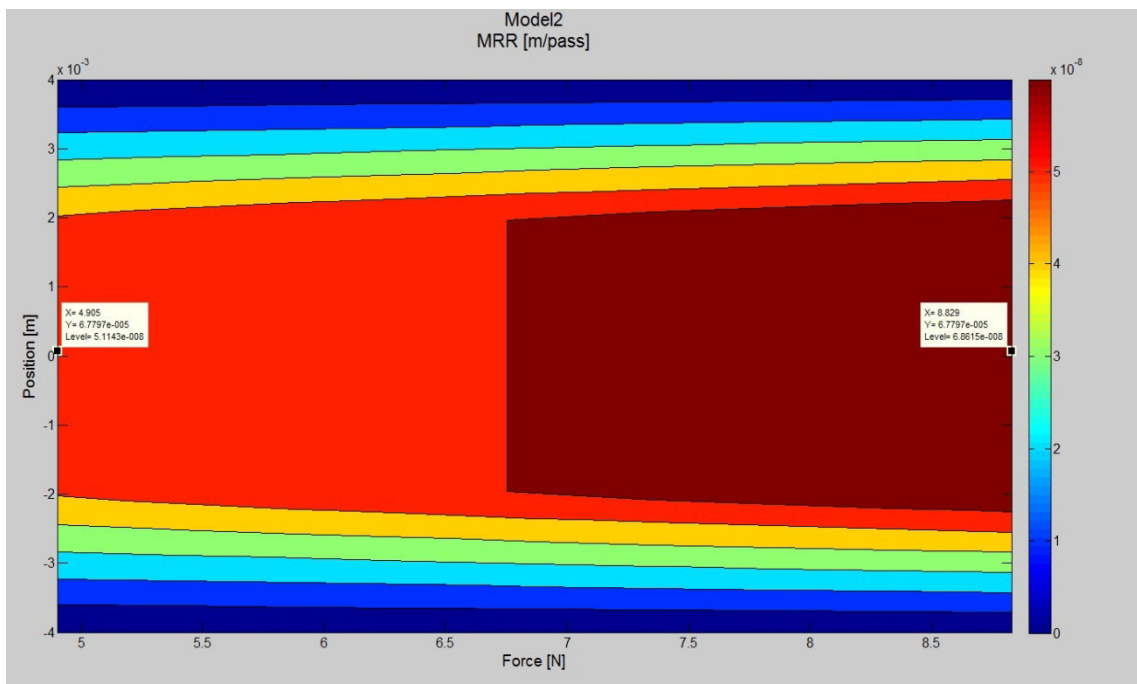


**FIGURE 12.99.** Contour plot of the estimation of the MRR for the second model employing the combination of parameters sample 8-42.

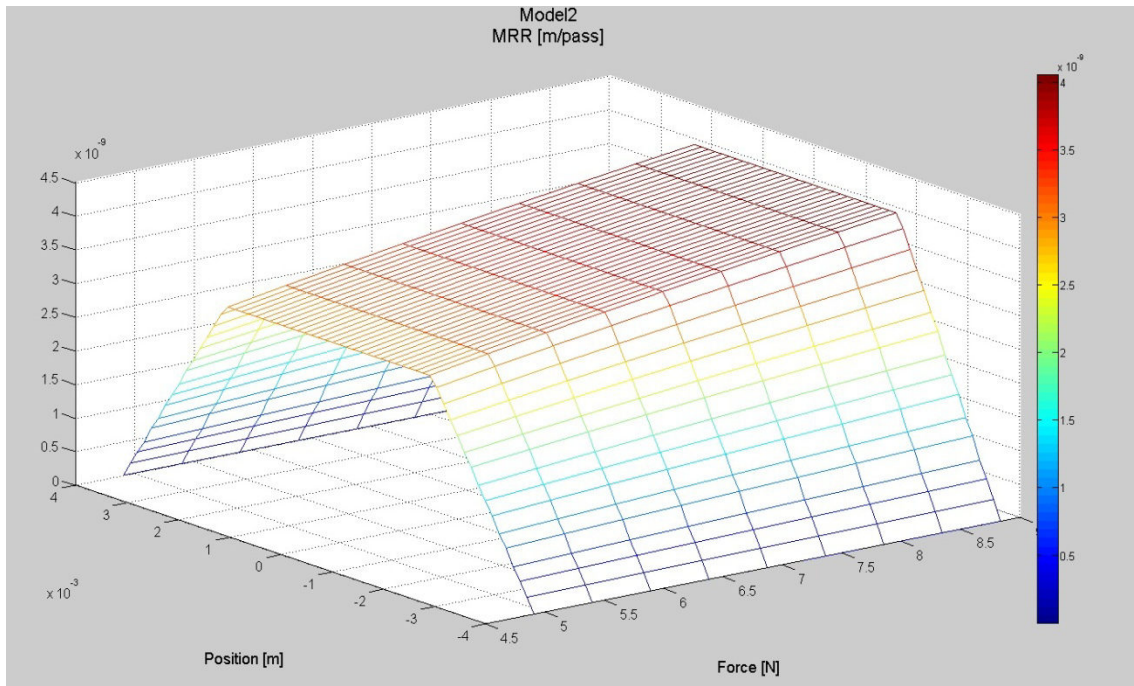


**FIGURE 12.100.** Surface plot of the estimation of the MRR for the second model employing the combination of parameters sample 9-43.

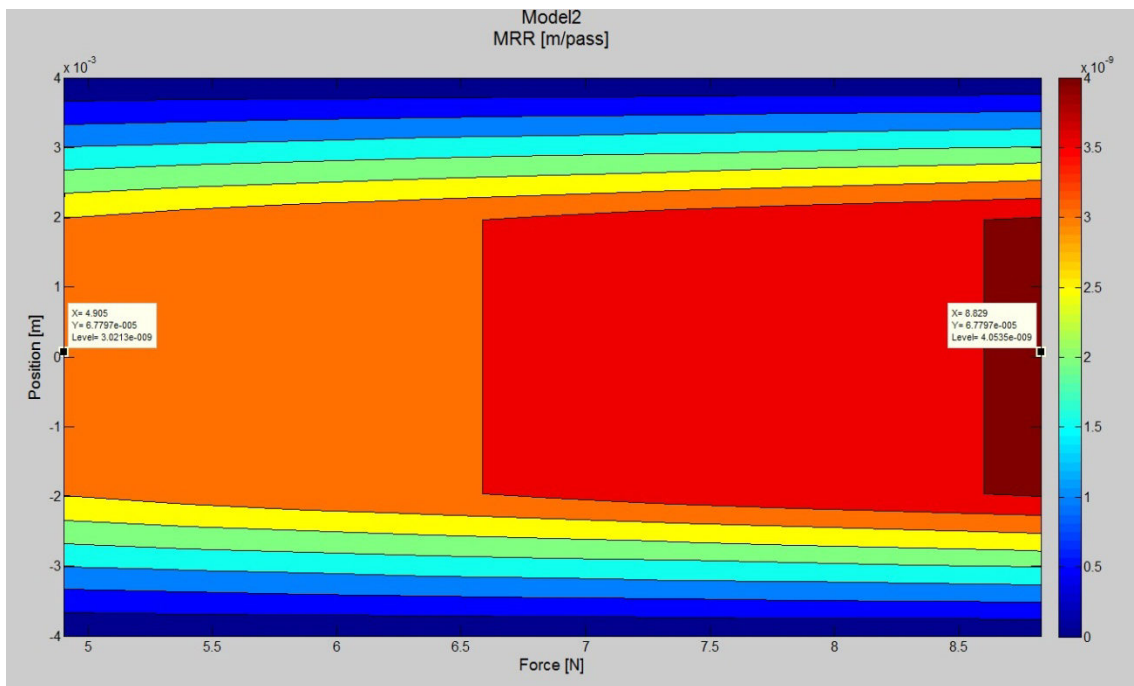


**FIGURE 12.101.** Contour plot of the estimation of the MRR for the second model employing the combination of parameters sample 9-43.

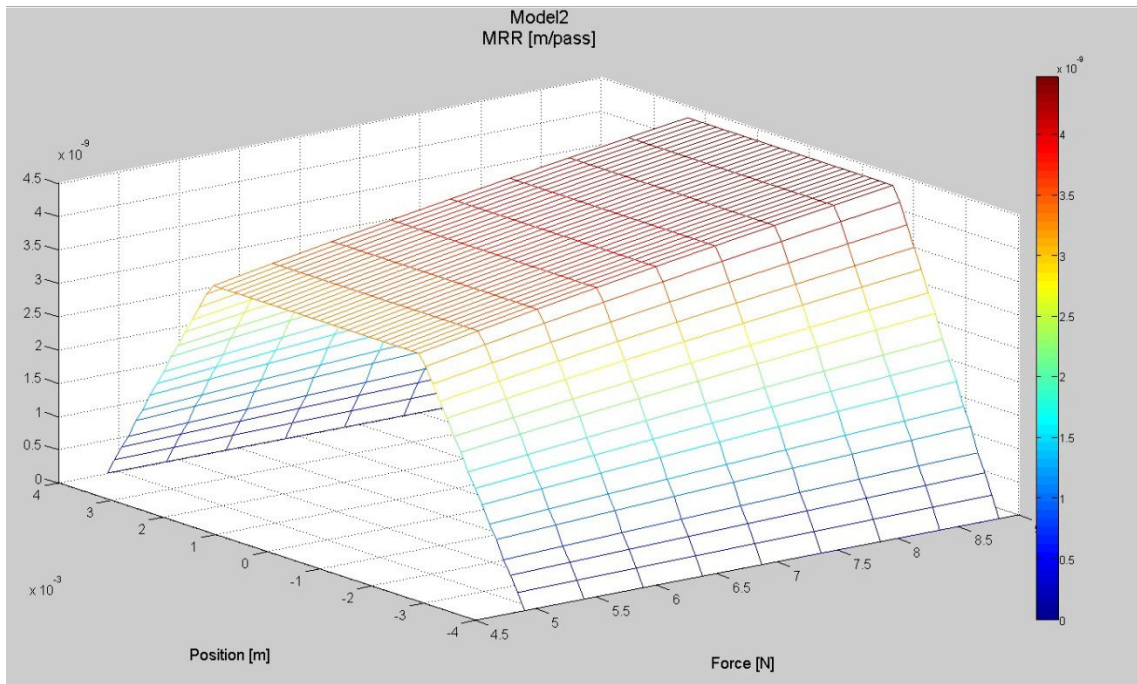


**FIGURE 12.102.** Surface plot of the estimation of the MRR for the second model employing the combination of parameters sample 12-12.

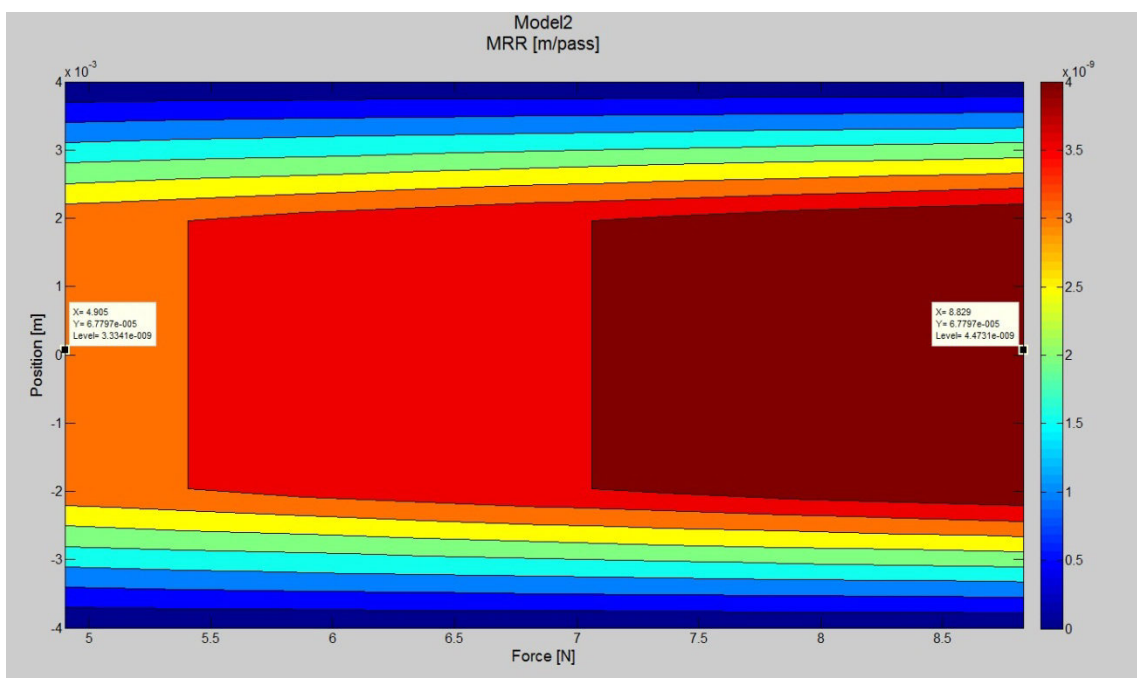


**FIGURE 12.102.** Contour plot of the estimation of the MRR for the second model employing the combination of parameters sample 12-12.

<b>Pressure (g)</b>	<b>Feed rate (mm/s)</b>	<b>Oscillation (1/min)</b>	<b>First measured MRR (<math>\mu\text{m}/\text{pass}</math>)</b>	<b>Second measured MRR (<math>\mu\text{m}/\text{pass}</math>)</b>	<b>Third measured MRR (<math>\mu\text{m}/\text{pass}</math>)</b>	<b>Prediction second model employing data from 8-42 (<math>\mu\text{m}/\text{pass}</math>)</b>
900	1.167	3500	0.009	0.010	0.009	0.068
500	1.167	3500	/	0.008	0.009	0.051

**TABLE 12.66.** Comparison between the detected MRR and the predictions of the second model.

<b>Pressure (g)</b>	<b>Feed rate (mm/s)</b>	<b>Oscillation (1/min)</b>	<b>First measured MRR (<math>\mu\text{m}/\text{pass}</math>)</b>	<b>Second measured MRR (<math>\mu\text{m}/\text{pass}</math>)</b>	<b>Third measured MRR (<math>\mu\text{m}/\text{pass}</math>)</b>	<b>Prediction second model employing data from 9-43 (<math>\mu\text{m}/\text{pass}</math>)</b>
900	1.167	3500	0.009	0.010	0.009	0.004
500	1.167	3500	/	0.008	0.009	0.003

**TABLE 12.67.** Comparison between the detected MRR and the predictions of the second model.

<b>Pressure (g)</b>	<b>Feed rate (mm/s)</b>	<b>Oscillation (1/min)</b>	<b>First measured MRR (<math>\mu\text{m}/\text{pass}</math>)</b>	<b>Second measured MRR (<math>\mu\text{m}/\text{pass}</math>)</b>	<b>Third measured MRR (<math>\mu\text{m}/\text{pass}</math>)</b>	<b>Prediction second model employing data from 12-12 (<math>\mu\text{m}/\text{pass}</math>)</b>
900	1.167	3500	0.009	0.010	0.009	0.004
500	1.167	3500	/	0.008	0.009	0.003

**TABLE 12.68.** Comparison between the detected MRR and the predictions of the second model.

### 12.7.5. Comparison between the experimental data and the prediction of the third model

The same considerations made for the previously two models are here true again, and the graphs with the predictions are shown below:

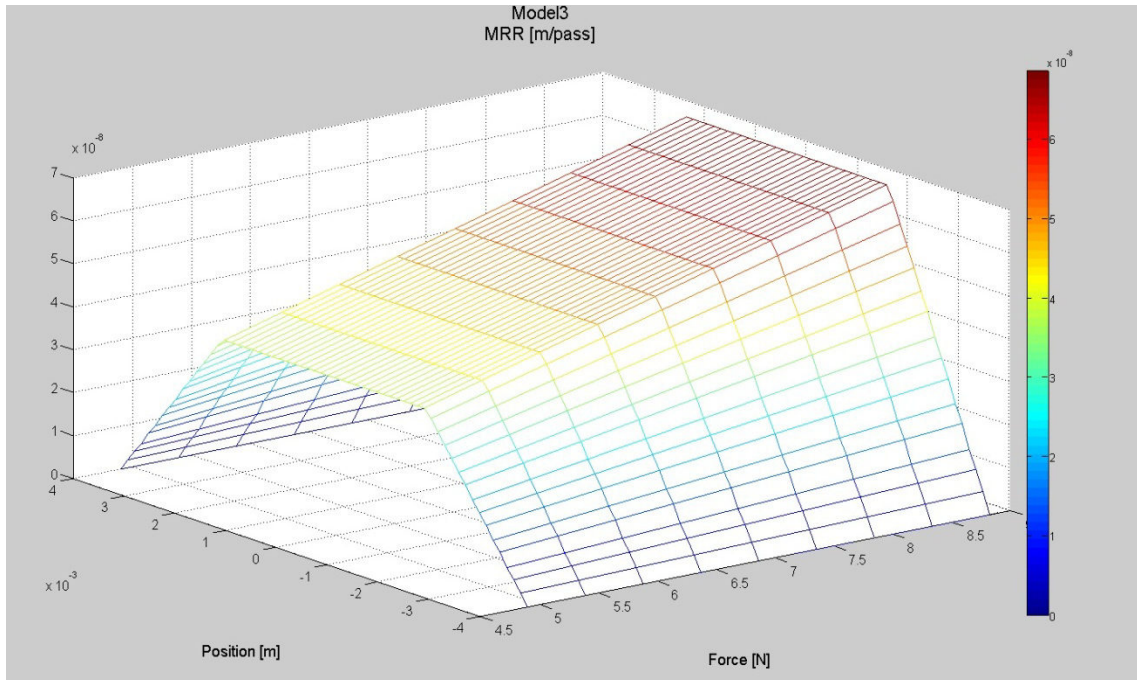


**FIGURE 12.104.** Surface plot of the estimation of the MRR for the third model employing the combination of parameters sample 8-42.

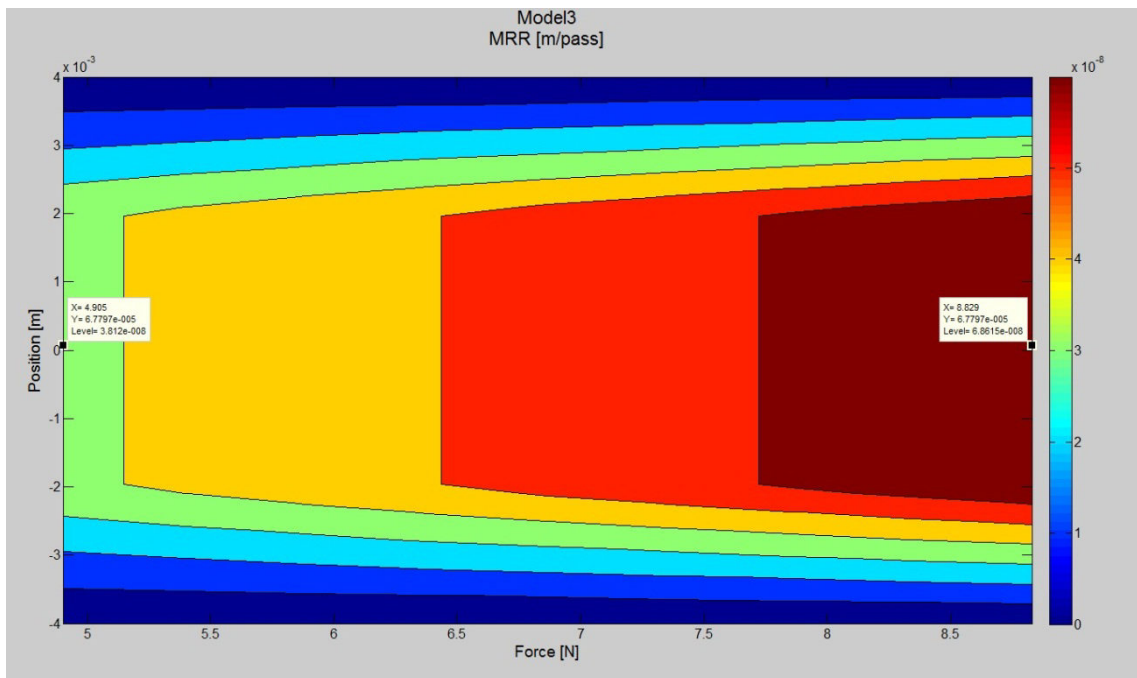


**FIGURE 12.105.** Contour plot of the estimation of the MRR for the third model employing the combination of parameters sample 8-42.

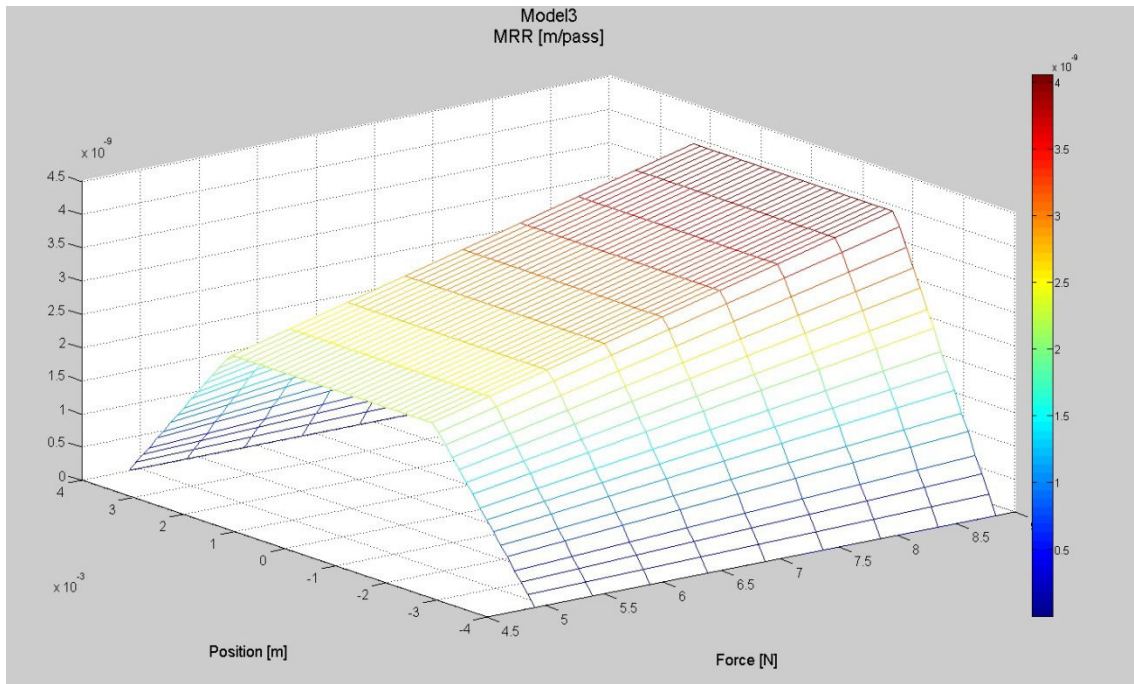


**FIGURE 12.106.** Surface plot of the estimation of the MRR for the third model employing the combination of parameters sample 9-43.

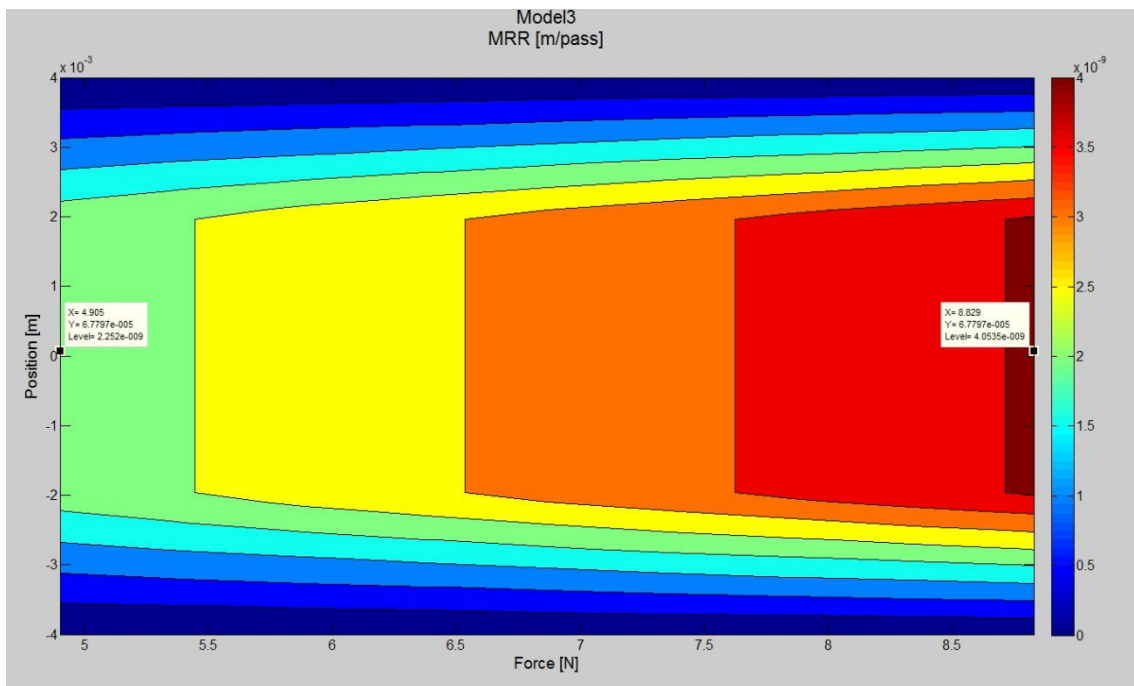


**FIGURE 12.107.** Contour plot of the estimation of the MRR for the third model employing the combination of parameters sample 9-43.



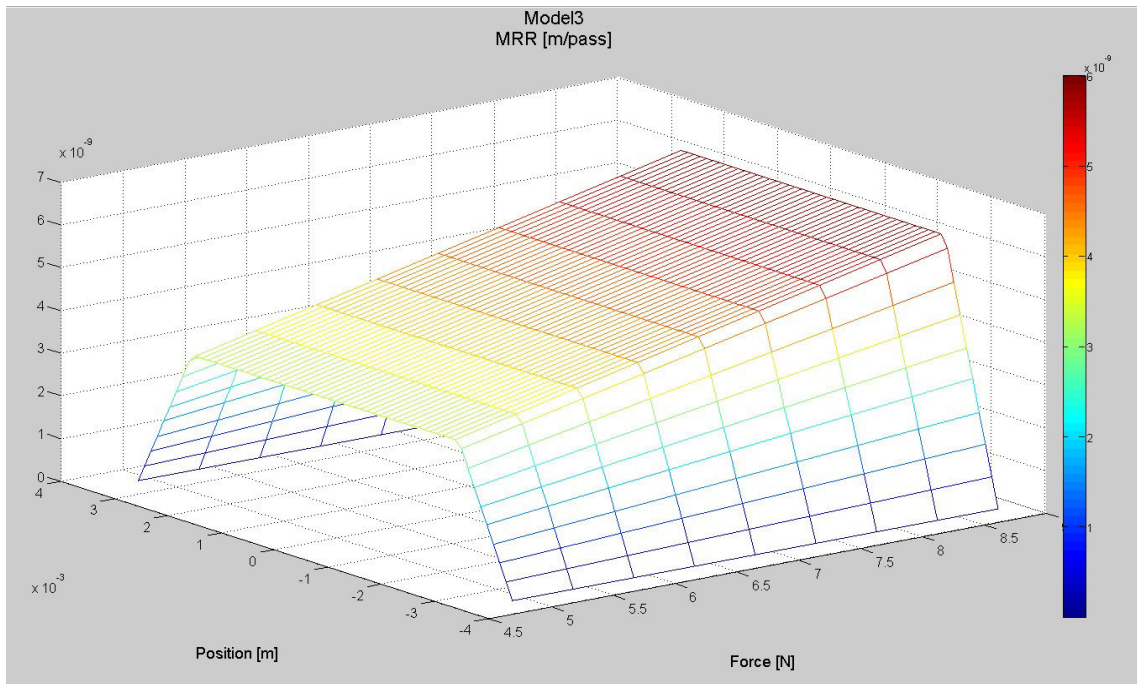


**FIGURE 12.108.** Surface plot of the estimation of the MRR for the third model employing the combination of parameters sample 12-12.

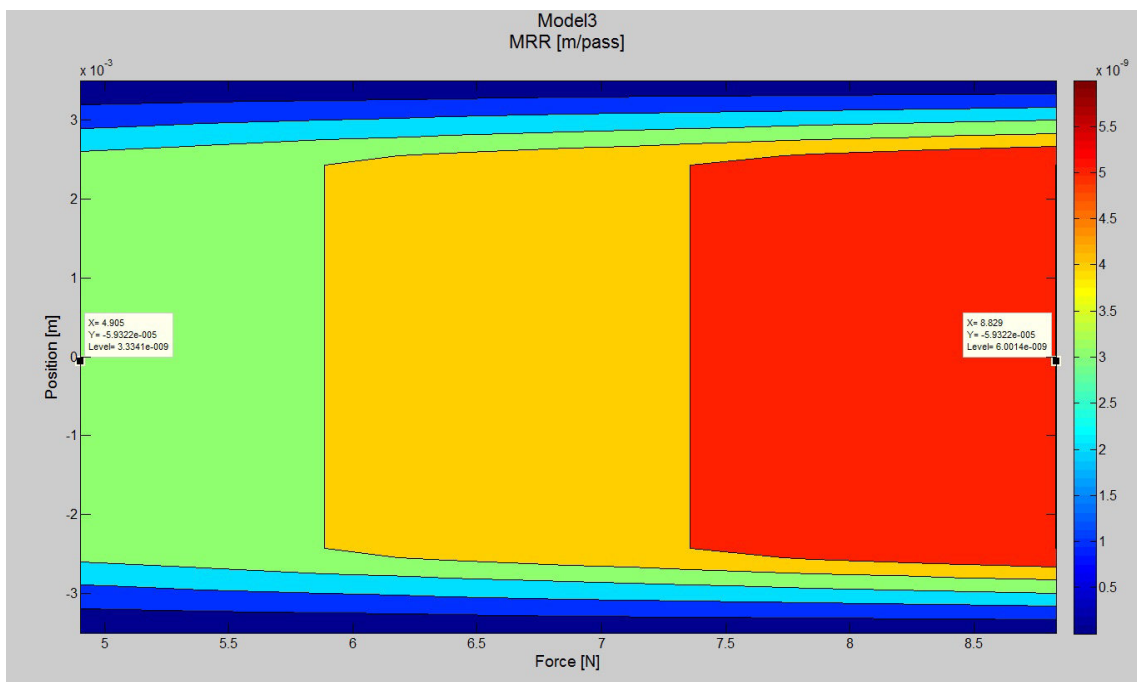


**FIGURE 12.109.** Contour plot of the estimation of the MRR for the third model employing the combination of parameters sample 12-12.

<b>Pressure (g)</b>	<b>Feed rate (mm/s)</b>	<b>Oscillation (1/min)</b>	<b>First measured MRR (<math>\mu\text{m}/\text{pass}</math>)</b>	<b>Second measured MRR (<math>\mu\text{m}/\text{pass}</math>)</b>	<b>Third measured MRR (<math>\mu\text{m}/\text{pass}</math>)</b>	<b>Prediction third model employing data from 8-42 (<math>\mu\text{m}/\text{pass}</math>)</b>
900	1.167	3500	0.009	0.010	0.009	0.069
500	1.167	3500	/	0.008	0.009	0.038

**TABLE 12.69.** Comparison between the detected MRR and the predictions of the third model.

<b>Pressure (g)</b>	<b>Feed rate (mm/s)</b>	<b>Oscillation (1/min)</b>	<b>First measured MRR (<math>\mu\text{m}/\text{pass}</math>)</b>	<b>Second measured MRR (<math>\mu\text{m}/\text{pass}</math>)</b>	<b>Third measured MRR (<math>\mu\text{m}/\text{pass}</math>)</b>	<b>Prediction third model employing data from 9-43 (<math>\mu\text{m}/\text{pass}</math>)</b>
900	1.167	3500	0.009	0.010	0.009	0.004
500	1.167	3500	/	0.008	0.009	0.002

**TABLE 12.70.** Comparison between the detected MRR and the predictions of the third model.

<b>Pressure (g)</b>	<b>Feed rate (mm/s)</b>	<b>Oscillation (1/min)</b>	<b>First measured MRR (<math>\mu\text{m}/\text{pass}</math>)</b>	<b>Second measured MRR (<math>\mu\text{m}/\text{pass}</math>)</b>	<b>Third measured MRR (<math>\mu\text{m}/\text{pass}</math>)</b>	<b>Prediction third model employing data from 12-12 (<math>\mu\text{m}/\text{pass}</math>)</b>
900	1.167	3500	0.009	0.010	0.009	0.006
500	1.167	3500	/	0.008	0.009	0.003

**TABLE 12.71.** Comparison between the detected MRR and the predictions of the third model.

#### 12.7.6. Conclusion regarding the verification of the three theoretical models for the MRR

In the previous three subchapters the verification of the three theoretical models implemented in MATLAB has been carried out. Three experimental combinations of parameters have been used to help the models to provide the estimation of the

material removal rate, otherwise only a proportional coefficient related to the MRR would have been obtained. The three combinations have been sample 8-42 (pressure=900 g; feed rate=0.167 mm/s; oscillation=3500 1/min; MRR=), sample 9-43 (pressure=900 g; feed rate=1.167 mm/s; oscillation=2000 1/min; MRR=), and sample 12-12 (pressure=500g; feed rate=0.667 mm/s; oscillation=2000 1/min; MRR=).

From these three combinations of parameters we have obtained by the same model six different predictions of the MRR as function of the down force.

It is clear from the comparison among the predictions of all the theoretical model and the experimental data that these models do not work well in no case. This does not mean that they are wrong. In fact, the experimental results related to the material removal have been strongly affected by the lack of flatness of the contact surface of the pad. That is, the fact which the pad surface was not perfectly parallel to the samples surface has implied that the pressure distribution was completely different from the theoretical one. In fact, two of the input parameters of the theoretical models are related to the geometry of the pad itself, that is, length and width of the pad. From these parameters and from the pressure applied during the polishing process the distribution of the pressures on the polishing area is calculated. But if the contact surface is not equal to the size of the pad surface the real pressure cannot be well estimated from the models. This clearly appears when the profiles of the polished area are analyzed. For everyone the polished area detected has a width very small compared with the real size of the pad. To have a better verification of the model, therefore, the test should be repeated with a pad that leaves on the workpiece surface a track closer to the real size of its contact surface.



**FIGURE 12.110.** Track left by the pad on the surface.

## 12.8. Analysis of the overlap zone

In this subchapter the analysis made on the sample 12 are taken into account and explained. In fact, in all the previous analysis all the samples have been taken into consideration except the sample 12. In fact, this sample was polished with the aim to see what happens to the polished surface when an overlap is present.

An overlap occurs when part of a progressing pad passes over a zone previously polished by the last pass (literally the pad overlap part of the previous polished zone). Below a drawing is introduced to clarify this concept:

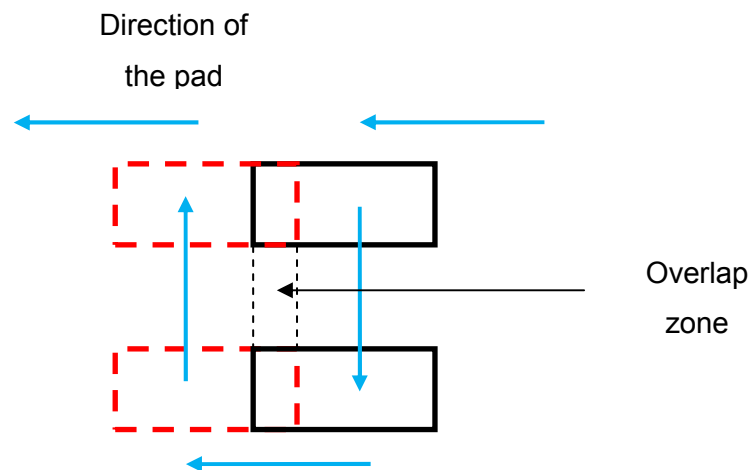


**FIGURE 12.111** .The overlap zone is showed.

This situation is the most common in the polishing process in flat conditions, in fact, generally, the pad move both along the feed rate direction and along the oscillation directions, causing therefore overlapping (as shown in the *figure 12.111*). For this reason is interesting to analyzed what happens in this zone to understand how this overlap affects the process.

Therefore, our purpose here is not to understand how the roughness behavior depends on the presence of the overlap, but how the track of the pad appears in this zone. In fact, it is expected that, since the pad spends more time in the overlap zone compared to the other parts of the polished area, the material removal will be more pronounced,

because it will be subjected to the pressure of the pad longer. This means that the left track in this case is expected to be different from the previous ones related to the other samples in absence of overlapping. In particular it is expected that in the zone where the overlap occurs (central zone in this case), the track will be deeper.

To verify these hypothesis, a profile measurements have to be done. As it happened for detecting the amount of material removal occurred during the polishing process, a profile before and after the polishing process has to be measured. In this case the polished surfaces in the sample 12 have been six, and have been polished with a combination of parameter equal to that employed for the sample zero (pressure=500 g, feed rate=0.667 mm/s, and oscillation=2000 1/min). The measurements for each surface have been three, and they were carried out with the employment of the Hommel.

As it happened for the material removal profiles, the two corresponding profiles (before and after polishing) have been aligned together and the track left by the pad has been analyzed.

Now, one of the analyzed alignment is shown below:

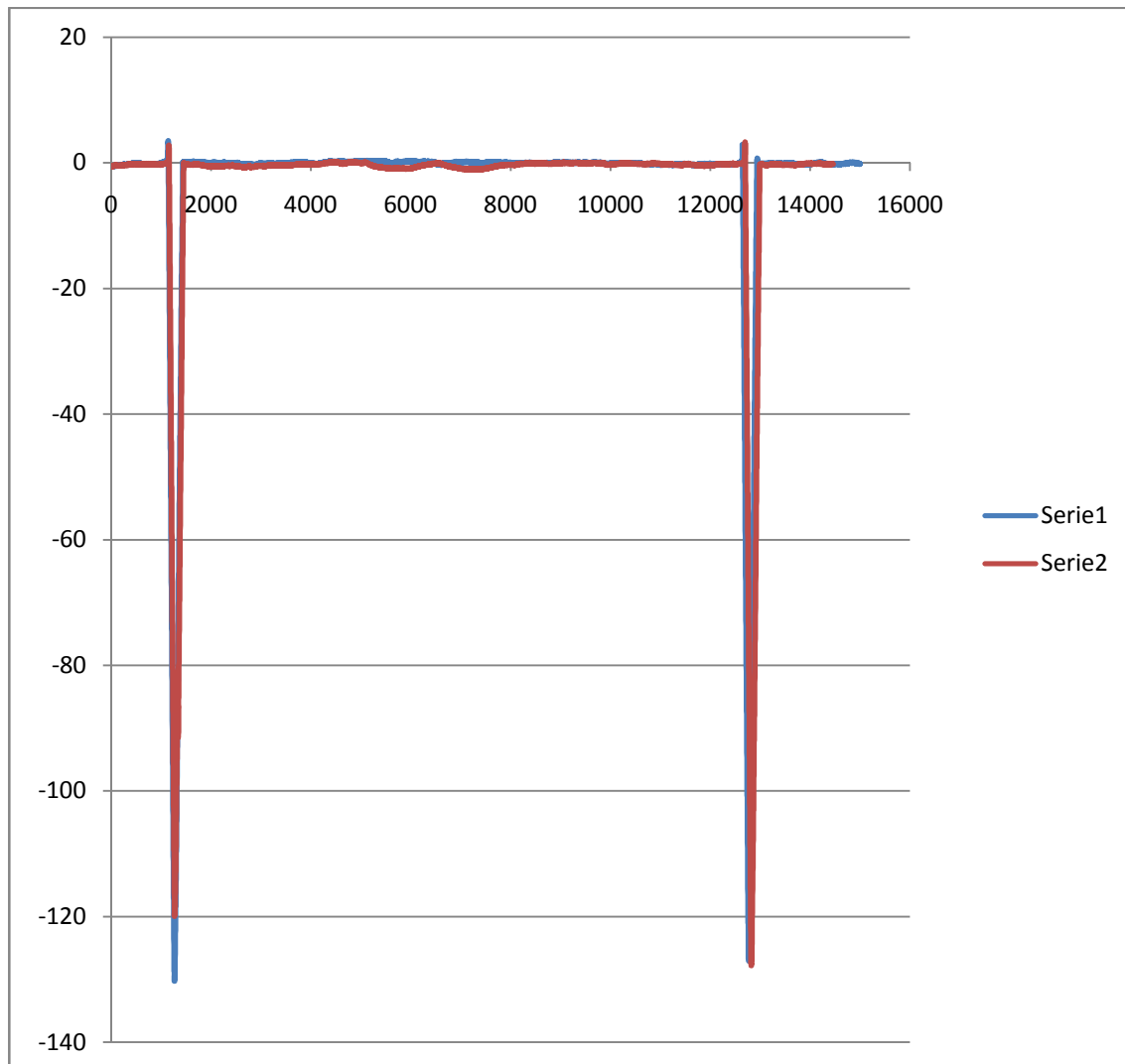


**FIGURE 12.112** . Alignment of two corresponding profiles of the sample 12 (pressure=500 g; feed rate=0,667 mm/s, oscillation

As it can be seen from the *figure 12.112*, the track is very different from the expected. In fact, the hypothesized deeper “hole” in correspondence of the overlapping zone does not occur. Also, the overall width produced by the pad during the process results smaller than the expected. In fact, the overlap employing during the process has been equal to the 50% of the width of the pad. This means that, if the width of the pad was 3 mm, the width covered during the process should be equal to 4,5 mm, and if the strokes are considered too, the overall width should be 5,5 mm (in fact the strokes employed during the process was equal to 0,5 mm for side). But as it can be seen from

the *figure 12.112*, the track left by the pad results to be less of 3,5 mm wide. This means that the no-flatness of the pad respect the workpiece surface has affected the results again. In fact, that small hill inside the track could be derived from the fact that only a part of the pad has been in contact with the polished surface. And this working part seems to be the left size, if the starting position of the pad is supposed to be situated between the  $10000\mu\text{m}$  and  $7000\mu\text{m}$ , shown in the *figure 12.112*, and the position where the pad shift during the process causing overlap is supposed to be between the  $5000\mu\text{m}$  and the  $8000\mu\text{m}$ . A figure is provided below to clarify the term “working part” of the pad.

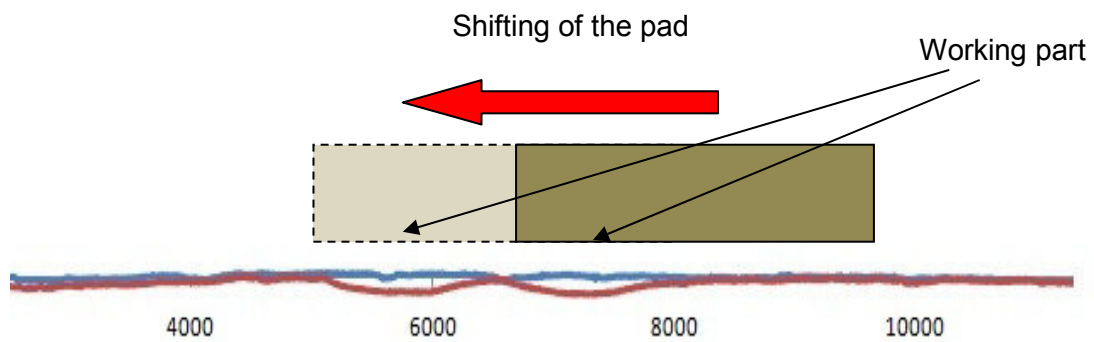


**FIGURE 12.113** . This figure is only to clarify what is meant by “working part” of the pad. It does not reproduce the real sizes of the pad itself.

Therefore, as it was happened for the verification of the model, also here to have a reliable behavior of the overlapping zone, the experimental tests should be repeated employing a polishing pad that guarantees a better contact pad surface-workpiece.

# CHAPTER THIRTEEN

## Conclusion

The purposes of this master thesis have been mainly two: to understand which are the polishing parameters that strongly affect the roughness behavior during a polishing process in flat kinematics conditions, and to verify the reliability of three theoretical models regarding the material removal rate. To detect them, an experimental planning involving twelve samples has been created. A setting of parameters of three polishing parameters (force, feed rate, and frequency of the pad) has been formulated to understand how their variation affected the polishing process. The levels of them have been chosen keeping a constant wavelength of the pad motion equal to 20  $\mu\text{m}$ . From the experimental results obtained by the tests some analysis have been carried out. The first analysis has regarded the extraction of the roughness curves deriving from the measurement made after the experimental test for each combination of parameters. The roughness parameters here detected have been: the  $R_a$  value, because it is the roughness parameter employed by STRECON to detect the goodness of its manufactures, the  $R_v$  value, because in ground sample like those employed in the tests, the depth of the valley has been supposed to strongly affect the required time to reach the final roughness value expected from the typology of used diamond paste, and the  $R_z$  value, to verify if it is mainly the depth of the valleys which affects the process or if there is a contribution from the height of the peaks as well. What has been observed from this first analysis, it has been that the depth of the valley strongly affect the required timing to reach the end of the process. Some stalemates have been observed caused by the presence of initial deep valley on the machining surface. This situation has been verified by three samples (sample 4, 5, 7) which have shown a lower decrease of the roughness. In these cases the required time to finish the process is longer respect to the other samples, especially if low levels of pressure are involved. This happens because the material removal required to reach good surfaces conditions in this case is bigger than for a sample without the presence of these deep valley, but, if the level of pressure is low the material removal will be low and the time to reach the end of the polishing process will be long. What we have seen from the comparison between the  $R_z$  curves and the  $R_v$  curves is that they present very similar trends. This means that the velocity of the reduction in the depth of the valley characterizes the roughness behavior of the machining surface in this case.



The second analysis has been done with the aim to detect which are the polishing parameters that more affect the process. Through a DOE analysis, it has been detected that the most important parameters which affect the polishing process are, in order of magnitude: pressure, frequency, the interaction frequency-feed rate, and the feed rate itself. It has been observed that with an increase of pressure and frequency the process reach the final roughness value in shorter time. Whereas the feed rate acts in opposition. Anyway, a great interaction between feed rate and frequency exists and it has to be taken into account in the process. Moreover, the variation of the system response with the variation of the parameters is not linear. This is demonstrated because when the sample 0 is polished (central value) the timing required to reach the final roughness value is shorter than expected by a linear variation of the response. Small timing values also have been obtained from the three sample polished keeping constant two of the three parameters to their high levels and varying the third one on its central value (an example is given by the sample 9 where pressure and feed rate have been kept constant to 900 g and 1.167 mm/s, whereas the frequency has been set on its central value of 33.33 1/s). these results mean that a stable region where small polishing time are obtained could exist. Nevertheless, these results have to be considered as an indication of where and how new experimental tests can be done. In fact, not all the data employed in the DOE analysis are experimental, because three samples (sample 4, 5, and 7) have not reach the real final roughness value for that diamond paste employed due to the initial presence of deep valley in the surface. Then this considerations have to be verify with other tests.

The third analysis regarding the roughness has been made to carry out some empirical model describing the roughness behavior. Two regression model has been purpose. The first, called preliminary regression models, has been found fitting the equations  $y = A + B \times \log(x)$  computed for each combinations of parameters. The second one instead has been fitted employing a MATLAB program capable to provide a regression model of second degree making the least squares regression. They has been compared and the second one reproduces better the roughness behavior for different combinations of parameters. Nevertheless, the data employed to create this model are incomplete due to the different starting roughness shown by the samples. To improve this model, more data are required, and then some new tests have to be run in the next future to reliably verify it. With this models the hypothesis that the roughness could depend on the number of strokes of the pad and not on the time has been verified. Combinations of parameters with the same pressure and same wavelength have been compared. Nevertheless, the obtained results have refused this hypothesis, because

for equal number of strokes the reached roughness value for two combinations of parameter related to each other has been detected to be different.

The second aim of this thesis has been to verify three theoretical MRR models found in the literature. To do it the profiles before and after the polishing process have been measured. The results show that there is no correspondence between the experimental data and the prediction of these models. But in this case the results have been affected by a variable, that is the pad surface of contact with the workpiece surface. In fact, during all the experimental tests it has never been completely parallel to the machining surface, but only a part of it touched the surface. This means that the real distribution of the pressure has been different respect to the theoretical one, in fact the models compute it through the geometry of the contact surface of the pad. The reason of this lack of parallelism has been mainly attributed to three causes: the first one is that no precise instrument has been possible to use to make the pad surface extremely flat, in fact only a cutter and sandpaper have been employed to adjust the shape of the pad. The second one is that maybe the wood has not been the material more adapt for that process, in fact from the literature it appears that for a polishing process the soft pad with a good stiffness work better than the others. This means that a more rigid pad could bring a better results because it is dimensionally more stable and the distribution of the pressure can be more similar to the theoretical hypothesized by the models. But to verify this, other experimental tests employing another kind of pad have to be run. Finally, the third reason could be related to the clamping system employed to the RAP polishing arm to keep the pad. In fact, to hold the pad attached to the polishing arm a screw is employed. When this one is screwed, it can penetrate into the pad for some millimeters weakening it. Moreover the size of this screw is smaller than the pad size, and this probably do not guarantee the perfectly clamp of the pad which could change continuously position during the process when an medium-high frequency is applied. Another clamping system capable to clamp a bigger size of the pad will be preferable.

Moreover, the comparison of the profiles for the MRR has not been possible for that sample which employed low values of pressure (100 g). This because the track of the pad on the polished surface was not clearly visible. Anyway, the pressure of 100 g is a very low value that is not used from STRECON to polish its manufactures.

Regarding the analysis of overlapping carried out with the sample 12, they have shown again the problem related with the lack of parallelism between the pad surface and the surface of the workpiece. In fact, in the *figure 12.112*, it is visible a hill is present in the

middle of the track. This means that the pad has polished the surface only with a restricted part of its surface, whereas the other size of it has not affected the process.

## References

- [1] SBT Lapping and Polishing, "Lapping and Polishing basis", Application Laboratory report 54.
- [2] M.J. Jackson and J.P. Davim, "Machining with Abrasives", ©Springer Science + Business Media, LLC 2011.
- [3] Version 2 ME, IIT Kharagpur, "Module 5, Abrasive Processes (Grinding).
- [4] [www.krebs-riedel.com](http://www.krebs-riedel.com).
- [5] [www.efunda.com](http://www.efunda.com).
- [6] Mark Irvin, "Diamond Lapping and Polishing", Hyprez ® Product Manager, Engis Corp.
- [7] [www.lapping-pdish.com](http://www.lapping-pdish.com).
- [8] [www.directindustry.com](http://www.directindustry.com).
- [9] [gsmachineries.tradeindia.com](http://gsmachineries.tradeindia.com).
- [10] [cnx.org](http://cnx.org).
- [11] [www.testbourn.com](http://www.testbourn.com).
- [12] [www.srate.com](http://www.srate.com).
- [13] [dismac.isten.ing.unipg.it](http://dismac.isten.ing.unipg.it).
- [14] V.K. Jain, "Magnetic field assisted abrasive based micro-/nano-finishing", Indian Institute of Technology, Mechanical Engineering, Kanpur, 208016, Uttar Pradesh, India.
- [15] [www.seekpart.com](http://www.seekpart.com).
- [16] [www.cheap-hack.com](http://www.cheap-hack.com).
- [17] [milano.olx.it](http://milano.olx.it).
- [18] Ron Amaral, Leonel Ho Chong, "Surface Roughness", December 2002, MatE 210, Dr. Guna Selvaduray.
- [19] [www.santo-plastic-mold.com](http://www.santo-plastic-mold.com).
- [20] [cnqinyou.en.made-in-china.com](http://cnqinyou.en.made-in-china.com).
- [21] [www.palmatech.co.kr](http://www.palmatech.co.kr).
- [22] [sg.misumi-ec.com](http://sg.misumi-ec.com).
- [23] [www.sciencephoto.com](http://www.sciencephoto.com).
- [24] [www.widepr.com](http://www.widepr.com).
- [25] Guanghui Fu, Abhijit Chandra, Sumit Guha, and Ghatu Subbhash, "A Plasticity-Based Model of Material Removal in Chemical-Mechanical Polishing (CMP)", IEE TRANSACTION ON SEMICONDUCTOR MANUFACTURING, VOL 14, NO.4, NOVEMBER 2001.

- [26] Jianfeng Luo and David A. Dornfeld, "Material Removal Mechanism in Chemical Mechanical Polishing: Theory and Modeling", IEE TRENDACTIONS ON SEMICONDUCTOR MANUFACTURING, VOL. 14, NO.2, MAY 2001.
- [27] Yongsong Xie, Bharat Bhushan, "Effects of particle size, polishing pad and contact pressure in free abrasive polishing", Computer Microtribology and Contamination Laboratory, Department of Mechanical Engineering, The Ohio State University, Columbus, OH 43210-1107, USA.
- [28] Roman Wechsler, "Manual: MATLAB Program for the Development of Empirical Models".
- [29] [www.mathworks.se](http://www.mathworks.se)
- [30] Private communication with STRECON.
- [31] [www.uddeholm.com](http://www.uddeholm.com).
- [32] [www.ricercaemisure.it](http://www.ricercaemisure.it).
- [33] [www.strecon.com](http://www.strecon.com)

## Acknowledgements

My gratitude goes to Dr. Giuliano Bissacco for having followed this thesis work.

Thank you to Professor Hans Nørgaard Hansen for having welcomed me.

Thank you to my family to have always supported me during this experience.

Thank you to Kamran Mohaghegh and Jacob Rasmussen to have helped me in the measurement analysis.

Thank you to STRECON staff for its availability shown.

Finally thank you to all DTU for the availability shown.